Durham E-Theses

Petrographic and Geochemical Analysis of the Carboniferous (Namurian) Holywell Shale of northeast Wales

NEWPORT, LEO,PHILIP

Petrographic and Geochemical Analysis of the Carboniferous (Namurian) Holywell Shale of northeast Wales

THIS THESIS WAS SUBMITTED

FOR THE DEGREE OF DOCTOR OF PHILOSOPHY

by

LEO PHILIP NEWPORT

2015

DEPARTMENT OF EARTH SCIENCES

DURHAM UNIVERSITY

Abstract

The potential of the Holywell Shale as a source-rock reservoir was explored using a multidisciplinary approach which focused on understanding the depositional setting of the Holywell Shale within the UK Namurian (mid-Carboniferous) Pennine Basin. The deposition of the Holywell Shale was examined to understand the supply and preservation of organic matter and detrital input into the basin both temporally and spatially. Both outcrop and borehole material was sampled and analysed using organic geochemical (e.g. total organic carbon, carbon isotopes, and RockEval™), inorganic geochemical (e.g. X-ray fluorescence) techniques in combination with detailed petrographic analysis.

Organic matter content of the Holywell Shale was highly variable (0.1 wt % to 10.3 wt %), with an average 2.0 wt % and predominantly Type III kerogens present. Carbon isotopes revealed a change in supply of organic matter to the basin from the strongly marine influenced Lower Holywell Shale (-31.1 ‰ to -25.6 ‰, average -28.8 ‰; containing some Type II kerogen) to the terrestrial dominated Upper Holywell Shale (-28.0 ‰ to -22.4 ‰, average -24.5 ‰; containing some Type IV kerogens). Trace element and RockEval™ pararmeters indicate that the Holywell Shale was deposited under predominantly oxic conditions with some periods of hypoxia. This resulted in relatively poor preservation of organic matter (low HI values < 301 mg/g and high OI values < 121 mg/g).

There is no clear relationship between organic matter source, quantity and quality within the Holywell Shale. The highest organic matter quantity with greatest preservation occurs within fossiliferous, clay-rich lithofacies associated with marine highstands. Although, the small-scale variability and heterogeneity of both organofacies and lithofacies mean that the reservoir quality of the Holywell Shale is inherently difficult to predict.

Contents

iv

List of Figures

Figures are listed here according first to the chapter in which they occur followed by the order they appear within that chapter (e.g. Chapter 4, Figure 2 would appear as Figure 4-2). Each figure has the corresponding page number where it can be found.

Chapter 4:

laminar organic matter with abundant silt sized quartz; E (sample CVS3H2; Arnsbergian; location Easting: 326050, Northing: 356880): black arrows denote possible diagenetic quartz (possibly from remineralisation of biogenic silica), with some other diagenetic minerals such as ferroan dolomite; F (sample RTS5H1; Arnsbergian; location Easting: 323365, Northing: 356900): large (sand/silt sized) detrital grains of quartz within a fine clay matrix…………………………………68

Chapter 5:

Figure 5-4: Point of Ayr No.3 shaft depths of samples, marine bands, regional substages and faults. Images represent different facies and microfacies (transmitted

Chapter 7:

List of Tables

Declaration and Copyright Statement

This thesis describes my own work, except where acknowledgement is made in the text, and is not the same as any work that has been submitted to this or any other university for any degree, diploma or other qualification.

6th August 2015

Acknowledgements

The project has been made possible through the continued funding of IGas Energy PLC. I am very grateful for the opportunities in addition to my PhD funding which IGas have provided such as hands-on experience on their shale gas exploration drill rig. Particular thanks to Matthew Wright for his help and support.

Many thanks to my team of supervisors Chris Greenwell, Jon Gluyas, Andy Aplin and Darren Gröcke for their support through the process, being there to discuss the project details and helping me improve as a researcher and scientist. I would like to also thank everyone who has provided helpful support and discussion on shale-related research including: Stuart, Fred, Howard, Jonny, Liam, Richard and Joao.

There are numerous people who have helped me at some stage of my PhD including sample preparation, analysis, teaching me techniques, and many have gone the extra mile to meet my (often difficult) requests. I would like to thank Ian Chaplin for his help with preparing thin sections; Leon Bowen for his help with training and problem-solving using scanning electron microscope techniques; Scott Renshaw, Tracey Gallagher and Colin Waters for their help with my enquiries and useful discussion on my visits to the British Geological Survey (Keyworth). Many thanks also to Martin Jones (Newcastle University) and Applied Petroleum Technology (Norway) for RockEval™ analysis and Alex Finlay and John Martin at Chemostrat for XRF analysis.

Finally I would like to thank my family and friends for all the love and support they have given me throughout this PhD – I couldn't have done it without you.

This thesis is dedicated to my wonderful wife Sarah.

"Science is not only a disciple of reason but, also, one of romance and passion"

-    *Stephen Hawking*

Chapter 1:

Introduction

1.1: Background

Over the last decade the development in production of hydrocarbons from unconventional sources has significantly expanded, specifically the shale-gas and shale-oil plays of the United States have become a significant hydrocarbon resource (Aplin & Macquaker, 2011; Jarvie, 2012).

Shale is a name commonly used to describe a broad range of fine grained rocks which are fissile. However, the fissile nature of a rock is a characteristic dependent on the degree of weathering and therefore the term shale should not be used as a group classification term for fine-grained sedimentary rocks which may or may not be fissile (Aplin & Macquaker, 2011; Lazar et al., 2015a). The term mudstone is a more suitable term to describe fine-grained sedimentary rocks where > 50 % of particles are less than 62.5 µm in size by weight/volume and encompasses a wide variation of composition, porosity, thickness and heterogeneity   (e.g. Folk, 1980; Hart et al., 2013; Lazar et al., 2015a; Milliken, 2014). These variations develop as a result of provenance (origin of material), depositional environment (i.e. marine settings, estuaries, lakes), and post depositional alteration processes (including compaction, cementation, mineral authigenesis and dissolution, and organic matter maturation) (Hart et al., 2013).

Mudstones commonly form source rocks for conventional hydrocarbon exploration. In a source rock the process of maturation of organic material (kerogen) with increase in temperature (oil window circa 50-150 °C, gas window circa 150-200 °C) and pressure (increasing with depth) generates hydrocarbons over time. In a conventional system, these hydrocarbons are then expelled where they typically migrate along permeable pathways until they reach an impermeable layer (sealing or cap-rock), become trapped and form an accumulation. However, mudstones are vertically anisotropic and have low

permeability (< 0.1 mD) which results in trapped hydrocarbons held within the rock, and without either natural or induced fractures (using methods such as hydraulic fracturing) hydrocarbons cannot be extracted at economic rates. Unlike conventional hydrocarbon systems where the source, reservoir and seal are typically different rock types; in unconventional shale-gas and shale-oil systems, the mudstone acts as source, reservoir and seal, resulting in the term source-rock reservoir (Hart et al., 2013).

Within the UK the main targets for the development of source-rock reservoirs are the Carboniferous Bowland-Hodder Formation and the Jurassic Weald Basin (Andrews, 2013). This study focuses on the Carboniferous mudstones of northeast Wales (Holywell Shale). The term Holywell Shale has been made obsolete and is now incorporated within the term Bowland Shale Formation (BGS Lexicon of named rock units). However, the term 'Bowland Shale Formation' covers a series of mudstones which were deposited diachronously within different basins and sub-basins across northern England, northeast Wales, and the English midlands. To avoid confusion when referring specifically to the Bowland Shale Formation where it occurs in northeast Wales (the study area for this thesis), the term Holywell Shale will be used.

1.2: Aims

This thesis investigates the potential of the Holywell Shale as a source-rock reservoir through analysis of the depositional setting (i.e. organic matter flux to the basin, type of organic matter present, mineralogy present and the lithofacies which occur). The aim in undertaking this research is to identify sedimentary facies and organic matter variations at and around biostratigraphic markers (marine bands) across the Holywell Shale. This will provide greater insight into the varying depositional settings which occurred within the basin during the Namurian, in particular, identify which settings provided the most

favourable conditions for optimum source-rock reservoir deposition. The identification of the varying depositional settings and conditions will help to further enhance the ability to predict the prospectivity of source rock reservoirs not only for the Holywell Shale but also across the Carboniferous basins of the UK. This requires a complex approach of combining petrographic imaging at varying scales with organic and inorganic geochemical techniques. The material used within this study was collected from both outcrop and core material of the Holywell Shale (Arnsbergian 326Ma – Yeadonian 314.5Ma) at the southwest edge of the Namurian Pennine Basin (UK). In order to achieve the principle aim of this project the following objectives will be addressed:

- The lithofacies of the Holywell Shale will be investigated and described, after Macquaker & Adams (2003), using optical and scanning electron microscope techniques. Combining the lithofacies descriptions with geochemical data (including Total Organic Carbon, RockEval™, carbon isotope values, XRF and C/N ratios) to determine the depositional environment, mineralogy and supply of organic matter for each lithofacies. This approach will allow the relationship (if any) between lithofacies and organic matter to be investigated and to determine the spatial and temporal variations which occur.

- Organic matter characteristics will be obtained using organic geochemical techniques including TOC, $\delta^{13}C$ and RockEval™ to characterise the kerogen type, source (terrestrial vs marine) and maturity of the Holywell Shale. This will allow the hydrocarbon generation potential of the Holywell Shale to be deduced.

- The quality of data obtained from outcrop material will be compared to data from material collected from 'legacy' core using identical analytical techniques

over the same stratigraphic interval (marine bands) to assess whether any variations which occur. The use of outcrop samples in geochemical studies of fine grained mudstones is common (e.g. Davies et al., 2012; Macquaker et al., 2007) by assessing the quality of the data compared to core material it will determine the suitability of this material within these studies as well as determine the reliability of comparisons between outcrop and borehole material, using the Holywell Shale as a case study.

1.3: Thesis outline

This thesis includes three main chapters (4, 5 & 6) which contain independent data, interpretations, and conclusions. These chapters have been written in the style of a scientific journal article with Chapter 4 in review and Chapters 5 and 6 in preparation for submission to separate academic journals. The thesis structure is as follows:

Chapter 2: An overview of the research problem, including a literature review of what is known about the mudstones of northeast Wales. The geological and palaeogeographical context of the study area is discussed.

Chapter 3: Detailed scientific methodologies used within Chapter 4, 5 and 6 of the thesis are outlined here. Details of specific methodologies specifically with regards to sampling procedures are discussed in more detail within the chapters.

Chapter 4: (manuscript submitted to *Marine and Petroleum Geology* in July 2015) discusses geochemical and petrographic data collected from outcrops of the Holywell Shale. A change in the source of organic matter from marine to terrestrial was shown using $\delta^{13}C$ isotopes. A negligible relationship between lithofacies and organic matter type/amount was observed. This results in the reservoir quality of the Holywell Shale being inherently difficult to predict.

Chapter 5: (manuscript pending submission to *Journal of the Geological Society, London*) examines the petroleum generation potential of the Holywell Shale using samples from boreholes. Samples were characterised principally using RockEval™ to determine the quantity, quality and preservation of organic matter.

Chapter 6: (manuscript in preparation to submit to *Geochemistry, Geophysics, Geosystems – G^3*) results from samples analysed in Chapters 4 and 5 were used to examine the differences between using samples from boreholes (differences between results from core and cuttings) and outcrops. The samples collected provide the ability to correlate marine bands between outcrops, core and cutting samples over a relatively short distance.

Chapter 7: provides a synthesis of all the material discussed within the chapters of the thesis and present findings, outcomes and conclusions. This chapter also poses questions and problems which have arisen as a result of this work, including suggestions for further work. There was also a further research approach which was adopted and became unfeasible throughout the time of this thesis, progress, findings and problems which arose are discussed.

Appendices: including complete data tables.

References: all references cited within the thesis will be included at the end.

Chapter 2:

Geological Background

2.1: Introduction

T̲he success of shale gas in the United States of America has led to attempts being made to replicate the successes in parts of Europe and the UK. However, the depositional and tectonic setting of the basins in the UK is much more complex (deposition within much smaller tectonically active basins). Understanding the deposition of organic mudstones within these basins is critical to being able to predict reservoir properties and therefore reservoir quality. Both industry and academics are working within mudstones to create a predictive tool to be able to identify mudstone characteristics which can be used for shale gas exploration. Within this thesis a combination of methods and techniques are used in an attempt to predict where organic rich mudstones occur and establish links to other rock properties.

2.2: Characteristics of shale gas systems

From the assessment criteria of successful shale gas plays mainly within the US, which make them good prospects for shale gas production, a broad range of parameters have been suggested to indicate a potential 'good' shale gas play. Some of these parameters are essential to ensure the success as a shale gas play whilst others are just desirable.

2.2.1: Organic Matter Quantity

The quantity of organic matter present within a mudstone is measured using total organic carbon (TOC). The TOC values (at present day) for a suitable shale gas target must exceed 1 wt % (Jarvie, 2012), whilst many authors suggest that a value at least 2 wt % is required (e.g. Andrews, 2013; Charpentier & Cook, 2011; Gilman & Robinson, 2011).

2.2.2: Organic Matter Type

The organic matter within mudstones is present as several organic compounds; kerogen (the portion of organic matter which is not soluble in both aqueous alkaline and common organic solvents; Dow, 1977; Tissot & Welte, 1984) normally represents 95% or more of the total organic matter in sedimentary rocks (in the absence of migrant hydrocarbons; Tyson, 1995). Another common organic constituent of sedimentary rocks is bitumen, a term which refers to long-chain soluble hydrocarbons which have the ability, with heat and pressure over time, to be broken down into other smaller chain hydrocarbons. The amount of bitumen (including asphaltenes and resins) present within the rock can be determined from gas chromatography- mass spectrometry (GC-MS; Tissot & Welte, 1984). Free hydrocarbons (gas and oil) also contribute to the TOC value, and can be present in cracks, pores or adsorbed to the surface of minerals and other organic matter compounds; the amount of free hydrocarbons can be determined from RockEval™ using the S_1x100/TOC (Jarvie & Baker, 1984).

There are three basic types of kerogen, Types I, II and III, originally defined from a study of coal macerals (van Krevelen, 1950). Within this thesis kerogen type was identified using RockEval™ pyrolysis parameters (Section 3.4). Successful shale gas systems in the US have organic matter composed predominantly of Type II kerogens (Jarvie, 2012).

- Type I kerogens are derived mainly from algal components (and bacterial components) dominated by amorphous liptinite macerals. They are typically deposited within a marine or lacustrine environment and upon maturation they produce mainly waxy oils (Dembicki, 2009). Type I kerogens can be identified

using RockEval™ pyrolysis as when they are thermally immature they have hydrogen indices greater than 600 mg/g (hydrocarbon/TOC).

- Type II kerogens are derived from algal and bacterial organic matter dominated by liptinite macerals such as exinite and sporinite. They are typically deposited within a marine environment (although not exclusively) and upon maturation they are oil-prone. Type II kerogens can be identified using RockEval™ pyrolysis as when they are thermally immature they have hydrogen indices in the range of 300 to 600 mg/g.

- Type III kerogens are generally derived from higher plant organic matter dominated by vitrinite macerals. They are typically deposited within a paralic marine environment (although not exclusively) and upon maturation they are gas-prone. Type III kerogens can be identified using RockEval™ pyrolysis as when they are thermally immature they have hydrogen indices in the range of 50 to 200 mg/g.

There are two further types of kerogen, Type IV and Type IIS kerogens.

- Type IV kerogens are dominated by inert organic matter that was recycled or extensively oxidised during deposition, and they have no hydrocarbon potential (Tissot & Welte, 1984). Type IV kerogens have low initial H/C ratios indicating the presence of oxidised and degraded organic matter. Type IV kerogens can be identified using RockEval™ pyrolysis, when thermally immature they have hydrogen indices below 50 mg/g.

- Type IIS kerogens are similar to Type II kerogen (see above) but contain uncommonly high organic sulphur (8 to 14 wt %, atomic $S/C \geq 0.04$). They are deposited under highly reducing conditions which results in sulphur substituted

for oxygen within the kerogen structure (Dembicki, 2009). Type IIS kerogens can generate oil at a lower thermal maturity than typical Type II kerogens which contain less than 6 wt % sulphur (Orr, 1986). Type IIS kerogens when they are thermally immature have hydrogen indices in the same range (300 to 600 mg/g) as Type II kerogens, and they can be distinguished by sulphur content. When Type IIS kerogens are plotted on a van Krevelen plot they can plot within the Type I kerogen range due to generally low oxygen indices and are then also distinguished using sulphur content (Williams, 1984).

2.2.3: Organic Matter Maturity

In order for free hydrocarbons to be present the mudstone source-rock reservoir has to be mature for hydrocarbon generation to occur. RockEval™ parameters hydrogen indices and T_{max} (the maximum temperature of hydrocarbon generation during pyrolysis; Section 3.4) can be used to indicate maturity (McCarthy et al., 2011). Within this thesis, maturities of samples are calculated using RockEval™ parameters.

Maturity can be also be calculated using vitrinite reflectance (VR; R_o = reflectance in oil %), determining the organic matter maturity by calculating percentage of incident light reflected by a polished vitrinite surface under petrographic analysis (in order for VR samples must contain vitrinite macerals; Dow, 1977). The oil window maturity occurs between 50 to 150 °C (approximately as this varies according to the kerogen type present) which corresponds to R_o values of 0.5 % for the onset of generation and terminating between 0.85 % and 1.1 %. The window for gas maturity is between 150 and 200 °C (approximately as this varies according to the kerogen type present) which corresponds to R_o values between 1.0 % to 3.0 %. In the US, examples of R_o

considered mature enough for shale gas exploration range from 1.1 to 3.5 % (Charpentier & Cook, 2011; Gilman & Robinson, 2011; Jarvie, 2012).

2.2.4: Mineralogy

Mineralogy is also important to consider in shale gas exploration, as hydraulic fracturing which is required to create artificial permeability and thereby create pathways for hydrocarbons to be released, will not be effective in clay rich mudstones. It has been suggested that at least 30 % silica and/or carbonates are required, with less than 35% clay minerals for successful fracture propagation (Andrews, 2013), whilst other authors suggested than 50 % clay (Bowker, 2007).

2.2.5: Porosity

Mudstones have generally low porosity, with the best producing shale gas source-rock reservoirs in the US having porosities typically around 4 to 7 % (< 15 %; Jarvie, 2012). Pores within shale can be classified into three different types: interparticle pores which occur between minerals; intraparticle pores which are located within minerals; and intraparticle pores which are located within organic matter (Loucks et al., 2012). Pores can be characterised in a variety of ways including mercury injection porosimetry (e.g. Yang & Aplin, 2010), nitrogen and CO_2 analyses (such as Brunauer–Emmett–Teller, or BET nitrogen porosimetry; e.g. Ross & Bustin, 2009), or through petrographic study using ion beam milling (Section 3.8) combined with scanning electron microscopy (e.g. Loucks et al., 2012).

2.2.6: Permeability

Mudstones also typically have low permeability (< 1000 ηD) and are anisotropic (Aplin & Macquaker, 2011; Jarvie, 2012; Yang & Aplin, 2007; Yang & Aplin, 2010). Permeability can be calculated using Darcy's Law (Equation 1). Hydraulic fracturing is

required to create an artificial fracture network along which hydrocarbons can be extracted. In some cases, natural fractures can aid hydrocarbon extraction, but open natural fractures are very rare and most naturally occurring fractures are healed with cements such as calcite (Bowker, 2007; Gale et al., 2007; Gale et al., 2014).

Equation 1: Darcy's Law for permeability. Q = total discharge (m3/s), k = intrinsic permeability (m2), A = cross-sectional area to flow (m2), μ = viscosity (Pa.s), ΔP = change in pressure.

$$Q = \frac{-kA}{\mu} \Delta P$$

2.3: Determining depositional environment using organic and inorganic geochemical analyses

Organic rich mudstones are typically deposited in high productivity zones with low siliciclastic input and often with low oxygen levels at the sea floor and within thre sediment to prevent organic matter oxidation and degradation. Cyclic variations in eustatic sea level are thought to correlate with these high productivity periods of deposition represented by marine bands at stratigraphical maximum flooding surfaces. It is important to constrain where these organic rich mudstones occur, and assess whether there is any correlation between a lithofacies type which would be good for hydraulic fracturing. A multifaceted approach to mudstone characterisation, including petrographic observations, would allow for greater understanding into the depositional environments of the Holywell Shale during the Carboniferous.

2.3.1: Using carbon isotopes to determine organic matter source

Carbon isotope signatures represent a ratio of ^{12}C: ^{13}C and can be used to distinguish between terrestrial and marine sources of organic matter (Tyson, 1995). Fractionation of carbon isotopes occurs during photosynthesis as C3 land plants incorporate ^{12}C from

inorganic carbon (CO_2) more readily than ^{13}C, this results in a shift of the ratio to more negative values. C4 plants are not considered as they evolved during the Palaeogene and therefore do not contribute to the isotopic signature within Carboniferous mudstones (such as the Holywell Shale). There are many factors which can affect the fractionation of carbon isotopes in organic matter.

- Positive ^{13}C shifts can indicate: high productivity; transgression; low nutrient flux; increased carbon burial; increased flux of siliciclastic material to shelf seas; and increased weathering rates of carbonate shelf environments.

- Negative ^{13}C shifts can indicate: increased ocean and atmospheric circulation; increased upwelling; input of dissolved inorganic carbon from rivers; periods of increased volcanic activity; weathering of black shale/coal; and gas hydrate dissociation.

It is important to note that carbon isotopes from pre-Neogene marine kerogens have signatures 5-7% lighter (more negative values) than younger marine material, which means that pre-Neogene marine material appears to have an isotope signature close to that of modern C3 land plants (-33 ‰ to -24 ‰). Whilst, pre-Neogene C3 plant signatures from kerogens exhibit isotope signatures up to 3‰ heavier (more positive values) than modern C3 plants (Koch et al., 1992; Tyson, 1995). These effects combine to provide the inverse correlation between marine and terrestrial signatures from the pre-Neogene and modern day samples.

Therefore, within the carbon isotope signatures of the Holywell Shale and other Carboniferous mudstones more negative 'lighter' isotope values (-35 ‰ to -30 ‰) represent a marine signature (and an algal source of carbon; Lewan, 1986) whilst more positive 'heavier' values (-24 ‰ to -22 ‰) represent a terrestrial signature (and a C3

plant source of carbon; Maynard, 1981; Peters-Kottig et al., 2006; Stephenson et al., 2008). Another consideration when interpreting carbon isotope data, particularly within organic mudstones such as the Holywell Shale, a negative isotopic shift may also be represented by a change from oxic to anoxic conditions (Tyson, 1995).

2.3.2: Determining the source of organic matter from RockEval™ pyrolysis

Hydrogen indices (HI; a RockEval™ derived parameter) can be used to characterise the origin of organic matter, based on the variation in H to C ratios of sources of organic matter (Tissot & Welte, 1984). Marine organisms and algae are mainly composed of proteins and lipid-rich organic material with corresponding high H/C ratios (1.1 to 1.5; Kerogen Types I, II and II/III), whilst terrestrial plants are mainly composed of carbohydrate-rich material with corresponding low H/C ratios (0.5 to 1.0; Kerogen Types III, IV; Peters & Moldowan, 1993; Tissot & Welte, 1984).

2.3.3: Determining the depositional environment from inorganic and petrographic techniques.

Previous research on mudstones has shown that the variation between terrestrial and marine signatures is not a direct representation of marine or non-marine conditions linked to glacio-eustatic changes in sea level. Instead, changes in carbon isotope may be influences by differences in material transport with distal locations having much lower portions of terrestrial influenced material (Davies et al., 2012). Combining carbon isotope data with detailed sedimentological observations of lithofacies and organic matter (using transmitted light and scanning electron microscope techniques) and elemental analysis (e.g. X-ray fluorescence) provides greater information regarding the depositional environment and the source of organic matter within organic-rich mudstones, such as the Holywell Shale (e.g. Davies et al., 2012; Könitzer et al., 2014a;

Schieber et al., 2000). Various proxies have been used to establish the detrital input, the amount of oxygen present at the time of deposition and therefore interpret the environment and paleogeography of the mudstone, these include Si/Al ratios, CaO content, Zr concentration, Ni/CO and V/Cr ratios (Jones & Manning, 1994).

Silica is found in quartz and clay minerals within mudstones and the relative portions of their elemental oxides (from X-ray fluorescence analysis; Section 3.6) can be used to represent a quartz to clay ratio (Si/Al). High Si/Al ratios indicate that the majority of the silica in the sample is present as quartz; whist low Si/Al ratios (i.e. more Al present) indicate more clay minerals present in the sample (Ross & Bustin, 2009). However, the ratio of Si/Al can be affected by other processes including diagenesis or biogenic input of non-crystalline opaline silica (e.g. Blood et al., 2015).

The amount of CaO present within the sample (determined from XRF analysis) is a proxy for the amount of carbonate present. High CaO can be used to suggest an increase in productivity or materials derived from nearby high productivity environments (such as surrounding carbonate shelves) if the material is detrital. However, CaO content can correspond to other detrital sources (such as biogenic carbonate from fossils and shell fragments) or diagenetic sources (such as early diagenetic cements). The use of this proxy in combination with petrography is essential to ensure accurate interpretation (e.g. Lazar et al., 2015a).

Trace element concentrations (in particular Ni/Co and V/Cr) can be used to infer water column oxygenation conditions at the time of mudstone deposition (Jones & Manning, 1994; Ross & Bustin, 2009). The Co and Cr portions are thought to represent a detrital composition and are unaffected by oxygen state whilst both Ni and V are affected by the oxygen state (Ross & Bustin, 2006). High Ni/Co (> 7) and high V/Cr (> 4.25)

reflect anoxic conditions, whilst Ni/Co ratios below 5 and V/Cr ratios below 2 reflect oxic conditions, the values between represent degrees of dysoxia within the water column (these values should not be applied strictly but used in combination with other observations; Lazar et al., 2015b).

2.4: Carboniferous basins, structure, and palaeogeography

The term Holywell Shale has been made obsolete and is now incorporated within the term Bowland Shale Formation (BGS Lexicon of named rock units). However, the term 'Bowland Shale Formation' covers a series of mudstones which were deposited diachronously within different basins and sub-basins across northern England, northeast Wales, and the English Midlands. To avoid confusion when referring specifically to the Bowland Shale Formation where it occurs in northeast Wales (the study area for this thesis), the term Holywell Shale will be used.

During the Carboniferous the landscape of the UK comprised a series of fault bounded blocks (horst) and basins (graben/ half-graben) which were created by of back-arc extension related to the Variscan Orogeny (410-280 Ma; Woodcock & Strachan, 2009). The episodic rifting and reactivation of earlier Caledonian NW-SE and NE-SW trending faults lasted from the late Devonian to early Permian (Fraser & Gawthorpe, 1990; 2003). Initial extension and rifting ceased in the mid-Carboniferous and subsequently the basins which had been created progressively filled during a thermal sag phase throughout the Namurian Stage (326 -313 Ma; Aitkenhead et al., 2002; Leeder & McMahon, 1988). The area which existed between the Southern Uplands High in the north, and the Wales-London-Brabant Massif (also referred to as St George's Land) in the south is referred to as the Pennine province (Figure 2-1).
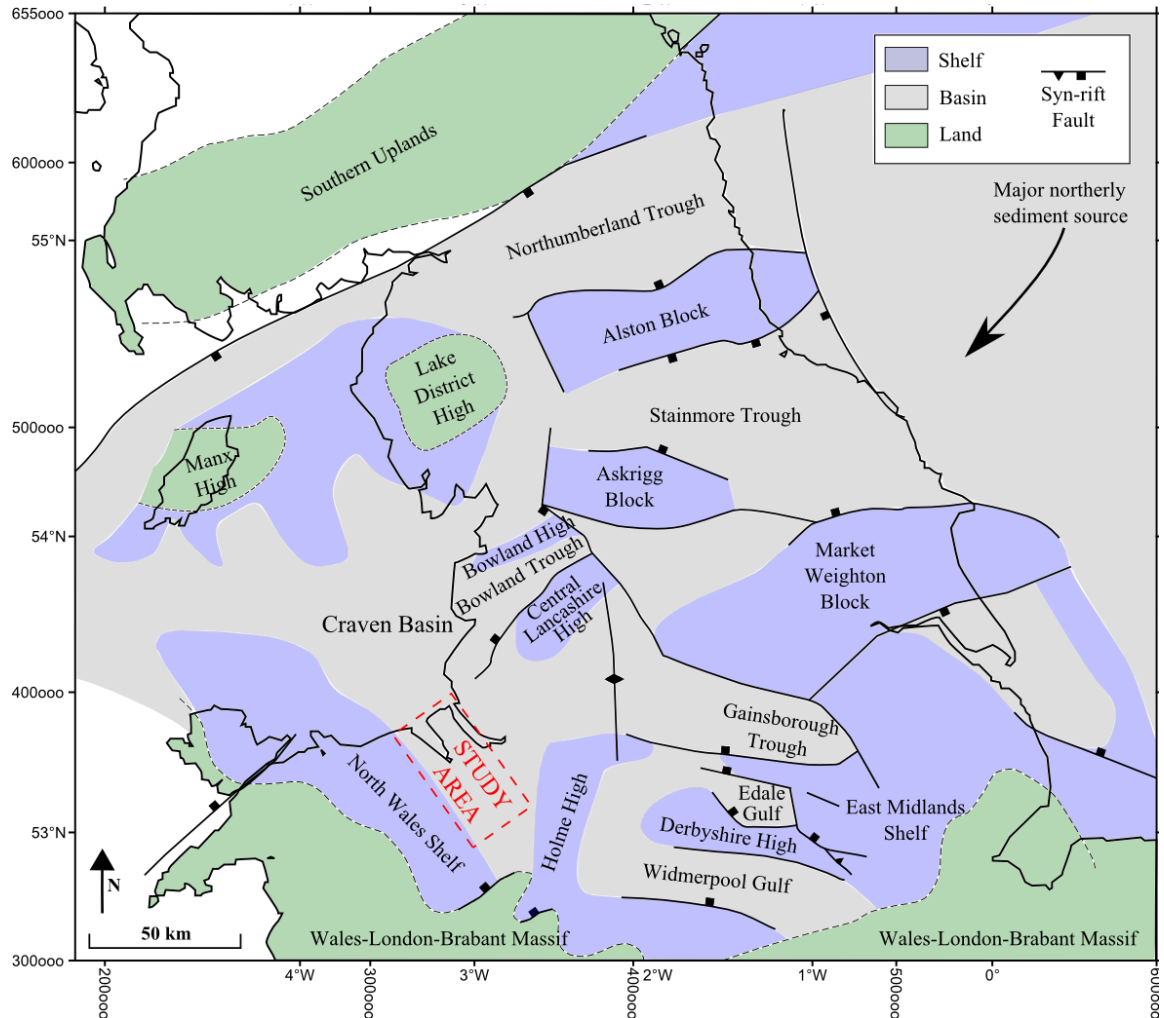
Figure 2-1: Structural framework and basins of the Pennine Province (Central Province Basin) in the early Carboniferous (adapted from Fraser & Gawthorpe, 2003; Waters et al., 2009). The study area for this thesis is marked in a red dashed box.

There were two dominant sediment sources throughout the Carboniferous which both had a significant effect on the Holywell Shale deposition. The largest source prograded across the UK southwards from the Dinantian to late-Namurian from a major river system which was feeding large quantities of feldspathic material from Scandinavia and Greenland which was deposited as the Millstone Grit Group (Figure 2-1; Jones, 1980; Smith et al., 2005). The Millstone Grit Group (locally, the Gwespyr Sandstone) did not reach the southern regions of the Pennine Province until the late Namurian (Yeadonian in northeast Wales). The second more locally sourced sediment was composed largely

of quartz arenite, was supplied from the south of the Pennine Region (Wales-London-Brabant Massif) and was most active in the earlier Namurian (Pendleian to Marsdenian, but can be separated into three parts: Pendleian to Arnsbergian, Arnsbergian to mid-Kinderscoutian, and Kinderscoutian to late Marsdenian) where it supplied the local Cefn-Y-Fedw Sandstone (Davies et al., 2004; Martinsen et al., 1995).

The edges of the Pennine Basin were rimmed by carbonate reef systems which prospered due to low levels of siliciclastic input across the shelf during the Dinantian. Throughout the Namurian, the increased fluviodeltaic and siliciclastic input led to predominantly marine mudstones being deposited in the deeper basin centres with sandstones prograding conformably across the Dinantian carbonate shelf into the basins (Davies et al., 2004). Finally, the early rift basins of the Pennine Province gradually filled and were overtopped and became incorporated into the larger Pennine Basin (Collinson, 1988; Guion & Fielding, 1988).

2.5: Carboniferous climate

During the Carboniferous the global climate is thought to have oscillated from periods of greenhouse conditions (where no ice caps existed) to icehouse conditions (where ice caps were present on the Gondwanan land mass at the South Pole; Fielding et al., 2008; Heckel, 1986). The climate in the UK during this period shows a transition from more humid conditions (during the Namurian) to more arid conditions (during the Westphalian) which is thought to relate principally to the geographical movement of the UK (at the southern edge of the Laurentian plate) northwards across the equator (Cope et al., 1992).

The large Gondwanan land-mass was situated over the South Pole during the Namurian and as a result, a large volume of ice accumulated on the continent. Fluctuations in the

glaciations appear to be relatively rapid with glacial periods of 1 − 8 Ma, with interglacial periods of similar length (Fielding et al., 2008; Rygel et al., 2008). These glaciations have been well documented across the world with particular work in eastern Australia demonstrating the dynamics of the fluctuations (Fielding et al., 2008). These glacials and interglacials had a significant effect on eustatic sea-levels which are recorded in northern hemisphere geology (and can be seen in the Holywell Shale – see section 2.6).

Glacial episodes in the Carboniferous began at the boundary between the Viséan and Namurian and continental ice grew in the southern hemisphere until the Early Permian and subsided by the Late Permian. There were four major glacial episodes recognised in the Carboniferous from the eastern Australian records which occur around the Pendleian to Arnsbergian (C1; ~ 326.6 Ma to ~ 325.6 Ma), Alportian to Kinderscoutian (C2; ~ 322 Ma to ~ 318 Ma), Marsdenian to Yeadonian (C3; ~ 316.3 Ma to ~ 314.6 Ma), and finally in the Langsettian (C4; ~ 313 Ma to ~ 308.7 Ma) (Fielding et al., 2008).

The Carboniferous glacial periods caused large scale eustatic sea-level fluctuations (indicated from erosional relief; Rygel et al., 2008). From the onset of the mid-Carboniferous glaciation, sea levels fluctuated by 10 to 50 m in the Asbian and Brigantian, whereas during the major glacial period throughout the Namurian there are significant sea-level fluctuations of 40 − 100 m (Rygel et al., 2008). These large sea-level fluctuations are likely to have played a significant role in deposition in the UK Pennine Basin and its sub-basins. The changes in sea-level correspond with stratigraphic variation which correspond to periods of varying basin connectivity, sediment input, primary productivity and oxygen levels.

2.6: North Wales stratigraphy

The oldest Carboniferous strata of northeast Wales is exposed in the west of the region with Dinantian Clwyd limestones comprising the flanks of the Clwydian range of hills. These limestones represent a sequence of carbonates occurring predominantly as shallow marine ramp and platform settings (Figure 2-2; Davies et al., 2004; Waters et al., 2009).

During the Pendleian, the Pentre Chert Formation was deposited in a setting largely devoid of siliciclastic input with significant amounts of sponges and radiolaria (biogenic silica) present (Davies et al., 2004). The formation disconformably succeeds the coeval platform Cefn Mawr Limestone; in places the Pentre Chert conformably succeeds the ammonoid-bearing Dinantian basinal turbiditic marine mudstones (Figure 2-2). In the south of the northeast Wales region the Pentre Chert is found thinly interbedded with the lowermost Cefn-Y-Fedw Sandstones (Davies et al., 2004).

The Cefn-Y-Fedw Sandstones are derived from the Wales-London-Brabant Massif to the south of the northeast Wales region (Figure 2-1). They represent a quartzitic series of fluvio-deltaic which record cyclical transgressive and regressive cycles with three main progradational events identified within the Pendleian, Alportian and Kinderscoutian (Figure 2-2; Davies et al., 2004).

The Holywell Shale Formation of north Wales (Pendleian to Yeadonian) succeeds the Pentre Chert, and occurs laterally transitional with the Cefn-Y-Fedw Sandstones (Figure 2-2; Davies et al., 2004). The formation represents a series of hemipelagic mudstones with ammonoid bearing strata (marine bands up to several metres thick) with relatively unfossiliferous mudstones from the strata between marine bands (which

commonly contain fish remains and plant debris) and subordinate thin sandstones and argillaceous limestones (Davies et al., 2004).

During the Yeadonian the Holywell Shale is laterally succeeded by the Gwespyr Sandstone Formation which represents the local occurrence of the dominant Millstone Grit Group deltas sourced from the north east finally reaching the region (Figure 2-2). The Gwespyr Sandstone represents a series of thickly bedded feldspathic sandstones, with thin argillaceous sandstones (Davies et al., 2004). As well as being very feldspathic, the sandstones are often micaceous with abundant plant fragments and contain bedding surfaces of carbonaceous material; they are often intensely bioturbated (Davies et al., 2004). The Namurian Millstone Grit Group sediments are conformably

succeeded by Langsettian (Westphalian A) claystones and coals (Figure 2-2).

Unit Name		Age (Ma)	Series	Stage ICS	Stage UK	Regional Substage	Ammonoid Biozone
Lower Coal Measures		310–312	Pennsylvanian	Moscovian	Westphalian	Langsettian	*G.listeri*
Gwespyr Sandstone		313–314					
Upper Holywell Shale		315	Pennsylvanian	Bashkirian	Namurian	Yeadonian (G1)	*G.subcrenatum* *C.cumbriense* (G1b) *C.cancellatum* (G1a)
		316				Marsdenian (R2)	*B.superbilinguis* (R2c) *B.bilinguis* (R2b) *B.gracilis* (R2a)
		317				Kinderscoutian (R1)	*R.reticulatum* (R1c) *R.nodosum* (R1b) *R.circumplicatile* (R1a)
Holywell Shale		318–321				Alportian (H2)	*Ht.prereticulatus* (H2c) *H.undulatum* (H2b)
Cefn-Y-Fedw Sandstone		322–323					*Hd.proteum* (H2a)
Lower Holywell Shale		324–325	Mississippian	Serpukhovian		Chokierian (H1)	*H.beyrichianum* (H1b) *I.subglobosum* (H1a)
		326				Arnsbergian (E2)	*N.nuculum* (E2c) *Ct.nitidus* (E2b) *E.bisulcatum* (E2a)
Pentre Chert						Pendleian (E1)	*Cr.malhamense* (E1c) *T.pseudobilingue* (E1b) *Cr.leion* (E1a)
Clwyd Limestone Group		327–331			Viséan	Brigantian	

Key
Coal (& Clay/seatearth)
Shale
—m— Marine band
Sandstone
Limestone

Figure 2-2: Simplified stratigraphic column (scale is not thickness) for the Namurian of northeast Wales with corresponding international stratigraphic units as well as the regional substages and corresponding ammonoid biozones (Davies et al., 2004).

The Namurian of the northeast Wales region was dominated by the cyclical deposition of hemi-pelagic mudstones of the Holywell Shale being succeeded by more paralic and deltaic facies of the Cefn-Y-Fedw Sandstones. The cyclical nature of the Holywell Shales with the Cefn-Y-Fedw Sandstones has been observed in other Carboniferous

geological formations across large areas of Europe since the early 20th century (Wright et al., 1927). Within the Pennine Basin, Ramsbottom (1977) recognised that the cycles were of eustatic origin due to periodic glaciation on the Gondwanan continent (Fielding et al., 2008; Heckel, 1986). Ramsbottom (1977) coined the terms cyclothem and mesothem to describe the transgressive and regressive episodes with 11 mesothems (boundaries of each major cycle) identified throughout the Namurian of the UK. Ramsbottom's mesothems are divided by the appearance of new ammonoid fauna. This approach assumes that distinctly new species of ammonoid fauna represent widespread flooding/highstand events which linked the smaller Carboniferous basins in an epicontinental seaway across northwest Europe (Ramsbottom, 1978).

The Namurian has 49 marine bands which have been identified across the basins of the Pennine Province (Central Province Basins). Of these 49 periods of widespread transgression 15 recorded marine bands are present in the northeast Wales region (Davies et al., 2004). These marine bands vary in thickness and expression dependant on factors such as global climate and palaeogeography. The marine bands of the region are most complete and developed within the late Kinderscoutian – Yeadonian/Langsettian boundary, although there are also marine bands from Pendleian – Alportian in the region showing cyclical marine influence throughout the Namurian.

The Holywell Shale occurs at surface across the northeast Wales region (Figure 2-3). Exposures commonly occur predominantly within river and road cuttings. The Holywell Shale is thickest to the north of the region and a 152 m complete succession with identified marine bands is found within the Point of Ayr No.3 Colliery Shaft and Abbey Mills No.1 and No.4 Boreholes (Figure 2-2; Davies et al., 2004). Offshore to the north within the Carboniferous Craven Basin (Figure 2-1) the Bowland Shale

Formation is present as a source rock for the oil and gas fields of the East Irish Sea (Armstrong et al., 1997; Waters et al., 2009).
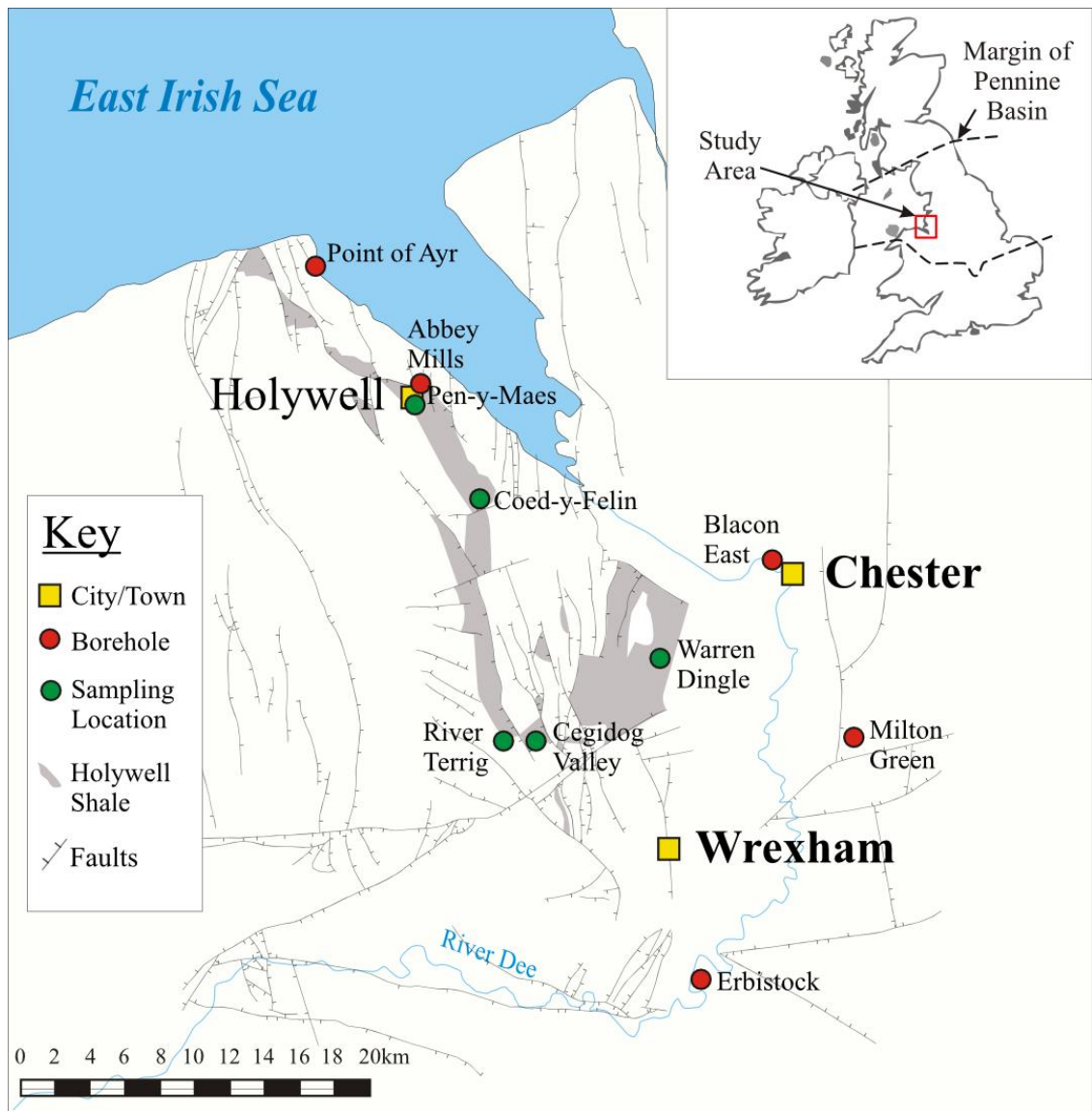
Figure 2-3: Map of the study area with the wider location (inset image), showing: the extent of the Holywell Shale (grey); main faults; outcrops and boreholes sampled in northeast Wales.

Chapter 3:

Methods

3.1: Sample collection

Samples used in this thesis were collected from both outcrop and borehole material. The detailed methods of collection are outlined below.

3.1.2: Outcrop sampling

In the northeast Wales region, the Holywell Shale is exposed at numerous outcrops. These outcrops are often difficult to find and gain pedestrian access to (once permission of the land owner was granted). Outcrops are most often exposed in stream cuttings across the region, but due to the limited amount of exposure (often less than 0.5 m x 0.5 m) and complex faulted nature of the region, direct correlation between exposures is inherently difficult. The only reliable method of correlating between the disparate outcrops (Figure 3-1) is to place them biostratigraphically using marine goniatite fauna, or marine bands.

Outcrop locations were selected due to the marine bands which they are reported to contain (Table 3-1). Each outcrop was a stream cutting and precise locations of each outcrop are detailed in Table 3-1; Figures 3-1 & 4-2.

At each sampling location (Figure 3-1) weathered material was removed until a 'fresh' more competent layer of mudstone was accessible. In some cases this resulted in over 20 cm of material being removed. Samples (up to 100 x 200 mm in size) were then collected from the competent material which was taken as being unweathered mudstone. However, caution must be used in determining the weathered state of a sample by its degree of competency due to lithological variation (clay vs. silt) and diagenetic variations (i.e. degree of cementation) which may make material more competent but do not directly relate to the degree of weathering a sample has undergone.

The following standard operating protocols were employed when sampling to ensure, as far as possible, repeatable sample collection occurred:

• Samples were taken from "clean/fresh" outcrop material where exposure allows.

• Samples were collected from horizons at each site at a 100mm stratigraphic interval.

• Samples collected were labelled in sealed plastic bags, or wrapped in cling film if the sample was too large.
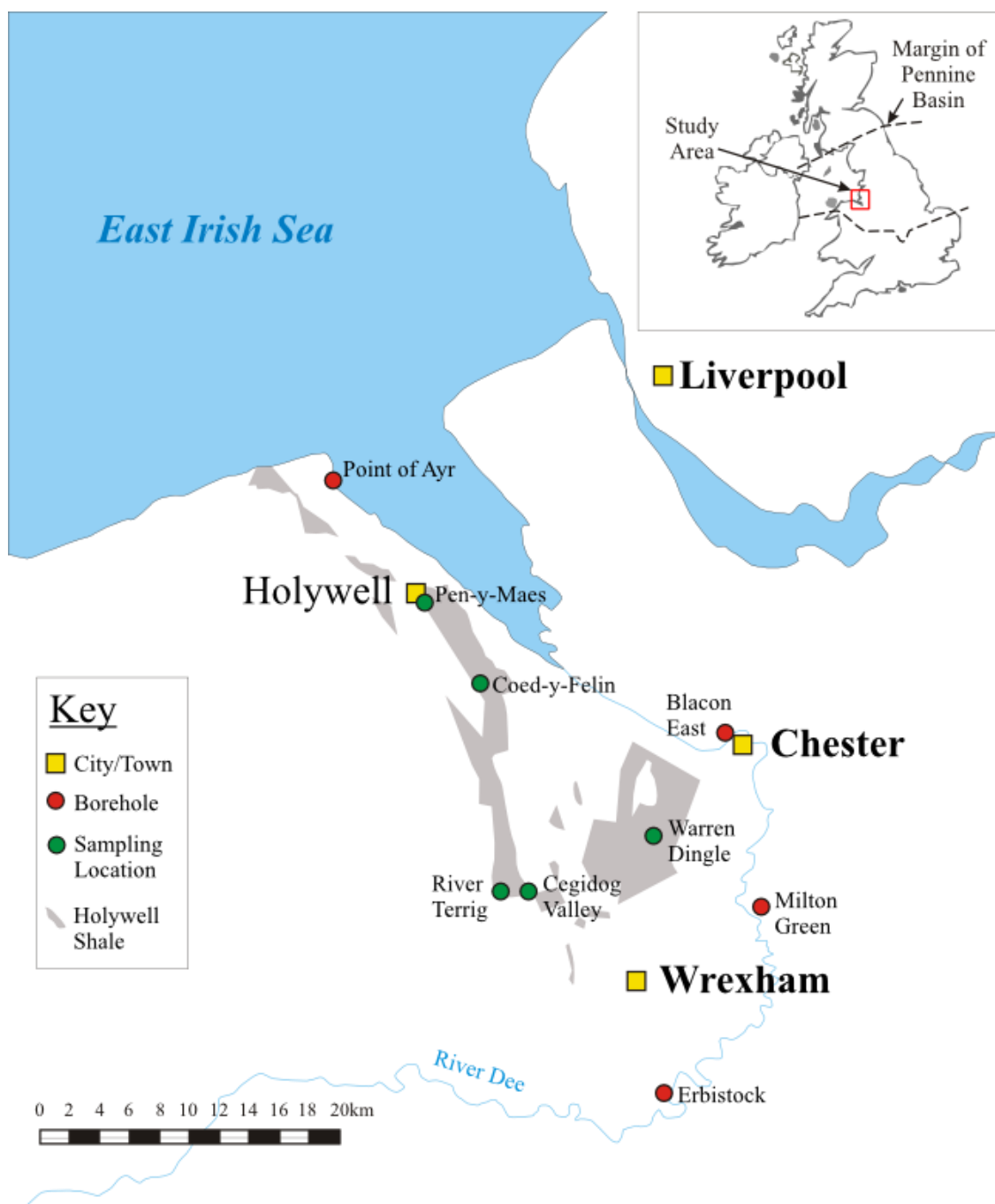
Figure 3-1: Map of the study area with the wider location (inset image), showing the extent of the Holywell Shale (grey), and the main outcrop locations studied and the boreholes sampled.

3.1.3: Borehole sampling

Samples were selected from the boreholes which were available at the British Geological Survey (BGS, Keyworth) core store. Details of available material were found using the online onshore borehole material database

(http://www.bgs.ac.uk/data/bmd/home.html). Sampling depths were identified from well logs and reports held by the BGS to ensure the samples were taken from material within the Namurian Holywell Shale or Bowland Shale Formation.

The cuttings within Blacon East borehole were spaced over a regular interval with a cutting sample collected every 50 ft (15.24 m; Table 3-1). Where enough material was available 5 g of cuttings were collected for analysis (Figure 3-1). The Erbistock borehole (Figure 3-1) had a more limited amount of cutting material and so cuttings from a range of depths were collected depending on the quantity of material available. The Namurian section within the Erbsitock borehole is substantially smaller than the Blacon East and Point of Ayr boreholes; and the biostratigraphic markers are also limited with only the G1a marine band (which appears to be the most extensive across the northeast Wales region) recognised (Figure 3-1; Andrews, 2013). The cuttings examined have been held at the British Geological Survey (BGS) since the material was collected in the 1980s and has been resampled by various companies and researchers. This means that in some cases the quantity of cuttings available is depleted. The cuttings are held at the BGS in standard cuttings sample bags (~75 x 100 mm) which are made of thick card and folded over at the top to stop any sample being lost. These cuttings are kept in depth order within long, thin cardboard boxes (100 x 1000 mm) and stored on racks in the core store. The material within the bags appears well dried and relatively undisturbed since extraction.

Table 3-1: Details of the locations of the boreholes and outcrops sampled (including the depth intervals for the boreholes), the type of material sampled in each case, and the marine bands which exist within the section sampled. Cuttings refer to the material which is brought to the surface during drilling operations by being suspended within drilling mud.

Borehole/ Outcrop	Location (Easting, Northing)	Marine bands	Sample depth range (m)	Material Type
Point of Ayr Colliery Shaft number 3	312700, 383800	G1b, G1a, R2b, R2a	65.5 to 333.8	BGS reference samples (from core)
Blacon East 1	337887, 366856	G1b, G1a, R2b, R2a	1205 to 1255	Cuttings
Erbistock 1	334767, 343213	G1a	807.7 to 1021.1	Cuttings
Pen-Y-Maes	319450, 376700	G1a	-	Outcrop sample
Warren Dingle	331800, 362340	G1a	-	Outcrop sample
Coed-Y-Felin	322370, 371500	R2a	-	Outcrop sample
River Terrig	323365, 356900	E2b	-	Outcrop sample
Cegidog Valley	326050, 356880	E2a	-	Outcrop sample

The Point of Ayr number 3 colliery shaft was sunk in the 1950's and is therefore not strictly a borehole but a mine shaft. This has the additional benefit that, in some cases, the precise offset of faults could be observed at the rock-face and are recorded in the sedimentary log (Magraw, 1954). However, the disadvantage is that there are no wireline logs available to compare with the logs for Blacon East and Erbistock boreholes (Figure 3-1).

The material available for sampling from Point of Ayr was reference material (due to the fossils which they contain Magraw, 1954) which comprises borehole specimens (< 100 mm in size). The reference samples are preserved in a sample tray at the BGS

with small individual card trays, labelled for identification. The samples have been largely undisturbed for 60 years which means that whilst the material is "legacy core" and not recently extracted, it is likely to be in a stable and relatively unweathered state. The Abbey Mills Boreholes (No.1 & 4) represent another source of reference material held by the BGS; however, the Abbey Mills Boreholes were not available for sampling.

The samples selected for sampling at Point of Ayr were chosen due to their marine band fauna allowing for direct comparison, at the same stratigraphic position, with other marine band fauna from outcrop. Selection of samples was dependent on the amount of material at the edges of fossil bearing samples which did not have fossils present such that they would not destroy or impede the identification of reference fossils. Each proposed sample had to be agreed with the BGS core store manager before sampling was permitted. The nature of the material meant that many of the Point of Ayr samples were collected from marine bands (Table 3-1).

3.2: Sample Preparation

Samples used in this thesis were prepared for various petrographic and geochemical analyses undertaken which required the preparation of powdered material and thin sections. The detailed methods of preparation are outlined below.

3.2.1: Powder Preparation

Most geochemical analysis methods used within this thesis required powdered samples. All samples were dried at room temperature, powdered using an agate mortar and pestle or ball mill until a fine uniform consistency was achieved.

3.2.2: Thin Section Preparation

Polished thin sections of select samples were created by cutting the shale sample into 10 mm thick slices using a bench-mounted circular disc with a fine diamond

impregnated blade and water. Instead of water, oil can be used in the cutting process to reduce the chance of hydrophilic clay swelling (which is where clay minerals such as smectite could disaggregate with water); however, this was not possible at Durham University. Samples were then trimmed to height and width to be able to fit a standard glass slide (25.4 x 76.2 mm).

Before attaching the sample to the glass slide, it was necessary to prepare the surface that the sample was bonded with. This involved polishing the cut rock sample surface using both a 20 µm and 10 µm abrasive, then the rock sample was further polished using a flat glass surface with a paste formed of 9.5 µm aluminium oxide powder mixed with water, this process was completed by hand in an even figure-of-eight pattern before the sample was washed with water and air dried. The next step was to 'lap' the glass (makes the glass frosted to allow for a better bond with the rock) then for the final polish the same process of polishing by hand using a flat glass surface and the 9.5 µm aluminium oxide paste before washing with water and air dried was repeated, before placing on a hot plate at 60 °C.

To mount the prepared rock sample on the prepared glass slide an epoxy resin (EpoTek 301) was used. The resin was mixed and then applied to the sample before it was bonded to the glass slide ensuring that there are no bubbles present between the rock sample and glass slide. Once the resin was set, the sample was re-sectioned. Re-sectioning involved cutting the rock sample (bonded to the slide) on a diamond impregnated disc to a thickness of 500 µm. The sample was then ground to a 100 µm thickness before the process of applying the final polish described previously by hand using 9.5 µm aluminium oxide paste on a glass slide was repeated to the finished thickness of 15 µm for optical thin sections and 50 µm for SEM thin sections. The sample was then either covered with a cover slip (used for optical microscope only) or

further polished using a 0.3 μm aluminium oxide paste (used on both optical and scanning electron microscopy – Sections 3.5 & 3.6).

3.3: Total organic carbon (TOC), total nitrogen (TN) & stable isotope analysis

Total organic carbon, total nitrogen content and stable isotope analysis of the samples were performed at Durham University using a Costech Elemental Analyser (ECS 4010) connected to a ThermoFinnigan Delta V Advantage isotope ratio mass spectrometer. Sample preparation for TOC, TN and $\delta^{13}C$ analyses involved weighing the mass of the sample followed by a 50 ml treatment of 3 M hydrochloric acid that de-calcified the powdered samples. Samples were then rinsed with de-ionised water until pH neutrality was obtained, subsequently dried in an oven at 60 °C, and after drying the samples required re-powdering.

Carbon isotope ratios were corrected for ^{17}O contribution and reported in the standard delta (δ) notation in per mil (‰) relative to Vienna Pee Dee Belemnite (VPDB). Total organic carbon data was obtained as part of the isotopic analysis using an internal standard (Glutamic Acid, 40.82 % C). Isotopic accuracy was monitored through routine analyses of in-house standards, which were stringently calibrated against international standards (e.g., USGS 40, USGS 24, IAEA 600, IAEA N1, IAEA N2): this provided a linear range in $\delta^{13}C$ between –46.7 ‰ and +2.9 ‰. Analytical uncertainty in carbon isotope analysis was typically ±0.1 ‰ for replicate analyses of the international standards and typically < 0.2 ‰ on replicate sample analysis.

Nitrogen isotope analysis was performed separately to the carbon isotope analysis. A carbon dioxide (CO_2) trap was installed in the Costech Elemental Analyser so that only N_2 gas entered the isotope ratio mass spectrometer, and nitrogen isotope ratios with a

signal strength over 1000 mV are only reported in this study. Total nitrogen data was obtained as part of the isotopic analysis using an internal standard (Glutamic Acid, 9.52 % N). Isotopic accuracy was monitored through routine analyses of in-house standards, which were stringently calibrated against international standards (e.g., USGS 40, USGS 24, IAEA 600, IAEA N1, IAEA N2): this provided a linear range in $\delta^{15}N$ between –4.5 ‰ and +20.4 ‰. Analytical uncertainty in nitrogen isotope analysis was typically ±0.1 ‰ for replicate analyses of the international standards and typically < 0.2 ‰ on replicate sample analysis.

3.4: Kerogen Type & Maturity

RockEval™ is a widely used technique in the petroleum industry due to the ability to get relatively quick and cheap results about organic matter parameters from which it is possible to deduce information about maturity, organic matter type (kerogen type), organic matter quality, and the ability for a source rock to generate further hydrocarbons (Behar et al., 2001). RockEval™ analysis was completed using a RockEval™ II (for outcrop samples, Chapter 4) by Martin Jones, Newcastle University. RockEval™ analysis was completed using a RockEval™ VI (for borehole samples, Chapter 5) by Geir Hansen, Applied Petroleum Technology (APT) Norway. The change was due in part to the RockEval™ VI machine having the capability to measure CO_2 to give an S_3 parameter (explained below), as well as the RockEval™ II at Newcastle University was unavailable at the time of analysis as it was undergoing maintenance.

RockEval™ is a pyrolysis based technique which allows the type and maturity of organic matter and thus the petroleum generation potential to be established (Espitalié et al., 1977). Between 50–100 mg of powdered whole rock samples (Section 3.1) were

pyrolysed in an inert Helium atmosphere from 180 °C to 600 °C, using a ramp rate of 25 °C per minute. The mass of hydrocarbon vapours produced at 300 °C (free hydrocarbons) was analysed using a flame ionising detector (FID), to give the S_1 peak of the pyrogram (Figure 3-2). The temperature was then increased from 300 °C to 550 °C in order to crack non-volatile organic matter, i.e. kerogen. The vaporised hydrocarbons measured by the FID during this heating phase represent the S_2 peak on the pyrogram (Figure 3-2). The temperature at which the S_2 peak reaches maximum generation is termed the T_{max}. The S_3 parameter is the amount of CO_2 measured on the thermal conductivity detector (TCD) produced during the phase of pyrolysis from 300 °C to 550 °C which indicates the quantity of oxygen in the kerogen. Further parameters were derived using the following equations (Tissot & Welte, 1984):

(i) Hydrogen index, HI = $(S_2/TOC)x100$; this parameter corresponds to the H/C ratio of samples. Kerogen type can be inferred from this parameter with Type I having the highest HI value and Type IV the lowest HI values. It can also indicate the origin of organic matter in samples as land plants have a low H/C ratio as they are mainly composed of long-chain carbohydrates, whereas marine organisms and algae are mainly composed of shorter-chain lipid- and protein-rich organic matter with high H/C ratios.

(ii) Oxygen index, OI = $(S_3/TOC)x100$; this parameter corresponds to the O/C ratio of samples. High OI values indicate oxidised organic matter and normally correspond with lower HI and poor organic matter preservation.

(iii) Production index, PI = $S_1/(S_1+S_2)$; this can be used to determine the amount of hydrocarbons which have been produced from kerogens.

(iv) Transformation index, TI = S_1/TOC; this parameter shows the amount of the total organic matter which has been converted into hydrocarbons.

(v)   Pyrolysate yield, PY = S_1+S_2; this corresponds to the amount of hydrocarbons which have been generated and the amount which the rock could still produce.
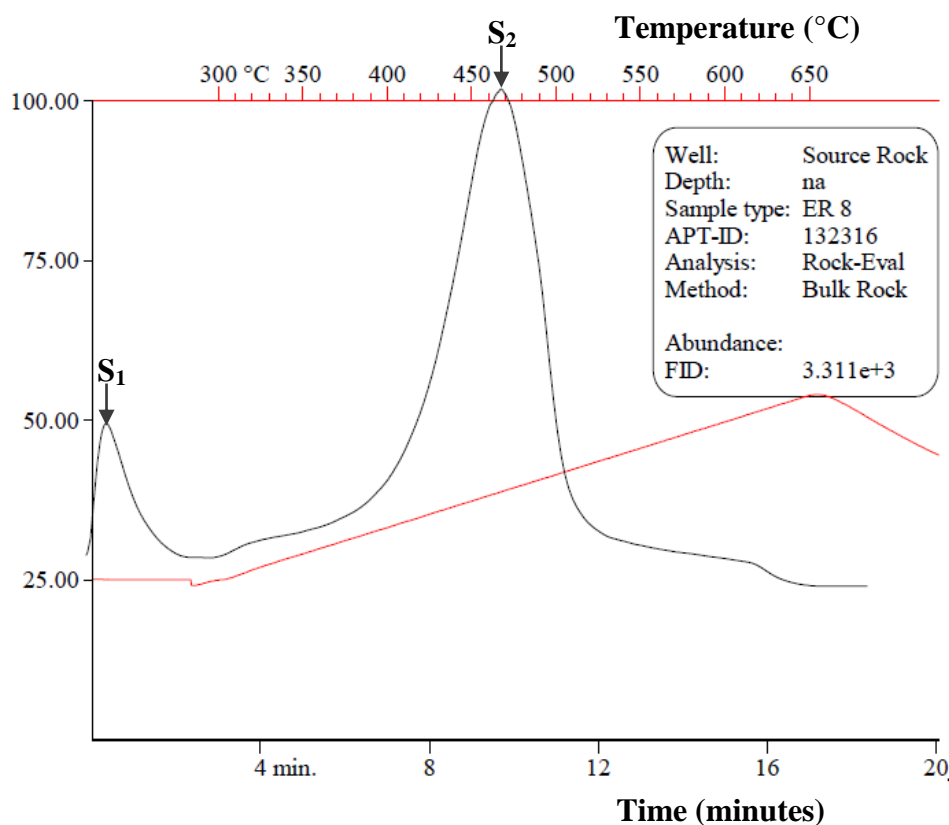
Figure 3-2: RockEval™ pyrogram with S_1 and S_2 peaks identified. Temperature is of the pyrolysis column, the T_{max} temperature is 39 °C ± 1 °C lower. The red line indicates the temperature programming, with flat lines showing when temperature was constant and inclined line showing when temperature was increased.

All experimental procedures for RockEval™ VI analysis follow the Norwegian Industry Guide to Organic Geochemical Analyses (NIGOGA), 4th Edition. A standard (Jet-Rock 1) was run as every tenth sample and checked against the acceptable range given in NIGOGA.

3.4.1: Thermogravimetric analysis (TGA) coupled with mass spectrometry

Thermogravimetric analysis was used initially (at Durham University) due to insufficient funds to acquire RockEval™ data externally. Thermogravimetric analysis

is a pyrolysis technique which uses a small aliquot (< 1 g) of powdered sample to determine mass loss over a programmed heating cycle (similar to RockEval™, Section 3.2). Mass spectrometry was used to analyse which elements were pyrolysed at different stages of heating. The mass spectrometer attached to the TGA machine used was limited and unable to give details about the hydrocarbons produced at different pyrolysis temperatures.

The theory behind using thermogravimetric analysis was that it could replicate RockEval™ analysis by pyrolysing samples in an inert helium atmosphere using the same heating programme (temperature ramp rate and holding temperatures) as described in Section 3.2 for RockEval™ analysis. The differences with the technique using TGA was that it was only possible to identify the S_1 and S_2 peaks by mass loss and was unable to isolate the organic matter portion of a sample, which is achieved in the RockEval™ technique by using an FID. To combat this, pyrolysis gas chromatography and mass spectrometry (GC-MS) was investigated (at Durham University) as the addition of an FID and TCD would allow organic matter to be analysed similar to RockEval™ and further information about the hydrocarbons produced could be ascertained. However, the pyrolysis oven and heated transfer line were not able to reach the temperatures required for longer chain hydrocarbons to remain in gas state, meaning that they would condense before being analysed.

3.5: Qualitative bulk powder X-ray diffraction

Mineral phases are commonly identified using X-ray diffraction techniques. X-rays are focused into an incident beam using slits and directed onto the surface of randomly oriented powdered sample. Rayleigh scattering occurs when the X-ray beam comes into contact with an atom's electron shells. Within a crystalline structure (n = a positive

integer), the atoms occur repeating at an Ångström distance (Å; 1 x 10^{-10}m) similar to the wavelength of X-rays (λ) thus their electron clouds are used as a diffraction grating for Rayleigh scattering. Within a crystalline structure, atoms occur in lattices which create planes which can be defined according to the Miller index (hkℓ). Bragg's Law of X-ray diffraction (Equation 2) states that a pair of parallel planes are separated by a distance (d; Figure 3-3). The Bragg angle (θ) can be described as the incidence angle between the X-ray wave and the atomic plane..

Equation 2: Bragg's Law of X-ray diffraction

$$n\lambda = 2d_{hkl} \sin\theta$$

Strong intensities recorded on an X-ray diffractogram are named Bragg's peaks which record the angles at which the Bragg condition is satisfied and the scattered X-rays interfere constructively (Figure 3-3). Random orientation of particles is necessary so that crystals which might preferentially align (e.g. plates/cylinders) and record greater peak intensity or broaden the recorded peak.
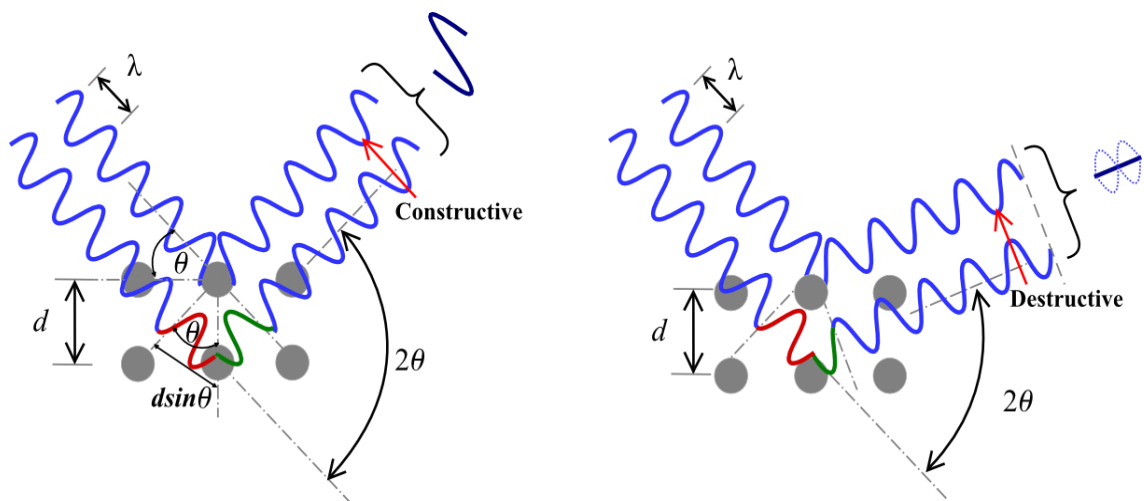
Figure 3-3: Schematic indicating scattering of X-rays by a crystal lattice and Bragg's Law, waves are X-ray paths. Left demonstrates constructive interference (red arrow shows peaks combine to give a greater signal). Right shows destructive interference which occurs when the phase of the waves shift and the signal is destroyed (red arrow shows destruction of signal).

Chapter 3

Powder X-ray diffraction (XRD) analysis of the outcrop samples was undertaken at Durham University using a Bruker D8 Advance (D8000 diffractometer), with a wavelength of 1.5406 nm (Cu K$_{\alpha1}$ radiation). The machine was calibrated using Al_2O_3, Y_2O_3, and SiO_2 standards. Bulk powder samples were continuously rotated and scanned from 5-90 ° (2θ), with measurements taken every 0.02 ° (2θ). Total scan time was 1256 seconds (20 minutes 56 seconds) with a time per step of 3.146 seconds. The clay fraction was not separated for further analysis in this study. Peak analysis was done in MS Excel manually using known diffraction patterns from the Inorganic Crystal Structure Database (ICSD).

3.6: X-Ray Fluorescence spectroscopy

X-ray fluorescence (XRF) spectroscopy analysis was conducted at Chemostrat Ltd using a SPECTRO XEPOS ED-XRF. Powdered samples (~ 4 g) were pressed into 30 mm diameter pellets. Major, minor and trace elements were measured using a solid state lithium-drifted silicon detector (Si (Li)). Analytical uncertainty was typically < 1 % relative standard deviation (RSD) and an accuracy of 2% to 5% RSD can be expected for major elements, with a less accurate performance being achieved for trace elements. Quantification limits are of less than a few parts per million (mg/g). XRF data was acquired for eleven major elements, e.g., Si, Ti, Al, Fe, Mn, Mg, Ca, Na, K, P and S, plus forty trace elements, e.g., Ag, As, Ba, Bi, Br, Cd, Ce, Cl, Co, Cr, Cs, Cu, Ga, Ge, Hf, Hg, I, In, La, Mo, Nb, Nd, Ni, Pb, Pr, Rb, Sb, Se, Sn, Sr, Ta, Te, Th, Tl, U, V, W, Y, Zn and Zr. However, some of the trace elements, e.g., Bi, Cd, Ge, Hg, I, In, Se, Sb and Te, are present in rocks at such low levels below limits of determination, that the data for these trace elements is semi-quantitative.

3.7: Optical Thin Section Analysis

Samples were scanned using a HP Deskjet F4200 series flatbed scanner to show visible variations in colour and structures. The images are taken at a 2400 DPI resolution with no magnification used in the process.

Textures in the thin sections were studied using a Leica DM 1B02 petrographic microscope, and images were captured using the attached digital camera (Leica DFC 320). The images were taken at varying magnifications, from 5 x to 50 x, using both transmitted and crossed polarisers.

3.8: Scanning Electron Microscopy (SEM)

Thin sections of selected samples were carbon coated (15 nm) using a Cressington 108Carbon/A carbon coater and examined using a Hitachi SU-70 High Resolution Analytical SEM with a Schottky Field Emission Gun (FEG), equipped with an Oxford Instrument Energy Dispersive X-ray (EDX) and microanalysis system (INCA Energy 700). The Schottky FEG comprises a Tungsten tip coated with ZnO which provides greater electron brightness (i.e. increased number of electrons directed at the sample area per second) and more coherent electron energies thus providing a greater signal to noise ratio than a traditional Tungsten filament. Details of the electron column including lenses for focusing the electron beam, the sample stage and detectors can be found in Figure 3-4.

The microscope uses the Schottky FEG to generate a high voltage electron beam which interacts with and penetrates the surface of the rock sample generating X-rays from a relatively broad and deep zone within the surface of the sample (Figure 3-5). The SEM has two detectors used in imaging, these are secondary electron (SE) and back scattered electron (BSE) detectors (Figure 3-4). Both were used in this thesis.
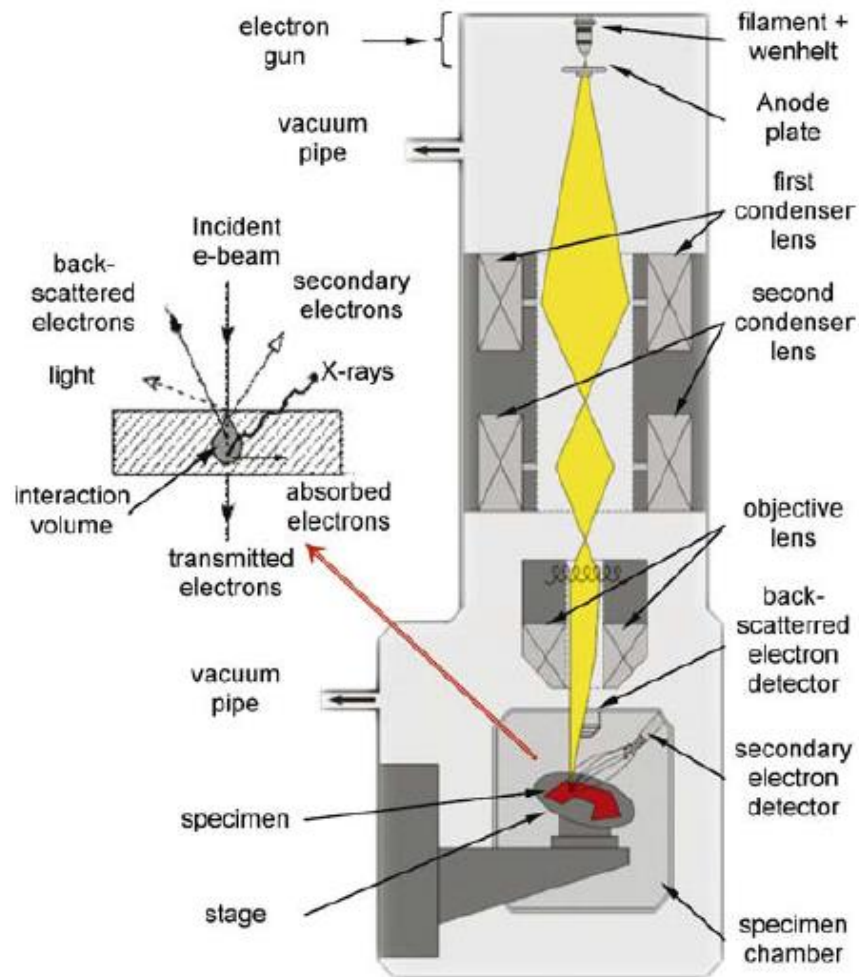
Figure 3-4: Scanning electron microscope schematic with the electron beam highlighted in yellow and the sample on the sample stage in red (from Sutton et al., 2007).

Secondary electron imaging utilises the low energy (50 eV) electrons emitted from a sample when it is bombarded with the high-voltage electron beam (20 kV). Secondary electrons move towards a detector due to a positive electrical bias and are focused onto phosphorous scintillators to increase the strength of the signal where it is detected. Secondary electron images give information about the topography of the surface that is being imaged with edges highlighted by brighter SE image due to edge effects. With SE it is possible to investigate surface topography, including grain edges and pores as well as etching/scratching to the surface of grains.

Backscatter electron imaging uses high energy beam electrons which are scattered back from the surface of the sample. The number of electrons backscattered depends on the sample composition according to atomic number and thus it can be used to investigate the mineralogy and texture (including: mineral/grain roundness, sphericity, size and distribution) of the samples.
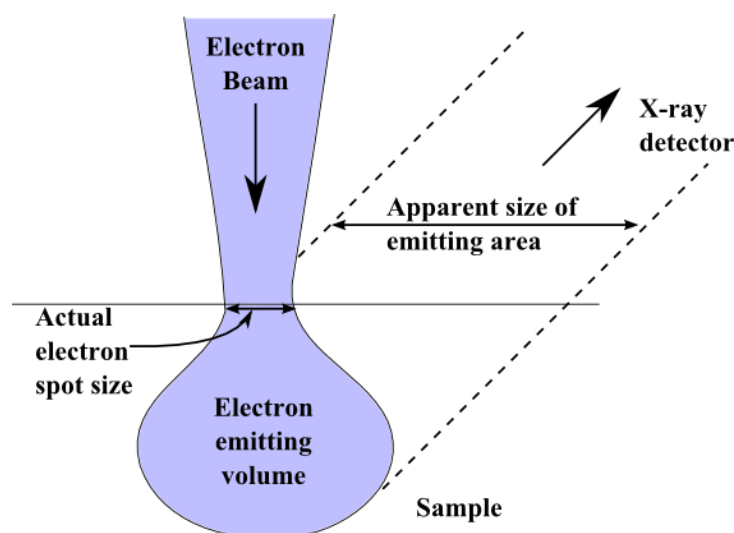
Figure 3-5: Interaction volume of the surface of a sample comparing electron beam spot size and the size of the area of emitted X-rays.

3.8.1: Energy Dispersive X-ray Spectroscopy (EDS)

Energy dispersive X-ray spectroscopy was conducted on SEM samples using an Oxford Instruments X-MaxN silicon drift detector (SDD) to give qualitative and semi-quantitative elemental analysis. The technique focuses high energy electrons on to the surface of the sample which causes secondary electrons to be expelled. This results in the atom shifting to an excited state; to return to its normal state an electron from a higher shell moves to fill the electron hole and radiation is emitted as an X-ray. Each atom has unique energy levels which occur in electron transfer leading to the wavelengths of the X-rays emitted being of a distinct length to be able to characterise each atom.

To be able to quantify the amount of an element in a sample, a pure cobalt standard is used to calibrate virtual standards built into the EDS INCA software. The concentration of an element within a sample (C_{spec}) is then compared to the constant (k) concentration of the standard (C_{std}) by equation 3 (Castaing, 1951). The number of counts from a sample (N_{spec}) is divided by the number of counts from the standard (N_{std}) multiplied by the known concentration of the standard.

Equation 3: Quantifying an element within a sample

$$C_{spec} = \frac{N_{spec}}{N_{std}} C_{std} = kC_{std}$$

Complications with quantifying elements can occur and matrix corrections are required to accommodate for this. Philibert (1963) proposed corrections for atomic number effects (Z), absorption (A) and fluorescence (F). Improved corrections were proposed by Pouchou & Pichoir (1984) which was a general model for calculating X-ray intensity (called PAP). The Oxford INCA software uses a correction called eXtended Pouchou & Pichoir (XPP) which is an extended PAP correction and provides a more accurate correction than the ZAF method particularly of lighter elements.
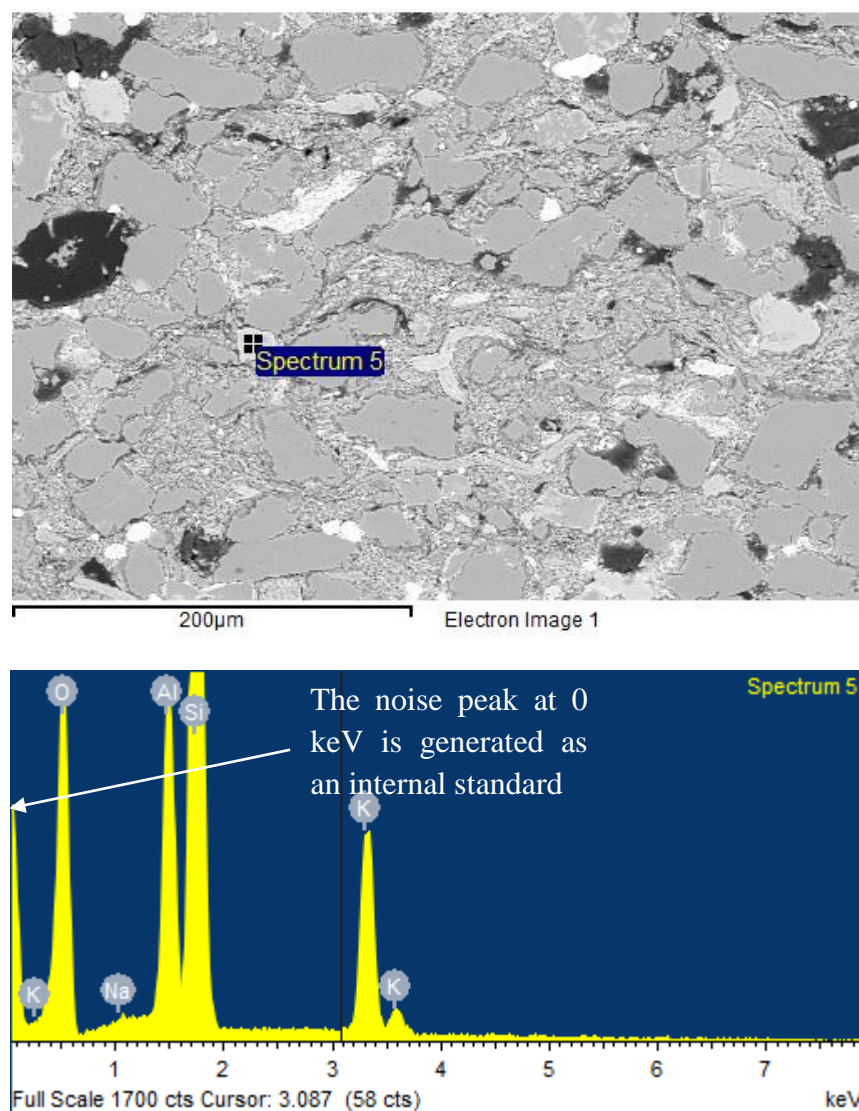
Figure 3-6: Electron Dispersive X-ray Spectroscopy (EDS) spectrum showing an alumina-silicate mineral (below) of the point Spectrum 5 on backscatter SEM image of a mudstone sample from the Holywell Shale (above).

For selected areas identified using the SEM, EDS was used to identify points (single minerals; Figure 3-6) and to create mineral maps using Oxford INCA software based on elemental distribution (Figure 3-7). Durham University acquired Oxford AZTEC software which allows quantitative EDS spectra maps (Figure 3-7) to be interpreted as minerals present within a sample and the identified minerals could be overlaid on the BSE image as different colours. However, this software was only available after the

majority of imaging, collection of EDS spectra and interpretation on Oxford INCA software had been conducted on most samples from the Holywell Shale.
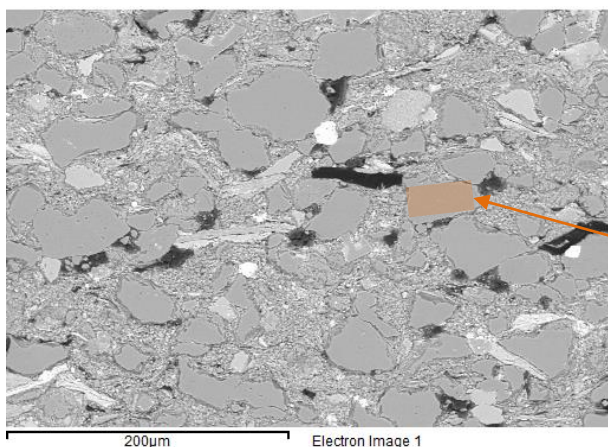
Backscatter SEM image of the area of EDS map.

Si and O EDS maps below (pg. 43) indicate that the sample has quartz (SiO$_2$) present.
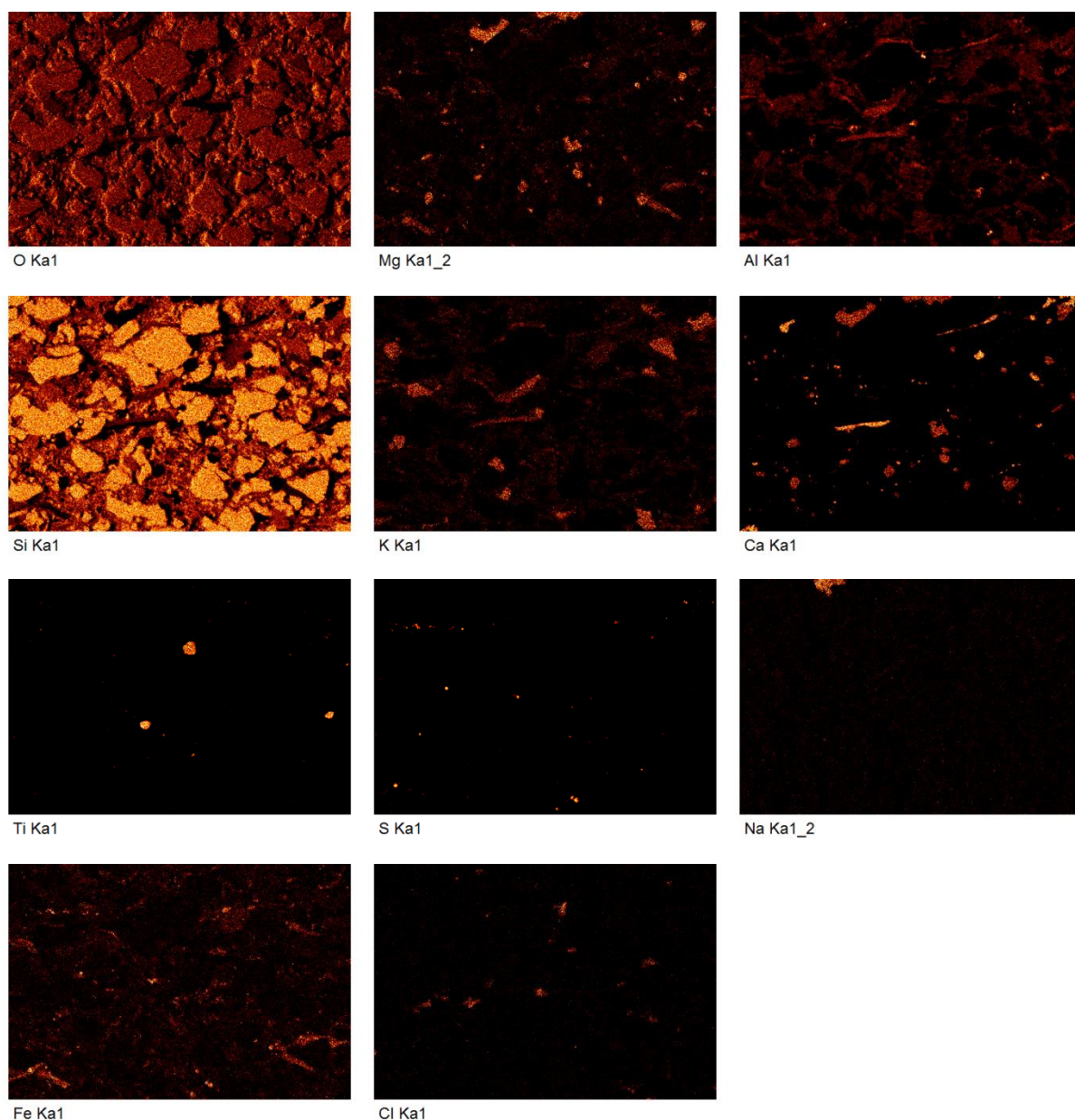
Figure 3-7: Backscatter electron image (pg. 46) above EDS element maps for the shaded area indicated on BSE image. The brighter the orange colours indicate a higher intensity of the element. Ka1 (or Ka1_2) notation after the element name refers to the X-rays detected which penetrate to the innermost 'K' electron shell of an atom and is normally the strongest intensity spectral line.

3.8.2: Broad Ion Beam (BIB) milling

Broad ion beam milling was conducted at Durham University using a Gatan Precision Ion Polishing System (PIPS- model 691). Broad ion beam milling was used to achieve a very fine polish on the surface of a sample before imaging on SEM. This very fine

polish allowed pores to be visible to a scale much smaller than is possible with techniques using abrasives. Samples were prepared initially as 50 μm thin sections on standard glass slide (25.4 x 76.2 mm). Selected areas of interest 3 mm in size were identified using optical and SEM analyses and then cut using an ultrasonic drill with Boron Nitride powder and water. The cut samples were then milled/ polished on the PIPS machine under vacuum with a 3 kV beam, 10 mA/cm^2 ion current density, 1 ° gun tilt and the sample was rotated at 2.5 rpm. The PIPS machine uses an argon ion gun (25 psi) to create a pair of ion beams which were aligned using a phosphorous fluorescent screen. Milling time (the time at which the sample was exposed to the ion beams under the conditions explained) was approximately 13 hours although this time varied depending on sample composition and quality of polish.

3.8.3: Focused Ion Beam (FIB)

Focused ion beam milling and SEM imaging was conducted using an FEI Helios Nanolab G3 DualBeam™ system. FIB imaging is very similar to SEM (Section 3.6) but uses positively charged Ga^+ ions instead of negatively charged electrons. Within the FEI Helios Nanolab G3 DualBeam™ system the electron column is at 0° and the ion column is at 52°. This allows ion beam milling whilst imaging with the electron column. FIB can be used to produce 3-dimensional reconstructions using backscatter electron images which can be used in combination with other imaging (SEM-EDS) to determine mineral type or organic matter present. The technique involves sputtering platinum (2 to 3 μm thick) at both 0° and 52° to protect the site of interest. The Ga^+ ion beam was then used at a high voltage and current (30 kV, 9.3 nA) to mill a trench 25 μm x 18 μm x 18 μm in order to image a 10 μm x 10 μm image. Then the sample is tilted to 0° to mill the site of interest. An electron image was collected every 1 μm slice through an area of interest 10 μm.

Chapter 4:

Geochemical and Lithological Controls on a Potential Shale Reservoir: Carboniferous Holywell Shale, Wales

4.1: Abstract

The Holywell Shale is part of the Carboniferous Bowland Shale Formation, identified as the main potential shale gas system in the UK. Here, geochemical and petrographic data from five outcrops of the lower and upper Holywell Shale across northeast Wales are reported. At outcrop, the Holywell Shale is immature to early oil mature and has total organic carbon (TOC) values ranging between 0.1 and 10.3 wt. %, with a mean of 1.9 wt.%. Carbon isotope data clearly differentiate terrestrial and marine organic matter and show that both occur throughout the Holywell, with terrestrial sources (Type III/IV) dominating the upper Holywell and marine sources dominating the lower Holywell (Type II/III). Trace element data indicate that bottom waters were oxygenated, resulting in poorly preserved organic matter, supported by C/N and HI data. A range of silt- and clay-rich lithofacies occur, which show no relationship to either the amount or type of organic matter. The data are interpreted in terms of a mixed supply of terrestrial and marine organic matter to marine depositional environments in which there was sufficient hydrodynamic energy to transport fine-grained sediment as bed load. The resulting mudstones exhibit a range of sedimentary textures with millimetre- to centimetre-scale silt-clay bed forms which show almost no relationship to organic matter type and amount. The small-scale variability and heterogeneity of both organofacies and lithofacies means that the reservoir quality of the Holywell Shale is inherently difficult to predict.

4.2: Introduction

Over the past decade the production of hydrocarbons from unconventional sources has increased significantly, specifically with the development and exploitation of mudstone source-rock reservoirs where hydrocarbons have been generated *in-situ* (Hart et al., 2013). A key shale gas target in the UK is the Carboniferous Bowland-Hodder

Formation of the Pennine Basin (Andrews, 2013). The present study focuses on the Holywell Shale deposits of northeast Wales, part of the Bowland Shale Formation, and investigates the way in which a complex interplay of sediment supply, depositional environment and provenance and preservation of organic matter influences the source-rock reservoir quality of this major mudstone unit.

The Carboniferous basins of northern England, including the Pennine Basin in which the Holywell Shale was deposited (Figure 4-1), were formed during the Dinantian (359.2–326.4 Ma) by a phase of rifting that was dominated by N-S extension acting along pre-existing NW-SE and NE-SW post-Caledonian weaknesses to create asymmetrical half-graben structures. Subsequent Namurian sedimentation (326.4–314.5 Ma) occurred during a period of post-rift thermal subsidence which created sufficient accommodation space for the accumulation of up to 2 km of sediments, including the Holywell Shale (Fraser & Gawthorpe, 1990; Williams & Eaton, 1993). The type-section for the Holywell Shale is contained within the Abbey Mills borehole with a maximum thickness of 152m (Davies et al., 2004; Waters, 2009).
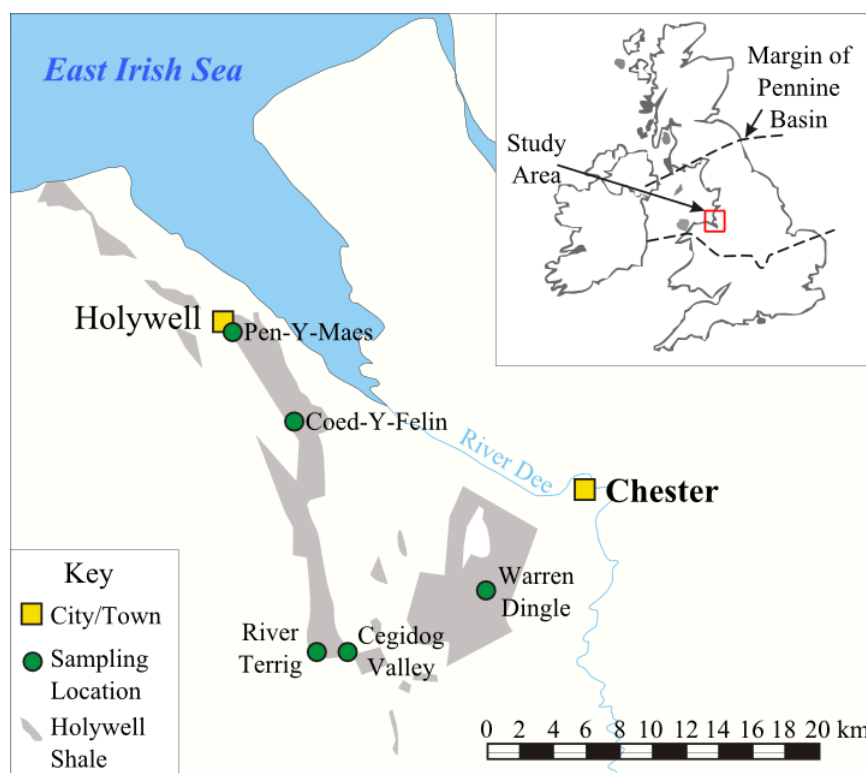
Figure 4-1: Map of the study area with the wider location (inset image), showing the subcrop extent of the Holywell Shale (grey) and the main outcrop locations studied.

Namurian sedimentation in northern England generally occurred in a shallow epicontinental seaway within a series of connected basins stretching across the UK and Ireland (Figure 4-2; Davies et al., 1999). Sediment was supplied from the north into deltaic systems and shallow seas and deposited in water depths of less than 100-200 m (Figure 4-2; Wells et al., 2005). Sea levels in the late Mississippian and early Pennsylvanian were also strongly influenced by a series of glacioeustatic cycles which resulted in global sea level variations of 60-100 m (Rygel et al., 2008) which are well recognised in the UK Namurian (Armstrong et al., 1997; Bott & Johnson, 1967; Church & Gawthorpe, 1994; Hampson et al., 1996; Jerrett & Hampson, 2007; Martinsen et al., 1995; Ramsbottom, 1977; Wright et al., 1927). The Holywell Shale was thus deposited as a succession of marine, brackish and non-marine mudstones on the southwest edge of the Pennine Basin (Figure 4-2; Collinson, 1988; Davies et al., 2004; Guion & Fielding, 1988). Maximum flooding surfaces are represented by a series of ammonoid-

bearing (goniatite) marine bands up to several metres thick, which contain assemblages of both benthic and planktonic fauna and which represent a range of fresh water to saline environments (Waters et al., 2009). These marine bands allow the Holywell Shale to be dated biostratigraphically (Figure 4-3; Davies et al., 2004; Ramsbottom, 1974; Ramsbottom et al., 1978; Waters & Condon, 2012).
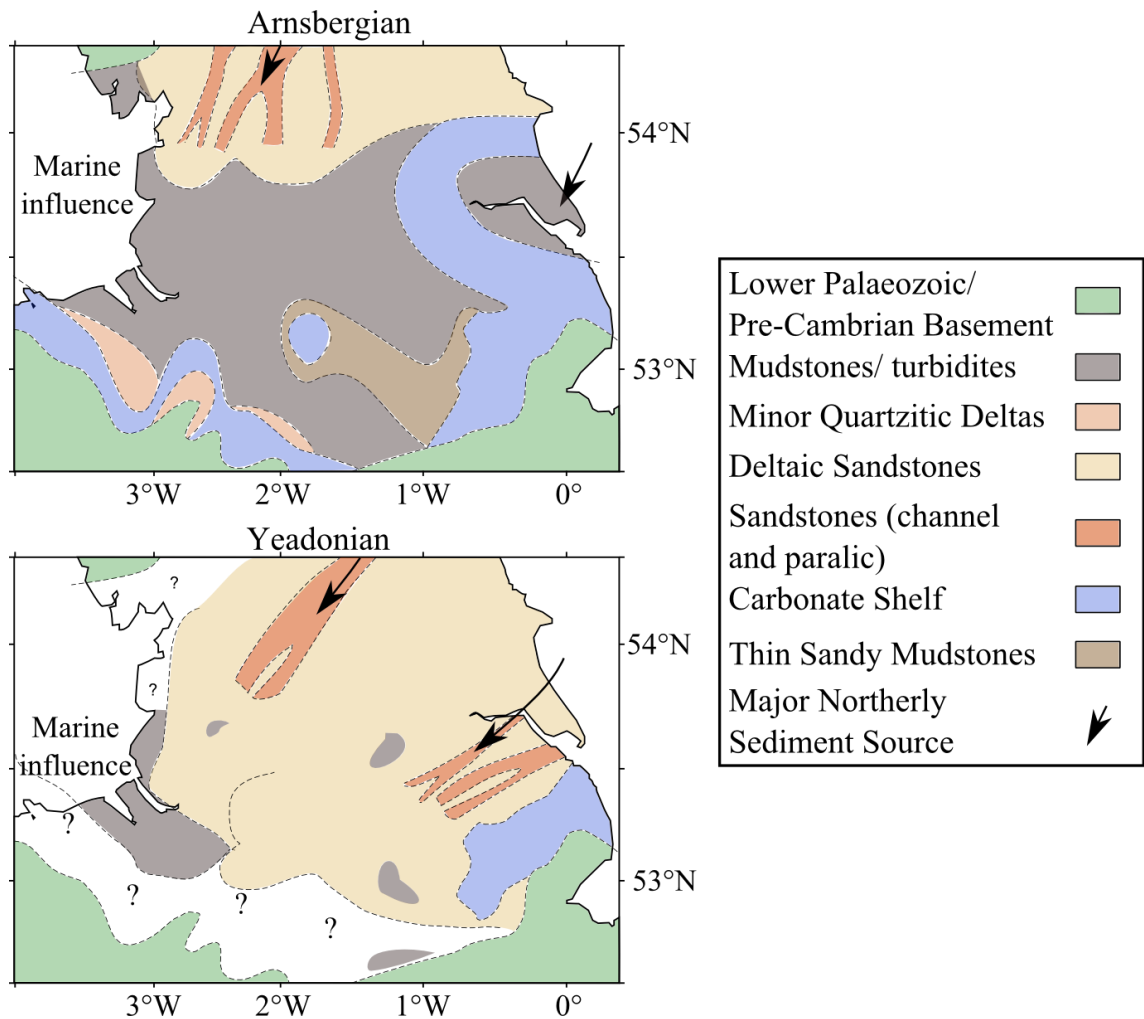
Figure 4-2: Palaeogeography of the Arnsbergian (top) and Yeadonian (bottom) showing the progradation of the major northerly sourced delta systems (adapted from Fraser & Gawthorpe, 2003).

Organic carbon contents of Namurian mud-rich sediments in northern England typically range from 1 to 3%, with values up to 8% (Andrews, 2013). Palynological and carbon isotope studies show that the organic matter is derived from both marine

and terrestrial sources (Stephenson et al., 2008; Davies et al., 2012). Previous work suggests that at least parts of the Lower Holywell Shale (E1c age; Figure 4-3) have petroleum potential and may have sourced oils in the Douglas and Lennox oilfields in the East Irish Sea (Armstrong et al., 1997).

The quality of shale reservoirs relates to both their gas/oil storage potential and the rate at which that petroleum can be delivered to a wellbore from matrix pores to a fracture network induced by hydraulic fracturing. These factors relate in turn to the nature and amount of organic matter in the rocks, and also their lithology and mineralogy (e.g. Passey et al., 2010). In a depositional system like the Holywell Shale, in which both water depth and the supply of both sediment and organic matter changed over short periods of geological time, controls on shale reservoir quality will be complex in both space and time, and thus difficult to predict. In this context, analysis was undertaken on a series of samples from both the Lower (Pendleian to Arnsbergian) and Upper (Marsdenian to Yeadonian) units of the Holywell Shale to determine whether there are relationships between the sedimentology and mineralogy of the rocks and the nature and amount of organic matter.

Unit Name		Sample Location (Easting, Northing)	Age (Ma)	Series	Stage ICS	Stage UK	Regional Substage	Ammonoid Biozone
Lower Coal Measures			310–312	Pennsylvanian	Moscovian	Westphalian	Langsettian	*G.listeri*
Gwespyr Sandstone			313–314					
Upper Holywell Shale		Pen-Y-Maes (319450, 376700) — Warren Dingle (331800, 362340) — Coed-Y-Felin (322370, 371500)	315		Bashkirian	Namurian	Yeadonian (G1)	*G.subcrenatum* *C.cumbriense* (G1b) *C.cancellatum* (G1a)
			316				Marsdenian (R2)	*B.superbilinguis* (R2c) *B.bilinguis* (R2b) *B.gracilis* (R2a)
			317				Kinderscoutian (R1)	*R.reticulatum* (R1c) *R.nodosum* (R1b) *R.circumplicatile* (R1a)
Holywell Shale			318–321				Alportian (H2)	*Ht.prereticulatus* (H2c) *H.undulatum* (H2b) *Hd.proteum* (H2a)
Cefn-Y-Fedw Sandstone			322–323					
Lower Holywell Shale		River Terrig (323350, 356850 to 323380, 356970) — Cegidog Valley (326050, 356880)	324–326	Mississippian	Serpukhovian		Chokierian (H1)	*H.beyrichianum* (H1b) *I.subglobosum* (H1a)
							Arnsbergian (E2)	*N.nuculum* (E2c) *Ct.nitidus* (E2b) *E.bisulcatum* (E2a)
							Pendleian (E1)	*Cr.malhamense* (E1c) *T.pseudobilingue* (E1b) *Cr.leion* (E1a)
Clwyd Limestone Group			327–331			Viséan	Brigantian	

Key
- Coal (& Clay/seatearth)
- Shale
- m — Marine band
- Sandstone
- Limestone

Figure 4-3: A simplified stratigraphic column of the Holywell Shale, Gwespyr and Cefn-Y-Fedw Sandstone units; Westphalian Lower Coal Measures; Viséan Limestones. Sample locations and their ages relative to Namurian regional chronostratigraphy and biostratigraphy (* denotes ammonoid biozone recorded within the Holywell Shale in the northeast Wales region; adapted from Davies et al., 2004; Jerrett & Hampson, 2007; Jones & Lloyd, 1942; Waters & Condon, 2012).

4.3: Methods

4.3.1: Sample Site Description

Samples were collected from outcrops of the Holywell Shale. Outcrop access was restricted due to the limited exposure of the Holywell Shale within northeast Wales

(Figure 4-1). The outcrops sampled consisted of narrow sections (< 1 m) within stream cuttings, where samples were taken from an area of ~ 0.5 m^2. In the case of River Terrig and Pen-Y-Maes, which were more extensive, multiple sites were sampled along the exposures and therefore, represent a more significant range in stratigraphy (Figure 4-3). Due to faulting, the River Terrig location does not represent a continuous sequence of deposition and the stratigraphic placement of this location is difficult as the E2b3 pelagic goniatite fauna (*Cravenoceratoides nititoides*) is only reported as present on the north side of the fault (RTS2 sampling site, with RTS3, RTS5, RTS6 sampling sites occurring close to the faulted zone) (Waters & Condon, 2012). It is not clear from outcrop analysis what type of faulting has occurred, it has been assumed that the fault is normal with the north side of the fault (with the fossil marine band present) downthrown therefore representing younger material than the southern side (RTS1 sample site) of the fault.

4.3.2: Sample Collection and Analysis

At each sampling location (Figures 4-1 & 4-3) samples were collected at random across the available exposure from base to top. Weathered material was removed until a fresh surface of mudstone was accessible: in some cases this resulted in over 20 cm of material being removed. All samples were dried at room temperature, powdered using an agate mortar and pestle and subsequently re-dried in an oven at 40 °C. Polished thin sections of select samples were created by cutting the shale sample into 1 cm thick slices and mounting them to glass slides using an epoxy resin (Epo Tek 301) and polishing to 15 μm for optical thin sections and 50 μm for SEM thin sections.

4.4: Results

4.4.1: Organic Geochemistry

The average TOC across the Holywell Shale in this study is 1.9 wt % with both the highest (10.3 wt %) and lowest (0.1 wt %) values recorded within the Upper Holywell Shale (Appendix A). The range of TOC within the Lower Holywell Shale is 0.6 wt % to 3.4 wt % with an average of 2.0 wt %. RockEval™ data show that the organic matter ranges from mixed Type II/III to Type III/IV and that the samples have maturities ranging from immature to oil mature (Figures 4-4 & 4-5). However, in eleven of the Holywell Shale samples, low values for RockEval™ S2 mean that kerogen type and maturity calculations are not accurate.
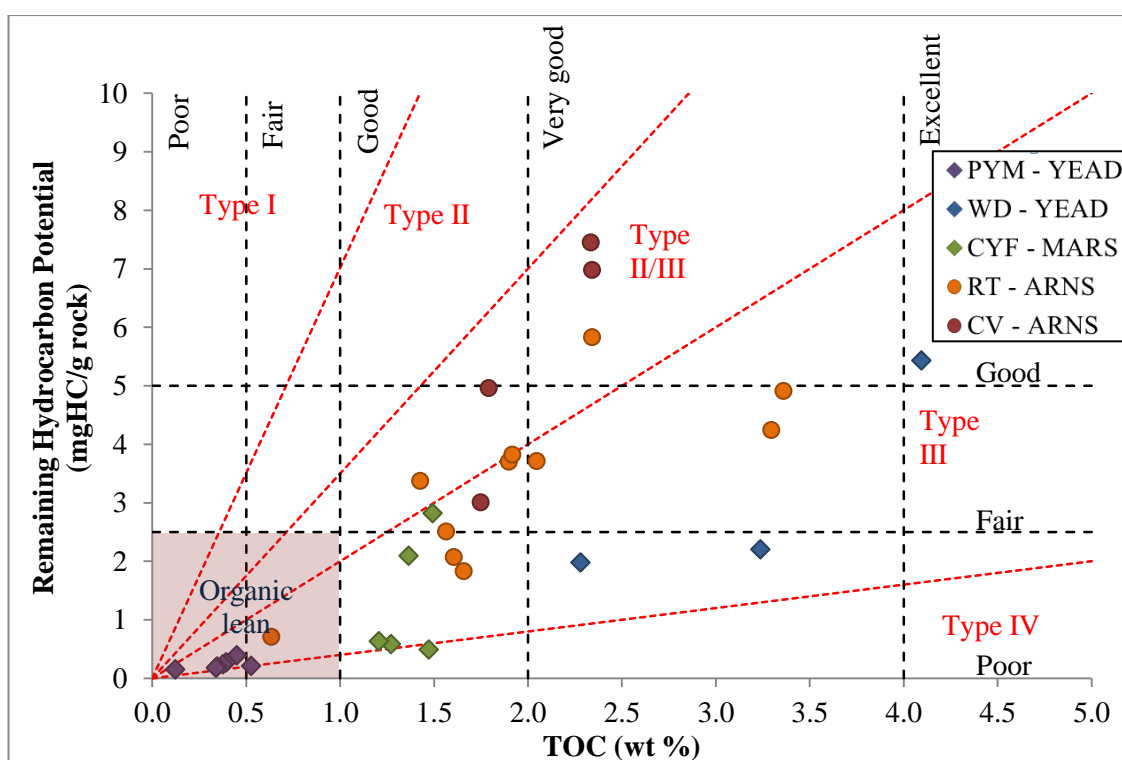
Figure 4-4: Kerogen quality plots indicating the kerogen type (in red) and generation ability of the remaining total organic matter (Y axis – which corresponds to S_2 from RockEval™). Warren Dingle (WD) sample WDS1H4 has been removed due to its high TOC value (10.31 wt %); it plots in the Type III kerogen region and is above good to excellent for TOC and remaining potential. The majority of samples are composed of type

III kerogens; five samples (3 Cegidog Valley (CV) and 2 River Terrig (RT) samples) demonstrate a mixed type II/III kerogen, with 3 samples from Coed-y-Felin (CYF) exhibiting type IV kerogen. PYM = Pen-Y-Maes. The shape of data points on the plot corresponds to Upper (diamond shape) and Lower (circle shape) Holywell Shale. Yeadonian (YEAD), Marsdenian (MARS), Arnsbergian (ARNS).
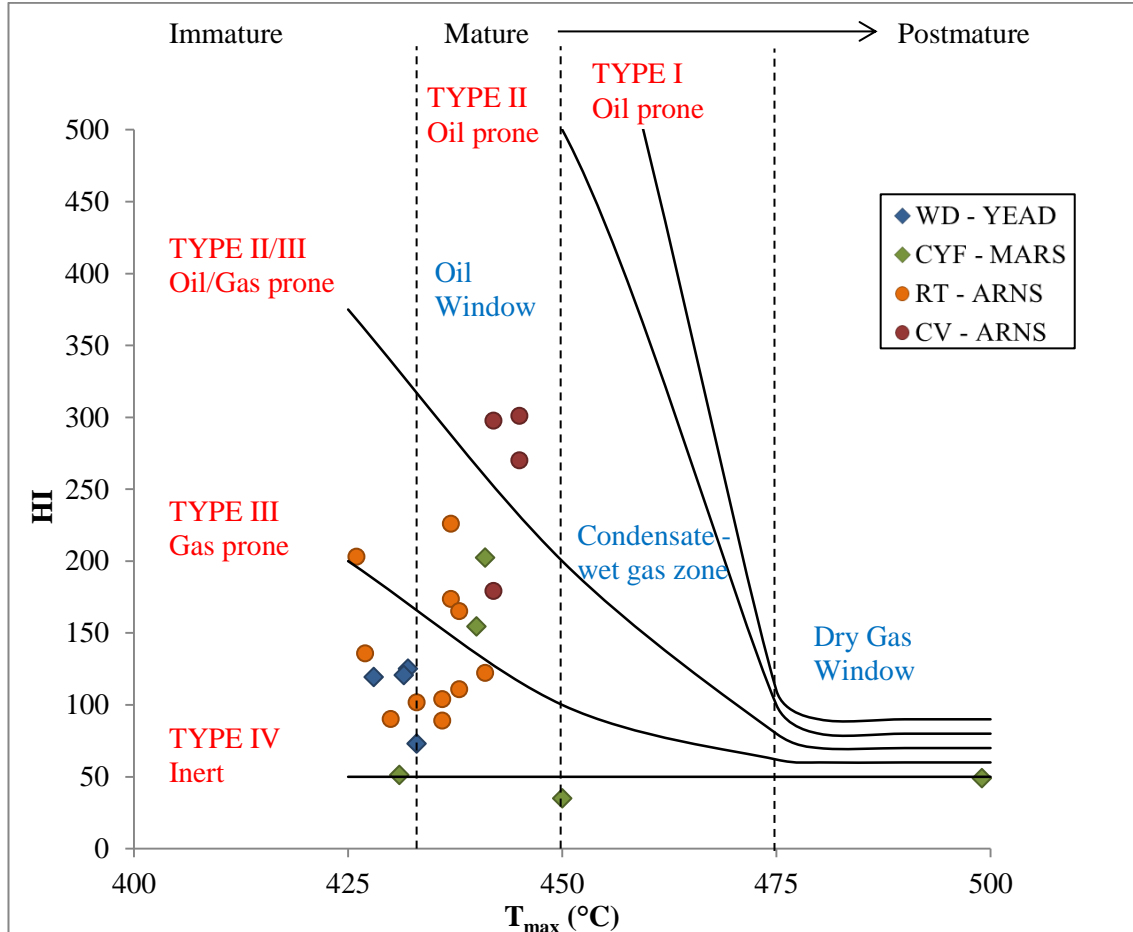
Figure 4-5: Plot of T_{max} and HI showing maturity and kerogen type. The T_{max} (x-axis) indicates the maturity the samples have reached and the black dotted lines indicate oil, condensate gas and dry gas windows. The majority of samples are immature to oil mature, with some Coed-Y-Felin (CYF) location samples showing anomalous HI and T_{max} values and Pen-Y-Maes (PYM) samples not included due to lack of organic matter present. RT = River Terrig; CV = Cegidog Valley. The shape of data points on the plot corresponds to Upper (diamond shape) and Lower (circle shape) Holywell Shale. Yeadonian (YEAD), Marsdenian (MARS), Arnsbergian (ARNS).

Carbon isotope signatures allow good insights to the provenance of the organic matter because terrestrially-derived kerogens in the Carboniferous have carbon isotopic values

of -24 ‰ to -22 ‰ compared with -35 ‰ to -30 ‰ for marine organic matter (Lewan, 1986; Peters-Kottig et al., 2006; Stephenson et al., 2008). In this study, there is a clear difference in the range of carbon isotope values between the Lower and Upper Holywell Shale. $\delta^{13}C$ values for organic matter in the Lower Holywell Shale range from -31.1 ‰ to -25.6 ‰ compared with -25.9 ‰ to -22.4 ‰ for the Upper Holywell Shale. Based on the range of carbon isotope values in Appendix A, it can be assumed that terrestrial and marine organic matter have $\delta^{13}C$ = -22.5 ‰ and -31 ‰ respectively, so that organic matter in the Lower Holywell Shale is 40 - 100 % marine and in the Upper Holywell is 0 - 40 % marine (Lewan, 1986; Maynard, 1981; Peters-Kottig et al., 2006; Stephenson et al., 2008).

Using $\delta^{13}C$ as a proxy for the source of the organic matter, plots of $\delta^{13}C$ versus TOC and HI are shown in Figures 4-6 and 4-7 respectively. There is no relationship between the amount of organic matter and its source. Whilst the end-member marine organic matter has higher HI values than the end-member terrestrial organic matter, the weak correlation between $\delta^{13}C$ and HI suggests variable degradation/preservation of both terrestrial and marine organic matter. Degradation of organic matter, either in the water column or at the seabed, is supported by the nitrogen contents of the sediments. A plot of total organic carbon versus total nitrogen shows a positive correlation and therefore implies that much of the sedimentary nitrogen is associated with organic matter (Figure 4-8). C/N ratios for marine organic matter typically range between 5 and 8 (Meyers et al., 2009). However, the C/N ratios for all samples (with the exception of Pen-Y-Maes) are in the range of 12.7 to 76.2 (Figure 4-9). Such high C/N ratios demonstrate the preservation of a carbon-rich, nitrogen-poor organic material which is most probably related, in these sediments, to the selective removal of nitrogen from organic matter during early diagenesis (Junium & Arthur, 2007; Meyers et al., 2009;

Van Mooy et al., 2002; Verardo & MacIntyre, 1994; Meyers et al., 2009; Rivera & Quan, 2014). It is notable that organic matter at Pen-Y-Maes, which represents the terrestrial end-member, has the lowest C/N ratios, perhaps reflecting the initial ratio of the organic matter. Note also that the $\delta^{15}N$ data range from 1.2 to 3.2 ‰ but show no relationship to either the source or amount of organic matter (Calvert, 2004).
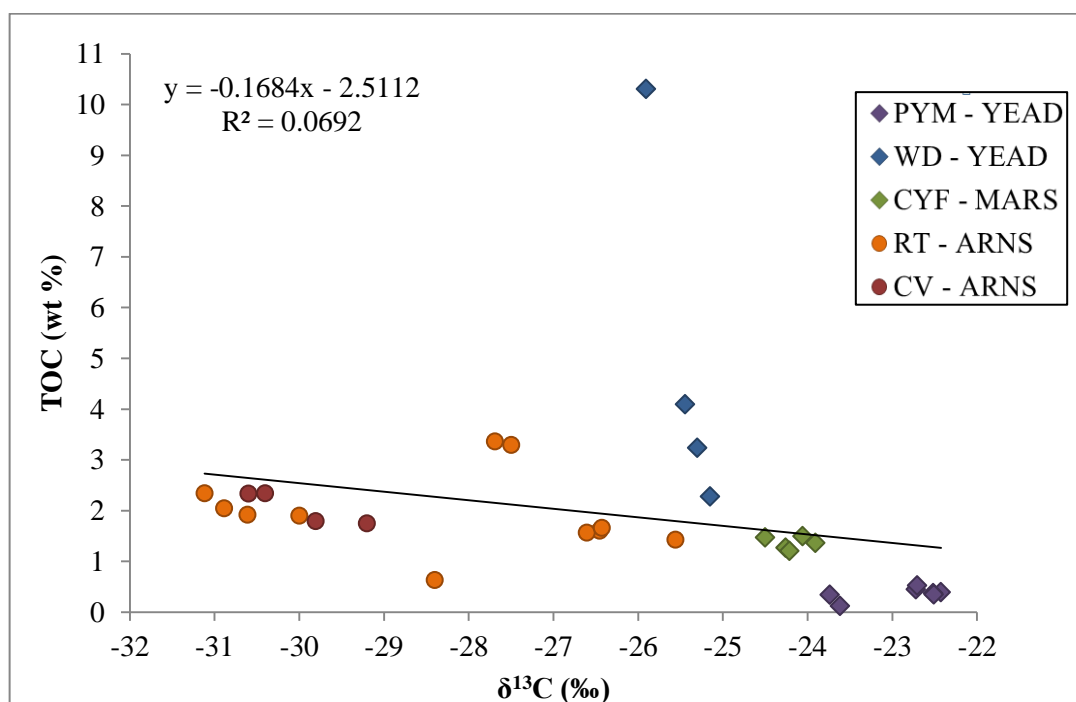
Figure 4-6: Total organic carbon versus carbon isotope composition of organic matter. Isotopically lighter results (-32 ‰) are indicative of a marine influence; isotopically heavier results (-22 ‰) indicate terrestrial organic matter. PYM = Pen-Y-Maes (n = 7); WD = Warren Dingle (n = 4); CYF = Coed-Y-Felin (n = 5); RT = River Terrig (n = 11); CV = Cegidog Valley (n = 4). The shape of data points on the plot corresponds to Upper (diamond shape) and Lower (circle shape) Holywell Shale. Yeadonian (YEAD), Marsdenian (MARS), Arnsbergian (ARNS).
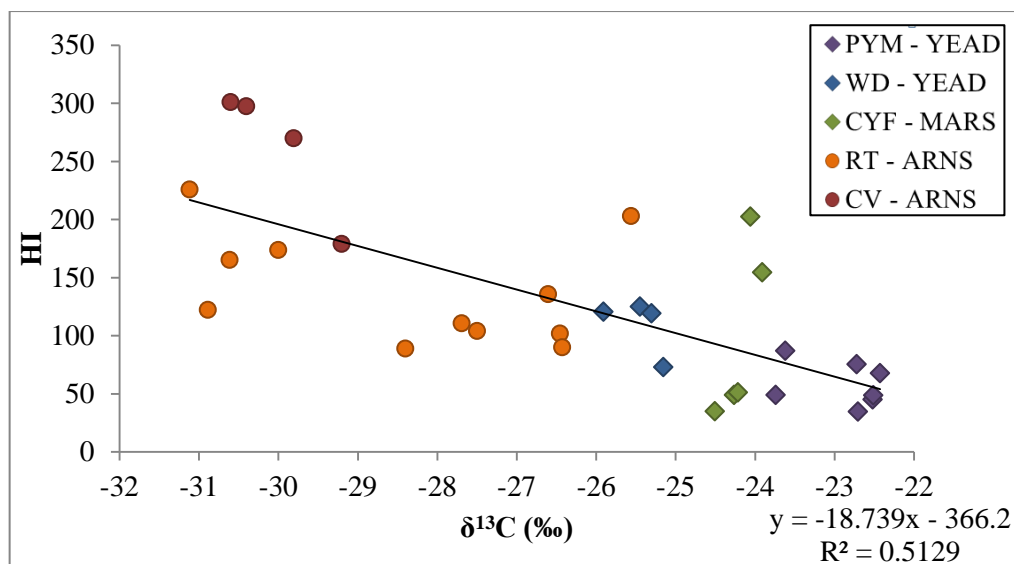
Figure 4-7: Hydrogen Index versus the carbon isotope composition of organic matter. PYM = Pen-Y-Maes (n = 7); WD = Warren Dingle (n = 4); CYF = Coed-Y-Felin (n = 5); RT = River Terrig (n = 11); CV = Cegidog Valley (n = 4). The shape of data points on the plot corresponds to Upper (diamond shape) and Lower (circle shape) Holywell Shale. Yeadonian (YEAD), Marsdenian (MARS), Arnsbergian (ARNS).
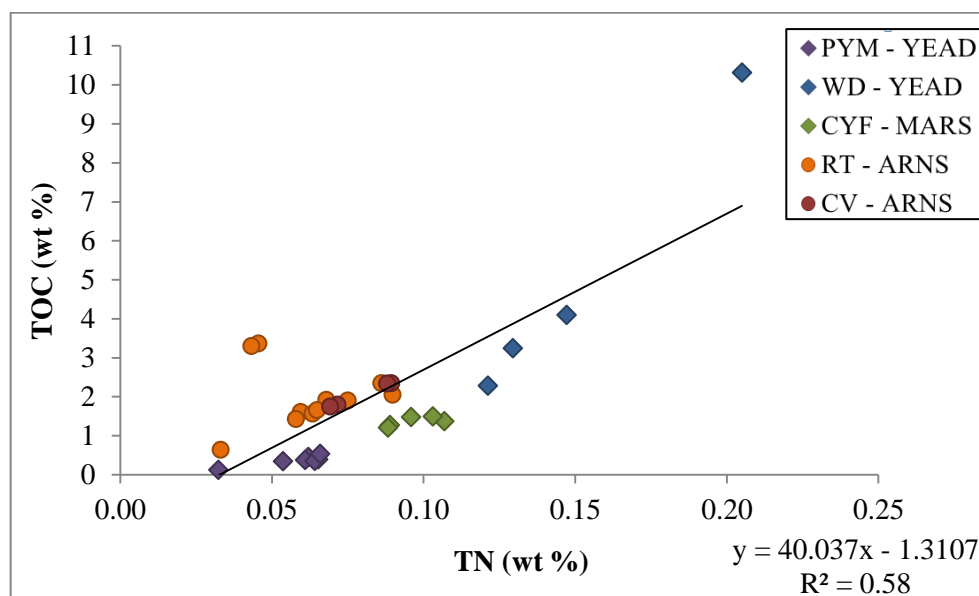
Figure 4-8: Total organic carbon versus total nitrogen. PYM = Pen-Y-Maes (n = 7); WD = Warren Dingle (n = 4); CYF = Coed-Y-Felin (n = 5); RT = River Terrig (n = 11); CV = Cegidog Valley (n = 4). The shape of data points on the plot corresponds to Upper (diamond shape) and Lower (circle shape) Holywell Shale. Yeadonian (YEAD), Marsdenian (MARS), Arnsbergian (ARNS).
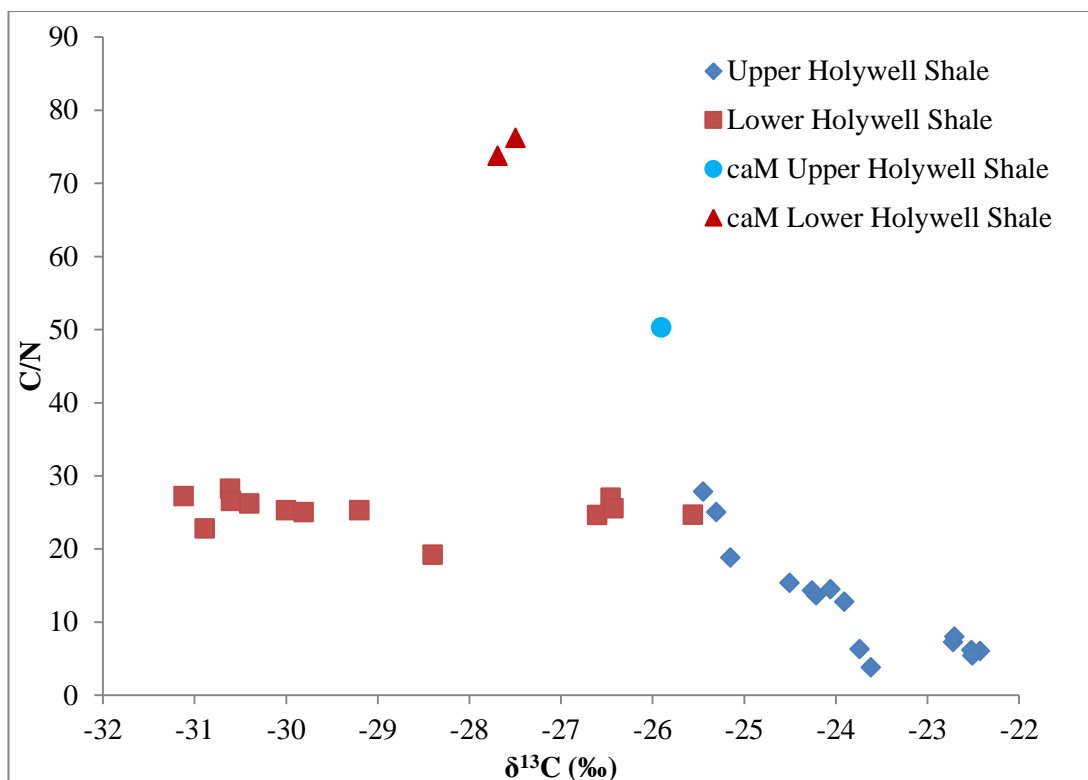
Figure 4-9: C/N ratio plotted with carbon isotope signature showing an increase in C/N with greater marine influence (more negative δ¹³C ‰). The three outlying points with anomalously high C/N ratios have high CaO (from XRF) and are labelled caM = calcite rich mudstone.

4.4.2: Lithology, Mineralogy and Inorganic Geochemistry

Thin sections reveal a small number of centimetre-scale lithofacies including silt-rich and clay-rich mudstones; millimetre-scale, silt-clay bedding structures are common and are strong evidence of sediment transport (Figure 4-10). Around one third of the samples contain significant amounts of carbonate (Appendix B), some of which appears to be detrital (Figure 4-12A) and some of which is fossiliferous (Figure 4-10: facies 2). Carbonate, which is mainly calcite but includes some diagenetic dolomite and ferroan dolomite, occurs primarily in the Lower Holywell Shale, with detrital calcite most probably derived from erosion of pre-existing carbonate platforms (Arthurton et al., 1988; Gross et al., 2015; Johnson et al., 2001; Rose and Dunham, 1977; Waters et al., 2009).

There are no clearly-defined relationships between mineralogy, lithology and the nature and abundance of organic matter in this set of Holywell Shales. In the Upper Holywell Shale, samples from Pen-Y-Maes are silt-rich (Figure 4-10) and have low concentrations of terrestrial organic matter (Figure 4-7; Appendix A). SEM studies show abundant, silt-grade detrital quartz and small amounts (less than 0.5 wt % TOC) of particulate organic matter, consistent with a terrestrial source (Figure 4-12B). Samples from Warren Dingle and Coed-Y-Felin have much lower Si/Al ratios and are thus more clay-rich. Compared with Pen-Y-Maes, they are substantially enriched in organic matter (1.2 wt % to 10.3 wt % TOC) and contain a mixture of terrestrial and marine organic matter, with up to 40 % marine organic matter (Figure 4-12C). The sample with 10.3 wt % TOC also contains almost 30 % calcite, including fossiliferous calcite.
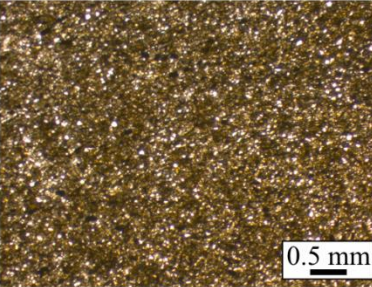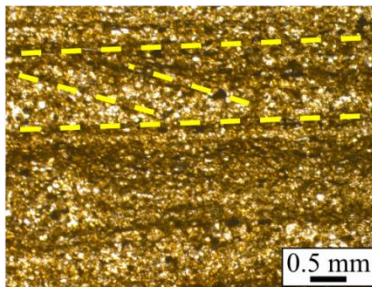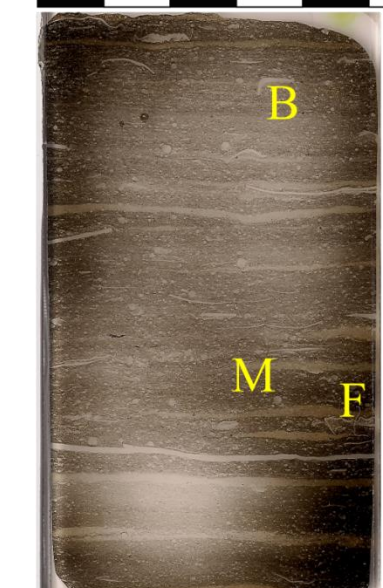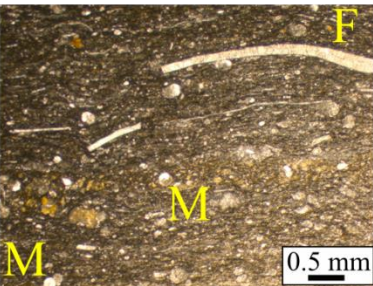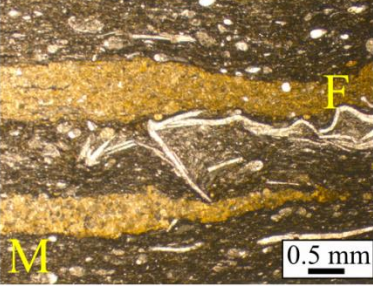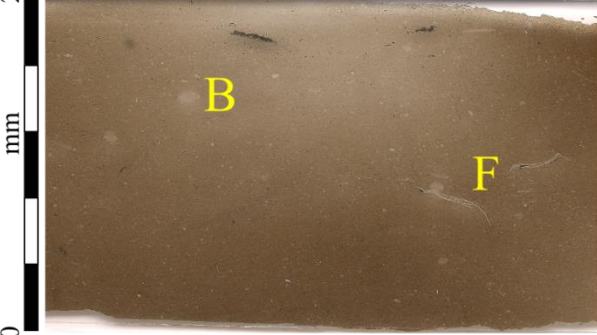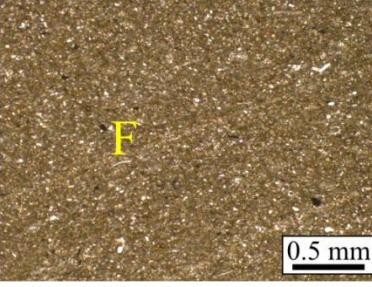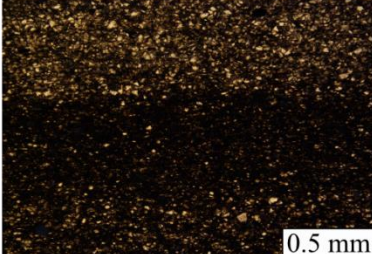
Facies 1a: Silt-bearing mudstone - homogeneous	**n = 5** TOC: 0.1 wt % to 0.5 wt % $\delta^{13}C$: -23.6 ‰ to -22.4 ‰ • Silt sized (50 μm) sub-rounded detrital quartz grains. • Dark and light coloured clay and silt rich bands. • Fragmentary terrestrial organic matter. • Organic matter clustering in isolated lenses.
Facies 1b: Silt-bearing- with graded bedding and sedimentary structures	**n = 2** TOC: 2.3 wt % to 0.3 wt % $\delta^{13}C$: -31.1 ‰ to -23.7 ‰ • Bedding grades from silt sized (50 μm) sub-rounded detrital calcite grains to clay sized (5 μm) calcite grains, occasional rounded quartz grain (<20 μm), and clusters of pyrite framboids. • Mixed, largely fragmentary organic matter (< 60 μm), with some amorphous organic matter aligning along bedding.
Facies 2: Fossiliferous, calcareous, clay rich mudstone	**n = 4** TOC: 1.6 wt % to 10.3 wt % $\delta^{13}C$: -26.5 ‰ to -25.3 ‰ • Microfossils (micro-goniatites < 250 μm) present. • Bone fragments present (< 5 mm). • Yellow stained bands under transmitted light. Composed of microfossil material. Yellow discolouration is possibly oil staining? • Amorphous organic matter aligns along bedding bending around larger grains along with clay minerals. • Discrete lenses and subtle continuous wavy lamination. Often lenticular fabric and beds distorting around fossils and large detrital grains. • Burrows present, often calcite filled.
Facies 3a: Clay rich mudstone – homogeneous	**n = 2** TOC: 3.4 wt % to 3.3 wt % $\delta^{13}C$: -27.7 ‰ to -27.5 ‰ • Massive/homogenous texture with no signs of bedding. • Often bioturbated with burrows present. • Mixed fragmentary and amorphous organic matter (< 20 μm).
Facies 3b: Clay rich mudstone – with discrete graded bedding and wavy lamination	**n = 9** TOC: 1.2 wt % to 2.3 wt % $\delta^{13}C$: -30.6 ‰ to -23.9 ‰ • Graded bedding with continuous parallel beds and continuous non-parallel wavy beds. • Small grain size and thinner beds compared with facies 1b

Figure 4-10 (found on page 64): Lithofacies within the Holywell Shale, thin section image and transmitted light image showing example of each individual facies. Example lithofacies are from both Upper and Lower Holywell Shale samples. Facies 1a: PYMS2H3; Yeadonian; location Easting: 319450, Northing: 376700. Facies 1b: RTS5H1 (left); Arnsbergian; location Easting: 323365, Northing: 356900; & PYMS1H5 (right); Yeadonian; location Easting: 319450, Northing: 376700. Facies 2: WDS1H4; Yeadonian; location Easting: 331800, Northing: 362340. Facies 3a: RTS6H1; Arnsbergian; location Easting: 323365, Northing: 356900. Facies 3b: CVS3H2; Arnsbergian; location Easting: 326050, Northing: 356880. Each lithofacies description includes the number of samples which have that lithofacies description (n), a range of TOC and δ^{13}C values identified within the Holywell Shale. Vertical arrow = fining upward sequence with increase in clay toward the top, inclined arrow = example of bedding feature such as lens, wavy lamination, dashed yellow lines = small scale cross-bedding, M = microfossil, F = bone or shell fragment, B = burrow.

It is possible to estimate clay mineral content for the Holywell Shale samples using Si/Al. A value for Si/Al from average shale based on 277 samples is 3.1, with clay mineral content around 60% (Ross & Bustin, 2009; Wedepohl, 1971). The Si/Al ratios for the Upper Holywell Shale are between 2.5 and 5 whereas the Lower Holywell Shale samples have Si/Al ratios from 5 to 15. This would suggest that the Lower Holywell Shale has clay mineral contents considerably lower than 60%, whereas the Upper Holywell Shale samples from Warren Dingle and Coed-Y-Felin locations have clay mineral contents higher than 60%.

In the Lower Holywell Shale, samples from Cegidog Valley contain primarily marine organic matter, with TOC contents between 1.8 and 2.4 wt % (Appendix A). Scanning electron micrographs indicate the presence of laminar organic matter and also abundant silt-grade detrital quartz (Figure 4-12D). Whilst it is difficult to differentiate detrital and diagenetic quartz without cathodoluminescence data (Milliken et al., 2012; Schieber et al., 2000), textural evidence suggests that some quartz grains may be recrystallized biogenic silica (Figure 4-12E).
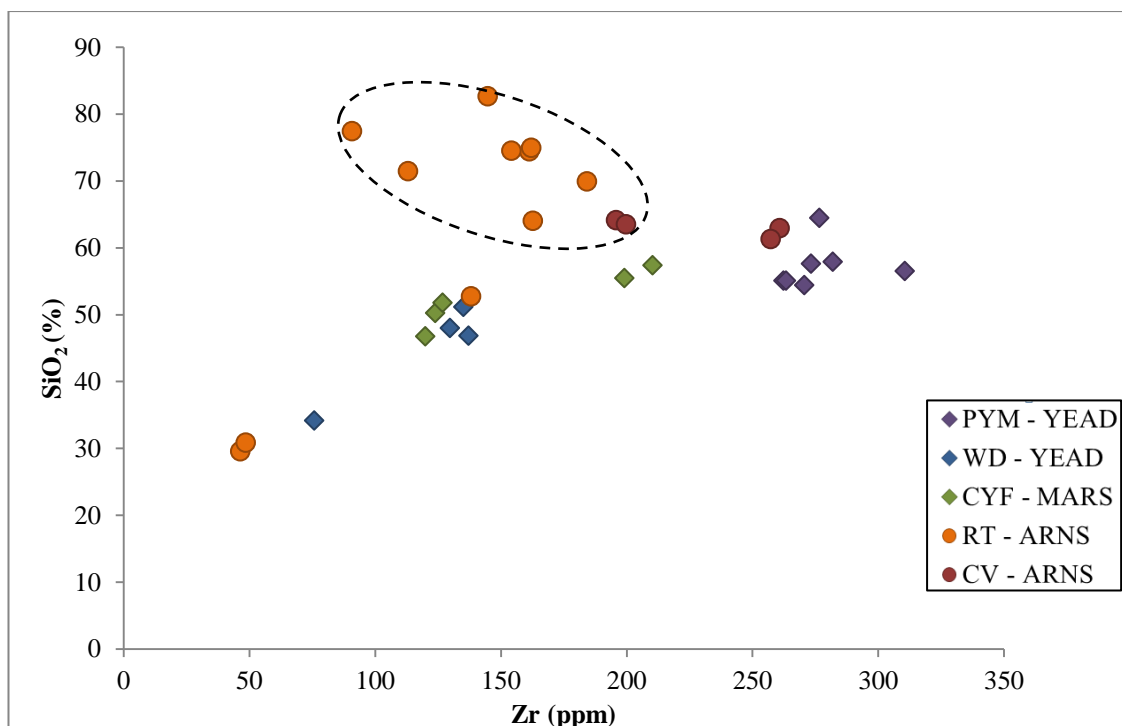
Figure 4-11: SiO$_2$ versus Zr. The strong correlation in most of the sample set is taken to indicate that the quartz is mainly or entirely detrital. Samples from River Terrig and Cegidog Valley are highlighted by the dashed oval line and are relatively enriched in silica, suggesting an input of biogenic silica in addition to detrital quartz. The shape of data points on the plot corresponds to Upper (diamond shape) and Lower (circle shape) Holywell Shale. Yeadonian (YEAD), Marsdenian (MARS), Arnsbergian (ARNS).

Lower Holywell Shale samples from River Terrig contain 0.6 - 3.4 wt % TOC (Appendix A). The organic matter is 40-100 % marine and there is no relationship between the source and amount of organic matter. Samples from River Terrig have the highest Si/Al ratios of the whole sample set, with SiO$_2$ contents up to 83 % (Appendix B). From a geomechanical and petrophysical perspective, it is important to understand whether the quartz is detrital or diagenetic, since the recrystallization of biogenic silica to quartz can lithify and strengthen the mudstone, with important consequences from the formation of hydraulic fractures (Jarvie et al., 2007). SEM evidence suggests that much of the quartz is detrital rather than diagenetic, with silt-grade and sometimes sand-grade quartz grains associated with a clay matrix

(Figure 12F). Figure 11 shows that eight samples from River Terrig are enriched in SiO_2 relative to Zr and are likely to contain some biogenically sourced quartz, samples from other areas only have quartz from detrital sources. The poor sorting of some samples from River Terrig suggests that they may have been deposited from mass wasting processes; in addition, some samples contain substantial carbonate which, based on its similar grain size to quartz, may have a detrital origin supplied from erosion of the underlying Clwyd Limestone.
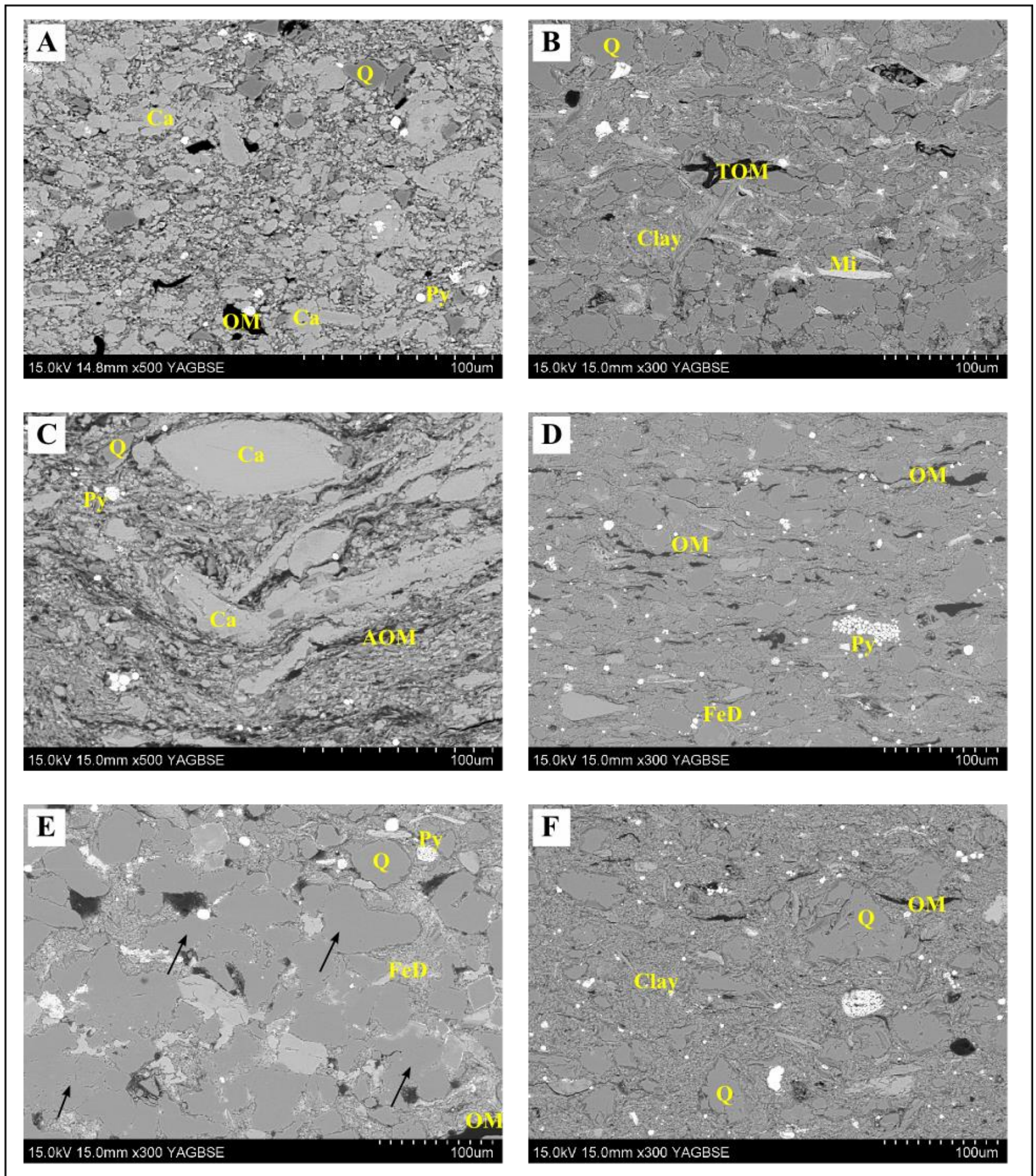
Figure 4-12: Backscatter electron microscope images of the Holywell Shale. Q = quartz, Ca = carbonate, Py = pyrite, OM = organic matter, AOM = amorphous, TOM = terrestrial, Mi = mica, FeD = ferroan dolomite. A (sample RTS6H1; Arnsbergian; location Easting: 323365, Northing: 356900): sample rich in detrital carbonate grains; B (sample PYMS1H5; Yeadonian; location Easting: 319450, Northing: 376700): sample with large detrital quartz grains; C (sample WDS1H4; Yeadonian; location Easting: 331800, Northing: 362340): carbonate grains occurring with large amounts of AOM; D (sample CVS2H1; Arnsbergian; location Easting: 326050, Northing: 356880): laminar organic matter with abundant silt sized quartz; E (sample CVS3H2; Arnsbergian; location Easting: 326050, Northing: 356880): black arrows denote possible diagenetic quartz (possibly from remineralisation of biogenic silica), with some other diagenetic minerals such as ferroan dolomite; F (sample RTS5H1; Arnsbergian; location Easting: 323365, Northing: 356900): large (sand/silt sized) detrital grains of quartz within a fine clay matrix.

Trace element data are shown in Appendix C. Particular focus is on trace elements which give insights to redox conditions at the sediment-water interface or the occurrence of sulphidic bottom- or pore-waters. In general, abundances of elements such as uranium, vanadium and zinc, are similar to those seen in average shale and generate no support for oxygen-depleted bottom waters (e.g. Jones and Manning, 1994). In detail, higher uranium concentrations and U/Th ratios in samples from Warren Dingle and some from River Terrig occur are typically higher in TOC and $CaCO_3$ than other samples, implying that these may be periods or areas where primary productivity was higher and/or where bottom water oxygen concentrations may have been reduced from fully saturated conditions.

4.5: Discussion

4.5.1: Depositional System

The combination of organic geochemical, inorganic geochemical and petrographic data indicate that controls on (a) organic matter quantity and quality and (b) lithology in the Holywell are complex and vary substantially on a wide range of spatial and temporal scales. Shale reservoir quality, which is largely controlled by these parameters, is thus highly variable and inherently difficult to predict at possible exploration sites.

Generally, and throughout the whole period of Holywell Shale deposition, a mixture of terrestrial and marine organic matter was supplied to a range of marine depositional environments in which there was sufficient hydrodynamic energy to transport fine-grained sediment as bed load. The resulting mudstones exhibit a range of sedimentary textures with millimetre- to centimetre-scale silt-clay bed forms but which show almost no relationship between texture and organic matter type or amount. Trace element data,

high C/N ratios and low HI values all indicate oxygenated bottom waters which allowed substantial degradation of organic matter at or close to the seabed, resulting in the poor preservation of organic matter and relatively low petroleum potentials. The combination of the early diagenetic destruction of organic matter plus its dual supply from both terrestrial and marine sources has resulted in weak relationships between the quantity and quality of preserved organic matter, and also between lithology and the organic matter amount and type. Similar observations were made by Davies et al. (2012) in a Marsdenian mud-rich sequence approximately 150 kilometres further north, albeit in an area more dominated by a terrestrial organic matter source.

Within this general framework, there are important details in the data. Organic matter in the lowermost (E2a age; *Eumorphoceras bisulcatum*) Holywell Shale, at Cegidog Valley, is dominantly marine. Based on its relatively low C/N ratio and relatively high HI, the organic matter is moderately well preserved. Abundances of silica and phosphate are higher than those in samples from other localities, and there is petrographic evidence for recrystallized biogenic silica (Figure 4-12E) and SiO_2/Zr ratios are slightly elevated compared with samples with purely detrital quartz. These characteristics suggest that primary productivity may have been elevated in this area at this time, but that relatively little organic matter (average 2.2 wt %) was preserved due to the oxygenated bottom waters indicated by, for example, low sedimentary uranium contents, low U/Th, V/Cr, and Ni/Co ratios (averages 0.25, 0.67, 0.37 respectively; Appendix C; Fisher & Wignall, 2001). In contrast, organic matter in Armstrong et al.'s (1997) study of E2a age samples from the Hope Mountain area 3 km east of Cegidog Valley has δ^{13}C values of -25.5 ‰, indicating a predominantly terrestrial source. Such a large isotopic difference over such a small distance suggests that supplies of organic matter were highly variable and resulted in quite different organofacies.

There is similar evidence (fossiliferous calcite; phosphate) for elevated primary productivity from the lower part of the sample set from River Terrig. Nevertheless, organic matter in the two most calcite-rich samples is only 40 % marine, implying a significant supply of terrestrial organic matter. Preservation of organic matter, based on very high C/N ratios and HI values of around 100-150, is poor. It indicates substantial destruction close to the sediment-water interface.

Elevated values of primary productivity are common where upwelling occurs on continental margins. Whilst this cannot be proven with these data, it is noted that the study area was situated at the southwest edge of the Pennine Basin. Furthermore, it is notable that some of the quartz in River Terrig samples comprises sand-size grains which float in a clay matrix (Figure 4-12F) which could be interpreted as deposition from downslope depositional processes such as mass wasting. These observations are consistent with other interpretations, including the lateral transport of clay-sand flocs as bedload on continental shelves (Schieber et al., 2007; 2010; Davies et al., 2012).

Organic matter in the upper Holywell shale is predominantly terrestrial but with a marine contribution up to 40 % (assuming that terrestrial and marine organic matter have δ13C = -22.5 ‰ and -31 ‰ respectively, 40% is the greatest potential marine contribution from carbon isotope values of -25.9 ‰). The more clay-rich samples, for example at Warren Dingle, are enriched in organic matter (2.2 – 10.8 wt %) and also have the greatest contribution of marine organic matter. The most organic-rich sample also contains fossiliferous carbonate and phosphate, suggesting a period of higher biological productivity; nevertheless, the high C/N ratio and low HI indicates an oxygenated depositional environment which was not conducive to the preservation of hydrogen-rich organic matter. Given their similar hydrodynamic properties, it can be

inferred that the coincidence of relatively elevated clay mineral and organic matter contents relate to hydrodynamic sorting, perhaps related to bedload transport across continental shelves (e.g. Tyson & Follows, 2000).

The silt-rich samples from Pen-y-Maes have less than 0.5 wt % TOC which is isotopically heavy and comprises angular, terrestrially sourced organic matter fragments. This facies is very similar to the Marsdenian silt-bearing, clay-rich mudstones with graded beds described by Davies et al. (2012). This litho/organofacies, deposited at the very end of the Namurian, represents a more proximal facies deposited at a time when major deltas were prograding from the north, ultimately depositing the Gwespyr sandstones in the Yeadonian and early Westphalian.

4.5.2: Reservoir Quality

The Holywell Shale was deposited in a relatively shallow water environment into which organic matter was supplied from both terrestrial and marine sources and in which the transport of fine-grained sediment was a dominant process. These complex, coupled processes resulted in a sediment system which is heterogeneous, in terms of both lithofacies and organofacies, on many spatial scales. There are no simple rules to describe relationships between lithofacies, mineralogy and organic matter amount and type. Equally, since shale reservoir quality relates to both gas storage (TOC, porosity) and gas delivery (mineralogy and induced fracture characteristics, permeability), there are no simple rules with which to predict reservoir quality variation laterally and stratigraphically. These rocks are dominantly clastic and are mixtures of silt-grade and clay-grade particles. Silt-rich units have high matrix permeabilities and will contribute to gas delivery, whereas clay-rich units have much lower permeabilities (Dewhurst et al., 1998; Yang and Aplin, 2007; 2010); silt-clay interbeds are highly anisotropic with

respect to permeability (Armitage et al., 2011). Units of all these types occur in each part of the Holywell Shale, on many spatial scales. Connecting the silt-rich parts of the system should enhance the large-scale permeability of the reservoir.

In terms of mineralogy and the way in which mudstones respond to hydraulic fracturing practices, recrystallized biogenic calcite and silica are often considered to embrittle fine-grained sediments and thus to enhance reservoir quality. Whilst calcite occurs in some of the Holywell Shale, abundances are typically less than 10%. Silica concentrations are very variable but reach up to 82% in some samples from the Lower Holywell Shale. However, it is unclear how much of the silica has a biogenic source. Our petrographic observations suggest that most silica is macroscopic and detrital, although a contribution from biogenic silica is certainly possible.

Hydrocarbons in shales are generally considered to be stored both as free oil/gas within the pore system and as adsorbed oil/gas associated with organic matter (e.g. Montgomery et al., 2005; Gasparik et al., 2012; Rexer et al., 2013). Organic matter contents in the Holywell Shale only average 1.9 wt % and only a small portion of the formation has TOC contents above 3 wt %. Silt-rich units represent the best reservoir quality in terms of permeability but are often depleted in organic matter. The prospectivity of silt-rich units is thus dependent on migration, trapping and sealing, as for a conventional play. In this context the Holywell Shale might be considered as a hybrid play (Jarvie, 2011). Whilst the Holywell Shale is immature to early oil mature, age equivalent units within the UK range from immature to mature for gas generation due to the complex tectonic, depositional and burial history of the Carboniferous Pennine Basin (Andrews, 2013; Gross et al., 2015; Słowakiewicz et al., 2015).

4.6: Conclusions

The Holywell Shale represents a mudstone succession with highly variable organofacies and lithofacies which was deposited along the south western edge of the Pennine Basin during the Namurian (Carboniferous). The continued progradation of the Namurian delta systems, combined with a reduced thermal subsidence rate, led to a reduction in accommodation space and an increase in the importance of terrestrially derived minerals and organic matter.

Organic and inorganic geochemical data, along with petrographic observations, demonstrate the highly variable supply and preservation of organic matter and lithology in the Holywell Shale. The general trend is a reduction in the amount of marine sourced organic matter from the Lower to Upper Holywell Shale, but with large spatial variations in organic matter supply at a given time. There is no relationship between amount of organic matter and its source.

The combination of mixed organic matter sources, poor preservation conditions along with early diagenetic destruction of organic matter mean that there are only weak relationships between organic matter quality and quantity. There are also only weak links between organic matter quantity, type and lithology. Trace element data, combined with low HI and high C/N ratios indicate oxygenated bottom waters which resulted in poorly preserved organic matter, despite an average TOC content of 1.9 wt %. Type II/III kerogens dominate the Lower Holywell Shale with Type III/IV in the Upper Holywell Shale. The greatest petroleum potential is found within the Lower Holywell Shale interval during periods or areas of higher primary productivity and reduced bottom water oxygen levels. The complexity of the sedimentary system in both space and time means that shale reservoir quality is inherently difficult to predict.

Chapter 5:

Lithological and geochemical variations across ammonoid biozones of the late Namurian (Marsdenian to Yeadonian) Holywell Shale, Wales: implications for shale reservoir quality

5.1: Abstract

The Carboniferous Bowland Shale Formation of northwest England has been identified as one of the largest potential shale gas targets in the UK. The Holywell Shale, part of the Bowland Shale Formation, represents a succession of marine, brackish and non-marine mudstones at the southwest edge of the Pennine Basin. Core and cuttings from 4 British Geological Survey (BGS) held boreholes (Blacon East; Erbistock; Milton Green; Point of Ayr No.3 shaft) were used in the study to assess the shale gas/oil potential of late-Carboniferous (Namurian) Holywell Shale using a multidisciplinary approach relating organic and inorganic geochemistry, and petrographic imaging of micro-scale fabrics.

The Holywell Shale, from the boreholes studied, has total organic carbon (TOC) contents ranging from 0.5 to 8.6 wt % (average 2.0 wt %). RockEval$^{™}$ data show that the organic matter is composed of Type III or Type II/III kerogen with T_{max} values of 430 to 451 °C indicating oil window maturity. Carbon isotope values range from -26.3 to -23 ‰ suggesting that the organic matter is from terrestrial and marine sources. The Point of Ayr samples in the northwest of the region have the highest shale gas potential due to their high TOC and S_2 values but are limited by relatively low hydrogen index (< 224 mg/g). The highest TOC values (> 2.6 wt %) in the Point of Ayr borehole samples occurred within the marine band facies correlate well with more negative carbon isotope values (e.g. -25 ‰; more marine sourced organic matter) and low Si/Al and Zr concentrations indicating higher clay content. Whereas samples not taken from marine bands were typically silt-rich with graded bedding, had the lowest TOC values (< 0.7 wt %) significantly less negative carbon isotope values (e.g. -23 ‰) and higher Si/Al and Zr concentration indicating terrestrially derived minerals and organic matter.

5.2: Introduction

The Carboniferous basins of northern England are considered to be the main targets for unconventional shale gas exploration within the UK with several recent studies into their viability as shale gas targets e.g. Andrews (2013), Gross et al. (2015), Könitzer et al. (2014a, b), Newport et al. (2016), Słowakiewicz et al. (2015). The Bowland Shale Formation (northern England) deposited within these basins is thought to represent a total estimated resource of 1329 trillion cubic feet (Tcf) gas initially in place (Andrews, 2013).

The Holywell Shale, part of the Bowland Shale Formation, is a named rock unit by the British Geological Survey (BGS). However, the Holywell Shale was not included in the Bowland-Hodder Shale gas report of Andrews (2013). For the purposes of this paper, and to avoid confusion, the Bowland Shale where it occurs in the Namurian (326.4 – 314.5 Ma) section of the boreholes sampled in this study is referred to as the Holywell Shale.

Section 2.6 of this thesis describes the stratigraphy of the northeast Wales region in detail. It can be briefly summarised here: across the region, the Pendleian units which succeed the Dinantian Clwyd Limestone Group of shallow marine to ramp carbonates varies, with the Pentre Chert and Cefn-Y-Fedw Sandstone laterally interfingering each other. The Holywell Shale, in places, lies conformably on top of the limestones and Pentre Chert. Elsewhere, the Holywell Shale laterally interfingers with the Cefn-Y-Fedw Sandstones (Pendleian to Marsdenian, 326.4 to ~ 315.5 Ma). The Holywell Shale is succeeded by the Gwespyr Sandstone (Yeadonian; Figure 5-1; Davies et al., 2004; Waters et al., 2009) which represents the arrival of the northerly sourced Millstone Grit Group deltas. The Gwespyr Sandstone is feldspathic; it commonly contains

carbonaceous flakes, micas, plant fragments and is often significantly bioturbated. The type section for the Holywell Shale a total thickness of 152 m is recorded within the combined Abbey Mills number 1 and 4 boreholes (unavailable for sampling in this study; Davies et al., 2004).
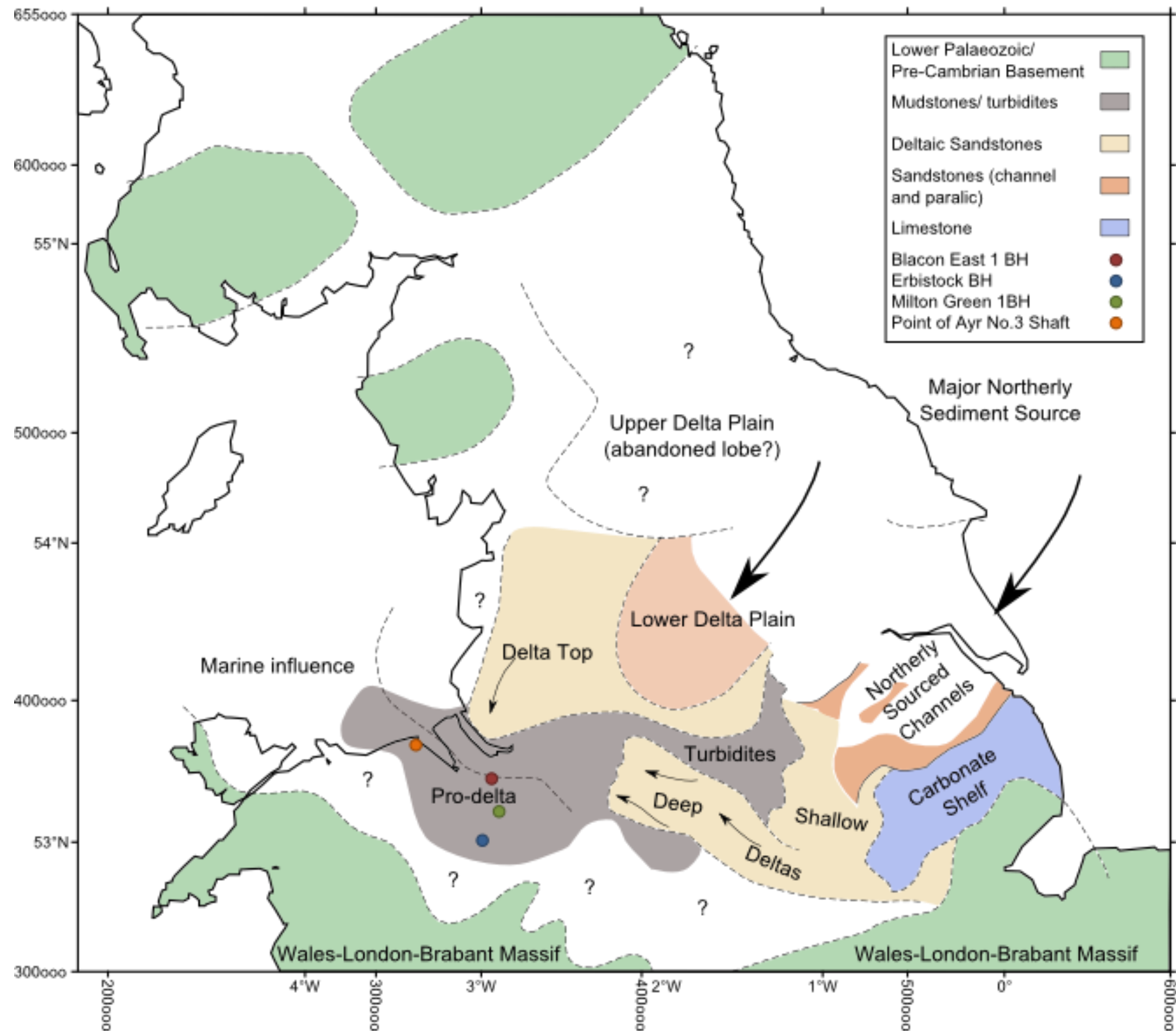
Figure 5-1: Simplified palaeo-facies map for the Marsdenian (LC1c; adapted from Fraser & Gawthorpe, 2003). Includes locations of each borehole: Point of Ayr = orange, Blacon East = red, Milton Green = green, Erbistock = blue.

The variation in deposition between shale and sandstone was delta driven and corresponds with eustatic changes in sea level (Ramsbottom, 1977). The Holywell Shale has faunal sequences representing the transition from paralic to full marine conditions: fish – *Planolites* – *Lingula* brachiopods – bivalves – ammonoids (Holdsworth & Collinson, 1988). Within this faunal sequence, thick shelled goniatite ammonoid species represent periods of widespread marine transgression (Davies et al., 2004; Gross et al., 2015). The occurrence of goniatite fossils within the UK Carboniferous basins is expansive and allows stratigraphical correlation (Davies et al., 2004).

The boreholes chosen for this study on the Holywell Shale are the Point of Ayr No.3 colliery shaft, Blacon East, Milton Green and Erbistock boreholes (Figure 5-1). Both the Point of Ayr and Blacon East boreholes contain identified marine bands of Marsdenian to Yeadonian regional substages (~ 317 – 314.5 Ma) within the Holywell Shale. These marine bands correlate with the LC1c seismic sequence stratigraphy unit of Fraser & Gawthorpe (1990; 2003). Other than these marine bands (which are not presently identified in Milton Green borehole, and only the *Gastrioceras subcrenatum* and uncertain *Cancelloceras cancellatum* (G1a) marine bands are identified in the Erbistock borehole; Penn, 1987) correlation between the boreholes is difficult (Figures 5-1, 5-2 & 5-3).

This paper aims to combine previously identified biostratigraphic markers (marine bands) (wireline and wellbore logs; Davies et al. 2004; Magraw, 1954; Penn, 1987; Waters, et al. 2009) and evaluate the stratigraphical (and where possible spatial) changes in lithofacies organic geochemistry: TOC, RockEval™ and carbon isotopes; and inorganic geochemistry: X-ray fluorescence across the Holywell Shale. These

techniques will also allow the potential for shale gas or oil generation within the

Holywell Shale to be examined.
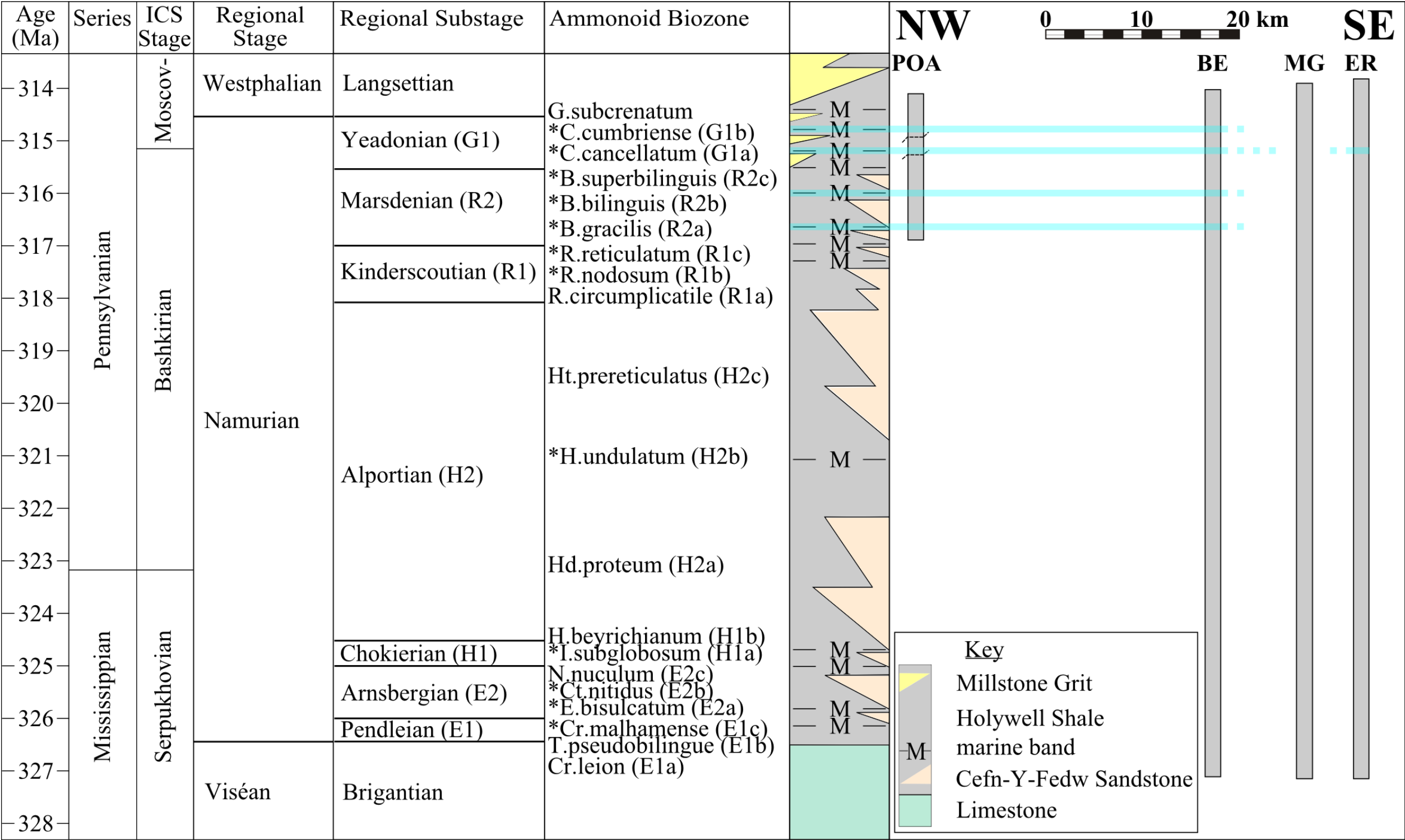
Figure 5-2: Namurian chronostratigraphy and ammonoid biozones (UK), the samples with * indicate marine bands that are identified within the northeast Wales region (Andrews, 2013). A simplified stratigraphical representation highlights the marine bands and lithologies present within the boreholes sampled: POA = Point of Ayr, BE = Blacon East, MG = Milton Green, ER = Erbistock (although no marine bands have been identified in the Milton Green borehole). Note: vertical scale is time (Ma); horizontal scale, equivalent to the distance (km) that boreholes are separated.
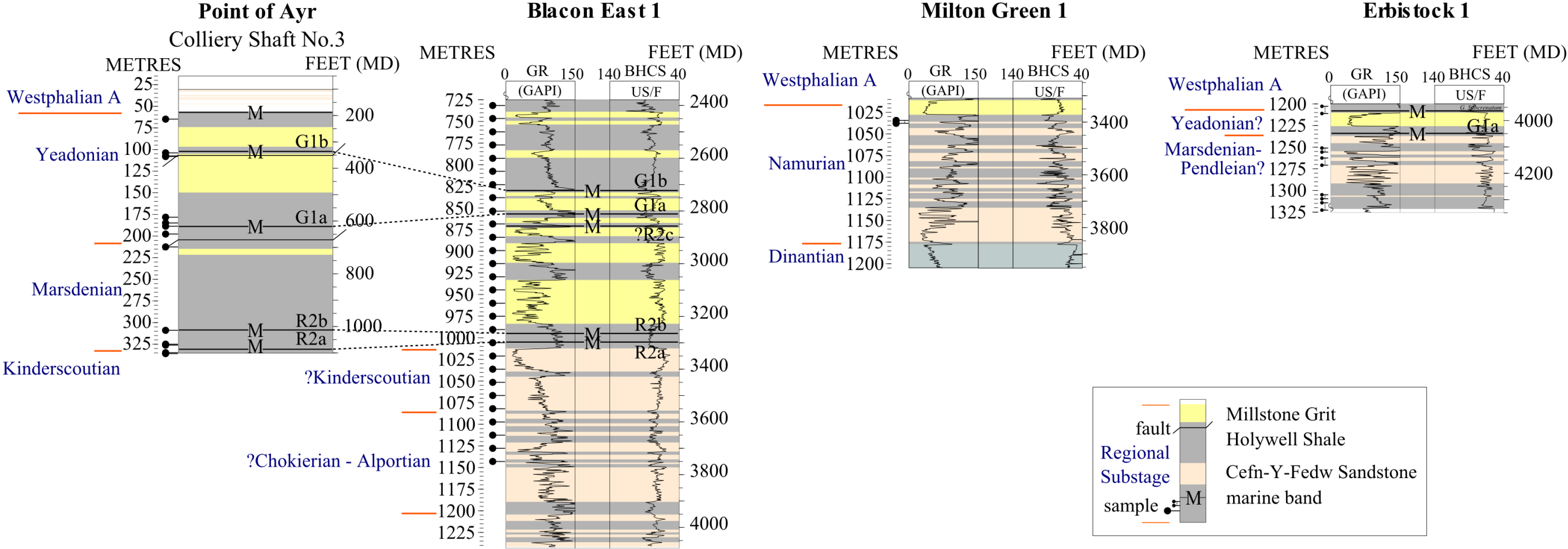
Figure 5-3: Log representation of all the boreholes used in this study across northeast Wales (Point of Ayr, Blacon East, Milton Green and Erbistock). Where possible, identified marine bands are labelled and correlated between Point of Ayr and Blacon East (dotted lines).

5.3: Methods

Detailed methods for the analyses used within this chapter can be found in Chapter 3 of this thesis.

5.3.1: Sample Collection and Analysis

For each borehole (Figure 5-1), samples were powdered using an agate ball mill. Core samples were taken from the Point of Ayr borehole and used for thin section preparation; all other borehole samples were cuttings which were unsuitable for petrographic analysis (Figure 5-3).

5.4: Results

5.4.1: Point of Ayr lithofacies

Due to the availability of material, it was only possible to make thin sections from Point of Ayr samples. The lithofacies present within the Point of Ayr No.3 Colliery shaft vary stratigraphically. There are two main lithofacies present within the Point of Ayr samples: clay-rich mudstone, and silt-rich mudstone; although these can be further subdivided by distinguishing features such as fossil content, fabric and textural variation.

Figure 5-4: Point of Ayr No.3 shaft depths of samples, marine bands, regional substages and faults. Images represent different facies and microfacies (transmitted light and SEM microscopy) of samples from the Point of Ayr No.3 shaft (depths indicated on each image refer to sampling depth (black round-headed pegs denote where a sample was taken). Vertical tapering arrows (in 65.53 m transmitted light image) refer to fining upwards grading; inclined arrows indicate coarse lenses; M = microfossils; OM = organic matter; Q = quartz; Mi = mica; Py = pyrite (predominantly occurring as framboids); Fe = iron oxide; Fs = feldspar; Ca = calcite (also occurs as Mg-rich calcite/dolomite). The Point of Ayr shaft samples continue in fig 5-5 below.
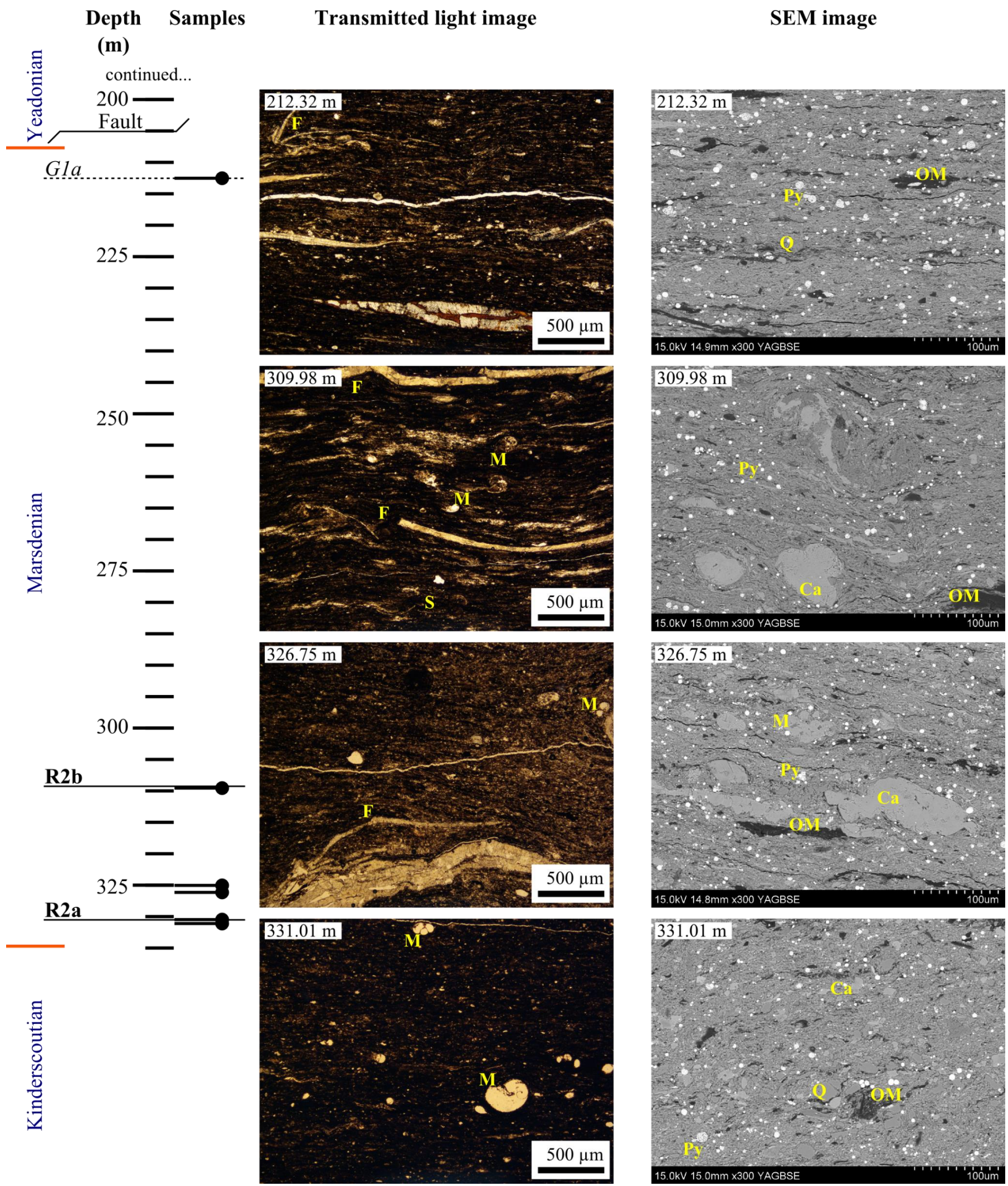
Figure 5-5: continued from fig 5-4. Point of Ayr No.3 shaft depths of samples, marine bands, regional substages and faults. Images represent different facies and microfacies (transmitted light and SEM microscopy) of samples from the Point of Ayr No.3 shaft (depths indicated on each image refer to sampling depth (black round-headed pegs denote where a sample was taken). Vertical tapering arrows (in 65.53 m transmitted light image) refer to fining upwards grading; inclined arrows indicate coarse lenses; M = microfossils; F = fossil fragments; S = shelly material; OM = organic matter; Q = quartz; Mi = mica; Py = pyrite (predominantly occurring as framboids); Fe = iron oxide; Fs = feldspar; Ca = calcite (also occurs as Mg-rich calcite/dolomite).

Samples which occur at marine bands tend to be clay-rich and fossiliferous, often containing shelly material or abundant ammonoid microfossils (described as spat by Holdsworth & Collinson, 1988; referred to by Könitzer et al., 2014a, b for the Carsington C4 borehole or Gross et al., 2015 for the Duffield borehole in the Widmerpool Gulf). These spat seem to occur simultaneously with goniatite fossils (identified within the Point of Ayr No.3 colliery shaft by Magraw, 1954), as the marine band samples within this study from the Point of Ayr were taken from reference materials which contain goniatite (ammonoid) fossils (< 30 mm).

Samples taken from mudstones which did not contain goniatites are quartz-rich, micaceous, often with graded bedding, and in some cases rich in silt-sized grains. The sample at 65.53 m reportedly contains non-marine shells (Magraw, 1954) and is micaceous (supported by the SEM image for this sample in Fig 5-4), occurring within a series of mudstones to siltstones and sandy-mudstones which are succeeded by the *Gastrioceras subcrenatum* marine band. The sample at 178.31 m reportedly contains small fragmentary mussels within silty-mudstone. This silty mudstone described by Magraw (1954) is present above the G1a (*Cancelloceras Cancellatum*) marine band for ~ 40 m and is often micaceous and containing some plant fragments.

The organic matter present within marine band and non-marine band facies within the Point of Ayr samples vary. SEM observations of organic matter occurring at the marine bands show largely amorphous organic matter which aligns with clay minerals along bedding (distorting around larger grains), with some indistinct fragments of organic matter (Figures 5-4, 5-5 & 5-6). Whereas the facies which do not occur at a marine band, have more dispersed and fragmentary organic matter with significantly less organic matter present than the marine band samples (Figures 5-4, 5-5 & 5-6).
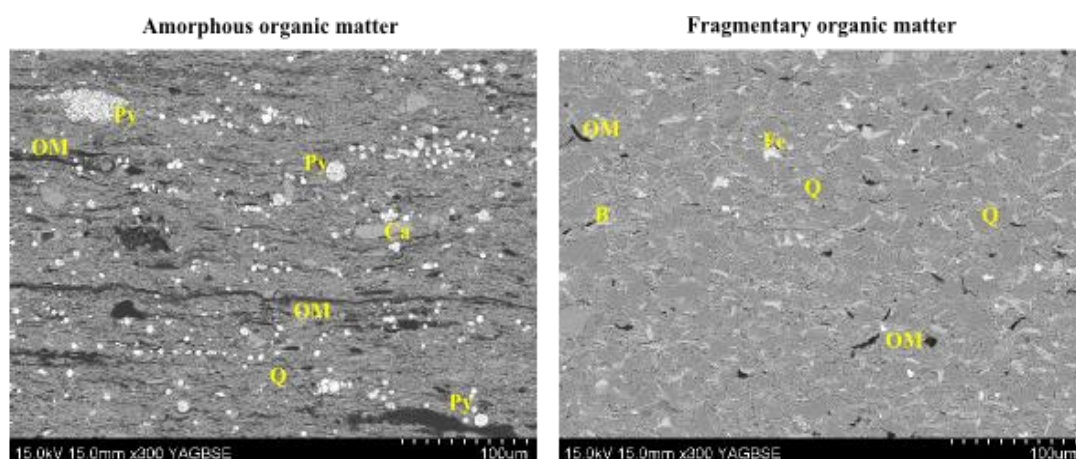
Figure 5-6: Two samples from the Point of Ayr borehole demonstrating the difference in organic matter (OM). Amorphous organic matter (left image: POA 7, 188.98 m depth) aligning along bedding in samples, quartz (Q), clay-rich, with calcite (Ca) fossiliferous and an abundance of pyrite framboids (Py). Fragmentary organic matter (right image: POA 6, 185.01 m depth) in silt-rich facies with terrestrially derived minerals such as biotite mica (B) and iron oxide (Fe).

There is repetition in facies throughout the Point of Ayr samples, with the same or very similar facies (clay-rich, fossiliferous) occurring in multiple marine bands. As well as this, the non-marine facies (quartz & mica-rich, siltstones and mudstones) repeat, commonly occurring in periods between marine bands. Across the zone where a marine band occurs, there can be variations in the fauna found; for example, at the G1b marine band, fish debris and planolites ichnofacies occur (Magraw, 1954). Elsewhere, plant debris and shelly material can occur stratigraphically close to marine bands (e.g. R2b, R2a; Magraw, 1954).

5.4.1: Organic Geochemistry

The TOC content of all samples ranges from 0.5 wt % to 8.6 wt % (average 2.0 wt %), with the Point of Ayr borehole containing both the highest and the lowest TOC samples recorded (Appendix E; Figure 5-4).

Carbon isotopes and RockEval™ data can be used to determine the provenance of organic matter. The carbon isotope signature allow differentiation between terrestrial and marine sources with terrestrial organic matter having carbon isotope signatures in the Carboniferous of -24 ‰ to -22 ‰ whereas marine organic matter carbon isotope signatures range from -35 ‰ to -30 ‰ (Lewan, 1986; Peters-Kottig et al., 2006; Stephenson et al., 2008). Within the four boreholes sampled, the carbon isotope values for the Holywell Shale range from -26.3 ‰ to -23.0 ‰ (Appendix E; Figure 5-4).

There is a weak positive correlation between lighter carbon isotope values (-26.3 ‰ to -23.8 ‰) and higher TOC values (0.8 to 1.7 wt %) in the Milton Green borehole. The Point of Ayr borehole shows a clear correlation between high TOC values (average 4.41 wt %) and the occurrence of lighter (more marine) carbon isotope signatures (ie. marine bands present). The Blacon East and Erbistock boreholes both have carbon isotopes in the range -26.3 ‰ to -23.2 ‰ and exhibit no significant correlation overall between identified marine bands, lighter carbon isotope values and high TOC values (Figure 5-4). The only minor exception to this is the R2a and R2b marine bands within the Blacon East borehole, which do show slightly lighter isotope values (-25.9 ‰ to -24.9 ‰) and the R2a marine band has the highest TOC value (2.5 wt %) for the Blacon East borehole (Figure 5-4). Samples not from marine bands have heavier carbon isotope values (average -24.4 ‰) and lower TOC values (average 0.9 wt %) with the majority of the organic matter being terrestrial in origin.

Within the Point of Ayr No.3 colliery shaft it was possible to separate the organic geochemical data stratigraphically by the marine bands present. A change can be observed in TOC across the marine bands sampled, with the G1a marine band exhibiting the highest TOC values and most negative carbon isotope signature (Figure 5-7). The marine band facies including the non-goniatite lingula brachiopod marine

sample (-24.5 ‰; 197.81 m depth) exhibited high TOC values (> 2.6 wt %) and more negative carbon isotope values. Whereas the samples which were not from marine bands had less negative carbon isotope signatures and significantly lower TOC values (< 0.7 wt %; Figure 5-7).
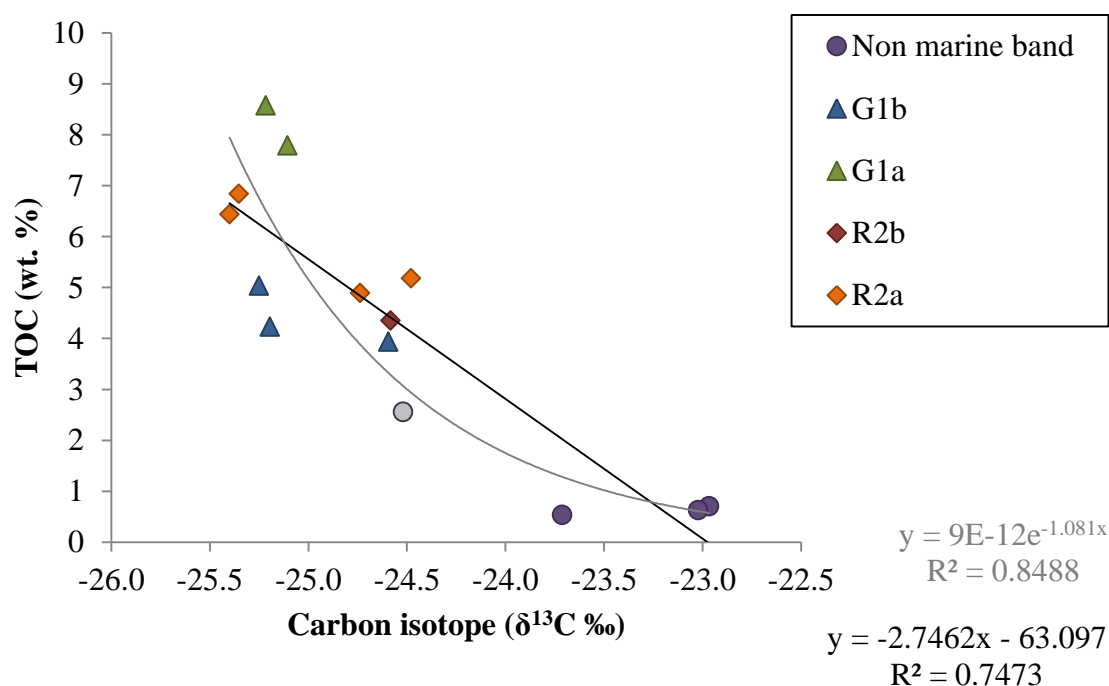
Figure 5-7: Point of Ayr No.3 shaft showing changes in TOC and carbon isotope signature with different marine bands recorded and non-marine band facies. The non-marine band sample (pale purple colour) at -24.5 ‰ is labelled non-marine as goniatite ammonoid fauna are absent; however, this sample contains lingula brachiopod marine fauna. There is a strong positive correlation between more negative carbon isotopes and higher TOC values (n = 14).

Most samples, especially those from Blacon East, Erbistock and Milton Green, have low S_2 values (< 2.5 mg HC/g rock) and will not generate substantial hydrocarbons (Figure 5-8). They are largely composed of a mixture of Type III and Type IV kerogens (Figure 5-10), which combined with low HI (23 to 155) and variable but often high OI (2.3 and 146) suggest limited marine organic matter input (average -24.6 ‰) with highly degraded marine organic matter where present and deposition in an oxygenated water column (Figure 5-10). Conversely, the Point of Ayr borehole and two Erbistock

samples from around the G1a marine band (~315.5 Ma) show much higher TOC (3.4 < 8.6 wt %) and S_2 values (5 < 19.2mg HC/g rock), suggesting a very good potential for hydrocarbon generation (Figure 5-8). Figure 5-9, T_{max} plotted against HI, shows that samples are composed from Type II/III to Type IV kerogens, but primarily of Type III gas-prone kerogens. However, all samples from Blacon East, Erbistock and Milton Green are oil window mature with some POA samples immature (Figure 5-9). The immature Point of Ayr samples correspond with the non-marine band quartz & mica-rich siltstone facies (Figure 5-4).
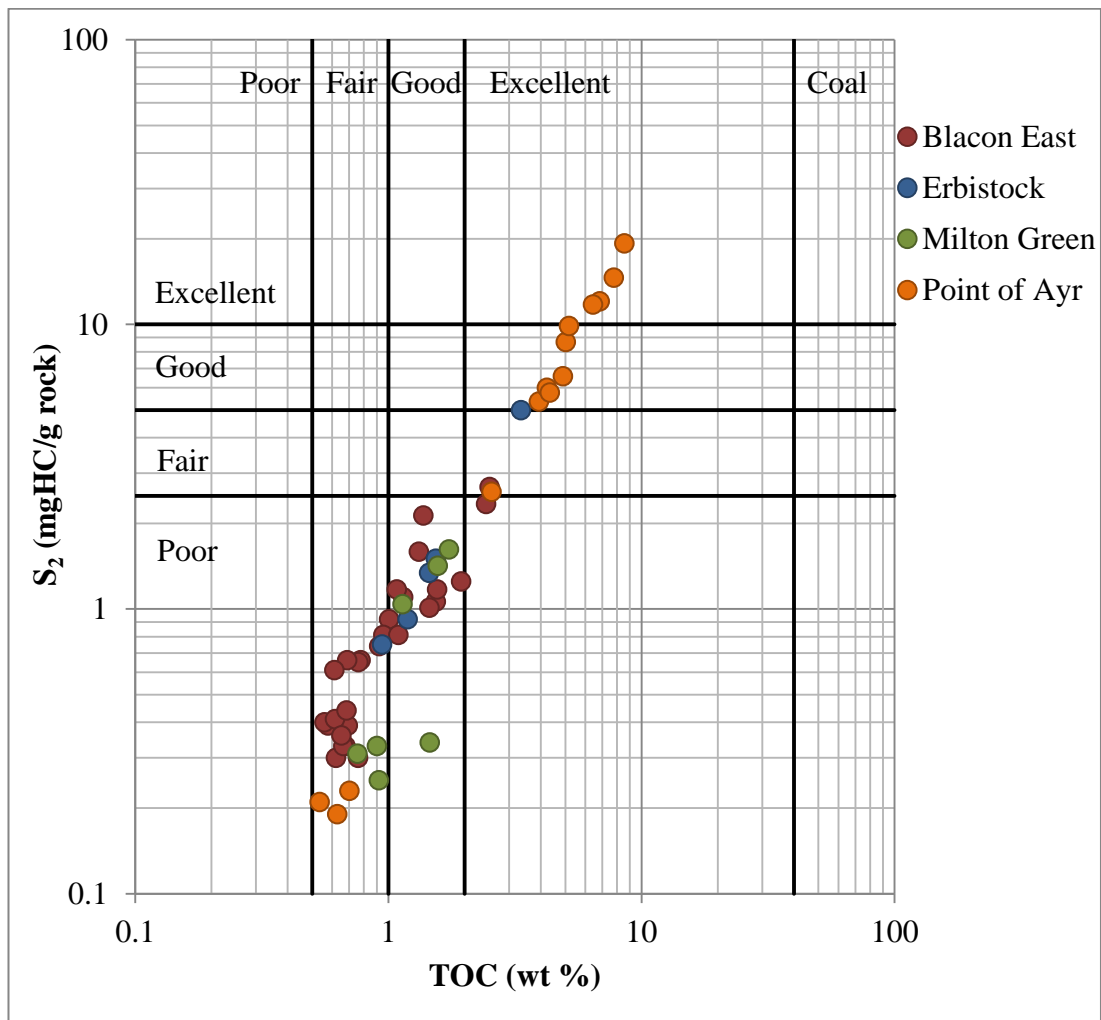
Figure 5-8: TOC vs. S_2 (hydrocarbons formed from thermal decomposition of kerogen; from RockEval™). The higher the S_2 values the greater the potential for hydrocarbon generation.

Chapter 5
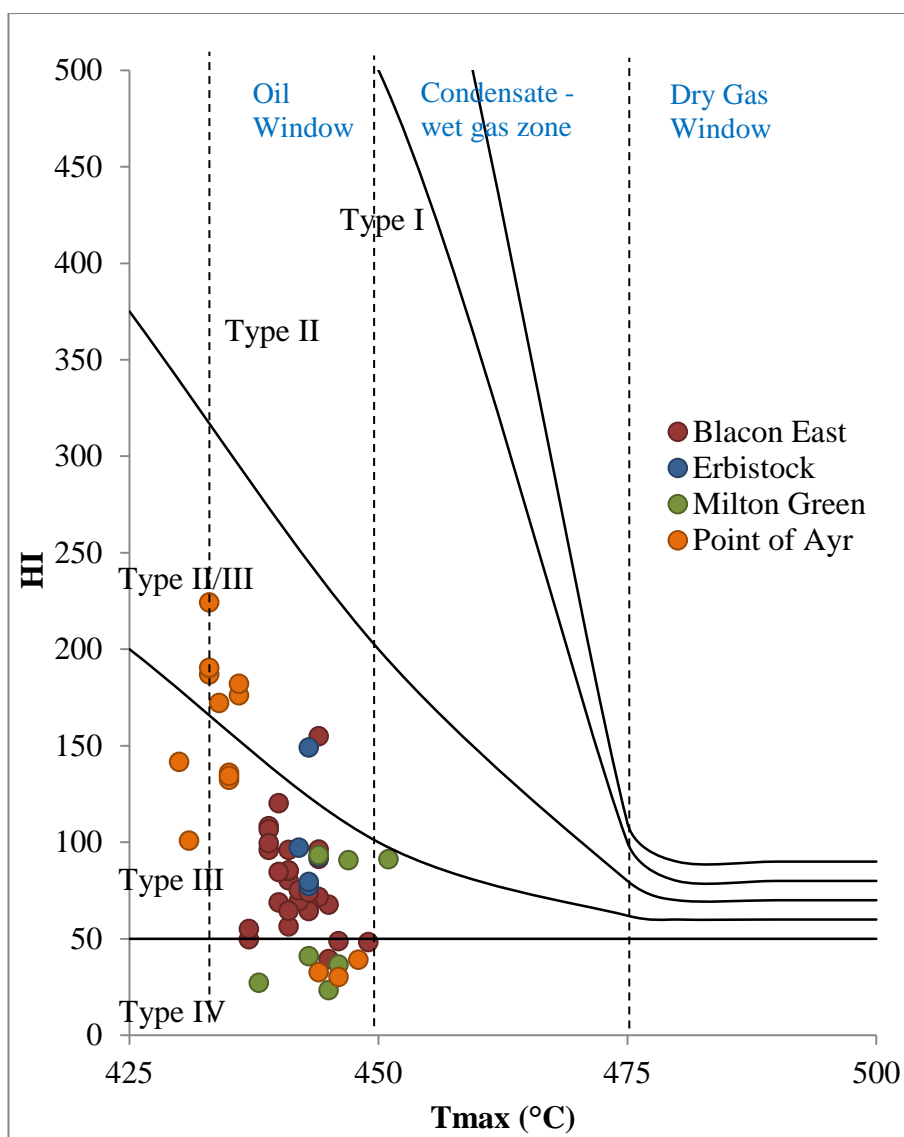
Figure 5-9: T_{max} vs hydrogen index (HI) data showing the kerogen type and range of thermal maturity within the Holywell Shale samples.

Hydrogen index (HI) and oxygen index (OI) are plotted as a modified van Krevelen diagram, with the addition of TOC to distinguish organic matter quantity and preservation (Figure 5-10; Tissot & Welte, 1984). There is a correlation between higher TOC and high HI values; increasing OI correlates with lower TOC (Figure 5-10). The HI of Milton Green and Erbistock samples is low, suggesting that organic matter preservation was poor. Point of Ayr has the highest and lowest HI values. The Point of Ayr samples with the lowest HI values correspond to the quartz & mica-rich siltstone facies (Figure 5-4).
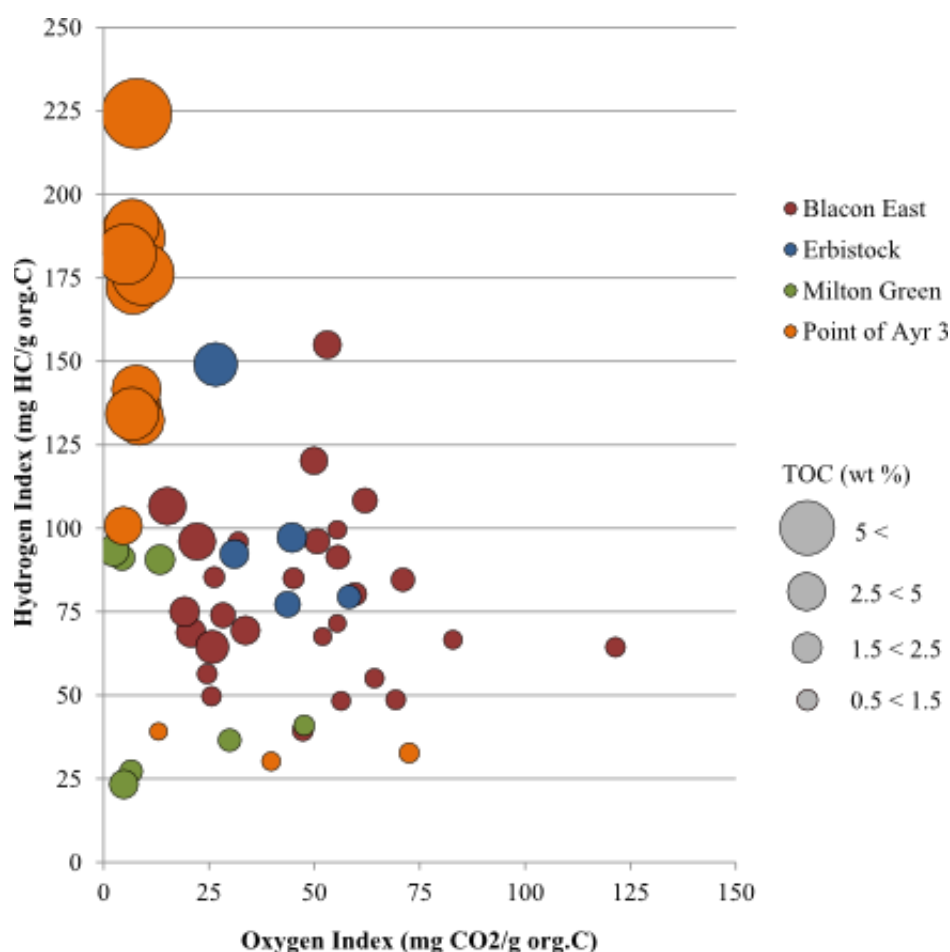
Figure 5-10: Modified Van Krevelen diagram (after Tissot & Welte, 1984). Colour denotes borehole; size of circle relates to TOC of the sample.

5.4.2: Lithology, Mineralogy and Inorganic Geochemistry

The amount of carbonate (calcite and dolomite) present in each borehole is relatively low (0.1 to 7.8 % CaO; 1.4 to 3.1 % MgO, although some MgO will occur in other minerals such as clays). Higher concentrations of CaO (calcite) suggest a more marine depositional environment. In samples from Point of Ayr borehole high CaO values (average 5 %) correlate with higher TOC values (average 5.7 wt %) and lighter carbon isotope values (average -25 ‰). However, the other three boreholes show no apparent correlation between the concentration of carbonate, TOC values and carbon isotope values.

There is almost no correlation (n = 50; R^2 correlation coefficient = 0.13) between TOC values and the Si/Al content of the Holywell Shale. High Si/Al ratio indicates that a higher percentage of silica exists as quartz, and conversely low Si/Al ratio indicates that a higher percentage of silica exists in clay minerals. The highest TOC values and lighter carbon isotope values from all boreholes only occur in the most clay-rich units, which have the lowest Si/Al concentrations (< 4.5).

U/Th, V/Cr, and Ni/Co ratios all imply that the Holywell Shale was not deposited in oxygen-depleted waters in the Blacon East, Erbistock and Milton Green boreholes, as well as the upper section in the Point of Ayr borehole (Appendices F & G; e.g. Jones & Manning, 1994). The exception are samples from the Point of Ayr, particularly the G1a, R2b and R2a marine bands, which have higher U/Th ratios suggesting a dysoxic environment of deposition with possible periods of anoxia (e.g. Jones & Manning, 1994). At Point of Ayr, higher TOC contents generally occur in samples with higher U/Th ratios. There is no significant correlation between the amount of CaO (calcite) present in the sample (and therefore more marine influenced depositional environment) and elevated U/Th ratios (degree of dysoxia). TOC/S could be used to give indications of anoxia and terrestrial/marine sources of organic matter (Gross et al., 2015). The TOC/S ratios for the Holywell Shale samples range from 0.5 to 33.6; values > 2.8 suggest more marine, reduced sulphur concentration (more oxic) and reduced salinity within the depositional environment (Gross et al., 2015). There is no overall statistical correlation between TOC/S values and carbon isotopes within the Holywell Shale.

Table 5-1: Proposed threshold values for palaeo-redox proxies (not to be applied strictly; adapted from Lazar et al., 2015b; Gross et al., 2015)

Bottom-water oxygenation	U/Th	V/Cr	Ni/Co	TOC/S
Anoxic (0 ml O_2/l H_2O)				
Threshold	1.25	4.25	7	(~ 1.5?)
Dysoxic (0 - 2 ml O_2/l H_2O)				
Threshold	0.75	2.00	5	2.8
Oxic (> 2 ml O_2/l H_2O)				

Table 5-2: Palaeo-redox proxy values for samples from the Blacon East borehole.

Depth (m)	Sample code	U/Th	V/Cr	Ni/Co	TOC/S
731.52	BE 3	0.12	1.26	2.78	10.10
746.76	BE 4	0.16	1.16	2.98	8.97
777.24	BE 6	0.17	1.14	2.86	14.06
792.48	BE 7	-	0.69	3.60	6.04
807.72	BE 8	0.14	1.20	2.62	12.28
822.96	BE 9	-	1.33	3.72	26.53
838.20	BE 10	0.14	1.14	2.77	4.20
853.44	BE 11	0.16	1.01	2.45	8.71
868.68	BE 12	0.23	1.11	2.76	3.14
883.92	BE 13	0.21	1.05	2.83	2.41
899.16	BE 14	-	0.72	2.85	1.85
914.40	BE 15	-	0.70	2.93	4.52
929.64	BE 16	0.42	1.80	4.25	2.07
960.12	BE18	0.14	0.79	2.87	0.89
990.60	BE 20	0.16	1.26	2.75	1.20
1005.84	BE 21	0.47	1.22	3.09	1.69
1021.08	BE 22	-	1.00	-	1.49
1036.32	BE 23	0.22	0.59	3.85	1.69
1051.56	BE 24	0.54	1.07	5.45	1.61
1066.80	BE 25	-	0.69	1.00	2.14
1082.04	BE 26	0.20	0.85	3.61	3.52
1097.28	BE 27	0.28	1.23	2.67	1.46
1112.52	BE 28	0.44	1.23	3.58	1.70
1143.00	BE 30	0.45	0.82	2.84	2.96

Table 5-3: Palaeo-redox proxy values for samples from the Erbistock borehole.

Depth (m)	Sample code	U/Th	V/Cr	Ni/Co	TOC/S
1203 < 1212	ER 4	0.13	1.29	2.99	8.23
1251 < 1256	ER 5	0.13	1.00	2.92	3.22
1263 < 1272	ER 6	0.14	0.84	3.57	2.06
1305 < 1311	ER 7	-	0.47	-	0.84
1314 < 1323	ER 8	0.18	0.88	1.44	1.73

Table 5-4: Palaeo-redox proxy values for samples from the Milton Green borehole.

Depth (m)	Sample code	U/Th	V/Cr	Ni/Co	TOC/S
1134.77	MG 1	0.15	0.59	2.66	0.46
1135.38	MG 3	-	0.94	3.06	4.37
1135.68	MG 4	0.20	0.98	2.61	0.94
1136.29	MG 6	0.13	0.85	2.10	0.74
1136.60	MG 7	0.16	0.82	-	0.93
1194.72	MG 8	0.69	0.84	-	1.48
1203.05	MG 9	-	-	-	3.29

Table 5-5: Palaeo-redox proxy values for samples from the Point of Ayr No.3 shaft.

Depth (m)	Sample code	U/Th	V/Cr	Ni/Co	TOC/S
65.53	POA 1	-	1.32	2.46	16.17
104.12	POA 2	0.66	1.16	3.20	1.97
106.68	POA 3	0.84	2.32	4.31	1.92
106.68	POA 4	0.91	2.32	3.41	1.07
178.31	POA 5	0.15	1.16	1.97	21.58
185.01	POA 6	-	1.18	2.57	33.57
188.98	POA 7	1.33	2.30	6.70	6.28
197.82	POA 8	1.19	1.44	2.64	1.08
212.32	POA 9	0.68	2.80	4.81	2.84
309.98	POA 10	1.03	2.16	3.21	1.80
325.22	POA 11	1.06	1.57	3.67	2.05
326.75	POA 12	1.78	1.80	4.35	1.74
331.01	POA 13	1.15	2.64	4.38	3.15
333.76	POA 14	1.45	2.93	4.44	2.62
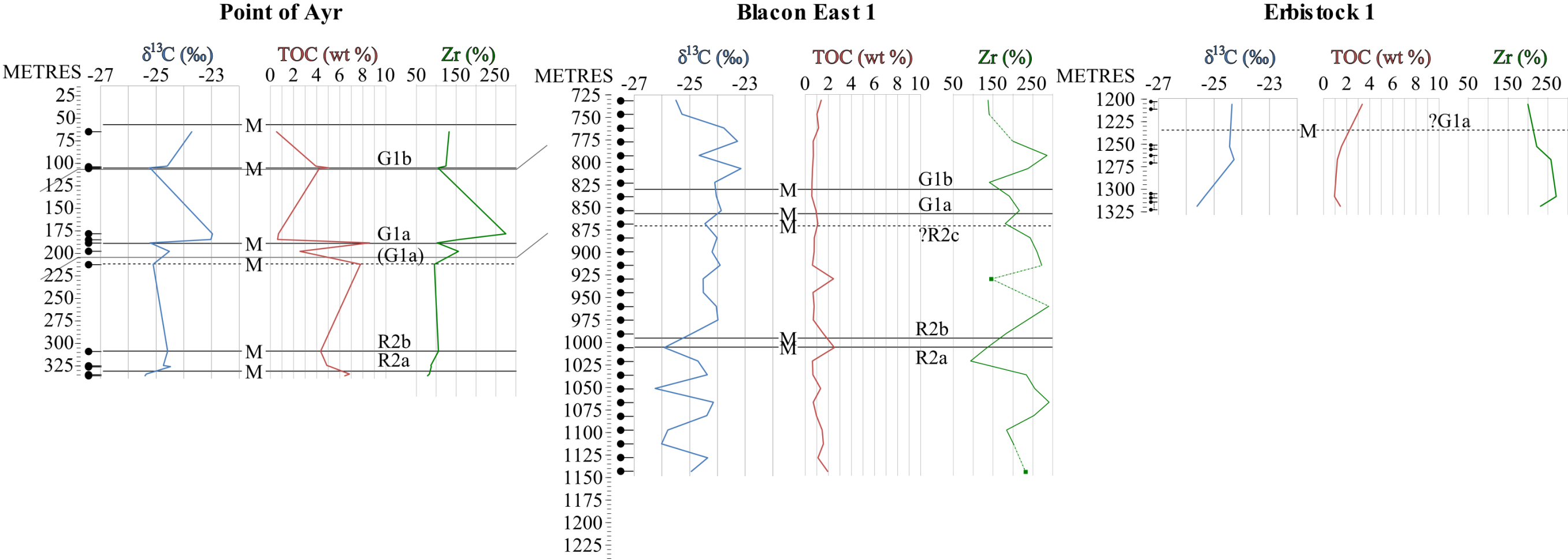
Figure 5-11: Within the boreholes studied geochemical trends with depth: Carbon isotope (δ^{13}C; blue line), TOC (wt %; red), Zr content (%; green). Marine bands are marked to show key links between chemostratigraphy and biostratigraphy. Points with dotted lines attached on the Zr plot in Blacon East are data points, but no data exists in between them and points on the solid line.

Zirconium (Zr) is used as a proxy for terrestrial input and abundance of silt-sized detrital components as Zr occurs primarily in zircon a dense, erosion-resistant mineral commonly derived from weathered igneous rocks or recycled sediments, hence its occurrence is indicative of terrestrial input from these sources. High Zr values can therefore be used to indicate a higher terrestrial input (Davies et al., 2012) and therefore discriminate between detrital (high Zr values) and biogenic (low Zr values) silica. High Zr values (> 200 ppm) correlate with the heaviest carbon isotope (most terrestrially sourced OM) samples of the Holywell Shale, which often have lower TOC values (average 0.9 wt %; Figure 5-11).
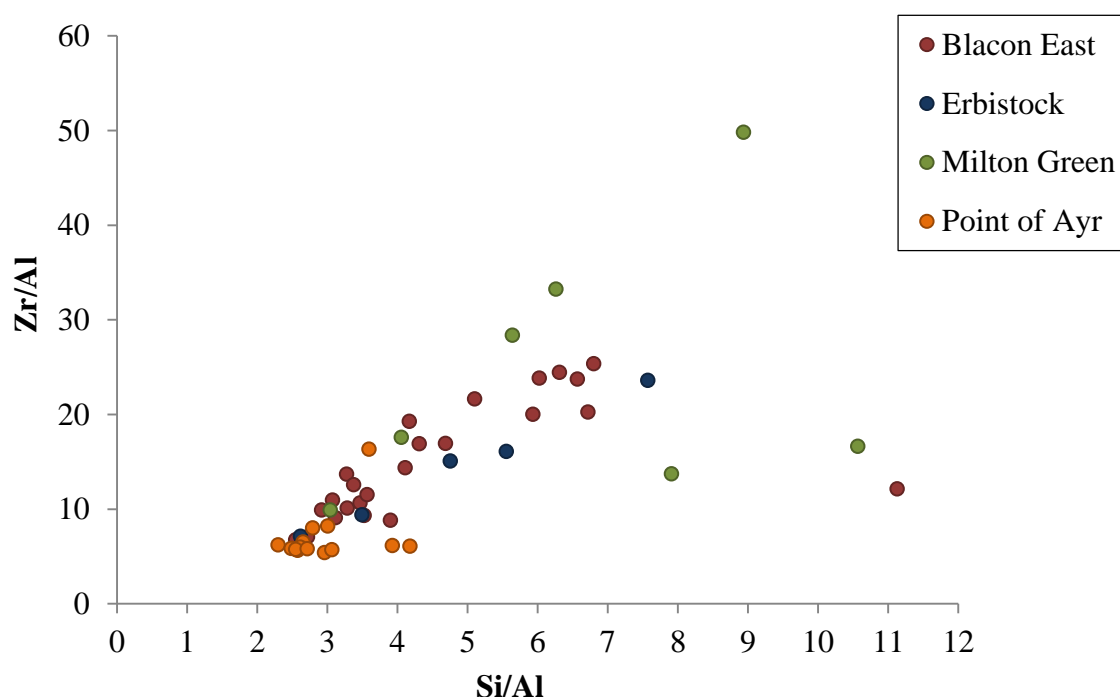
Figure 5-12: Silica and zirconium to aluminium ratios plotted to distinguish between biogenic and terrestrially sourced silica. Low Zr/Al indicates low terrestrial input, combined with high Si/Al indicates a biogenic source for the silica present.

The petrography of the Point of Ayr reveals that these high Zr concentration samples occur with silt-rich facies (Figure 5-5). Samples which are clay-dominated and often with lenticular fabric have Zr values < 125 ppm (Figures 5-4 & 5-5). These correlate

with high TOC values and the lightest carbon isotope values (more marine; Figures 5-11, 5-4 & 5-5). Within the Point of Ayr borehole some samples contain high Si/Al ratios (> 3.9), light carbon isotope values (average -25.4 ‰), but low Zr concentrations (< 85 ppm) suggesting that the origin of the silica is biogenic rather than terrestrial (Figures 5-12 & 5-13).

Titanium (Ti) concentrations can be used to support the Zr trend as they suggest a presence of terrestrially-sourced minerals and organic material in correlation with Zr values and carbon isotope values (Appendices F & G).
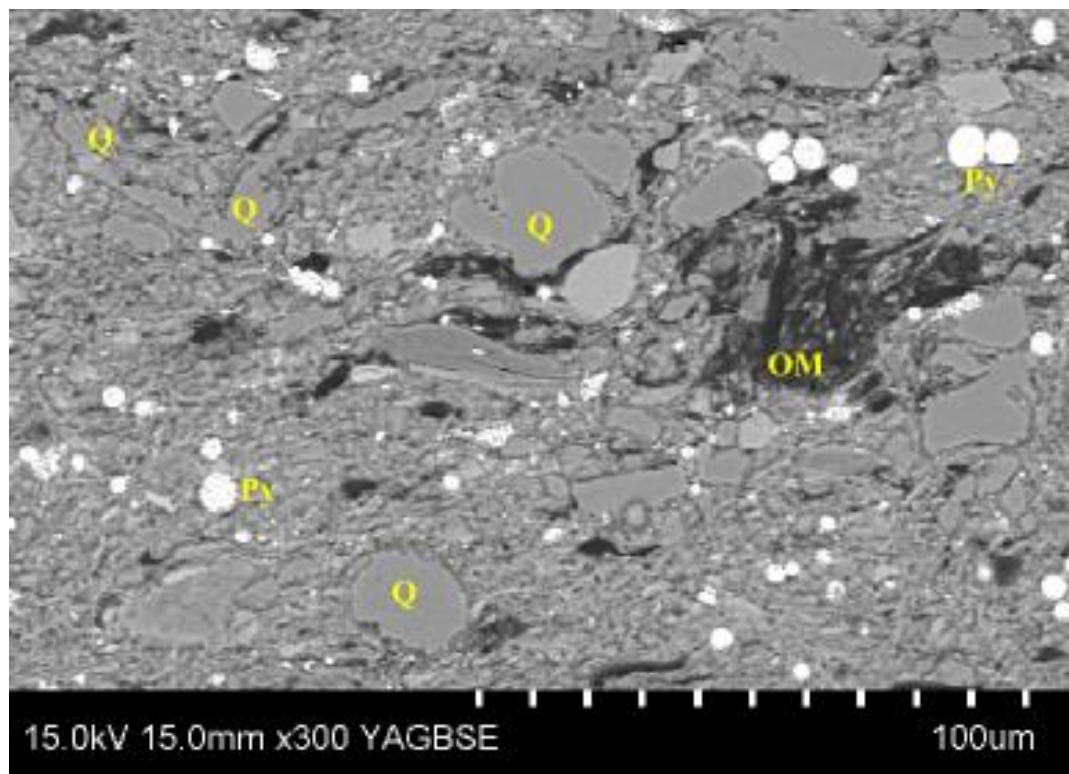
Figure 5-13: Point of Ayr borehole sample (POA 14, 333.76 m depth – R2a marine band; fossiliferous, clay-rich mudstone) which contains high Si/Al ratio, but low Zr concentration. The quartz (Q) present in the sample is rough edged and appears to be of biogenic source rather than terrestrial detrital grains. Pyrite (Py) occurs as framboids and is common; organic matter (OM) is largely of amorphous origin.

5.5: Discussion

Exploration for shale gas is in relative infancy in Europe, but experience from numerous wells drilled in the US have made it possible to suggest a range of precursors required for shale gas exploration (e.g. Andrews, 2013; Charpentier & Cook, 2011; Jarvie, 2012). The suggested parameters for prospective source rock reservoirs are: Type II kerogen (Type II are preferable due to the amount of gas they are capable of generating); TOC values > 2.0 wt %; original hydrogen index (HI_o) > 250 mg/g (high original HI correlates with higher H/C ratios resulting in a greater potential for hydrocarbon generation); carbonate-rich/ biogenic silica-rich (brittle components to improve the hydraulic fracturing ability of the rock); clay-poor (clay minerals reduce the efficiency of hydraulic fracturing).

Whilst none of the boreholes sampled meet all these criteria, the Point of Ayr borehole and three marine-influenced samples within Erbistock and Blacon East boreholes do meet some of the criteria. Kerogens within the Holywell Shale are mainly Type III which is not preferable, but still viable as a target for shale gas exploration (Figure 5-9). Type II (oil prone) kerogens have the potential to generate more kerogens than Type III (gas prone) because as Type II kerogen reach the end of the oil window, they begin early gas generation. As well as this, some (20 to 30 %) of the bitumen and oil produced in the oil window is retained and later cracked to gas (Dembicki, 2013). TOC values for the Holywell Shale range from 0.5 to 8.6 wt % (average 2.0 wt %), these values are in a very similar range reported for other UK Namurian mudstones within the Bowland Shale Formation (Armstrong et al., 1997; Davies et al., 2012; Könitzer, 2014a, b). However, in the Holywell Shale samples of this study, HI values are all much lower than required, with a maximum value of 224 mg/g in the Point of Ayr borehole.

The extremely low OI values (5 to 9 mg/g) of the high TOC Point of Ayr samples means that they plot as Type I kerogen or a much more mature source-rock on the modified van Krevelen diagram (Figure 5-10). Whilst the T_{max} vs HI plot (Figure 5-9) shows that the same samples are Type III kerogens. One possible explanation for this difference is that the kerogens are in fact Type IIS which have initially low OI and initially high HI due to deposition under reducing conditions but have high sulphur contents (8 to 14 %). However, the sulphur content of the Holywell Shale samples (between 0 and 4 %, average 1 %) is too low for this to be the case (Dembicki, 2009). An alternative explanation is that the organic matter present is a mixture of kerogen types (Dembicki, 2009). Type III kerogens typically have relatively low HI (150 mg/g) and high OI (115 mg/g; Dembicki, 2009). Within the Holywell Shale samples the average HI is 93 mg/g, and the average OI is 34 mg/g. This may indicate that HI is in line with values for Type III kerogens whilst OI is significantly lower than typical Type III kerogens. This suggests that while organic matter is less oxidised than typical Type III kerogens, the HI values show that the atomic H/C ratios are low and thus the hydrocarbon generation potential is more limited.

The Point of Ayr borehole has strong indications of a distal pro-delta mudstone facies with clay-rich, increased amorphous organic matter content and fossil debris input occurring at each eustatic marine band cycle. The carbon isotope values for these clay-rich facies (average -25.0 ‰), is similar to observations by Davies et al. (2012) of a mudstone dominated succession (Marsdenian) in west Yorkshire. Whilst the clay-rich lithofacies are marine sediments, the amorphous organic matter which they contain is poorly preserved as demonstrated by low HI values (average 162 mg/g). The silt-rich lithofacies present within Point of Ayr is associated low TOC values (average 0.6 wt %), low TOC/S, increased terrestrial OM (average -23.2 ‰) and high Zr combine to

suggest a terrestrial-dominated system possibly with periods of reduced marine influence (Figure 5-1).

The other three boreholes (Blacon East, Milton Green and Erbistock) have lower TOC values (average 1.2 wt %) but similar ranges in carbon isotope values (average -24.8 ‰) as the Point of Ayr borehole samples (with Milton Green isotopically lighter in some samples). The influence of the prograding Marsdenian deltas from the southeast (from the Wales-London-Brabant Massif) and from the northeast (Millstone Grit Group) during the Namurian had a significant effect on the marginal areas to the southeast of the region (Erbistock and Milton Green; Figure 5-1; Waters et al., 2009). However, the Point of Ayr borehole is located further into the basin which may have limited the influence of the prograding deltas and led to reduced siliciclastic input (Figure 5-1).

Gross et al. (2015) suggested that TOC/S ratios can be used to distinguish between fully marine and turbidite/limited marine mudstones. Sulphur content in shale is generally due to low oxygen at the time of deposition either in the bottom waters or in the sediment. TOC/S reflects this oxygenation state, although sulphur content in shale can be affected by other processes (Ross & Bustin, 2009). TOC/S ratios above 2.8 only occurring in limited marine, reduced salinity and reduced sulphur facies in between marine bands within the Bowland Shale Formation (Gross et al, 2015). TOC/S for the boreholes sampled range from 0.46 (hypoxic, high sulphur) to 33.57 (most oxic, low sulphur; Appendix E). There is a weak correlation between TOC/S and $\delta^{13}C$ values, with the highest TOC/S ratios corresponding to the least negative carbon isotope values (terrestrial influenced). TOC/S ratios for the Point of Ayr borehole silt-rich mudstone samples (Figures 5-4 & 5-5) are high (Table 5-5) indicating deposition within a

terrestrial dominated environment. Within these silt-rich facies, organic matter quantity is reduced (TOC values 0.5 to 0.7 wt %) and the organic matter present is oxidised (indicated by low sulphur 0.02 to 0.03 % and high OI 40 to 73 mg/g) resulting in poor preservation of organic matter. Point of Ayr samples which have marine goniatite fauna present (-25.4 ‰ to -24.5 ‰, Figures 5-4 & 5-5) have low TOC/S ratios (Table 5-5).

The most organic rich samples of the Holywell Shale are from marine bands within the Point of Ayr borehole (TOC < 8.6 wt %). In the majority of the marine band samples there is an association between high TOC content and clay-rich lithofacies dominated by marine microfauna and containing low Zr values (Zr average 97.2 ppm; low Si/Al ratios, 2.3 to 4.2; Figures 5-4 & 5-5). The fossiliferous organic-rich clay-rich mudstones (marine bands) also have modest generation potential (low HI average 168 mg/g). This association between high TOC, high clay content and low HI is also noted within the Bowland Shale Formation (Pendleian, ~ 326 Ma to Arnsbergian, ~ 325 Ma) in the Widmerpool Gulf (Gross et al., 2015). Whilst the marine bands represent the best target for shale gas exploration within the Holywell Shale, they are far from the ideal parameters previously outlined (Andrews, 2013; Jarvie, 2012).

Shale gas source-rock reservoir targets have to be gas-mature to be able to produce hydrocarbons, or oil mature for shale oil production. T_{max} values can be used as a proxy for maturity of the samples, which for the all Holywell Shale samples is oil window maturity, with the exception of most Point of Ayr samples which are immature (Figure 5-9). In the oil window S_1/TOC is below the 100mg/g threshold above which suggests free oil (i.e. oil beyond that adsorbed to kerogens) is present (Jarvie et al., 2007; Michael, 2013). Oil saturation values of the Holywell Shale range from 3.2 to 34.6 mg/g, whilst not above the required threshold of 100mg/g for shale oil production,

they are notably higher than comparable Namurian shale (Słowakiewicz et al. 2015) suggesting that in comparison the Holywell Shale is a preferable source rock.

The potential for the kerogen within the mudstone to generate further hydrocarbons is determined by the RockEval™ S_2 parameter (Appendix E). The majority of Point of Ayr and some Erbistock samples show good to excellent S_2 values (> 5 mg HC/g rock; Figure 5-8) indicating that with greater maturity (i.e. deeper burial) these samples could produce further hydrocarbons. For all other Holywell Shale samples S_2 values are poor (< 1.5 mg HC/g rock) and are likely to be the limiting factor for source-rock reservoir potential.

5.6: Conclusions

There are two main lithofacies present within the Holywell Shale samples: clay-rich mudstone, and silt-rich mudstone; although these can be further subdivided by distinguishing features such as fossil content, fabric and textural variation. Samples which occur at marine bands tend to be clay-rich (with lower Si/Al ratios and low Zr concentrations) and fossiliferous, often containing shelly material or abundant ammonoid microfossils. Samples taken from mudstones which did not contain goniatites are quartz-rich, micaceous, often with graded bedding, and in some cases rich in silt-sized grains, which also correlate with higher Si/Al ratios and Zr concentrations. Organic matter occurring at the marine bands (clay-rich, fossiliferous) show largely amorphous organic matter which aligns with clay minerals along bedding (distorting around larger grains). Whereas, non-marine band facies (silt-rich), have more dispersed and fragmentary organic matter with significantly lower TOC values.

The TOC content of all samples ranges from 0.5 wt % to 8.6 wt % (average 2.0 wt %), with the Point of Ayr borehole containing both the highest and the lowest TOC samples

recorded. Within the four boreholes sampled, the carbon isotope values for the Holywell Shale range from -26.3 ‰ to -23.0 ‰. The marine band facies exhibited high TOC values (> 2.6 wt %) and more negative carbon isotope values (e.g. -25 ‰). Whereas the samples which were not from marine bands had less negative carbon isotope signatures (e.g. -23 ‰) and significantly lower TOC values (< 0.7 wt %).

Spatially, the data suggests that for the Marsdenian/Yeadonian (317 Ma to 314.5 Ma) the marine influence is strongest in the northwest of the northeast Wales region and terrestrial input greatest in the southeast of the region which was more proximal to the Wales-London-Brabant Massif and Milton Green high. This is consistent with the source of Marsdenian/Yeadonian deltas from the southeast and Millstone Grit deltas from the northeast (Figure 5-1; Davies et al., 2004; Fraser and Gawthorpe, 2003).

Kerogen type (established from TOC and RockEval™ parameters) for the Holywell Shale is predominantly type III with some outliers plotting as type II. All samples are oil mature, with the exception of Point of Ayr samples which are immature. U/Th, V/Cr, and Ni/Co ratios all imply that the Holywell Shale was not deposited in oxygen-depleted waters). The exception are samples from the Point of Ayr, particularly the G1a, R2b and R2a marine bands, which have higher U/Th ratios suggesting a dysoxic environment of deposition with possible periods of anoxia. These trace element proxies combine with relatively low TOC, low HI and high OI values to suggest preservation of organic matter in the Holywell Shale is poor (e.g. Blacon East and Erbistock boreholes) with the exception of the marine band facies within the Point of Ayr borehole.

Chapter 6:

Lithological variations within the Holywell Shale (Carboniferous, UK): A predictive tool for geochemical and lithofacies characteristics

6.1: Abstract

This study assesses geochemical data collected from outcrop material in comparison to core material from the same stratigraphic position within an organic-rich mudstone using marine bands to correlate. Material from the Holywell Shale (Carboniferous, northeast Wales UK) was used as the basis for this study. The main geochemical analyses used within this study were carbon isotopes, total organic carbon, RockEval™ and X-Ray Fluorescence. Detailed petrographic analysis using natural light transmitted light microscopy and scanning electron microscopy (including EDS) was used to support the geochemical data and provide further context of the results. It was possible to correlate between specific data (such as TOC, HI, Zr etc.) as well as general trends (δ^{13}C) between outcrop and borehole material from an individual marine band (G1a) and across multiple marine bands. Two end-member facies were identified as: silt-rich and clay-rich fossiliferous. These facies had very different geochemical characteristics. However, the geochemical data for each facies was consistent throughout temporal and spatial variation (across the Holywell Shale and the wider Carboniferous Pennine Basin). The changes in geochemical data are likely to represent changes in the lithofacies and palaeogeographic location. The ability to correlate geochemical data was extended to samples which were taken from cutting material and thus had no petrographic analysis. The geochemical characteristics correlated well and demonstrated that it is possible to use geochemical characteristics as a predictive tool to determine facies variations in samples where it was not possible to observe petrographic variations. Overall this study demonstrates that a combination of outcrop and borehole material analysed using petrographic and geochemical techniques can be used to assess fine grained sedimentary rocks in terms of facies,

palaeoenvironmental interpretation and reconstruction as well as predicting reservoir quality and sweet spots/horizons.

6.2: Introduction

Shale gas and shale oil exploration, termed 'unconventional' describes hydrocarbon exploration where the target is the shale source rock rather than a conventional permeable and porous reservoir (such as sandstone or limestone). In the majority of these unconventional reservoirs, hydraulic fracturing 'fracking' is required in order for the wells to produce hydrocarbons at economic rates.

Shale is a general term used for fissile, fine-grained sedimentary rocks. A more accurate system of describing these fine grained systems is to use the generic term 'mudstone' as proposed by Lazar et al. (2015a). Mudstones, in conventional petroleum systems, are typically of interest as the source rock from which hydrocarbons are generated and then migrate to a reservoir rock where they are trapped by a seal (which can also be a mudstone; Hart et al., 2013). In unconventional shale gas and shale oil systems the gas and/or oil are generated within the source rock and are not completely expelled, in this sense, unconventional shale reservoirs can be described as source-rock reservoirs (Hart et al., 2013).

Within the UK several mudstones have been identified as potential shale gas or oil targets, although at present exploration is in its infancy. Currently, the largest potential UK shale gas target is the Bowland Shale Formation of central and northern England (Andrews, 2013). The Bowland Shale Formation can be locally subdivided into units such as the Holywell Shale (where it occurs in north Wales), and the Edale Shale (where it occurs in the Derbyshire/Pennine region) (Waters et al., 2009).

The Holywell Shale is exposed at the surface in outcrops across the northeast Wales region which have been previously studied, including the identification of marine bands where present (Chapter 4 – Newport et al., 2016; e.g. Armstrong et al., 1997; Jerrett & Hampson, 2007;Waters & Condon, 2012; Figures 6-1 & 6-2). The Holywell shale is also present within several boreholes that penetrate the Namurian strata in the region; the Abbey Mills number 1 and 4 boreholes (unable for sampling within this study; easting, northing: 319400, 377500) provide the type section for the Holywell Shale as they contain the most complete continuous succession of 152 m (Davies et al., 2004).

The aim of this paper is to compare data from core and cutting material from boreholes, against those samples collected at outcrop (Figure 6-1; Appendices A-G). In Chapter 5 the detailed vertical variation in biostratigraphy and geochemical data are discussed for each of the sets of borehole samples accessed for this study. In Chapter 4 the geochemical data for each outcrop visited are assessed. This study aims to compare and contrast the two datasets (Chapters 4 & 5) to determine whether similar lithofacies and geochemical characteristics can be found within both core and outcrops at the same stratigraphic horizons across the northeast Wales region. This could then be used as a powerful tool to predict the lithofacies within borehole cutting material by correlating the geochemistry.

6.3: Methods
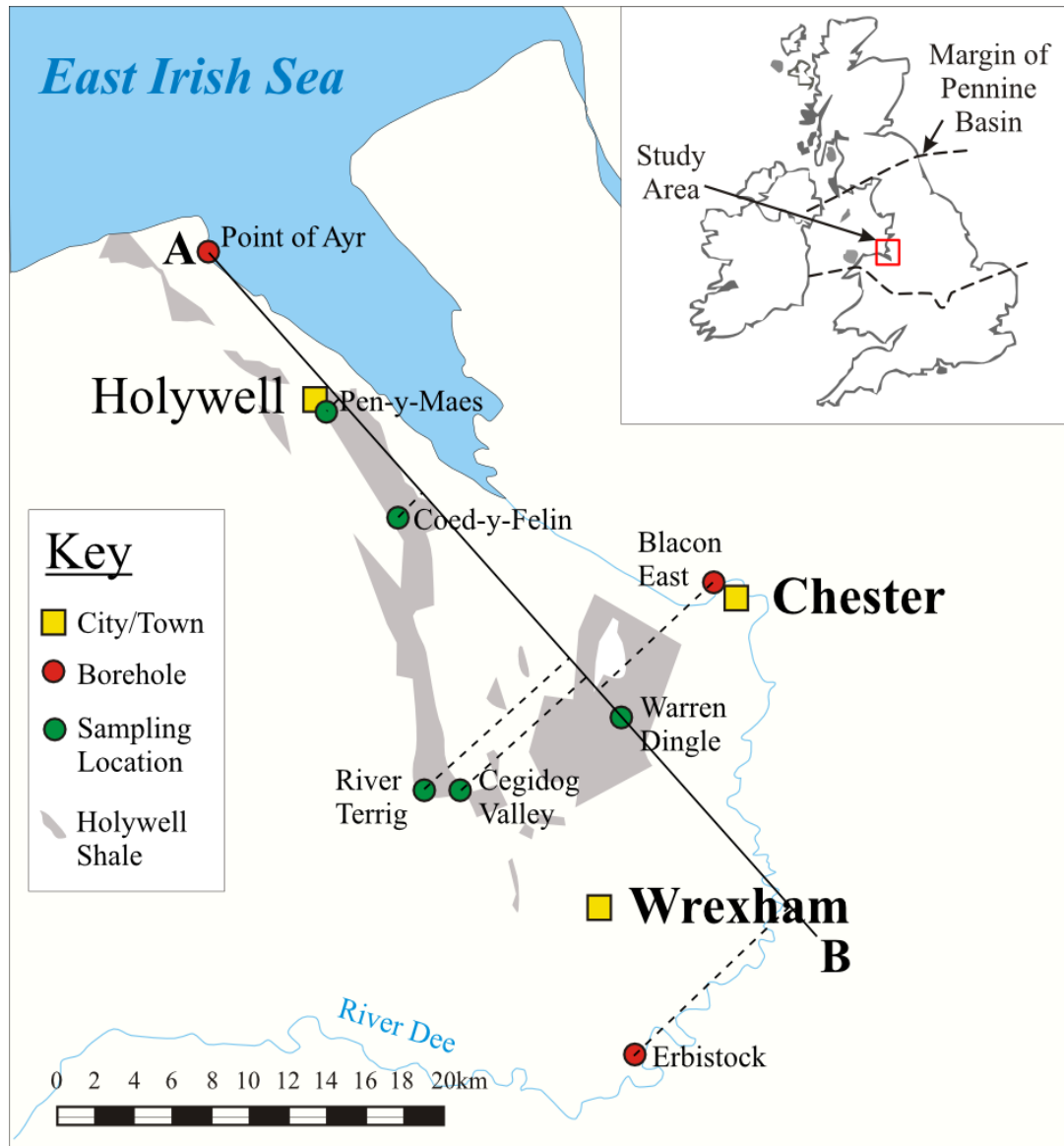
Figure 6-1: Map of outcrops and boreholes sampled in northeast Wales with a correlation line, A-B (48 km with some locations sitting off-line by 11 km). Inset image shows the setting within the UK for context and the dotted lines represent the edges of the Carboniferous Pennine Basin.

6.3.1: Sample Collection

Samples were collected from selected outcrops and boreholes across the northeast Wales region (Figure 6-1). Details of the material collection methods used, along with the location of outcrop and borehole material, the details including age of the

associated marine bands sampled and, for boreholes, the depth range at which samples were taken are outlined in Chapter 3, Table 3-1.

6.2.1.1: Borehole sampling

Borehole sampling procedures and the reasons behind the sampling strategy are outlined within chapter 3 of this thesis (Section 3.1.3).

6.3.1.2: Outcrop sampling

Outcrop sampling procedures and the reasons behind the sampling strategy are outlined within Chapter 3 of this thesis (Section 3.1.2). The collection of sample from outcrop rather than borehole material was relatively simple and inexpensive (if the cost of drilling is taken account of). Whilst there are associated problems relating to outcrop collection including accessibility of sites such as permissive access or protected status (i.e. Site of Specific Scientific Interest SSSI), these are significantly less costly obstacles to address than those associated with drilling. The main issue with outcrop material, however, is the difficulty in ensuring that the material sampled is 'fresh' meaning it has not been weathered or eroded due to exposure at the earth's surface.
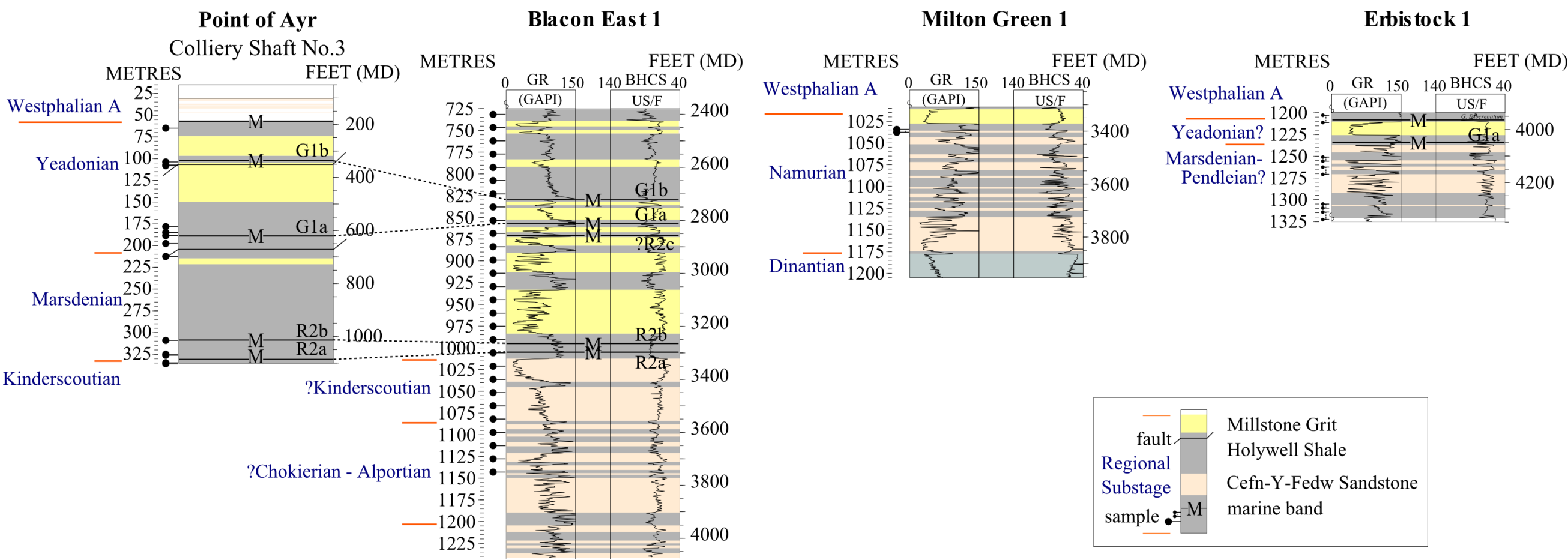
Figure 6-2: Point of Ayr, Blacon East and Erbistock borehole gamma ray (GR) and compensated sonic (BHCS) logs, stratigraphy and correlations of marine bands. Sampled horizons are marked, in the case of Erbistock this includes a range of depths of cuttings sampled.

6.3.2: Correlating between locations

The locations of the Holywell Shale boreholes and outcrops sampled are from the northeast Wales region (Figure 6-1). All boreholes and outcrop locations were chosen as they contained identified marine bands which allowed for biostratigraphical correlation between each location (Figures 6-2 & 6-3; Andrews, 2013; Magraw, 1954; Waters & Condon, 2012).

The most reliable marker for Namurian mudstones in the UK are the ammonoid (goniatite) marine bands. Of the 49 Namurian ammonoid marine bands which are recorded in the Central Province basins (UK), 15 have been identified within boreholes and outcrops of the northeast Wales region (Davies et al. 2004). Some of these marine bands are also recorded across Europe and the US (e.g. Caney Shale, Oklahoma), which means that wider correlations may be possible (Craig et al., 1979; Gordon, 1962). The marine bands are marked by specific goniatite ammonoid species, which planispirally coil and are identifiable by their distinctive suture patterns. The rapid evolution of the goniatite species, widespread distribution and anagenesis mean that distinctive changes in ammonoid species (in the region of Milankovich cycles 100/400 Ka) can be used as accurate biostratigraphic markers (House, 1996; Waters & Condon, 2012).

No seismic data is available for this region and therefore the borehole data cannot be integrated with the larger scale surfaces and packages. Within several of the boreholes sampled in this study both gamma ray and sonic velocity logs were available (Figure 6-2). Gamma ray (measured in API units) is used to determine rock types due to the naturally occurring radioactive materials present in them (e.g. uranium, thorium, potassium, radium, and radon; Rider & Kennedy, 2011). Whilst, sonic velocity logs

(measured in µs/ft) can be used to calculate porosity (Rider & Kennedy, 2011). High gamma (> 90° API) and low sonic velocity due are indicative of mudstones due to their high acoustic impedance due to the clay minerals present (Figure 6-2). The borehole logs supported by the lithological information from core and cuttings can also be used to correlate broadly between the formations present.

6.3.3: Analytical methods

Organic and inorganic geochemical analysis techniques and petrographic and scanning electron microscope techniques (described in detail in the methods section, Chapter 3) were used to evaluate similarities and differences between outcrop and core samples within this chapter.

Within the ideal faunal succession of Holdsworth & Collinson (1988), which represents the change in fauna from fully marine thick-shelled goniatites through regression to paralic species, there are many observations of lithofacies and within those lithofacies, microfacies occur. The goniatites which denote the sampled marine bands within the boreholes are present over several metres in some cases (< 8.6 m). Typical shale microfacies according to the classification proposed by Macquaker & Adams (2003) found around marine bands within the Holywell Shale are: clay rich mudstone, and silt bearing mudstone (Chapters 4 & 5). The mudstone microfacies can be described in terms of their mineralogy: siliceous, argillaceous or calcareous. However, within this classification several sub-categorisations, similarly used in the Bowland Shale Formation by Davies et al. (2012) & Könitzer et al. (2011; 2014a, b) can be made within these microfacies to further constrain the samples, these include: homogeneous, lenticular bedding, graded bedding (particularly within silt-rich samples), abundant microfossils, shell fragments.

NW   SE

POA   PYM   CYF   RT   CV   BE   WD   ER

0   10   20 km

Key

Millstone Grit
Holywell Shale
marine band
Cefn-Y-Fedw Sandstone
Limestone

Age (Ma)	Regional Stage	Regional Substage	Ammonoid Biozone
314	Westphalian	Langsettian	G.subcrenatum
315	Namurian	Yeadonian (G1)	*C.cumbriense (G1b)
			*C.cancellatum (G1a)
316		Marsdenian (R2)	*B.superbilinguis (R2c)
			*B.bilinguis (R2b)
			*B.gracilis (R2a)
317		Kinderscoutian (R1)	*R.reticulatum (R1c)
			*R.nodosum (R1b)
318			R.circumplicatile (R1a)
319			Ht.prereticulatus (H2c)
320		Alportian (H2)	
321			*H.undulatum (H2b)
322			
323			Hd.proteum (H2a)
324			H.beyrichianum (H1b)
325		Chokierian (H1)	*I.subglobosum (H1a)
		Arnsbergian (E2)	N.nuculum (E2c)
			*Ct.nitidus (E2b)
326			*E.bisulcatum (E2a)
		Pendleian (E1)	*Cr.malhamense (E1c)
			T.pseudobilingue (E1b)
327	Viséan	Brigantian	Cr.leion (E1a)
328			

Figure 6-3 (found on page 115): Namurian chronostratigraphy and ammonoid biozones (UK), the samples with * indicate marine bands that are identified within the northeast Wales region, including outcrop names which refer to their locations and the ammonoid biozones present (Chapter 4; Davies et al., 2004; Waters & Condon, 2012). A simplified stratigraphical representation highlights the marine bands and lithologies present. Boreholes and outcrops sampled and the marine bands which are contained within each; boreholes: POA = Point of Ayr, BE = Blacon East, ER = Erbistock; outcrops: PYM = Pen-Y-Maes, CYF = Coed-Y-Felin, RT = River Terrig, CV = Cegidog Valley, WD = Warren Dingle. Note: vertical scale is time (Ma); horizontal scale, equivalent to the A-B line in Figure 6-1, is given in km at the top of the figure.

6.4: Results

6.4.1: Lithology, Mineralogy and Inorganic Geochemistry

It is apparent from petrographic analysis that the lithofacies and microfacies of samples from both borehole and outcrop are directly comparable (Figure 6-4). Similar lithofacies from boreholes and outcrops will allow direct comparisons of geochemical results for a more accurate view of how the geochemical data vary between borehole and outcrop samples.

Similar lithofacies appear to be very similar in terms of lithofacies, with silt-rich facies having similar mineralogical constituents (detrital grains of quartz, mica and feldspar) occurring often with graded bedding (Figure 6-4). The marine band fossiliferous facies which is also observed in both outcrop and borehole samples appear very similar with microfossil goniatite spat, shell fragments and calcispheres (Figure 6-4; similar to those observed by Könitzer et al., 2011).The mineralogical constituents of the fossiliferous clay-rich facies are similar too, with a clay matrix encompassing many biogenic (fossils and fragments) components, which are rich in calcite, phosphate and relatively low in quartz minerals.

Borehole

Outcrop

Silt -rich facies with graded bedding

Clay rich facies, fossiliferous
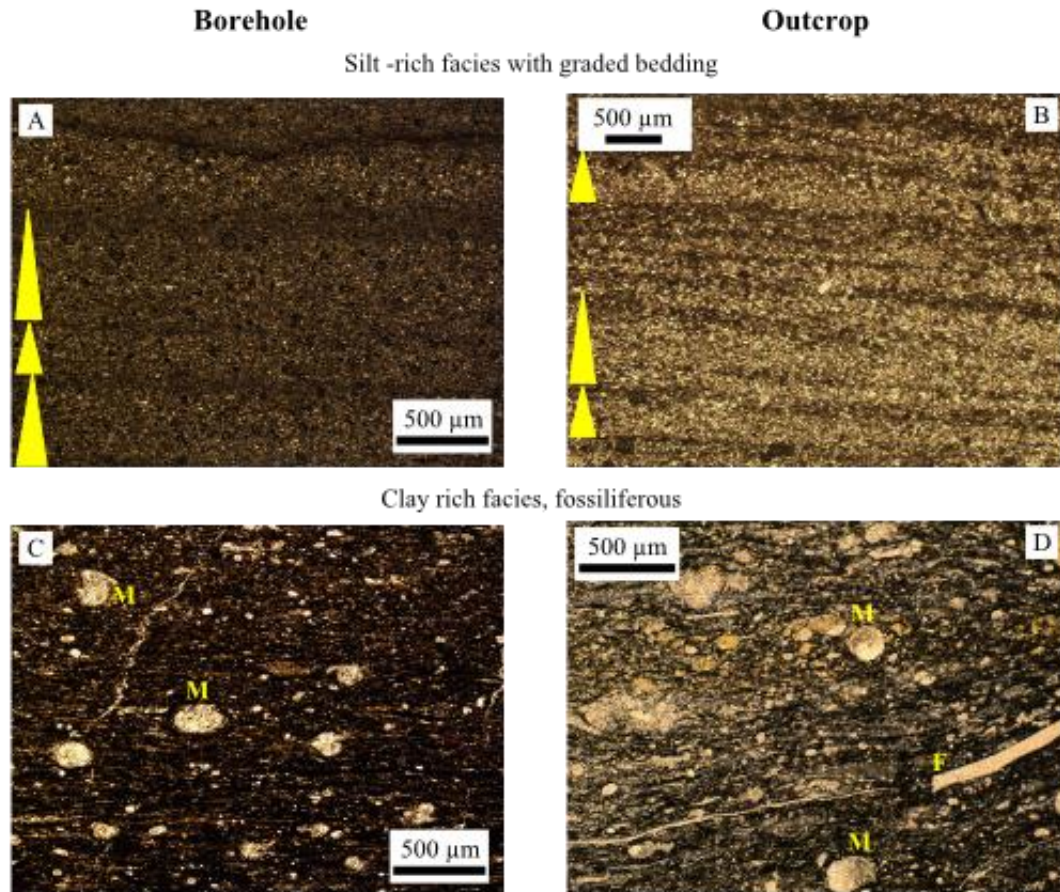
Figure 6-4: Thin section images of borehole samples (left; A = Point of Ayr – POA6, 185 m; C = Point of Ayr – POA7, 189 m) and outcrop samples (right; B = Pen-Y-Maes – PYMS1H5; D = Warren Dingle – WDS1H4) described after Macquaker & Adams (2003), Davies et al. (2012), Könitzer (2014a). M = microfossil, F = shell fragments, vertical arrow = examples of graded bedding (finer towards the top), dotted line denotes small scale cross bedding. All sections shown are taken from samples which occur at the G1a marine band. Samples A and B demonstrate silt-rich microfacies with graded bedding (fining upwards), terrestrially sourced minerals (including plagioclase feldspars) and fragments of terrestrial organic matter. Samples C and D show clay-rich mudstones with amorphous organic matter which aligns with clay minerals along bedding. An abundance of goniatite microfossils and larger fragments of shells occur in a lenticular fabric.

It is possible to observe variations in the inorganic geochemistry which correlate with the different facies and their mineralogy (Figures 6-4 to 6-8). The silt rich facies demonstrates similar Si/Al values for both borehole (average 3.3) and outcrop (average 3.4). The highly fossiliferous facies observed also have similar Si/Al ratios in borehole

(average 2.7) and outcrop (average 2.6). Si/Al doesn't directly correlate with facies and values within the Holywell Shale range from 2.3 to 14.9 (average 4.64), with large variations in Si and Al content suggesting diagenetic alteration or an increase in silica from biogenic sources.

Zirconium (Zr) is used as a proxy for terrestrial input and abundance of silt-sized detrital components as Zr occurs primarily in Zircon, a dense, erosion-resistant mineral commonly derived from weathered igneous rocks or recycled sediments, hence its occurrence is indicative of terrestrial input from these sources. High Zr values can therefore be used to indicate a higher terrestrial input (Davies et al., 2012). Zr values in the Holywell Shale range from 30.4 ppm to 405.3 ppm.
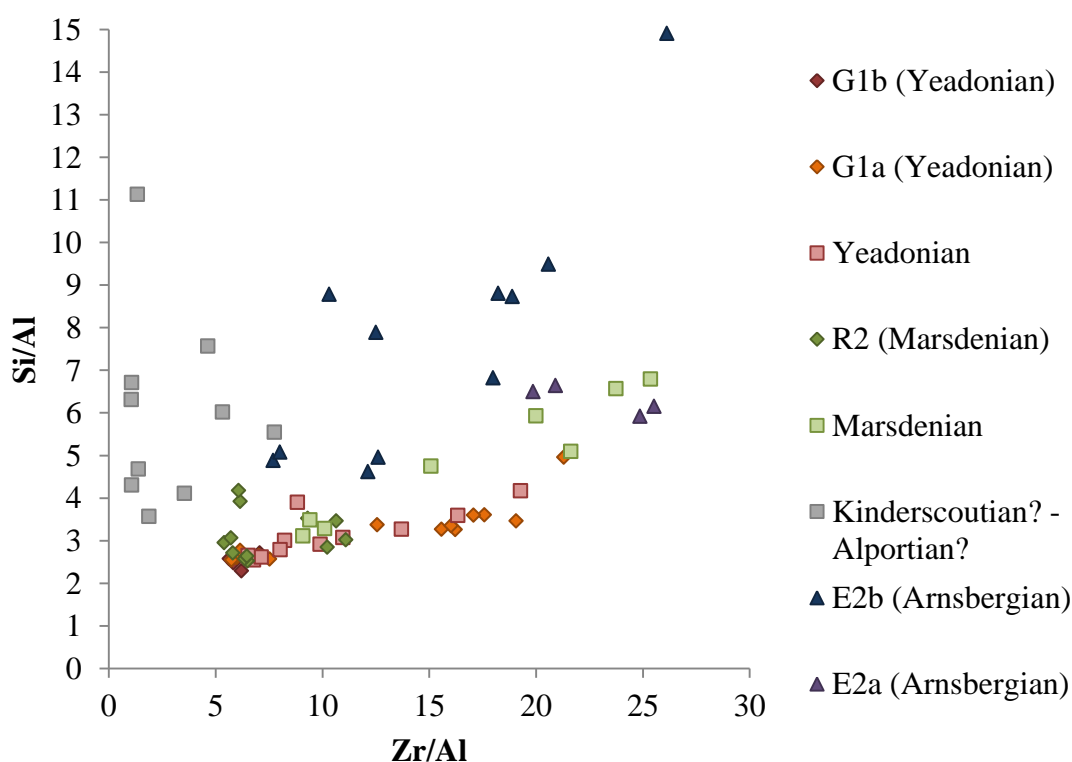
Figure 6-5: Zr/Al plotted against Si/Al. This plot demonstrates that the Arnsbergian and Kinderscoutian (?) – Alportian (?) aged samples have higher Si/Al ratios. Marsdenian to Yeadonian aged samples have a linear relationship where Si/Al ratio increases with Zr/Al ratio.

Marsdenian to Yeadonian samples appear to have a linear relationship, as Si/Al ratio

increases, so does Zr/Al ratios (Figure 6-5). This suggests that an increase in silica in

these samples is directly related to an increase in Zr, thus a terrestrial source of detrital

silica. However, the same is not the case for samples from Kinderscoutian (?) age and

Arnsbergian aged samples which have not got a strong correlation between Si/Al and

Zr/Al ratios (Figure 6-5). The samples are all relatively enriched in Si (higher Si/Al

ratio) compared to the samples from Marsdenian to Yeadonian ages (Figure 6-5). This

suggests an additional source for silica within these samples, which when combined

with low and very variable Zr/Al ratios could suggest a non-detrital or biogenic source

of silica.
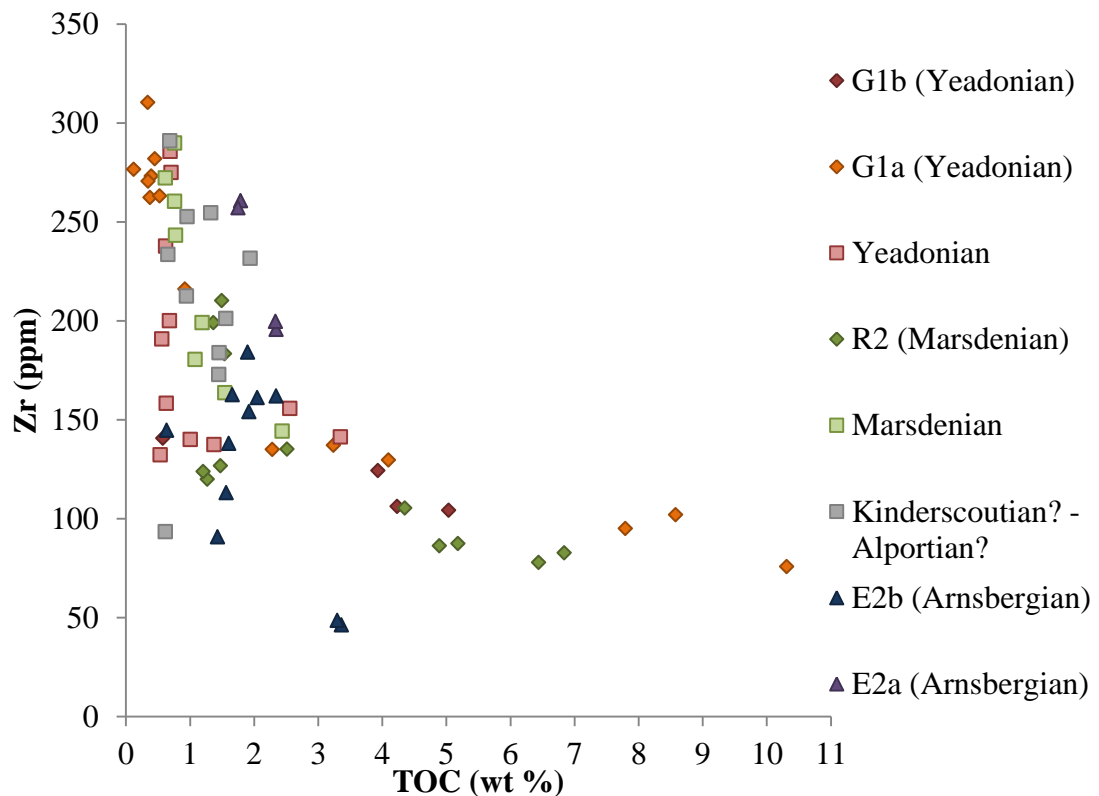
**Figure 6-6: TOC plotted with Zr. The plot shows that marine band samples which have
relatively high TOC values correspond with the lowest Zr concentrations.**

Samples higher in Zr are associated with the silt-rich facies (Figure 6-4, samples A and

B). These samples have the lowest TOC values and are often Type III or IV kerogens

with very limited generation potential. Samples with higher TOC which occur at marine bands and therefore are likely to be fossiliferous, clay-rich facies have lower Zr values (Figure 6-6).
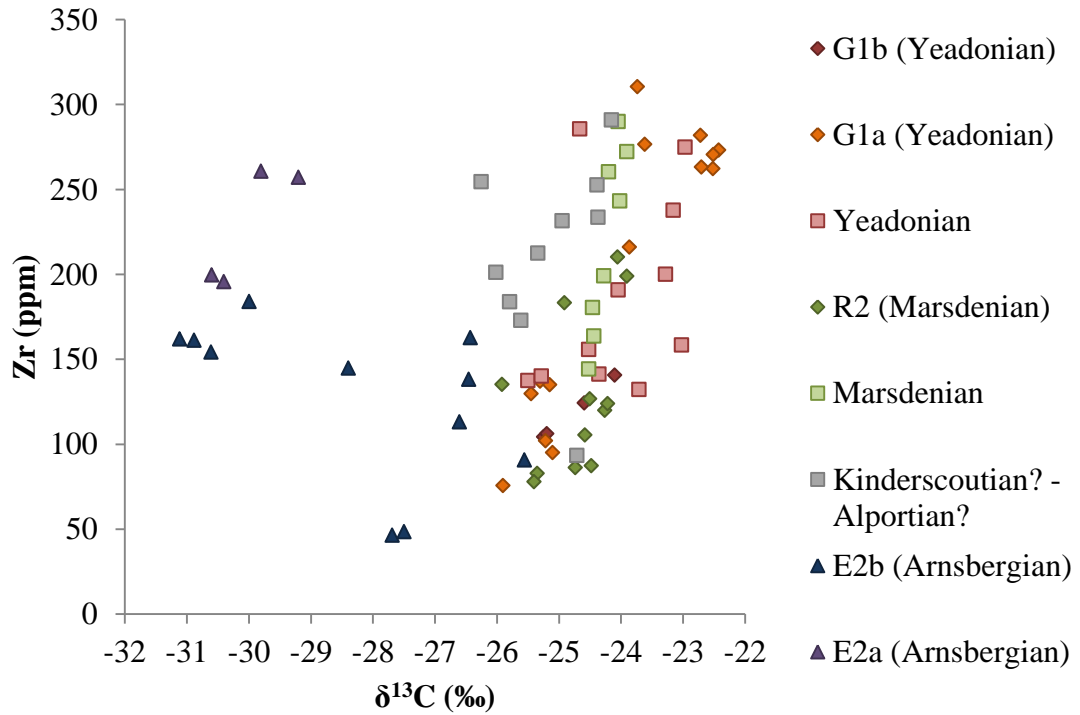
Figure 6-7: Carbon isotopes plotted with Zr concentration. There is a correlation for heavier (more positive) carbon isotopes with age, Yeadonian samples are heaviest, with Arnsbergian lightest. Marine band facies are the exception, and represented by more negative carbon isotope values. There is no strong link between carbon isotope values and Zr including the marine band facies.

There is no correlation between carbon isotope values and Zr concentrations (Figure 6-7). Whilst it is observable that facies has a significant association with Zr concentrations, the Zr concentrations for both Arnsbergian and Yeadonian aged samples can be similar. This temporal shift in carbon isotope values could be indicative of a more significant change.

There is a weak trend between marine band samples, fossiliferous facies, increased CaO (wt %) and low Zr concentrations (Figure 6-8). It is likely that the increased CaO

at marine bands is due to biogenic production of shell fragments. Samples which are not associated with marine bands and have elevated CaO concentrations are likely to have CaO from a detrital or diagenetic source.
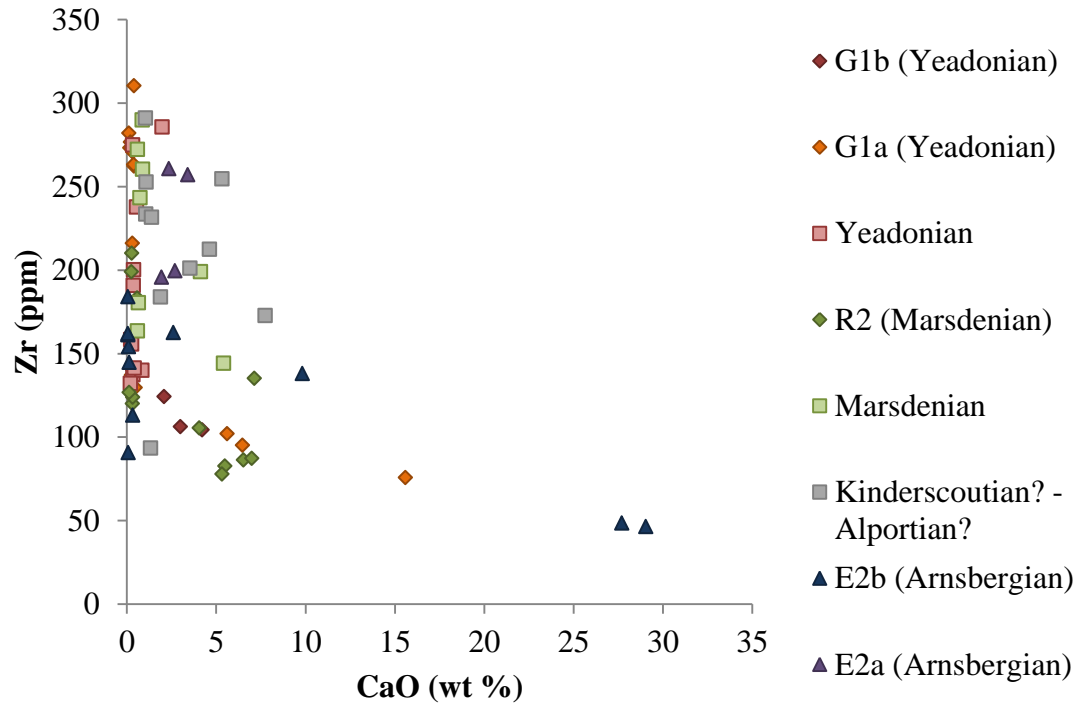
Figure 6-8: CaO plotted against Zr concentrations. There are weak trends between increased CaO and low Zr concentrations, which also correspond with only the marine band facies.

Trace elements (e.g. U/Th, Ni/Co, V/Cr) demonstrate that the Holywell Shale was largely deposited in an oxic water column, with some dysoxic periods and very few samples deposited in anoxic conditions, primarily associated with marine bands often with higher TOC values (Figures 6-9 to 6-11).

Table 6-1: Proposed threshold values for palaeo-redox proxies (not to be applied strictly; adapted from Lazar et al., 2015b; Gross et al., 2015)

Bottom-water oxygenation	U/Th	V/Cr	Ni/Co	TOC/S
Anoxic (0 ml O_2/l H_2O)				
Threshold	1.25	4.25	7	(~ 1.5?)
Dysoxic (0 - 2 ml O_2/l H_2O)				
Threshold	0.75	2.00	5	2.8
Oxic (> 2 ml O_2/l H_2O)				

Figure 6-9: U/Th plotted against carbon isotopes. Using values from Table 6-1, the blue box represents a proxy for oxic conditions of deposition; the yellow box indicates dysoxic deposition; the red box indicates anoxic conditions of deposition. Marine bands within the Marsdenian and Yeadonian appear to be most anoxic. N.B. some data points are missing due to unreadably low values from XRF.
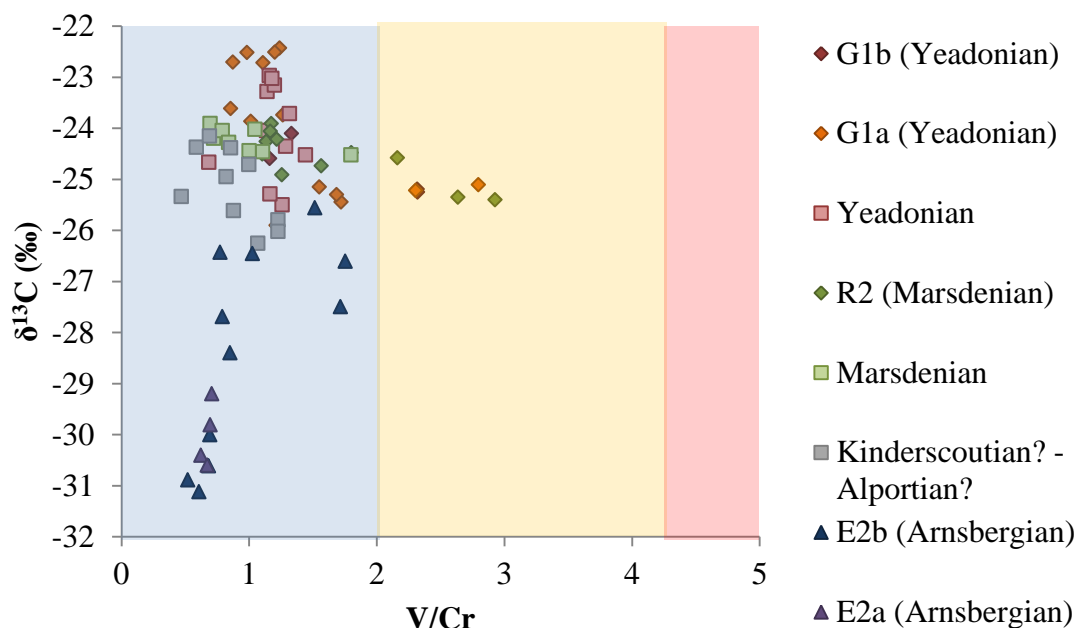
Figure 6-10: V/Cr plotted against carbon isotopes. Using values from Table 6-1, the blue box represents a proxy for oxic conditions of deposition; the yellow box indicates dysoxic deposition; the red box indicates anoxic conditions of deposition. Marine bands within the Marsdenian and Yeadonian appear to be most dysoxic, with most samples oxic and none anoxic. N.B. some data points are missing due to unreadably low values from XRF.
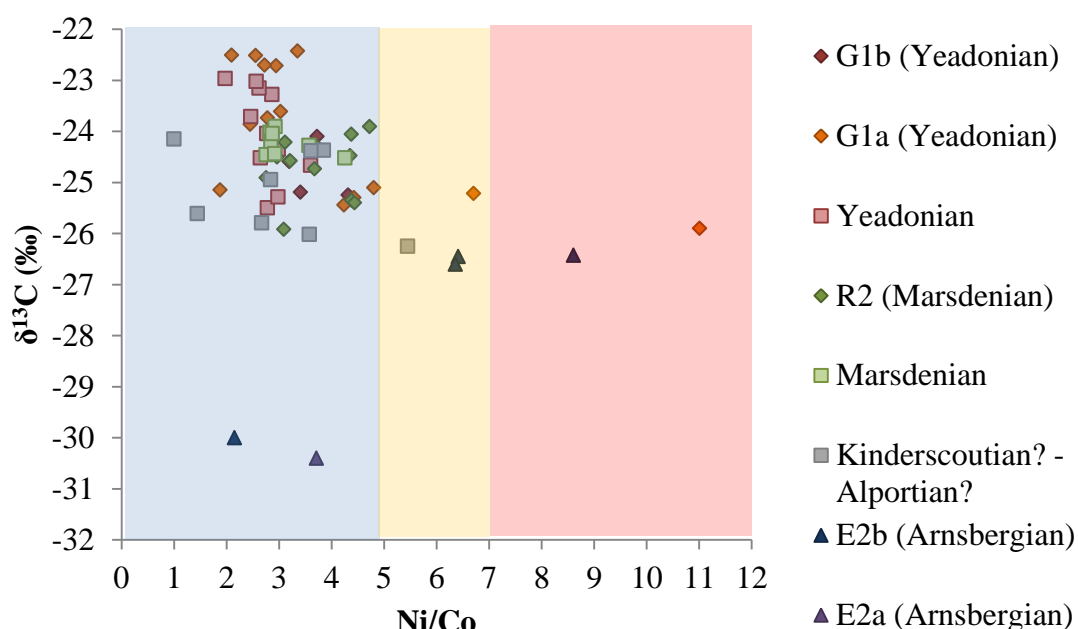
Figure 6-11: Ni/Co plotted against carbon isotopes. Using values from Table 6-1, the blue box represents a proxy for oxic conditions of deposition; the yellow box indicates dysoxic deposition; the red box indicates anoxic conditions of deposition. Marine bands within the

Yeadonian and Arnsbergian appear to be most anoxic, with most samples oxic and few dysoxic. N.B. some data points are missing due to unreadably low values from XRF.

6.4.2: Organic Geochemistry

6.4.2.1: Carbon isotopes

Based on the carbon isotope values recorded within the Holywell Shale and other Namurian shales of the UK, a range of values are used to determine terrestrially derived or marine sourced organic matter. Organic matter with a largely terrestrial influence is commonly in the range from -22 ‰ to -24 ‰, with marine sourced organic matter having a range of isotope values between -30 ‰ and -35 ‰ (Stephenson et al., 2008). Within the Holywell Shale, as previously reported in Chapters 4 and 5 of this thesis, the range of carbon isotopes is between -22 ‰ and -31 ‰. Marine bands, identified as biostratigraphical markers (Figure 6-2 & 6-3), are thought to represent rapid transgression and are often used to signify the maximum flooding surface (Jerrett & Hampson, 2007; Leeder, 1988; Gross et al., 2015; Martinsen et al 1995). The marine bands within the Holywell Shale (Figure 6-2 & 6-3) coincide with the most negative (lightest) carbon isotope values (Figure 6-12 & 6-13). The overall trend in carbon isotopes throughout the Namurian is an increasingly terrestrial supply (heavier isotopes) with marine bands present throughout (Figure 6-12 & 6-13; Stephenson et al., 2008).
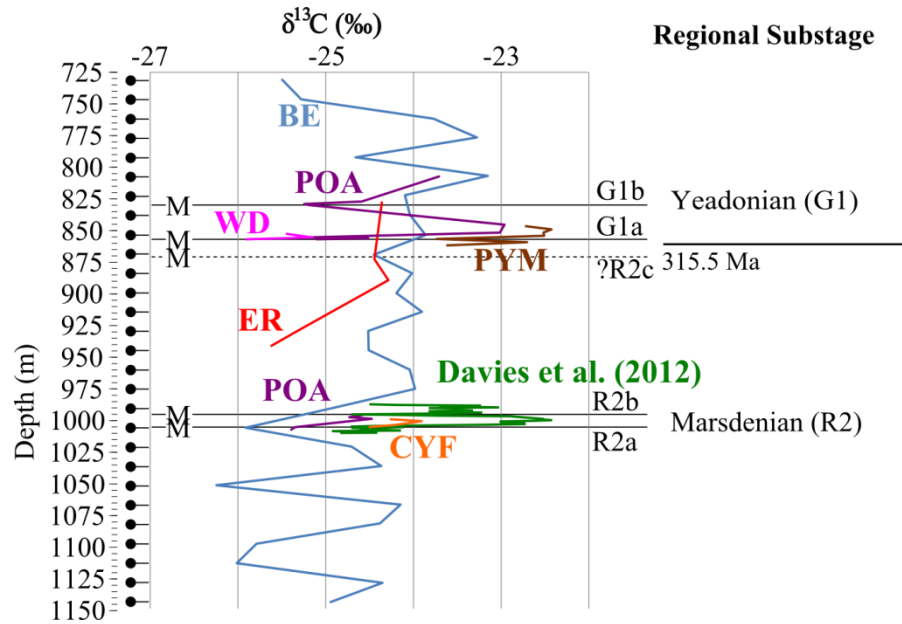
Figure 6-12: δ¹³C variations with depth and time. Depth is based on the Blacon East borehole (BE -blue line) which is the most continuous record of carbon isotope values available. Marine bands from the Holywell Shale allow correlation with other boreholes (Point of Ayr - purple and Erbistock - red) as well as outcrop locations from northeast Wales (Pen-Y-Maes = PYM - brown, Warren Dingle = WD - pink and Coed-Y-Felin = CYF - orange) and Yorkshire (Pule Hill; Davies et al., 2012).
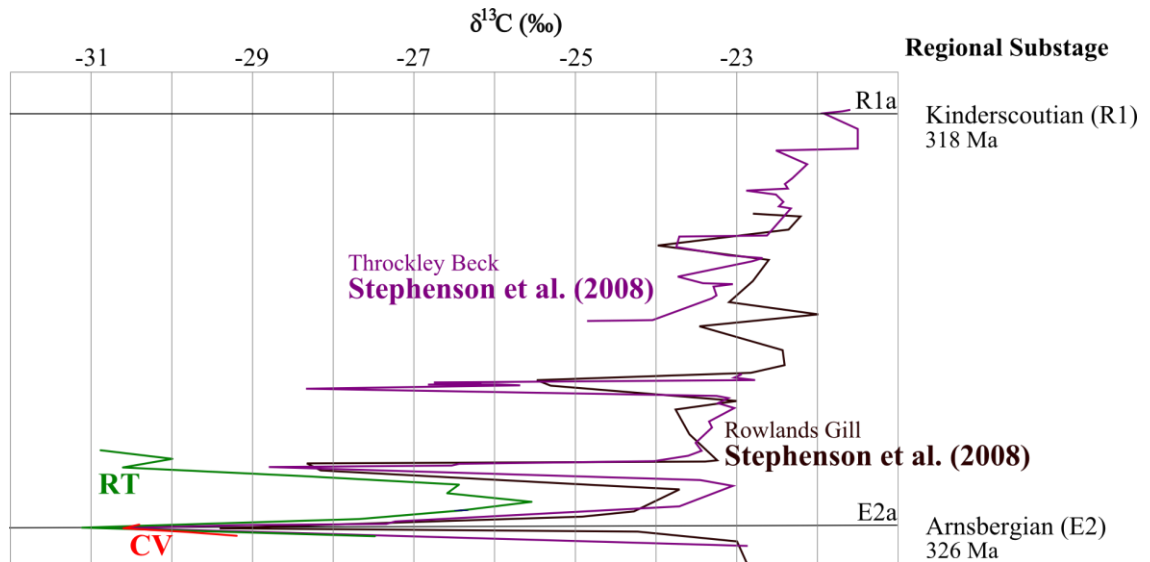
Figure 6-13: δ¹³C variations with depth and time. Marine bands of the Lower Holywell Shale from boreholes (Stephenson et al., 2008 – purple & maroon) allow correlation with outcrop locations from northeast Wales (River Terrig = RT – green, Cegidog Valley = CV – red).
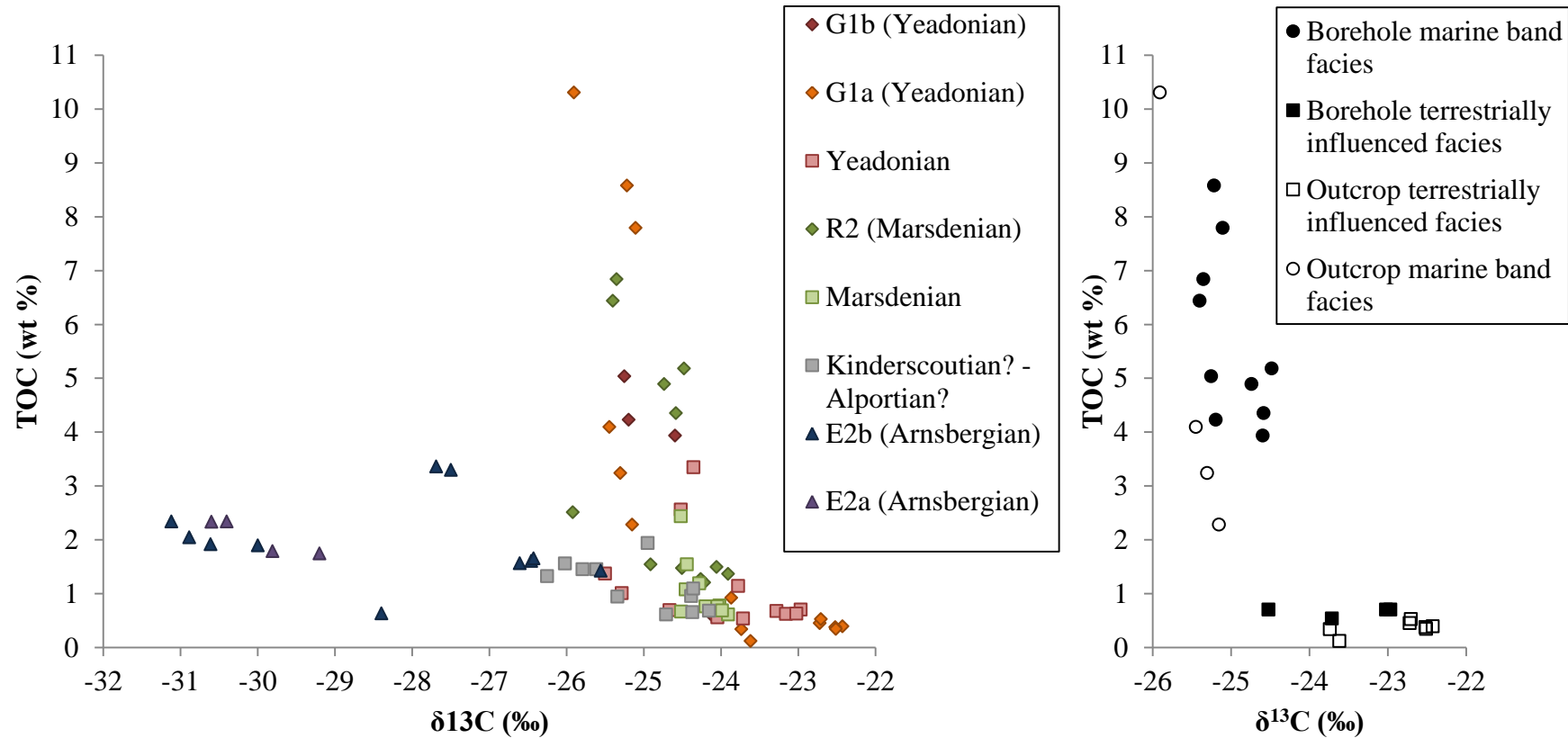
Figure 6-14A (left): Total organic carbon versus carbon isotope composition of organic matter. Higher TOC values occur within marine band facies between -26 ‰ and -24 ‰ isotope values. Holywell Shale samples are highlighted corresponding to which marine band they were sampled from. The samples which were not taken from marine bands (within boreholes) are highlighted as Upper Holywell Shale. Figure 6-14B (right): Total organic carbon versus carbon isotope composition of organic matter (from -26 ‰ to -22 ‰) limited to petrographic samples of the Upper Holywell Shale which have either terrestrially influenced, silt-rich facies; or fossiliferous claystone, marine band facies.

6.4.2.2: Total organic carbon (TOC)

TOC is a key parameter in determining the potential for a mudstone to be considered for shale gas exploration with a minimum value of 2.0 wt % often used (Andrews, 2013; Jarvie, 2012). The Holywell Shale TOC values range from 0.1 wt % to 10.3 wt % (average 2.0 wt %; Appendices A & E). Figure 6-14A shows that TOC values are highest (average 2.6 wt %) between -26 ‰ and -24 ‰ carbon isotope values. A more general trend is that the TOC values increase with increasing marine influence (lighter $\delta^{13}C$; Figure 6-14B).

6.4.2.3: RockEval™

Hydrogen Index is a proxy for H/C ratio which can be used to indicate the hydrocarbon generation potential and kerogen type. Low HI values indicate a low H/C ratio which means that the kerogen in the sample is unlikely to yield large amounts of hydrocarbons. There is a weak correlation between HI and $\delta^{13}C$, showing broadly increasing HI with lighter carbon isotopes (more marine; Figure 6-15A). There is also an increase in HI between -26 ‰ and -24 ‰ carbon isotope values (Figure 6-15B) which corresponds to the increase in TOC observed in Figure 6-14A. This positive trend in HI values and TOC values corresponds with the marine bands sampled from boreholes and outcrops (Figure 6-2 & 6-3). This trend is exaggerated by lithofacies variations which demonstrate the strongest marine influenced facies with the highest HI and TOC and silt-rich facies with the strongest terrestrial influence with lower HI and TOC values (Figure 6-4 & 6-15B).
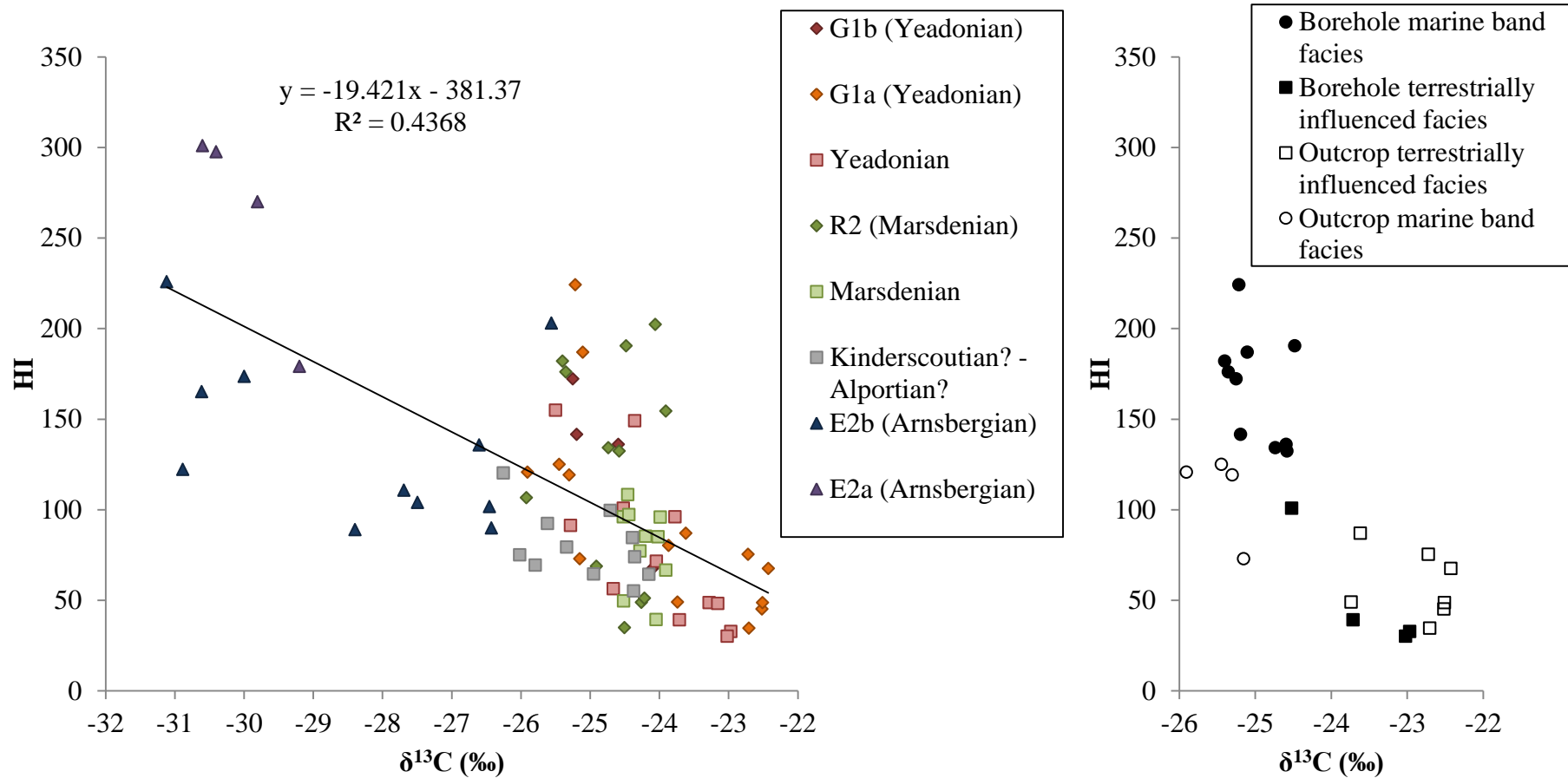
Figure 6-15A (left): Hydrogen Index (HI) versus the carbon isotope composition of organic matter. There is a weak positive correlation of more negative carbon isotope values with increasing HI values. Figure 6-15B (right): HI versus the carbon isotope composition of organic matter for the Upper Holywell Shale samples which correspond to petrographic samples. The samples with the most negative carbon isotope values correlate with the highest HI samples, which are fossiliferous, clay-rich marine band facies from petrographic analysis. The most positive carbon isotope samples correlate with the lowest HI values and silt-rich terrestrially influenced facies (Figure 6-4).

The kerogen type for the Holywell Shale samples can be calculated using HI and T_{max} from RockEval™ (Figure 6-16). Whilst there is a spread in the data from each stage throughout the Namurian, there are some trends. The majority of Yeadonian samples are composed of Type III gas-prone kerogens, whereas Marsdenian samples are Type II/III. The Arnsbergian samples range from Type III to Type II (E2a marine band). Most samples lie in the oil window, with some samples immature for hydrocarbon generation (Figure 6-16). The sample with erroneously high T_{max} value (499 °C) is due to low S_2 values giving a broad, unclear peak (Figure 6-16 & 6-17; Appendices A & E).
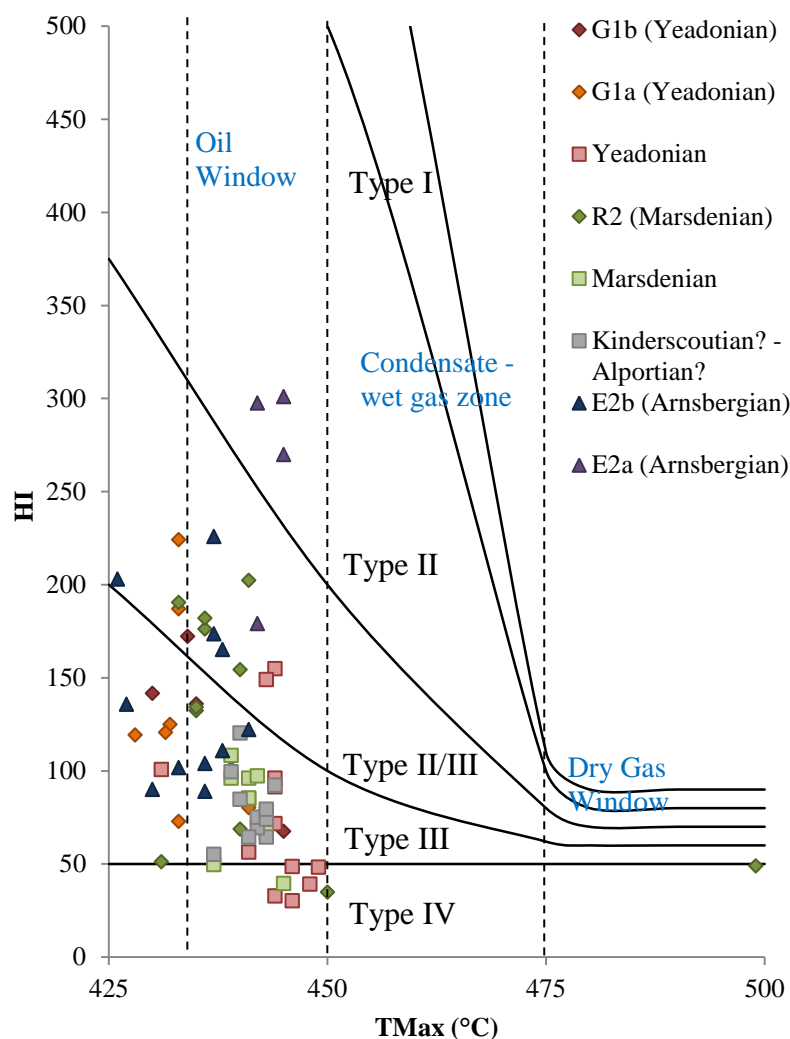
Figure 6-16: T_{max} vs hydrogen index (HI) data showing the kerogen type and range of thermal maturity within the Holywell Shale samples.

The potential for the Holywell Shale to yield further hydrocarbons can be assessed using S_2 values from RockEval™. Figure 6-17 shows that increases in TOC values correspond with an increase in S_2 values. The majority of samples have good or better TOC values (> 1 wt %), with a third of samples excellent (> 2 wt %). However, only five samples have excellent (> 10 mg HC/g rock) S_2 values, with the majority plotting as poor (< 2.5 mg HC/g rock). The boreholes and outcrops have similar comparable values of TOC and S_2. The hydrocarbon potential for different kerogen type demonstrates that Type II/III and Type III kerogens have the best potential in terms

their high TOC values corresponding with high S_2 values (Figure 6-17). However, the Type II samples have lower TOC values compared to the Type II/III and Type III samples. This suggests the samples with the most organic matter content (TOC) are gas prone Type III kerogens. These samples occur predominantly in the marine band facies of the Upper Holywell Shale, whilst the Type II facies occur only in the Arnsbergian (Lower Holywell Shale) facies. The Type IV inert kerogens are typically low in S_2 and TOC (Figure 6-17).
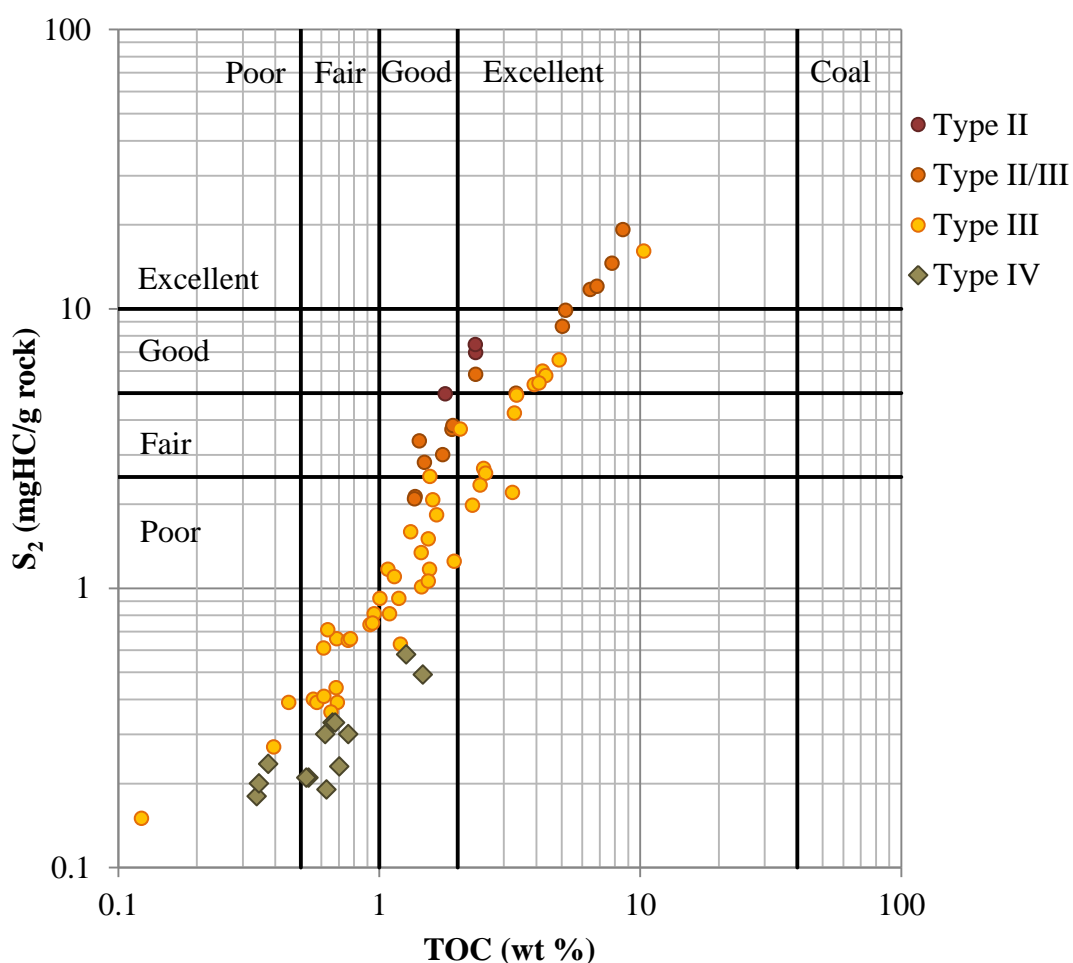
Figure 6-17: TOC versus S_2 (hydrocarbons formed from thermal decomposition of kerogen; from RockEval™). The higher the S_2 values the greater the potential for hydrocarbon generation. Samples are separated according to kerogen type (taken from Figure 6-16).

The overall trend for organic matter throughout the Namurian from the organic geochemical data is for a predominantly gas prone kerogen type with the greatest generation potential in the marine band facies of the Upper Holywell Shale.

6.5: Discussion

6.5.1: Variations across a single marine band (G1a)

Samples from both outcrop (at Pen-Y-Maes and Warren Dingle) and in boreholes (Point of Ayr and Blacon East) contain goniatites from the G1a marine band which have been previously identified (Figure 6-2 & 6-3; Magraw, 1954; Waters & Condon, 2012).

The G1a marine band appears to vary in thickness across the northeast Wales region. At outcrop, exposure is often small and the extent of the marine band is less easy to constrain (Warren Dingle and Pen-Y-Maes). Within the Point of Ayr borehole, the G1a marine band occurs in samples 7 and 9 (POA7 & POA9) and is marked at each point by marine fossils occurring < 3 m thickness of dark, fossiliferous clay-rich mudstone. The lithofacies which occur at or around the marine band often contain non-goniatite fossils and fish bones (e.g. sample POA 8 containing lingula brachiopod and fish debris). Succeeding the marine band, a relatively rapid transition to silt-rich facies (POA 6 and Pen-Y-Maes samples) occurs. This is probably linked to a transition to lowstand deposition.

**Table 6-2: Table of geochemical parameters from fossiliferous, clay-rich lithofacies which
occur at the G1a marine band in both borehole and outcrop.**

Clay-rich (fossiliferous) facies	TOC (wt %)	$\delta^{13}C$ (‰)	C/N	HI	Zr (ppm)	Si/Al	U/Th
Point of Ayr 7	8.6	-25.2	51.0	224.2	102.0	2.6	1.3
Point of Ayr 9	7.8	-25.1	43.2	187.0	95.2	2.6	0.7
Warren Dingle 2	3.2	-25.3	25.0	119.2	137.2	2.6	0.6
Warren Dingle 4	10.3	-25.9	50.3	120.7	75.7	2.8	2.5

**Table 6-3: Table of geochemical parameters from silt-rich lithofacies which occur at the
G1a marine band in both borehole and outcrop.**

Silt-rich facies	TOC (wt %)	$\delta^{13}C$ (‰)	C/N	HI	Zr (ppm)	Si/Al	U/Th
Point of Ayr 6	0.6	-23.0	6.6	30.2	158.4	3.0	-
Pen-Y-Maes 3	0.4	-22.5	6.2	45.2	262.4	3.3	0.1
Pen-Y-Maes 5	0.3	-23.7	6.3	49.0	310.5	3.5	0.1

In samples found at or around marine bands which are contemporaneous these silt-rich
and clay-rich facies can be observed. At the G1a marine band it can be observed that
they have significantly different geochemical attributes in each case (Tables 6-2 and 6-
3). The clay-rich facies which occur with abundance in fossiliferous material have high
TOC values, and carbon isotope values which represent a relatively more marine source
of organic matter (Table 6-2). The organic matter content of the G1a clay-rich,
fossiliferous samples from both the outcrop (Warren Dingle, average 5 wt %) and
borehole (Point of Ayr, average 8.2 wt %) samples is significantly higher than the
general TOC average for the Holywell Shale (2 wt %). These clay-rich samples also
have high HI values and high ratios of C/N indicating a high productivity at the time of
deposition and water column hypoxia enabling better preservation (or lack of oxidation
– which corresponds with elevated U/Th ratios in some cases) of organic matter (Table

6-2; e.g. Murphy et al., 2000). The clay-rich samples also correlate with lower Zr concentrations and relatively low Si/Al ratios (Table 6-2).

Silt-rich lithofacies deposited at the G1a marine band are in contrast to the clay-rich facies and indicate an environment with higher energy of deposition (with current ripples and graded bedding often observed in samples: Point of Ayr 6 and Pen-Y-Maes samples; Figure 6-18). The samples contain an abundance of terrestrially sourced minerals (large detrital angular quartz grains and feldspar grains) and organic matter observed in the samples is fragmentary and dispersed throughout the sample. The TOC values for the silt-rich facies are very low; the organic matter contained is oxidised and poorly preserved indicated by low HI values and U/Th ratios (Table 6-3). The silt-rich and higher energy depositional setting indicates an increase in siliciclastic input, with relatively high Si/Al ratios and the highest Zr concentrations recorded (Table 6-3). The carbon isotope values for the silt-rich facies are the most positive (suggesting the organic matter contained is likely to be strongly terrestrially influenced/derived; Table 6-3).
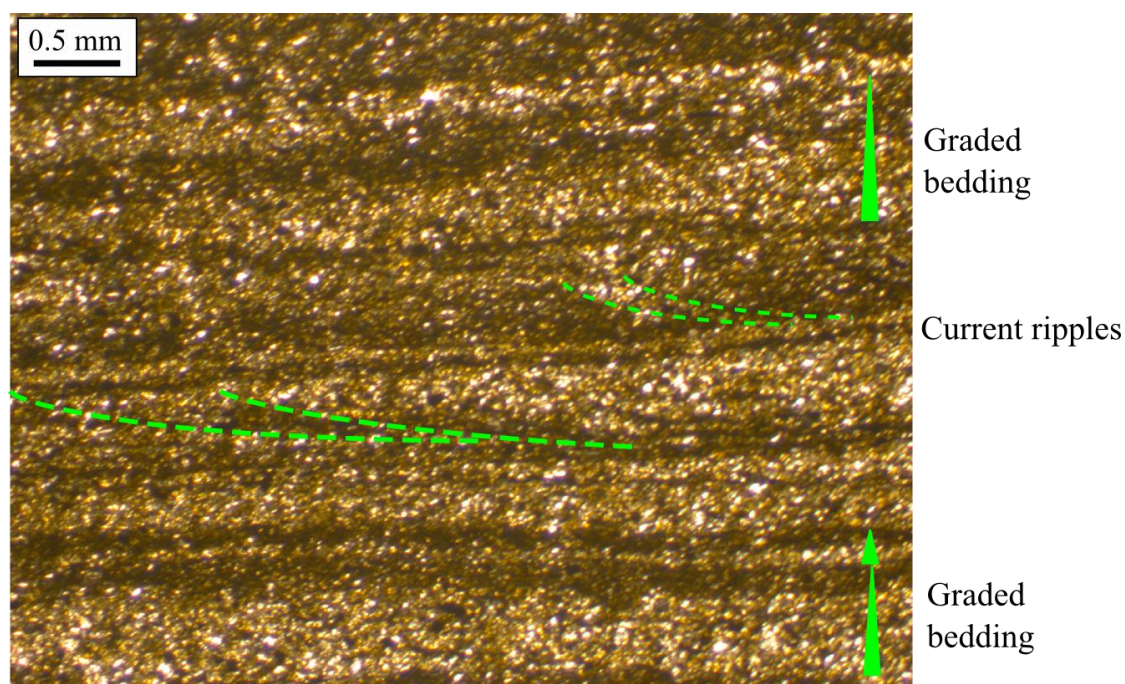
Figure 6-18: Pen-Y-Maes silt-rich lithofacies with graded bedding and current ripples (suggesting flow direction from left to right).

Samples which occur at the G1a marine band show a wide range in carbon isotope values (-25.9 to -22.4 ‰; average -23.8 ‰). However, when the trend of these isotope values are plotted (Figure 6-12) they correlate with the positive and negative carbon isotope excursions seen within the borehole records. The carbon isotope variations at the G1a marine band are strongly linked to facies. However, there are variations in the carbon isotope values and other geochemical parameters within samples of the same facies (clay-rich: Table 6-2; silt-rich: Table 6-3). This variation in carbon isotope values could be due to the position of the outcrops in relation to the paleogeography of the Pennine Basin at the time of deposition, with the terrestrial dominated Millstone Grit Group (locally, the Gwespyr Sandstone) advancing from the north east introducing significantly more terrestrially derived minerals and organic matter to the basin (Figure 6-19).
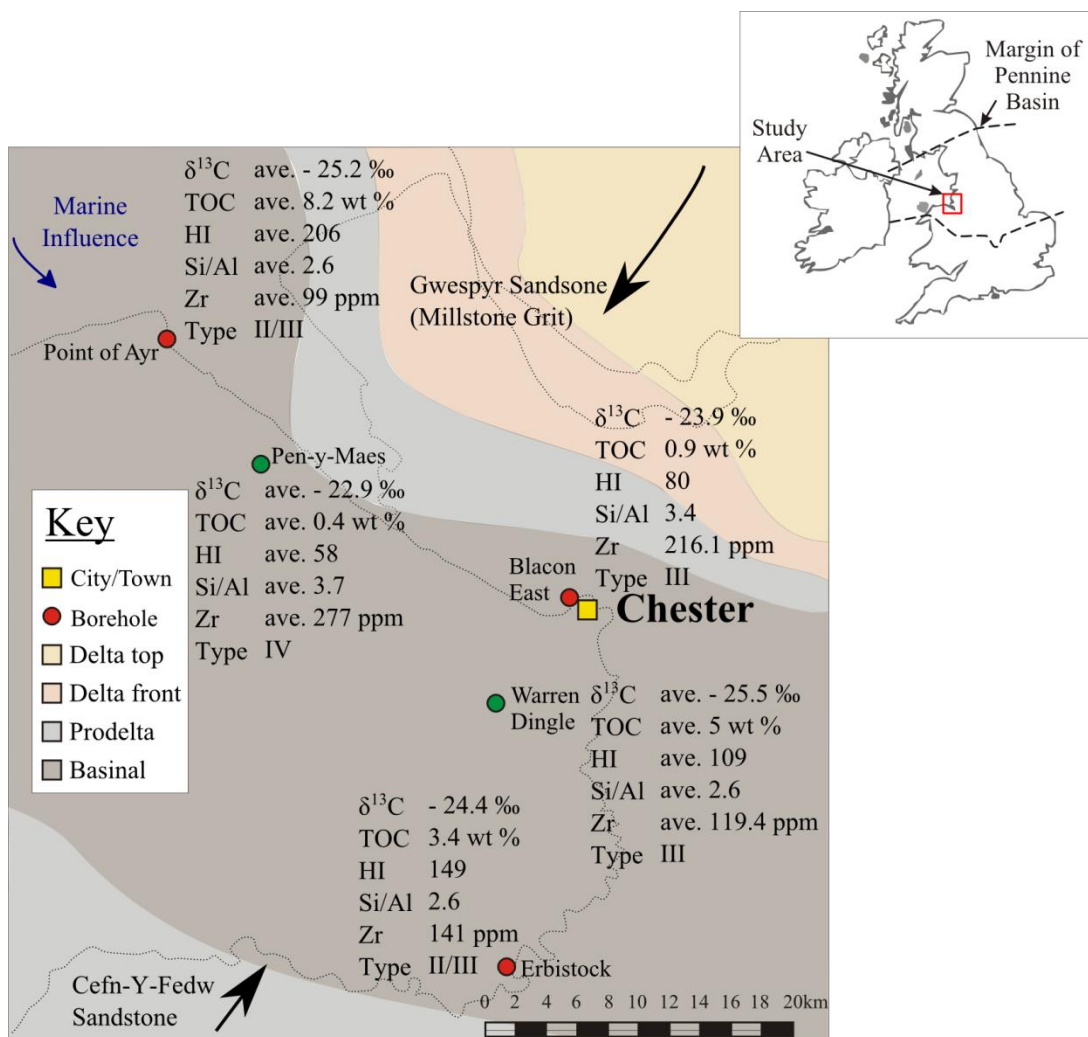
Figure 6-19: Palaeogeographical reconstruction for the G1a marine band (Yeadonian - 315 Ma) in northeast Wales. Combining the lithofacies observation with the trends observed in the carbon isotope values (Figure 6-12), the other geochemical results and petrographic analysis (Figure 6-4), the variations in terrestrial vs marine influence can be used to refine the palaeogeographic interpretation of Fraser & Gawthorpe (2003).

The geochemical data from each borehole and outcrop which are contemporaneously deposited around the G1a marine band in the Yeadonian, when combined with a palaeogeographical reconstruction of the Yeadonian of northeast Wales reveal spatial variations. It is apparent from samples which occur at the Warren Dingle and Point of Ayr locations that the lithofacies and organofacies have significant marine influence (Figure 6-19; Tables 6-2 & 6-3). Contrary to this are samples from Pen-Y-Maes, which

correlate with the sample POA 6 which occurs above the main G1a fauna in the Point of Ayr borehole.

Within other boreholes (Blacon East and Erbistock) the G1a marine band was not directly sampled, this makes direct comparison between these datasets difficult. However, Figures 6-12 & 6-19 demonstrate that the carbon isotope values (-24.4 ‰ to -23.9 ‰, average -24.1 ‰) for both Blacon East and Erbistock correlate well with the values for the Point of Ayr borehole (average -24.5 ‰).

The samples from Blacon East and Erbistock were cuttings and as such have no petrography. Using the geochemical data from samples at the G1a marine band within these boreholes (Blacon East and Erbistock) it is possible to predict the lithofacies and organofacies present within these samples and correlate them spatially (Figure 6-19).

Geochemical values from the sample within the Blacon East borehole correlate most favourably with the samples from Pen-Y-Maes (and the sample from Point of Ayr 6) with similarly low TOC, carbon isotope values, and low HI indicating organic matter input was low and is poorly preserved (Figure 6-19). The Si/Al and Zr concentrations also correlate with the silt-rich lithofacies of Pen-Y-Maes (and the sample from Point of Ayr 6). Similarly, the Erbistock sample correlates quite well with the Point of Ayr and Warren Dingle samples, although carbon isotope and Zr values suggest a slightly less strong marine influence (Figure 6-19). The ability to predict the facies using geochemical analyses has far reaching consequences for unconventional shale gas exploration, including the prediction of "sweet spot" horizons within the UK Carboniferous basins.

6.5.2: Variations across the Holywell Shale

The Blacon East borehole represents the largest dataset, in terms of both the amount of samples taken and the time period covered, within the Holywell Shale (Figure 6-2 & 6-3). This borehole forms the basis of comparison in geochemical data between other borehole and outcrop datasets throughout the Namurian (e.g. Figure 6-12).

The Blacon East borehole shows an overall trend towards more positive carbon isotope values through time (Figure 6-12). This is likely to be due to an increase in terrestrial organic input through time due to the advancement in millstone grit deltaic environments from the north east (Figure 5-1; Fraser and Gawthorpe, 2003). This trend towards more positive carbon isotope values is also mirrored in other boreholes (Erbistock and Point of Ayr; Figure 6-12). Erbistock shows a broader trend than that of Blacon East which is likely to be due to the limited sampling density (Figure 6-2).

The Point of Ayr borehole shows more pronounced excursions between positive and negative carbon isotope values surrounding the G1a and G1b marine bands, but not at the R2a and R2b marine band (Figure 6-12). The Blacon East borehole on average shows more terrestrial sediment input (Si/Al, 4.6; Zr, 208.4, CaO, 1.6) than the Point of Ayr borehole (Si/Al, 3; Zr, 121, CaO, 3.6); in line with the palaeogeography described at the G1a marine band (Figure 6-19). However, immediately following the G1a marine band a significant positive carbon isotope excursion occurs within the Point of Ayr which is not seen within the Blacon East record. The large positive carbon isotope excursion is also seen within the Pen-Y-Maes outcrop record (Figure 6-12) which is geographically closer to the Point of Ayr than Blacon East borehole (Figure 6-1 & 6-19). Therefore the positive excursion is likely to record a palaeogeographically limited event (such as a turbidite deposit) rather than a basin wide fluctuation (such as a

significant marine regression). SEM petrographic images from samples from borehole and outcrop (Point of Ayr and Pen-Y-Maes) at the positive carbon isotope excursion show similar attributes. Both contain predominantly silt sized grains of quartz, fragmentary organic matter and small quantities of micas and other aluminosilicates (Figure 6-4). This supports a possible turbidity current being shed from the advancing deltas of the feldspathic Millstone Grit Group to the western part of the Holywell area (Figure 6-19).
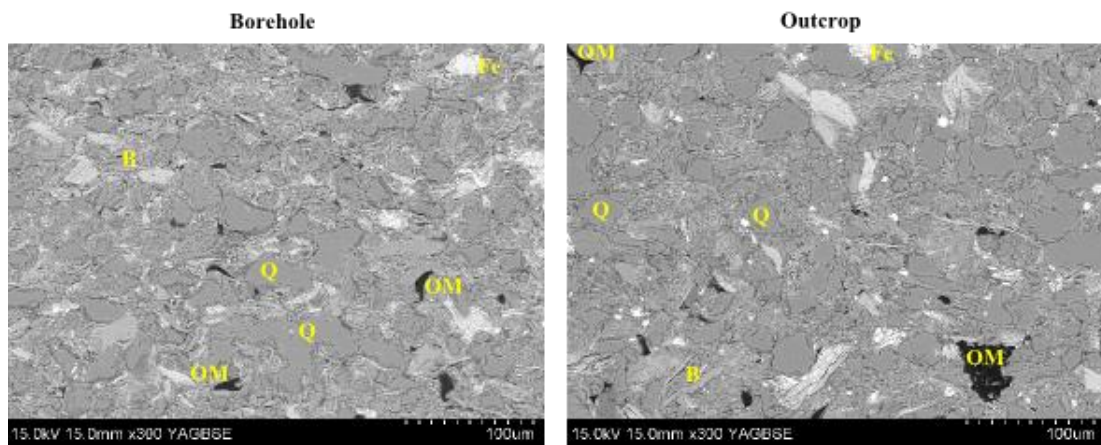
Figure 6-20: Borehole (Point of Ayr) and outcrop (Pen-Y-Maes) SEM images of heavy carbon isotope samples between G1a and G1b marine bands (Figure 6-4). Both samples are dominated by silt-sized quartz grains with fragmentary organic matter. Q = quartz, OM = organic matter, B = biotite mica, Fe = iron oxide.

In comparison to other studies of carbon isotopes from the Namurian Pennine Basin (Davies et al., 2012 & Stephenson et al., 2008) the carbon isotope records from both outcrop and core material show the same trends (Figure 6-12 & 6-13).

Between the R2a and R2b marine bands Blacon East, Point of Ayr and Coed-Y-Felin records show the same trend as the reported values for Pule Hill (west Yorkshire) outcrop (Figure 6-12; Davies et al., 2012). Whilst the trends appear similar the average $\delta^{13}C$ values for each record varies (Blacon east, -25.4 ‰; Point of Ayr, -25 ‰; Coed-Y-Felin, -24.2 ‰; Pule Hill, -23.4 ‰; Davies et al., 2012). These variations are likely

to be a result of different paleogeographic positions within the Pennine Basin and/or
similar changes in the depositional mechanisms at each location (Fraser & Gawthorpe,
2003; Davies et al., 2012; Figure 5-1).

Whilst the carbon isotope trends indicate marine and terrestrial organic matter input
which varies through the Namurian, a significant control on carbon isotope values
appears to be facies (as noted also in the Marsdenian of northern England by Davies et
al., 2012). Throughout the Holywell Shale there are significant changes across
identified marine bands and non-marine band facies. Lithofacies variations are broadly
from clay-rich fossiliferous facies to silt-rich facies. However, there is an underlying
broad trend in carbon isotopes from Arnsbergian to Yeadonian towards more positive
isotopes (which is independent of facies control). This suggests a change in carbon
isotope values from marine to terrestrial, which would correspond to a reduction in
accommodation space within the basin combined with the advance of northerly sourced
Millstone Grit deltas supplying an increasing amount of terrestrial material (minerals
and organic matter). However, it is possible that the trend is linked to a more significant
variation in carbon isotope values.

Figure 6-13 shows the similarity in carbon isotope trends between two outcrops of the
Holywell Shale (River Terrig and Cegidog Valley) with the two borehole records of
Stephenson et al. (2008; Throckley Beck and Rowlands Gill- northeast England)
around the E2a marine band. The similarity in these records (Holywell- River Terrig,
Cegidog Valley and Stephenson et al., 2008- Throckley Beck and Rowlands Gill) are
unlikely to have related deposition mechanisms due to the geographical separation and
lithological variation, thus the record is more likely to represent perturbation in the
global carbon cycle. The carbon isotope records of Throckley Beck and Rowlands Gill
show an overall trend in positive carbon isotopes, which was also observed within the

Blacon East borehole carbon isotope record albeit at different time periods (Figure 6-12 & 6-13). The similar trend noted within the records, whilst different in time, may be due to the same effect with the delay in the Holywell Shale samples related to the palaeogeography of the UK during the Carboniferous as the northeast England (location of Stephenson et al., 2008 data) was influenced by the advancing millstone grit deltas earlier (Fraser & Gawthorpe, 1990; 2003).

The outcrops River Terrig and Cegidog Valley represent the most marine samples from the whole of the Holywell Shale (Figure 6-14A & B). Within the Lower Holywell (Outcrop- River Terrig, Cegidog Valley; Appendices A & E) a broad increase in TOC values with lighter carbon isotope values (more marine; Figure 6-14A & B). In the Upper Holywell (Outcrop- Pen-Y-Maes, Warren Dingle, Coed-Y-Felin and Borehole-Point of Ayr, Blacon East, Erbistock) the $\delta^{13}C$ values show a less marine influence than the Lower Holywell and show a significant enrichment in TOC values occurring between -26 ‰ and -24 ‰ carbon isotope values (Figure 6-14B). These high TOC values directly relate to the marine bands G1a, G1b, R2a and R2b recorded in both outcrop and borehole material (Figure 6-14A & B; Appendices A & E). The enrichment may be due to the same mechanism described for the G1a marine band which suggest high productivity at the time of deposition and water column hypoxia within the basin at these time intervals (marine bands) although the effect varies due to palaeogeographical location (e.g. Murphy et al., 2000). This is further supported by the elevated HI values (better preservation of OM; Figure 6-15A & B) which correlate to the marine bands between -26 ‰ and -24 ‰ carbon isotope values indicating enhanced preservation of organic matter in association with marine organic matter supply. High HI values are also noted in association with samples from the E2a marine band suggesting a similar mechanism may be in place (Figure 6-15A & B).

The change in carbon isotope values between the marine band facies of the Lower Holywell Shale (E2 – Arnsbergian aged samples) and Upper Holywell Shale (Marsdenian and Yeadonian aged samples – R2 to G1b) demonstrates a shift in carbon isotopes to more positive values at marine bands (Figures 6-14A & B). This also correlates with a shift in carbon isotope values for silt-rich (non-marine band) facies to more positive values (Figures 6-4). Samples from other UK locations mirror this trend in carbon isotope values shifting throughout the Namurian, from more negative values in the Arnsbergian to more positive values in the Marsdenian and Yeadonian (Figures 6-12 & 6-13).

Throughout the Namurian there were widespread periods of southern hemisphere glaciation of Gondwana (Isbell et al., 2003). These glaciations are recorded in deposits in South America and eastern Australia, as well as incised valleys suggesting globally large fluctuations in sea-level (Fielding et al., 2008; Gonzalez, 2001; Rygel et al., 2008). As well as this the carbon isotope signature of carbonate brachiopod shells from across the USA to Russia and China shows a positive shift across the Namurian (Frank et al., 2008).

The glaciation-eustatic fluctuation in sea level has been recorded within the UK as cyclical events of transgression and regression represented by changes from mudstones with marine ammonoid fauna to paralic sandstone facies (Ramsbottom, 1977). The change in carbon isotope values from marine band facies within the Holywell Shale from more negative (-30 ‰; Arnsbergian) to a more positive (-25 ‰; Marsdenian and Yeadonian) demonstrates that a global shift in carbon isotope values has occurred throughout the Namurian.

6.6: Conclusions

Samples from the Holywell Shale demonstrate that it is possible to correlate lithofacies and geochemical variations across marine bands within the same basin, and across the larger area of the Carboniferous Pennine Basin. The lithofacies and organofacies sampled allowed two end-members to be identified within the Holywell Shale; a marine band facies which was clay-rich, fossiliferous and a silt-rich facies with sedimentary features and bedding.

The two end-member facies have distinctive geochemical trends. The clay-rich, fossiliferous facies has the highest organic matter content (TOC), the strongest marine carbon isotope signatures (more negative) and evidence (using trace element proxies e.g. U/Th) for a hypoxic environment of deposition with high primary production (e.g. high C/N ratios) as well as low siliciclastic inputs. Whereas the silt-rich facies contained very low organic matter content (TOC), the strongest terrestrial carbon isotope signatures (more positive) and evidence (using trace element proxies) for an oxic environment of deposition further supported by the poor preservation of organic matter (low HI) as well as increased terrestrial inputs of minerals and organic matter (e.g. silt-sized detrital quartz and feldspar grains, high Zr concentrations and fragmentary organic matter).

The results from the Holywell Shale demonstrate that it is possible to correlate specific data (such as TOC, HI, Zr etc.) as well as general trends ($\delta^{13}C$) between outcrop and borehole material from an individual marine band (G1a) and across multiple marine bands within a mudstone succession. This is significant as a comparison of geochemical data from core samples (where detailed petrographical characterisation is

possible) to cuttings can be used as a predictive tool to infer a lithofacies, organofacies and environment of deposition for the cutting material.

The variation in carbon isotope values across the Holywell Shale is strongly influenced by changes in lithofacies present. The marine band samples from the Marsdenian and Yeadonian within the Holywell Shale are significantly more positive than the most marine signatures of the Arnsbergian. The carbon isotope data shows that there is an underlying trend towards more positive values throughout the Namurian which correlates with published examples from across the UK Carboniferous Pennine Basin (Davies et al., 2012; Stephenson et al., 2008). This shift in carbon isotope values across the Namurian can be attributed in part to local (i.e. UK) factors such as the reduction of accommodation space through time due to the progradation of Namurian deltas and reduced thermal subsidence of the basin. However, the carbon isotope trend seen within the Holywell Shale strongly correlates with the timings of major southern hemisphere glaciation (C2 glaciation; Fielding et al., 2008; Rygel et al., 2008) and as such is likely to reflect the global positive shift in carbon isotope values.

Chapter 7:

Thesis Summary

7.1: Introduction

Throughout this thesis the principle focus has been the application of petrographic and geochemical techniques in assessing the suitability of the Holywell Shale as a potential shale gas resource. Through this key scientific theories have been tested, and in the process of determining whether the Holywell Shale holds any potential as a future shale gas resource for the UK, greater insights have been gained into the deposition of the Holywell Shale within the complex setting at the south western fringe of the Namurian Pennine Basin. Through organic and inorganic geochemical observations combined with detailed petrographic observations show the Holywell Shale to have a complex depositional setting. The results of this research can be applied to understanding the wider science of mudstones and unconventional exploration.

In this chapter the main findings from these studies are brought together, methodological limitations are discussed (in particular around some work that was undertaken but did not feature in the results chapters) and the opportunity for future work is suggested.

The Holywell Shale was characterised using a combination of techniques:

- Organic geochemistry (e.g. TOC, RockEval™, $\delta^{13}C$) was used to characterise the source, quantity and preservation of the organic matter within the mudstone. The key method used throughout all chapters of this thesis to determine organic matter source was carbon isotopes ($\delta^{13}C$). The main indication this method provided was the separation of the organic matter present as being from a marine or terrestrial source(s). The key method used throughout to determine the quantity of organic matter was TOC (present

day) analysis. RockEval™ and the associated parameters (e.g. HI, OI, T_{max}) was used to describe the kerogen type present, the degree of preservation of the organic matter and in places used to indicate the source of the organic matter.

- Inorganic geochemistry was used to characterise the mineralogy and trace elemental composition of the mudstones. This allowed the determination of mineral origins (from detrital, diagenetic, or biogenic sources) supporting petrographic analysis (using proxies such as Si/Al and Zr concentration); as well as providing further information about the oxygen state of the water column and sediment at the time of deposition (using proxies such as V/Cr and Ni/Co).

- Petrography using visual analysis of textures under natural light, microscopy using transmitted light and electron microscopy were used to characterise the mudstones according to lithofacies and organofacies (after Macquaker & Adams, 2003). Lithofacies and organic matter observations were then used to support the organic and inorganic geochemical observations previously described.

7.2: Deposition of the Holywell Shale during the Namurian (326.5 to 314.5 Ma)

The Holywell Shale represents a mudstone sequence with highly variable organofacies and lithofacies. A varied supply of minerals and organic matter from both terrestrial and marine sources was observed using organic, inorganic geochemistry and petrography. Variations in organic matter and mineral supply between the Upper and Lower Holywell Shale described in Chapters 4, 5 and 6 reflect the effect of reduced thermal subsidence of the Namurian basins leading to a

reduction in accommodation space with an increase of terrestrially derived minerals from prograding deltas (from both the north and south of the basin) and a reduction in the amount of marine sourced organic matter from the Lower (Pendleian to Alportian) to Upper (Kinderscoutian to Yeadonian) Holywell Shale.

Lithofacies variations within the samples coincided with marine bands, samples which occurred at marine bands and/or contained marine goniatite microfossils were characterised by lighter carbon isotope signatures (particularly prevalent in the Lower Holywell Shale samples). Samples which were not strongly marine influenced (between marine bands, characterised by heavier isotopic signatures) correlated with silt-rich lithofacies which were often coarser grained and had a significant amount of angular immature terrestrial sediment input (e.g. feldspars, iron oxide, titanium) and correlated with high concentrations of zirconium (likewise, more marine carbon isotope ratios correlated with low zirconium concentrations). This correlation between lithofacies, organic matter input, carbon isotope values and zirconium concentrations directly supports the observations of Davies et al. (2012) in similarly aged mudstones to the north east of the study area (Marsdenian age, ~ 316 Ma; west Yorkshire, UK).

The variation in carbon isotope values across the Holywell Shale is strongly influenced by changes in lithofacies present. The marine band samples from the Marsdenian and Yeadonian within the Holywell Shale are significantly more positive than the most marine signatures of the Arnsbergian. The carbon isotope data shows that there is an underlying trend towards more positive values throughout the Namurian which correlates with published examples from across the UK Carboniferous Pennine Basin (Davies et al., 2012; Stephenson et al., 2008). This shift in carbon isotope values across the Namurian can be attributed in part to local

(i.e. UK) factors such as the reduction of accommodation space through time due to the progradation of Namurian deltas and reduced thermal subsidence of the basin. However, the carbon isotope trend seen within the Holywell Shale strongly correlates with the timings of major southern hemisphere glaciation (C2 glaciation; Fielding et al., 2008; Rygel et al., 2008) and as such is likely to reflect the global positive shift in carbon isotope values.

7.3: The Hydrocarbon Potential of the Holywell Shale

Understanding the depositional environment is vital in understanding the reservoir quality and, therefore, the hydrocarbon potential of the Holywell Shale as an unconventional source-rock reservoir.

Using proposed values for source-rock reservoir evaluation parameters from experience in the US (e.g. Charpentier & Cook, 2011; Dembicki, 2009; Jarvie, 2012) it was possible to determine the potential of the Holywell Shale as a source-rock reservoir. The parameters focus around having a suitable type of organic matter (ideally kerogen Type II), the required minimum quantity of organic matter (present day TOC values greater than 2 wt %), and the maturity of the organic matter present (within the oil/gas window). In addition to the organic matter requirements there are also mineralogical constraints and rock properties (such as desirable porosity and permeability values) to consider in order for successful hydraulic fracturing to economically produce the hydrocarbons. As discussed in Chapters 2, 4, 5 and 6 of this thesis with the conclusions that the Holywell Shale samples demonstrate highly variable supply and preservation of organic material both temporally and spatially throughout the Namurian.

RockEval™ parameters (e.g. oxygen index which is a proxy for O/C ratio in organic samples) combined with inorganic geochemical analyses (e.g. sulphur which commonly occurs within marine reducing environments) and trace element ratios (e.g. U/Th, Ni/Co) were used to investigate the oxygenation state of the water column and sediment at the time of deposition. Sub-oxic environments of deposition prevent organic matter being oxidised or degraded by bacteria during deposition. Oxic environments often have poor organic matter preservation, whereas hypoxic or anoxic conditions allow for greater preservation of organic matter. The Holywell Shale was deposited under predominantly oxic conditions, with some periods of hypoxia occurring during marine bands and the most organic rich samples within boreholes (Point of Ayr) and outcrops (Warren Dingle). Despite of the oxic conditions, the quantity of organic matter present as indicated by the TOC values of the Holywell Shale was relatively high (an average TOC of 2.0 wt % and a range of 0.1 to 10.3 wt %; Appendices A & E).

RockEval™ hydrogen index and T_{max} parameters can be used to characterise the type of organic matter present within the Holywell Shale samples. Kerogen is organic matter which comprises 95% of all organic constituents of these mudstones and is defined as the portion which is insoluble in common alkaline and organic solvents (Tyson, 1995). The differences between kerogen types are outlined in Chapter 2 of this thesis. The organic matter found within the Holywell Shale is composed predominantly of Type III kerogens; with some Type II and Type II/III mixed kerogens and occasionally Type IV kerogens present (Figure 6-16). Type II/III kerogens dominate the Lower Holywell Shale samples, whereas Type IV are only found in the Upper Holywell Shale (Figure 6-16). Type II kerogens have the greatest potential to produce hydrocarbons, but they are only present in three

samples from the Cegidog Valley (Lower Holywell Shale) outcrop location. The Holywell Shale, therefore, has reduced potential as a source of shale gas although Type III kerogens found in the majority of samples (both Upper and Lower Holywell) still have gas generation potential albeit not as significant as Type II kerogens with the same maturity (gas window).

The greatest petroleum potential (as determined by RockEval™ parameters) is found within the Lower Holywell Shale samples during periods or areas of higher primary productivity and reduced bottom water oxygen levels. However, due to the largely oxidised and degraded organic matter present in the Holywell Shale (low HI values, often high OI values), and the complexity of the sedimentary system, both temporally and spatially, mean that shale reservoir quality of the Holywell Shale is inherently difficult to predict.

Mineralogical observations from outcrop and borehole samples outlined in Chapters 4 and 5 highlighted that the highest organic matter concentrations of the Holywell Shale occurred at marine bands in fossiliferous clay-rich mudstones. The clay-rich nature of the samples mean that they are unsuitable horizons to target for hydraulic fracturing, this has a considerable negative effect on the suitability of the Holywell Shale as a target for shale-gas. Only weak links between organic matter quantity, organic matter quality, organic matter type and lithologies exist within the Holywell Shale. This results in target horizons being difficult to predict at a basin scale in part due to variations occuring at a much smaller scale (< 10 m).

7.4: Lithofacies and geochemical variations across the Holywell Shale: towards a predictive tool

Correlation between boreholes and outcrops was possible using biostratigraphy (ammonoid marine bands). Petrographical analysis was able to identify the same lithofacies present in borehole material and outcrop material (Chapters 5 & 6). Geochemical data (both organic and inorganic) demonstrate that it is possible to correlate specific data (such as TOC, HI, Zr etc.) as well as trends in terrestrial and marine sediment and organic matter supply (e.g. $\delta^{13}C$, C/N, Ni/Co) between outcrop and borehole material from an individual marine band (G1a) and across multiple marine bands (Chapter 6; Figure 6-19).

Using identical geochemical analysis techniques on Holywell Shale samples collected from both boreholes and outcrops variations in geochemical results from analyses such as TOC, $\delta^{13}C$, HI, S_2, Zr and Si/Al were assessed across a single marine band with the conclusion that when variations occur they are likely to represent changes in the lithofacies and palaeogeographic location.

The two end-member facies of the Holywell Shale have distinctive geochemical trends. The clay-rich, fossiliferous facies has the highest organic matter content (TOC), the strongest marine carbon isotope signatures (more negative) and evidence (using trace element proxies e.g. U/Th) for a hypoxic environment of deposition with high primary production (e.g. high C/N ratios) as well as low siliciclastic inputs. Whereas the silt-rich facies contained very low organic matter content (TOC), the strongest terrestrial carbon isotope signatures (more positive) and evidence (using trace element proxies) for an oxic environment of deposition further supported by the poor preservation of organic matter (low HI) as well as increased terrestrial inputs of

minerals and organic matter (e.g. silt-sized detrital quartz and feldspar grains, high Zr concentrations and fragmentary organic matter).

The results from the Holywell Shale demonstrate that it is possible to correlate specific data (such as TOC, HI, Zr etc.) as well as general trends ($\delta^{13}C$) between outcrop and borehole material from an individual marine band (G1a) and across multiple marine bands within a mudstone succession. This is significant as a comparison of geochemical data from core samples (where detailed petrographical characterisation is possible) to cuttings can be used as a predictive tool to infer a lithofacies, organofacies and environment of deposition for the cutting material.

7.5: Key Conclusions

- The Holywell Shale represents a mudstone sequence deposited throughout the Namurian with highly variable organofacies and lithofacies suggesting complex variations in the supply of detrital material and organic matter, as well as preservation conditions present, both temporally and spatially within the basin.

- The organic matter content of the Holywell Shale measured using total organic carbon (TOC) analysis was an average 2.0 wt % with a range of 0.1 to 10.3 wt %. No apparent relationship existed between the amount of organic matter present and the source of the organic matter (marine vs. terrestrial or mixed).

- RockEval™ hydrogen index and T_{max} were used to determine kerogen type in the Holywell Shale. The kerogens present in the Holywell Shale were composed predominantly of Type III kerogens with some Type II/III mixed

kerogens. Type II kerogens occurred only within the Lower Holywell Shale whilst Type IV kerogens occurred only within the Upper Holywell Shale.

- A change from predominantly marine organic matter and low input of terrestrially derived material of the Lower Holywell Shale to the mixed (both marine and terrestrial sources) organic matter and high input of terrestrially derived material of the Upper Holywell Shale occurred. This change is likely to be a result of palaeogeographical changes related to the progressive influx of prograding deltas from the northeast (Millstone Grit Series) during the Namurian.

- The Holywell Shale was deposited under predominantly oxic conditions. Some periods of hypoxia are present within the most organic rich samples at maximum flooding surfaces (i.e. marine bands; noted in both borehole (Point of Ayr) and outcrop (Warren Dingle) material).

- Due to the predominately oxic conditions of the Holywell preservation conditions for organic matter were not optimal. The majority of organic matter present within the Holywell Shale is largely oxidised and degraded (determined principally from RockEval™ parameters; low HI values, average 104 mg/g, often high OI values, average 34 mg/g). This lack of preservation within the Holywell Shale combined with the highly variable (both temporally and spatially) sedimentary system means that the shale reservoir quality of the Holywell is inherently difficult to predict.

- The most organic-rich samples with the greatest potential to generate hydrocarbons of the Holywell Shale occur within the most clay-rich lithofacies (typically associated with marine bands). The mineralogy of these

organic-rich units (clay-rich) is unfavourable for the extraction of the hydrocarbons by hydraulic fracturing.

- There are only weak links between the lithology and the organic matter type, quantity, and quality present within the Holywell. Low quantities of the desired kerogen (Type II) and poor preservation of organic matter combined with the unsuitable clay-rich lithofacies of the organic-rich units result in the prospectivity of the Holywell Shale as a target for unconventional shale gas being severely reduced.

- Samples from the boreholes and outcrops of the Holywell Shale demonstrate that it is possible to correlate geochemical data effectively across the same basin as well as the larger Carboniferous Pennine Basin. Lithofacies observations identify two end-member facies for the Holywell Shale, silt-rich and clay-rich, fossiliferous. The two end-member facies have common geochemical trends across all samples from the Holywell Shale and those of Davies et al., 2012 and Stephenson et al., 2008 in northern England.

    o Marine band samples within the Holywell Shale are predominantly clay-rich, fossiliferous facies, with lighter carbon isotope values, higher TOC values, high HI and C/N, low in Zr concentration and low Si/Al ratios. These characteristics are prevalent across all samples from outcrops and boreholes (core and cutting material).

    o Between marine band samples within the Holywell Shale are predominantly silt-rich facies with immature terrestrial sediment input (including detrital feldspars and angular quartz grains), heavier carbon isotope values, low TOC values, low HI and C/N, high in Zr concentration and higher Si/Al ratios. These characteristics are

prevalent across all samples from outcrops and boreholes (core and cutting material).

- Whilst carbon isotope values vary with changes in lithofacies, an overall trend to more positive carbon isotope values in the Upper Holywell Shale (Marsdenian and Yeadonian) compared with the Lower Holywell Shale (Arnsbergian). The carbon isotope correlates with published examples from across the UK Carboniferous Pennine Basin (Davies et al., 2012; Stephenson et al., 2008). This shift in carbon isotope values across the Namurian can be attributed in part to local (i.e. UK) factors such as the reduction of accommodation space through time due to the progradation of Namurian deltas and reduced thermal subsidence of the basin. However, the carbon isotope trend seen within the Holywell Shale strongly correlates with the timings of major southern hemisphere glaciation (C2 glaciation; Fielding et al., 2008; Rygel et al., 2008; Frank et al., 2008) and as such is likely to reflect the global positive shift in carbon isotope values.

7.5 Methodological limitations

7.5.1: The use of TGA to replicate RockEval™

The theory behind using thermogravimetric analysis was to provide a cheaper alternative to RockEval™. The attempt to replicate RockEval™ analysis by pyrolysing samples in an inert helium atmosphere using the same heating programme (temperature ramp rate and holding temperatures) as described in Section 3.2 for RockEval™ analysis had limited success. The mass spectrometer attached to the TGA machine used was unable to give details about the hydrocarbons produced at different pyrolysis temperatures. The main differences between

RockEval™ and the technique using TGA was that it was only possible to identify the S_1 and S_2 peaks by mass loss and was unable to isolate the organic matter portion of a sample, which is achieved in the RockEval™ technique by using a flame ionising detector (FID). To combat this, pyrolysis gas chromatography and mass spectrometry (GC-MS) was investigated (at Durham University) as the addition of an FID and thermal conductivity detector (TCD) would allow organic matter to be analysed similar to RockEval™ and further information about the hydrocarbons produced could be ascertained. However, the pyrolysis oven and heated transfer line were not able to reach the temperatures (550 °C) required for longer chain hydrocarbons to remain in gas state, meaning that they would condense before being analysed.

7.5.2: Broad ion beam milling technique and its application within this study

Broad ion beam milling is a technique which can be used to detail pore size, shape, and position of pores. Pores can occur within mudstones as inter-particle pores where they occur between mineral grains, as intra-particle pores occurring within mineral grains, and intra-organic matter pores occurring within organic matter (Loucks et al., 2012).

The broad ion beam milling technique is detailed in Chapter 3 of this thesis. The use of the technique caused time-consuming obstacles which were unsurmountable with the time constraints on this PhD project, and an insufficient quantity of data were collected for detailed analysis or comparison to be included. Here the issues are outlined and the ways in which to combat them for future studies are suggested.

The largest obstacle to using the method was obtaining suitable samples. The method used to obtain a sample to perform broad ion beam milling was to use a thick (500 μm) thin section mounted on a glass slide as outlined in the methods section of this thesis (Section 3.2.2). After the thin section had been characterised using other petrography techniques (such as optical petrography and SEM) an area of interest (3 mm x 3 mm) was identified; an ultrasonic drill was used in combination with water and boron nitride to cut out the section of interest from the rest of the sample. This process was delicate, sensitive and time consuming (details in Section 3.8.2) and it was in this step the majority of problems were encountered.

In cutting a sample on the ultrasonic drill, the correct frequencies had to be found to activate the boron nitride into cutting. Initial cutting had to be approached slowly and with care to avoid damaging the surface of the polished rock sample. During cutting, the frequency had to be altered to cut through the sample and in particular, through the glass, which often caused vibrations.

The result of the cutting method was that often the sample would be damaged, either the surface (usually at the edges), or the sample would split in a variety of ways (Figure 7-1A). Commonly the sample would be delaminated where it had been bonded to the glass slide (Figure 7-1B); attempts were made to combat this by reattaching the sample to the slide after drilling. However this process also encountered problems as it was difficult to ensure that the sample was reattached the correct way up and due to the boron nitride delaminating the rock sample from the slide the surface to re-bond was often not flat which resulted in the sample surface not being flat/parallel to the glass slide which severely impacted the success of the ion beam milling process. Other problems encountered in the ultrasonic drilling

process included the glass slide to splinter or shatter underneath the 3mm rock sample (Figure 7-1C), or the glass slide to shatter, split (Figure 7-1D).
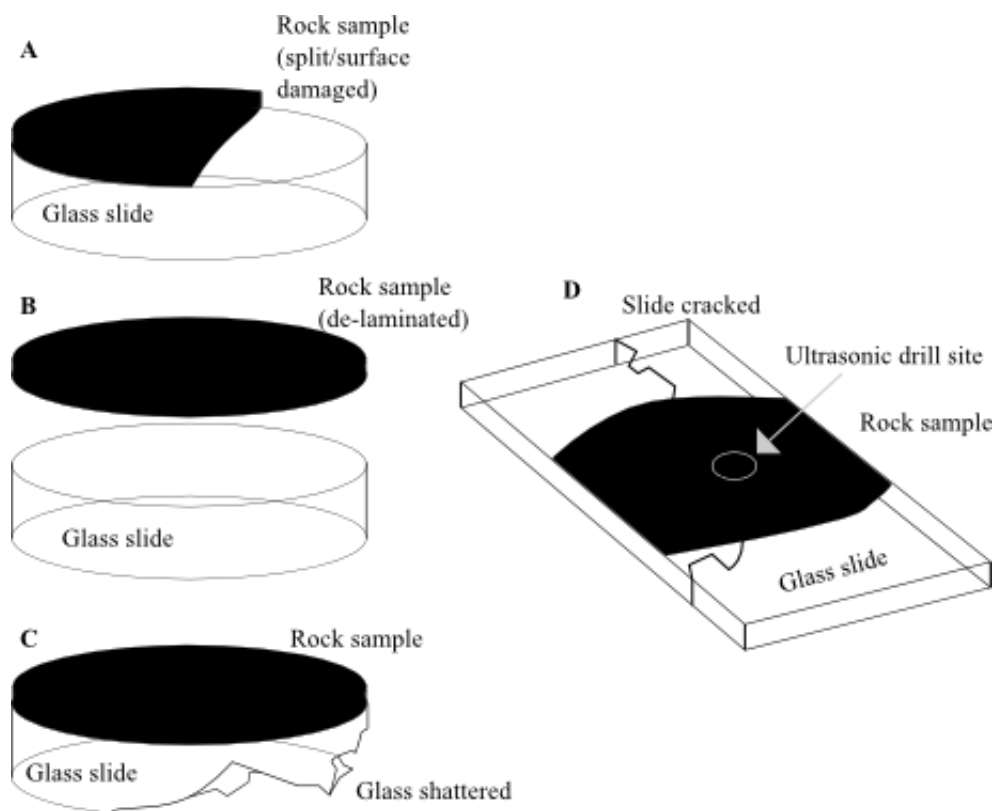
Figure 7-1: Problems encountered on the ultrasonic drill included A- sample to split or the surface of the sample to be damaged; B- rock sample becomes delaminated from the glass slide; C- the slide to break or shatter underneath the milled out sample; D- the entire sample and slide to break whilst drilling.

The reason the cutting process was required was due to the Gatan Precision Ion Polishing System (PIPS) machine having a 3mm maximum sample size to fit inside the sample chamber. The cutting process also allowed petrographical analysis to occur prior to milling in order to characterise the sample and select a suitable site(s) of interest. A method which could be used to eliminate the requirement for the ultrasonic drill process would be to use the off-cut sample from the thin section preparation. The off-cut sample would then be bonded in resin if necessary to hold it

together during the process and a 3 mm x 3 mm square of the sample cut on a fine cutting/grinding disc, in a similar way to preparing a thin section sample. The sample could then be ground and polished in the same way as a thin section before inserting into the PIPS machine.

Other problems encountered with the BIB technique were related to the PIPS machine which was used to mill/polish the sample. PIPS machine set-up varied depending on the mineral constituents of the sample and the polish which the sample had prior to milling. Samples with harder minerals or a poor quality manual polish were more difficult to polish on the PIPS machine and therefore required extended periods of time to achieve a suitable polish. The variations in set-up and run time for the PIPS machine (a minimum of 11 hours initial polish time was required for each sample) meant that a lot of time was needed to ensure samples were prepared properly to achieve good quality images of the pores under the SEM (Figures 7-2 and 7-3).
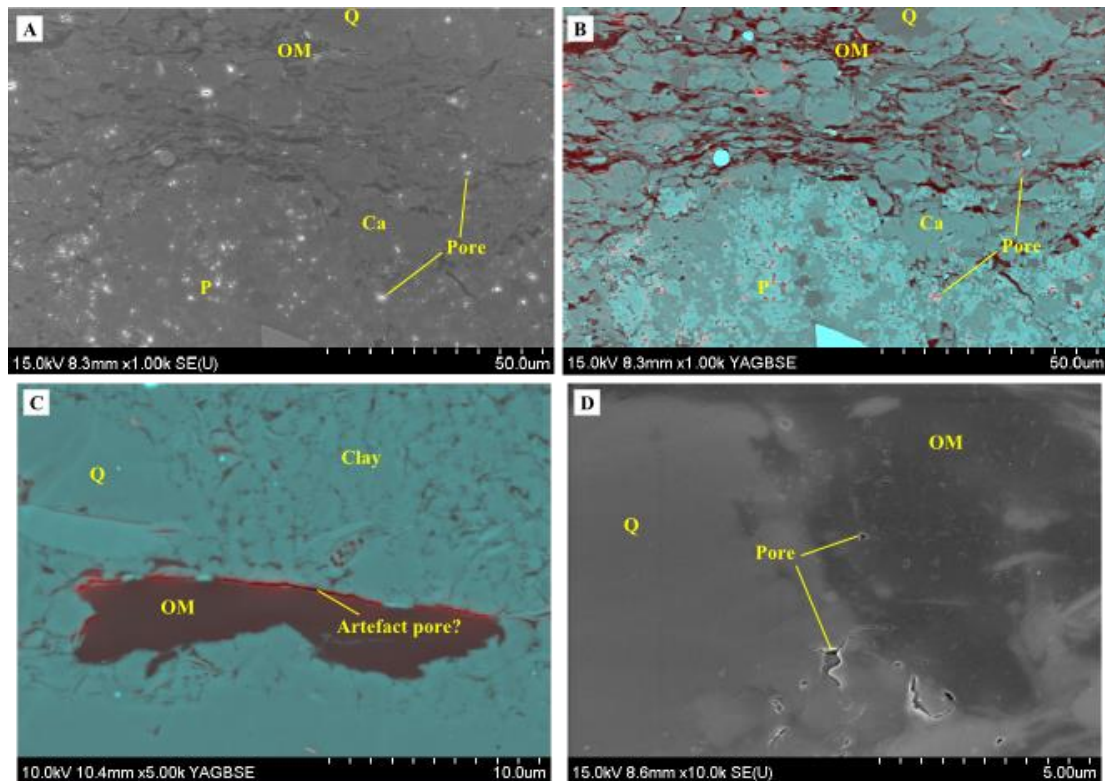
Figure 7-2: Good BIB polishes allowed imaging of pore in minerals and organic matter. A- Holywell Shale sample with intra-particle pores in predominantly calcium phosphate (bone type mineral; CaPO$_4$) minerals as well as inter-particle pores occurring between calcite grains (SE image, grey is mineral and white highlight is pore). B- The same image as A but coloured to highlight pores (red) and minerals (blue) using BSE image blending. C- Artefact pore within Holywell Shale sample occurring at the edge of organic matter where it contacts the mineral grains, suggesting shrinkage of organic matter. D- Intra-particle and intra-organic matter pores highlighted occurring within the Holywell Shale.
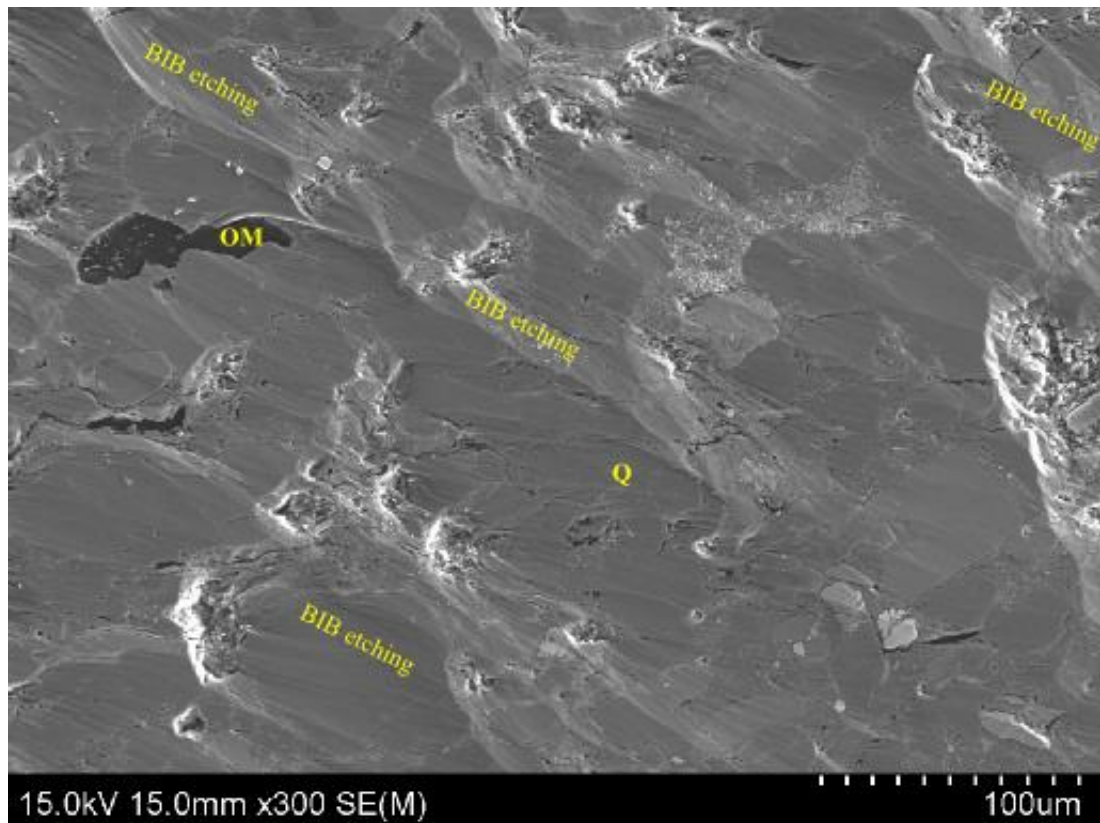
Figure 7-3: BIB polishing has left an uneven surface meaning that it is not possible to image pores accurately. An effort to correct this on the PIPS machine was attempted, but was not successful.

When the initial polish was unsuccessful (Figure 7-3) further polishing using different settings on the PIPS machine were used. Commonly this involved adjusting the beam current/voltage to remove more material, or lowering the voltage to give a finer polish. As well as this, adjusting the argon ion beam angles meant that more or less ablation of the surface could be achieved. The efforts to correct a bad polish were unsuccessful without more time to perfect the technique.

7.6: Further work

Throughout the process of this PhD research many questions and avenues of research have arisen, only some of which the time constraints of the project allowed to be explored. An explanation of the work which was started but not completed and key

questions raised by the research herein will be outlined. The remaining outcrop material collected as part of this study is currently stored at the Department of Earth Science (Durham University), whilst the remaining core material has been returned to the BGS at Keyworth, Nottingham.

1. Palynofacies analysis and pyrolysis gas chromatography can give further insights into the nature of the organic matter, kerogen type from visual analysis (particularly vitrinite reflectance data) and whether unconventional light or heavy hydrocarbons could be produced from the Holywell Shale. However, a lack of time, expertise and funds meant that this was not possible within the constraints of this project. Previous work on the Bowland Shale Formation have used palynofacies and chromatography to characterise the organic matter present as well as depositional environments (Könitzer, 2014a, b; Gross et al., 2015). Previous work by Armstrong et al. (1997) also used chromatography on a limited number of Holywell Shale samples to attempt to establish whether the Holywell Shale was a source rock for the East Irish Sea conventional oil and gas targets. Armstrong et al. (1997) concluded that the Lower Holywell Shale indicated good correlation (in terms of hydrocarbon product) with hydrocarbon accumulations in the Douglas and Lennox fields of the East Irish Sea. The existence of remaining material from this study would allow this analysis to be considered in the future. The Holywell at outcrop and in many of the boreholes in northeast Wales is within the immature to oil window, with variable generation potential (poor to moderate). This might meant that the proposed analyses may not add significant value to the research already conducted within this thesis.

2. The unknown source of siliceous material for the deposition of the localised Pentre Chert within the region as well as the various diagenetic observations within the petrographic analysis of Holywell Shale samples highlights the fact that no reported data regarding the diagenetic history of the Holywell Shale, or for that matter, the Bowland Shale Formation currently exists. Detailed cathodoluminescence studies of the diagenetic fabrics observed within SEM samples would greatly improve the documentation of the burial history of the Holywell Shale and this would have a significant impact on the prospectivity of the play (e.g. Milliken et al., 2012).

    Detailed studies into the diagenetic history of different parts of the Bowland Shale Formation, with the knowledge of the supply and nature of sediment and organic matter gained from this and previous studies (e.g. Könitzer, 2014a; Davies et al., 2012; Gross et al., 2015; Słowakiewicz et al., 2015) providing the foundation, would greatly benefit the exploration of unconventional source-rock reservoirs such as the Bowland Shale Formation. Diagenesis has a significant effect on the physical properties of mudstones, such as the porosity and permeability as well as brittleness and other properties, which ultimately contribute to the ability to hydraulically fracture and produce hydrocarbons.

3. Porosity (< 15%, but normally in the range 4 to 7 %; Jarvie, 2012) and permeability (< 1000 ηD; Jarvie, 2012) of mudstones is vital for successful hydrocarbon production. The nature of pores related to organic matter and minerals within mudstones can be observed and quantified using a variety of techniques including micro-X-ray computed tomography (CT) scanning, focused and broad ion beam milling techniques combined with SEM imaging

(e.g. Curtis et al., 2012). A study into the pore spaces in immature/early oil mature mudstones (Holywell Shale) was attempted using broad ion beam techniques. The broad ion beam milling techniques were very time consuming and the problems with the technique are previously outlined (Section 7.5.2). Focused ion beam techniques are often used in combination with other SEM techniques to provide in-depth slice-and-view images to give small-scale 3-dimensional information about pore spaces, organic matter and minerals (e.g. Loucks et al., 2012). Using Aviso software it is possible to quantify and observe pores and pore connectivity in 3-dimensions, this can be combined with EDS data to create 3-dimensional coloured mineral maps. This would provide a greater understanding of 3D pore structure within the Holywell Shale and other organic-rich mudstones, which is vital in understanding hydrocarbon storage and transport within these rocks.

4. Qualitative X-ray diffraction was completed on Holywell Shale outcrops to give greater certainty and understanding of the mineral constituents within the Holywell Shale. Quantitative X-ray diffraction could be used to provide further knowledge of the constituent mineral proportions, and allow this to be related to lithofacies variation which occurs within the Holywell Shale. An example of this use would be to combine this technique with a diagenetic study of the Holywell Shale to characterise detrital mineral grains from authigenic grains and to determine the presence and quantity of mineral cements within the mudstone.

Appendices

Appendix A: Organic geochemical parameters for outcrop samples of the Holywell Shale

Outcrop	Sample	TOC	$\delta^{13}C$	S_1	S_2
		(wt %)	(‰)	(mg/g)	(mg/g)
Pen-Y-Maes	PYMS1H1	0.5	-22.7	0.1	0.4
	PYMS1H2	0.4	-22.4	0.1	0.3
	PYMS1H3	0.4	-22.5	0.1	0.2
	PYMS1H4	0.3	-22.5	0.1	0.2
	PYMS1H5	0.3	-23.7	0.1	0.2
	PYMS2H1	0.5	-22.7	0.1	0.2
	PYMS2H2	0.1	-23.6	0.1	0.2
Warren Dingle	WDS1H1	4.1	-25.4	0.4	5.4
	WDS1H2	3.2	-25.3	0.3	2.2
	WDS1H3	2.3	-25.2	0.3	2.0
	WDS1H4	10.3	-25.9	0.9	16.1
Coed-Y-Felin	CYFS1H1	1.3	-24.3	0.1	0.6
	CYFS1H2	1.4	-23.9	0.2	2.1
	CYFS1H2i	1.5	-24.1	0.2	2.8
	CYFS1H3	1.2	-24.2	0.2	0.6
	CYFS1H4	1.5	-24.5	0.2	0.5
River Terrig	RTS1H2	2.0	-30.9	0.2	3.7
	RTS1H3	1.9	-30.0	0.1	3.7
	RTS1H4	1.9	-30.6	0.2	3.8
	RTS1H5	0.6	-28.4	0.1	0.7
	RTS2H1	1.6	-26.5	0.2	2.1
	RTS2H2	1.6	-26.6	0.3	2.5
	RTS2H3	1.4	-25.6	0.5	3.4
	RTS2H4	1.7	-26.4	0.2	1.8
	RTS3H1	3.4	-27.7	0.2	4.9
	RTS5H1	2.3	-31.1	0.1	5.8
	RTS6H1	3.3	-27.5	0.3	4.2
Cegidog Valley	CVS1H1	2.3	-30.4	0.2	7.0
	CVS2H1	2.3	-30.6	0.3	7.5
	CVS3H1	1.8	-29.8	0.2	5.0
	CVS3H2	1.7	-29.2	0.2	3.0

Outcrop	Sample	T_max	HI	S_1/TOC	TOC/S
		(°C)	(mg/g)	(%)	
Pen-Y-Maes	PYMS1H1	386	75	0.2	36.1
	PYMS1H2	-	68	0.3	107.7
	PYMS1H3	-	45	0.2	204.5
	PYMS1H4	-	49	0.2	44.9
	PYMS1H5	312	49	0.2	137.3
	PYMS2H1	529	35	0.1	94.0
	PYMS2H2	-	87	0.5	16.3
Warren Dingle	WDS1H1	432	125	0.1	11.0
	WDS1H2	428	119	0.1	3.1
	WDS1H3	433	73	0.1	29.8
	WDS1H4	432	121	0.1	13.2
Coed-Y-Felin	CYCS1H1	499	49	0.1	0.4
	CYCS1H2	440	154	0.1	50.9
	CYCS1H2i	441	202	0.1	68.1
	CYCS1H3	431	51	0.1	0.4
	CYCS1H4	450	35	0.1	2.1
River Terrig	RTS1H2	441	122	0.1	37.6
	RTS1H3	437	174	0.1	49.1
	RTS1H4	438	165	0.1	46.9
	RTS1H5	436	89	0.1	28.8
	RTS2H1	433	102	0.1	3.8
	RTS2H2	427	136	0.2	57.6
	RTS2H3	426	203	0.3	50.0
	RTS2H4	430	90	0.1	6.1
	RTS3H1	438	111	0.1	9.0
	RTS5H1	437	226	0.0	20.8
	RTS6H1	436	104	0.1	11.1
Cegidog Valley	CVS1H1	442	298	0.1	2.5
	CVS2H1	445	301	0.1	3.3
	CVS3H1	445	270	0.1	5.1
	CVS3H2	442	179	0.1	4.6

Appendix B: Inorganic geochemical parameter ratios for outcrop samples of the Holywell Shale

Outcrop	Sample	Si/Al	U/Th	V/Cr	Ni/Co	Fe/Ti	Fe/S
Pen-Y-Maes	PYMS1H1	3.6	0.1	1.1	2.9	5.6	449.4
	PYMS1H2	3.6	0.1	1.2	3.4	5.3	1459.7
	PYMS1H3	3.3	0.1	1.0	2.6	5.7	3143.3
	PYMS1H4	3.3	0.2	1.2	2.1	5.6	754.3
	PYMS1H5	3.5	0.1	1.3	2.8	5.5	2217.4
	PYMS2H1	3.4	0.2	0.9	2.7	6.0	1076.9
	PYMS2H2	5.0	-	0.9	3.0	5.1	536.5
Warren Dingle	WDS1H1	2.6	0.8	1.7	4.2	8.0	17.7
	WDS1H2	2.6	0.6	1.7	4.4	7.1	5.7
	WDS1H3	2.7	0.5	1.6	1.9	8.3	93.9
	WDS1H4	2.8	2.5	1.2	11.0	7.7	5.0
Coed-Y-Felin	CYFS1H1	2.5	0.6	1.1	3.7	8.8	2.4
	CYFS1H2	2.8	0.2	1.2	4.7	3.4	136.8
	CYFS1H2i	3.0	0.3	1.2	4.4	3.4	156.8
	CYFS1H3	2.6	0.7	1.2	3.1	8.5	2.5
	CYFS1H4	2.6	0.5	1.1	3.0	4.3	5.3
River Terrig	RTS1H2	9.5	0.9	0.5	-	4.9	44.5
	RTS1H3	6.8	0.8	0.7	2.1	3.3	50.5
	RTS1H4	8.8	0.8	0.7	-	3.8	46.9
	RTS1H5	14.9	1.4	0.8	-	4.4	71.1
	RTS2H1	4.6	0.4	1.0	6.4	4.2	7.0
	RTS2H2	7.9	0.6	1.8	6.4	5.2	103.1
	RTS2H3	8.8	0.5	1.5	-	2.2	38.6
	RTS2H4	5.0	0.6	0.8	8.6	4.4	13.6
	RTS3H1	4.9	2.3	0.8	-	6.4	5.5
	RTS5H1	8.7	0.6	0.6	-	3.9	17.8
	RTS6H1	5.1	1.5	1.7	-	7.3	7.3
Cegidog Valley	CVS1H1	6.5	0.3	0.6	3.7	5.8	3.8
	CVS2H1	6.6	0.1	0.7	-	5.5	4.6
	CVS3H1	6.2	0.3	0.7	-	5.8	10.8
	CVS3H2	5.9	0.2	0.7	-	5.8	10.3

Outcrop	Sample	Al$_2$O$_3$	SiO$_2$	TiO$_2$	Fe$_2$O$_3$	MnO	MgO
		%	%	%	%	%	%
Pen-Y-Maes	PYMS1H1	16.0	57.9	1.0	5.6	0.1	1.8
	PYMS1H2	16.0	57.6	1.0	5.3	0.1	1.8
	PYMS1H3	16.8	55.1	1.0	5.8	0.0	1.9
	PYMS1H4	16.7	54.4	1.0	5.8	0.1	1.9
	PYMS1H5	16.3	56.5	1.0	5.5	0.1	1.8
	PYMS2H1	16.4	55.1	1.0	6.0	0.1	1.9
	PYMS2H2	13.0	64.5	0.8	4.0	0.0	1.5
Warren Dingle	WDS1H1	18.7	48.0	0.8	6.6	0.1	1.4
	WDS1H2	18.2	46.8	0.8	5.9	0.0	1.5
	WDS1H3	19.2	51.1	0.9	7.2	0.0	1.6
	WDS1H4	12.3	34.2	0.5	3.9	0.1	1.4
Coed-Y-Felin	CYCS1H1	18.5	46.8	0.8	7.0	0.1	1.7
	CYCS1H2	19.5	55.5	1.1	3.7	0.0	2.0
	CYCS1H2i	19.0	57.4	1.0	3.4	0.0	2.0
	CYCS1H3	19.5	50.2	0.8	7.0	0.1	2.0
	CYCS1H4	19.6	51.8	0.9	3.8	0.0	1.4
River Terrig	RTS1H2	7.8	74.4	0.5	2.4	0.0	1.0
	RTS1H3	10.2	69.9	0.6	2.0	0.0	1.3
	RTS1H4	8.5	74.5	0.5	1.9	0.0	1.0
	RTS1H5	5.5	82.7	0.4	1.6	0.0	0.5
	RTS2H1	11.4	52.7	0.7	3.0	0.0	1.9
	RTS2H2	9.1	71.4	0.5	2.8	0.0	1.2
	RTS2H3	8.8	77.5	0.5	1.1	0.0	1.0
	RTS2H4	12.9	64.0	0.8	3.7	0.0	1.9
	RTS3H1	6.0	29.6	0.3	2.0	0.1	1.4
	RTS5H1	8.6	75.0	0.5	2.0	0.0	1.1
	RTS6H1	6.1	30.8	0.3	2.2	0.1	1.3
Cegidog Valley	CVS1H1	9.9	64.1	0.6	3.5	0.0	2.2
	CVS2H1	9.6	63.5	0.6	3.3	0.0	2.5
	CVS3H1	10.2	62.9	0.7	3.8	0.1	2.5
	CVS3H2	10.3	61.3	0.7	3.9	0.1	2.6

Outcrop	Sample	CaO	Na$_2$O	K$_2$O	P$_2$O$_5$	Cl	S
		%	%	%	%	%	%
Pen-Y-Maes	PYMS1H1	0.1	0.6	2.6	0.1	0.0	0.0
	PYMS1H2	0.2	1.0	2.5	0.1	0.0	0.0
	PYMS1H3	0.4	0.9	2.6	0.1	0.0	0.0
	PYMS1H4	0.3	0.6	2.7	0.2	0.0	0.0
	PYMS1H5	0.4	0.8	2.3	0.1	0.0	0.0
	PYMS2H1	0.4	0.7	2.6	0.1	0.0	0.0
	PYMS2H2	0.2	1.3	1.7	0.1	0.0	0.0
Warren Dingle	WDS1H1	0.5	0.0	3.1	0.1	0.1	0.4
	WDS1H2	0.3	0.0	3.6	0.1	0.0	1.0
	WDS1H3	0.2	0.0	3.6	0.2	0.0	0.1
	WDS1H4	15.6	0.0	2.1	1.7	0.1	0.8
Coed-Y-Felin	CYCS1H1	0.3	0.0	2.8	0.0	0.0	2.9
	CYCS1H2	0.3	0.0	3.5	0.0	0.0	0.0
	CYCS1H2i	0.3	0.0	3.3	0.0	0.0	0.0
	CYCS1H3	0.3	0.0	2.8	0.1	0.0	2.8
	CYCS1H4	0.1	0.0	3.1	0.0	0.0	0.7
River Terrig	RTS1H2	0.1	0.0	2.1	0.3	0.0	0.1
	RTS1H3	0.1	0.0	2.7	0.3	0.0	0.0
	RTS1H4	0.1	0.0	2.3	0.3	0.0	0.0
	RTS1H5	0.1	0.0	1.3	0.4	-	0.0
	RTS2H1	9.8	0.0	3.0	0.2	0.0	0.4
	RTS2H2	0.3	0.0	2.2	0.1	0.0	0.0
	RTS2H3	0.1	0.0	2.2	0.0	0.0	0.0
	RTS2H4	2.6	0.0	3.4	0.1	0.1	0.3
	RTS3H1	29.0	0.0	1.5	0.5	0.0	0.4
	RTS5H1	0.1	0.0	2.3	0.3	0.0	0.1
	RTS6H1	27.7	0.0	1.5	0.3	0.0	0.3
Cegidog Valley	CVS1H1	1.9	0.0	2.7	0.2	0.0	0.9
	CVS2H1	2.7	0.0	2.6	0.3	0.0	0.7
	CVS3H1	2.4	0.0	2.6	0.3	0.0	0.4
	CVS3H2	3.4	0.0	2.7	0.3	0.0	0.4

Appendix C: Inorganic trace element geochemical parameters for outcrop samples of the Holywell Shale

Outcrop	Sample	As	Ba	Ce	Co	Cr	Cu	Ga
		ppm	ppm	ppm	ppm	ppm	ppm	ppm
Pen-Y-Maes	PYMS1H1	10.0	407.2	105.3	12.3	90.3	39.0	14.8
	PYMS1H2	11.0	371.3	94.9	10.8	82.5	32.3	15.5
	PYMS1H3	10.2	385.9	114.5	17.2	95.6	33.2	16.0
	PYMS1H4	10.5	388.4	78.6	20.4	85.0	33.4	15.8
	PYMS1H5	11.2	399.1	82.2	14.1	81.2	26.2	16.1
	PYMS2H1	17.3	487.4	100.4	17.5	88.8	35.1	17.4
	PYMS2H2	6.0	275.8	66.2	9.0	63.5	25.2	9.5
Warren Dingle	WDS1H1	61.1	514.7	122.5	25.6	168.6	114.5	24.1
	WDS1H2	42.2	487.7	91.6	14.3	139.2	176.2	22.4
	WDS1H3	39.5	549.8	93.0	24.6	147.3	81.6	24.3
	WDS1H4	17.1	959.9	44.8	14.7	258.4	135.1	18.8
Coed-Y-Felin	CYFS1H1	41.6	388.2	97.6	31.3	113.7	83.8	26.3
	CYFS1H2	3.9	447.7	118.2	11.4	132.2	44.5	21.5
	CYFS1H2i	2.5	460.2	131.9	12.0	109.0	45.6	21.3
	CYFS1H3	35.9	363.1	101.5	36.0	113.1	87.2	25.6
	CYFS1H4	29.4	358.0	123.3	7.1	117.6	19.4	23.6
River Terrig	RTS1H2	6.2	348.6	79.0	-	80.5	25.3	4.5
	RTS1H3	5.8	545.6	84.9	5.1	86.4	33.5	7.7
	RTS1H4	6.3	379.1	59.2	-	71.7	25.3	5.1
	RTS1H5	7.2	226.9	59.7	-	72.7	24.0	1.0
	RTS2H1	2.7	272.3	42.3	6.7	87.2	27.9	10.6
	RTS2H2	6.9	282.9	55.3	7.9	77.4	62.1	7.0
	RTS2H3	2.4	335.7	43.4	-	63.5	13.9	3.4
	RTS2H4	8.6	507.7	55.0	6.4	105.9	26.5	12.3
	RTS3H1	4.7	155.4	43.4	-	51.0	20.5	8.9
	RTS5H1	5.8	323.9	52.1	-	80.2	10.6	5.6
	RTS6H1	3.2	514.2	25.9	-	45.9	29.0	9.2
Cegidog Valley	CVS1H1	9.3	295.9	66.8	10.3	87.8	26.2	10.1
	CVS2H1	7.2	293.2	56.2	-	87.2	23.0	4.9
	CVS3H1	7.2	273.8	55.3	-	91.2	21.5	7.4
	CVS3H2	7.8	299.0	91.2	-	90.8	26.6	6.3

Outcrop	Sample	La	Nb	Ni	Pb	Rb	Sr	Th
		ppm	ppm	ppm	ppm	ppm	ppm	ppm
Pen-Y-Maes	PYMS1H1	44.7	14.7	36.1	15.8	108.5	98.3	11.0
	PYMS1H2	52.0	15.4	36.0	7.4	106.4	103.8	10.6
	PYMS1H3	58.2	15.2	43.9	8.1	106.3	111.4	11.9
	PYMS1H4	52.7	15.4	42.8	8.8	106.2	108.7	11.6
	PYMS1H5	42.8	14.8	39.0	6.5	97.0	106.7	12.1
	PYMS2H1	38.7	15.1	47.5	12.3	109.1	107.0	11.9
	PYMS2H2	33.9	11.0	27.1	27.4	60.7	74.0	5.9
Warren Dingle	WDS1H1	57.4	11.3	108.3	102.0	163.1	68.1	13.5
	WDS1H2	43.8	12.7	63.5	63.5	182.0	70.0	14.6
	WDS1H3	42.2	12.5	46.2	52.4	183.1	71.2	15.1
	WDS1H4	25.6	7.2	162.0	24.7	102.3	281.7	5.2
Coed-Y-Felin	CYCS1H1	53.0	11.9	115.3	61.6	144.5	77.2	15.5
	CYCS1H2	44.7	16.9	53.9	26.4	174.1	84.9	15.9
	CYCS1H2i	78.7	17.1	52.4	30.8	163.5	81.2	15.1
	CYCS1H3	45.3	12.3	112.2	54.7	145.9	78.0	15.3
	CYCS1H4	53.7	12.7	21.0	73.8	163.9	80.7	13.3
River Terrig	RTS1H2	50.6	8.0	13.0	22.9	76.8	81.4	5.4
	RTS1H3	49.4	9.5	10.9	30.7	98.5	116.2	8.0
	RTS1H4	43.6	7.7	12.3	34.2	82.5	89.5	6.5
	RTS1H5	36.9	3.9	3.6	38.8	40.5	120.0	4.1
	RTS2H1	33.6	10.8	43.0	17.2	118.5	146.6	7.4
	RTS2H2	42.9	8.0	50.3	25.3	92.2	48.7	5.7
	RTS2H3	42.2	8.1	10.1	50.0	89.8	58.9	6.1
	RTS2H4	43.7	12.9	55.2	19.3	138.5	78.8	6.3
	RTS3H1	33.6	4.3	29.9	13.1	61.9	346.6	4.3
	RTS5H1	32.7	8.0	15.3	18.5	85.8	77.1	5.7
	RTS6H1	28.6	4.6	33.2	13.6	63.3	333.0	5.0
Cegidog Valley	CVS1H1	35.9	10.1	38.2	18.0	100.8	67.0	8.0
	CVS2H1	30.4	9.2	33.0	20.1	98.1	72.9	9.1
	CVS3H1	36.6	10.1	28.0	14.7	95.8	68.9	7.6
	CVS3H2	44.1	9.7	35.3	16.6	98.1	79.7	10.7

Outcrop	Sample	U	V	Y	Zn	Zr
		ppm	ppm	ppm	ppm	ppm
Pen-Y-Maes	PYMS1H1	1.6	100.2	36.1	86.1	282.0
	PYMS1H2	1.2	102.1	37.7	71.1	273.3
	PYMS1H3	1.1	94.0	36.3	71.9	262.4
	PYMS1H4	2.4	102.0	39.0	86.2	270.7
	PYMS1H5	1.8	102.7	35.7	69.5	310.5
	PYMS2H1	2.0	77.5	36.9	91.7	263.3
	PYMS2H2	-	54.3	27.6	63.7	276.6
Warren Dingle	WDS1H1	10.8	290.0	62.8	57.5	129.7
	WDS1H2	8.7	234.7	33.7	49.5	137.2
	WDS1H3	6.9	228.3	33.0	55.3	135.1
	WDS1H4	12.8	313.0	48.7	60.2	75.7
Coed-Y-Felin	CYCS1H1	9.7	129.0	25.5	71.2	120.0
	CYCS1H2	3.0	155.0	42.3	84.2	199.1
	CYCS1H2i	4.1	127.2	41.7	69.2	210.3
	CYCS1H3	10.1	137.5	25.1	52.2	123.9
	CYCS1H4	6.7	129.7	25.6	27.7	126.8
River Terrig	RTS1H2	4.6	41.9	23.3	11.9	161.3
	RTS1H3	6.1	59.8	50.3	13.4	184.2
	RTS1H4	5.1	48.8	27.4	13.7	154.2
	RTS1H5	5.9	61.8	21.6	10.1	144.8
	RTS2H1	2.9	89.4	31.5	26.6	138.2
	RTS2H2	3.6	135.8	34.6	22.6	113.1
	RTS2H3	3.0	96.3	18.3	11.3	90.8
	RTS2H4	3.6	81.9	25.4	42.9	162.7
	RTS3H1	10.0	40.3	34.0	10.5	46.4
	RTS5H1	3.4	48.6	20.2	9.2	162.0
	RTS6H1	7.6	78.8	33.9	11.4	48.6
Cegidog Valley	CVS1H1	2.4	54.7	30.8	16.5	195.8
	CVS2H1	1.3	58.6	32.4	16.5	199.7
	CVS3H1	2.4	63.4	34.4	17.8	260.9
	CVS3H2	2.4	64.2	33.9	19.3	257.2

Appendix D: Qualitative X-ray diffraction of Holywell Shale outcrop samples. x = mineral present, - = mineral absent.

	Sample	Quartz	Illite	Kaolinite	Chlorite	Calcite	Pyrite	Albite
Upper Holywell Shale	PYMS1H1	x	x	x	x	-	-	x
	PYMS1H2	x	x	x	x	-	-	x
	PYMS1H3	x	x	x	x	-	-	x
	PYMS1H4	x	x	x	x	-	-	x
	PYMS1H5	x	x	x	x	-	-	x
	PYMS2H1	x	x	x	x	-	-	x
	WDS1H1	x	x	x	-	-	x	-
	WDS1H2	x	x	x	-	-	x	-
	WDS1H3	x	x	x	-	-	-	-
	WDS1H4	x	x	x	x	x	x	-
	CYFS1H1	x	x	x	x	-	x	-
	CYFS1H2	x	x	x	x	-	-	-
	CYFS1H2i	x	x	x	x	-	-	-
	CYFS1H3	x	x	x	x	-	x	-
	CYFS1H4	x	x	x	x	-	-	-
Lower Holywell Shale	RTS1H2	x	x	-	-	-	-	-
	RTS1H3	x	x	-	-	-	-	-
	RTS1H4	x	x	-	-	-	-	-
	RTS1H5	x	x	x	-	-	-	-
	RTS2H1	x	x	x	x	x	-	-
	RTS2H2	x	x	-	-	-	-	-
	RTS2H3	x	x	-	-	-	-	-
	RTS2H4	x	x	x	x	x	x	-
	RTS3H1	x	x	x	x	x	x	-
	RTS5H1	x	x	-	-	-	-	-
	RTS6H1	x	x	-	-	x	-	-
	CVS1H1	x	x	x	-	-	x	-
	CVS2H1	x	x	x	-	-	x	-
	CVS3H1	x	x	x	-	-	x	-
	CVS3H2	x	x	x	x	-	x	-

Appendix E: Organic geochemical parameters for borehole samples

of the Holywell Shale

Well	Sample depth (ft)	Sample depth (m)	TOC (wt %)	$\delta^{13}C$ (‰)	S_1 (mg/g)	S_2 (mg/g)	S_3 (mg/g)
Blacon East	2400	731.5	1.4	-25.5	0.2	2.1	0.7
	2450	746.8	1.0	-25.3	0.1	0.9	0.6
	2500	762.0	1.1	-23.8	0.1	1.1	0.6
	2550	777.2	0.7	-23.3	0.1	0.3	0.5
	2600	792.5	0.7	-24.7	0.1	0.4	0.2
	2650	807.7	0.6	-23.2	0.1	0.3	0.4
	2700	823.0	0.6	-24.1	0.1	0.4	0.3
	2750	838.2	0.6	-24.0	0.0	0.4	0.3
	2800	853.4	0.9	-23.9	0.1	0.7	0.6
	2850	868.7	1.1	-24.5	0.1	1.2	0.7
	2900	883.9	0.8	-24.0	0.1	0.7	0.4
	2950	899.2	0.8	-24.2	0.1	0.7	0.2
	3000	914.4	0.6	-23.9	0.1	0.4	0.5
	3050	929.6	2.4	-24.5	0.4	2.3	0.5
	3100	944.9	0.7	-24.5	0.1	0.3	0.2
	3150	960.1	0.8	-24.0	0.1	0.3	0.4
	3200	975.4	0.7	-24.0	0.1	0.7	0.2
	3250	990.6	1.5	-24.9	0.3	1.1	0.3
	3300	1005.8	2.5	-25.9	0.5	2.7	0.4
	3350	1021.1	0.6	-24.7	0.1	0.6	0.3
	3400	1036.3	0.7	-24.4	0.1	0.4	0.4
	3450	1051.6	1.3	-26.3	0.4	1.6	0.7
	3500	1066.8	0.7	-24.2	0.1	0.4	0.8
	3550	1082.0	1.0	-24.4	0.1	0.8	0.7
	3600	1097.3	1.5	-25.8	0.2	1.0	0.5
	3650	1112.5	1.6	-26.0	0.2	1.2	0.3
	3700	1127.8	1.1	-24.4	0.1	0.8	0.3
	3750	1143.0	1.9	-25.0	0.1	1.3	0.5
Erbistock	3960	1205.0	3.3	-24.4	0.4	5.0	0.9
	4110	1255.0	1.5	-24.4	0.1	1.5	0.7
	4155	1265.0	1.2	-24.3	0.1	0.9	0.5
	4290	1310.0	0.9	-25.3	0.1	0.8	0.6
	4325	1320.0	1.5	-25.6	0.2	1.3	0.5
Milton Green	3723	1134.8	0.9	-23.8	0.1	0.3	0.1
	3725	1135.4	1.1	-23.9	0.1	1.0	0.1
	3726	1135.7	1.7	-26.0	0.2	1.6	0.0
	3728	1136.3	0.8	-24.0	0.1	0.3	0.4

Well	Sample depth (ft)	Sample depth (m)	TOC (wt %)	$\delta^{13}C$ (‰)	S_1 (mg/g)	S_2 (mg/g)	S_3 (mg/g)
	3729	1136.6	0.9	-24.7	0.1	0.3	0.3
	3919.7	1194.7	1.6	-27.8	0.4	1.4	0.2
	3947	1203.0	1.5	-28.0	0.1	0.3	0.1
Point of Ayr 3 Colliery shaft	215	65.5	0.5	-23.7	0.0	0.2	0.1
	341.6	104.1	3.9	-24.6	0.3	5.4	0.3
	350	106.7	5.0	-25.3	0.8	8.7	0.4
	350	106.7	4.2	-25.2	0.8	6.0	0.3
	585	178.3	0.7	-23.0	0.1	0.2	0.5
	607	185.0	0.6	-23.0	0.0	0.2	0.3
	620	189.0	8.6	-25.2	1.0	19.2	0.7
	649	197.8	2.6	-24.5	0.2	2.6	0.1
	696.6	212.3	7.8	-25.1	0.9	14.6	0.5
	1017	310.0	4.4	-24.6	0.9	5.8	0.4
	1067	325.2	4.9	-24.7	1.2	6.6	0.3
	1072	326.7	5.2	-24.5	1.5	9.9	0.4
	1086	331.0	6.8	-25.4	2.0	12.1	0.6
	1095	333.8	6.4	-25.4	2.2	11.7	0.3

Well	Sample depth (ft)	Sample depth (m)	T_{max} (°C)	HI (mg/g)	OI (mg/g)	S1/TOC (%)	TOC/S
Blacon East	2400	731.5	444	155	53	10.9	10.1
	2450	746.8	444	91	56	11.9	9.0
	2500	762.0	444	96	51	9.6	-
	2550	777.2	446	49	69	7.4	14.1
	2600	792.5	441	56	25	8.7	6.0
	2650	807.7	449	48	56	9.7	12.3
	2700	823.0	445	68	52	8.7	26.5
	2750	838.2	444	72	55	7.2	4.2
	2800	853.4	441	80	60	9.8	8.7
	2850	868.7	439	108	62	13.0	3.1
	2900	883.9	441	85	45	16.7	2.4
	2950	899.2	441	85	26	18.4	1.9
	3000	914.4	443	67	83	14.6	4.5
	3050	929.6	439	96	22	15.6	2.1
	3100	944.9	437	50	26	15.1	-
	3150	960.1	445	39	47	17.1	0.9
	3200	975.4	441	96	32	16.0	-
	3250	990.6	440	69	21	17.5	1.2
	3300	1005.8	439	107	15	21.1	1.7
	3350	1021.1	439	100	55	22.8	1.5
	3400	1036.3	437	55	64	10.7	1.7
	3450	1051.6	440	120	50	26.5	1.6
	3500	1066.8	443	64	121	20.5	2.1
	3550	1082.0	440	85	71	11.5	3.5
	3600	1097.3	442	69	34	11.7	1.5
	3650	1112.5	442	75	19	10.9	1.7
	3700	1127.8	443	74	28	12.8	-
	3750	1143.0	441	64	26	6.7	3.0
Erbistock	3960	1205.0	443	149	27	12.8	8.2
	4110	1255.0	442	97	45	7.8	3.2
	4155	1265.0	443	77	44	7.6	2.1
	4290	1310.0	443	79	58	13.8	0.8
	4325	1320.0	444	92	31	11.0	1.7
Milton Green	3723	1134.8	438	27	7	9.8	0.5
	3725	1135.4	451	91	4	12.3	4.4
	3726	1135.7	444	93	2	10.9	0.9
	3728	1136.3	443	41	48	13.2	0.7
	3729	1136.6	446	37	30	13.3	0.9
	3919.7	1194.7	447	91	13	27.4	1.5
	3947	1203.0	445	23	5	7.5	3.3

Well	Sample depth (ft)	Sample depth (m)	T_{max} (°C)	HI (mg/g)	OI (mg/g)	S1/TOC (%)	TOC/S
Point of Ayr 3	215	65.5	448	39	13	3.7	16.2
Colliery shaft	341.6	104.1	435	136	8	7.6	2.0
	350	106.7	434	172	7	15.7	1.9
	350	106.7	430	142	8	17.7	1.1
	585	178.3	444	33	73	7.1	21.6
	607	185.0	446	30	40	3.2	33.6
	620	189.0	433	224	8	11.4	6.3
	649	197.8	431	101	5	8.6	1.1
	696.6	212.3	433	187	7	11.0	2.8
	1017	310.0	435	132	9	20.2	1.8
	1067	325.2	435	134	7	24.5	2.1
	1072	326.7	433	190	7	28.9	1.7
	1086	331.0	436	176	9	29.8	3.1
	1095	333.8	436	182	5	34.6	2.6

Appendix F: Inorganic geochemical parameters for borehole samples of the Holywell Shale

Well	Sample depth	Sample depth	Al$_2$O$_3$	SiO$_2$	TiO$_2$	Fe$_2$O$_3$	MnO	MgO
	(ft)	(m)	%	%	%	%	%	%
Blacon East	2400	731.5	20.3	51.8	0.8	9.0	0.2	2.3
	2450	746.8	15.9	62.0	0.6	6.4	0.1	1.6
	2500	762.0	-	-	-	-	-	-
	2550	777.2	18.3	56.2	0.9	7.1	0.1	2.3
	2600	792.5	14.8	61.9	0.8	5.3	0.1	2.1
	2650	807.7	17.4	56.8	1.0	6.7	0.1	2.3
	2700	823.0	19.9	54.1	0.8	7.9	0.1	2.6
	2750	838.2	19.3	56.3	0.9	6.7	0.1	2.2
	2800	853.4	17.2	58.0	0.9	6.6	0.1	2.4
	2850	868.7	17.9	58.6	0.8	6.5	0.1	2.3
	2900	883.9	12.2	72.2	0.7	4.2	0.0	1.6
	2950	899.2	11.0	72.1	0.6	3.5	0.0	1.6
	3000	914.4	10.7	73.0	0.6	3.9	0.0	1.7
	3050	929.6	15.9	49.4	0.7	6.1	0.1	3.1
	3100	944.9	-	-	-	-	-	-
	3150	960.1	13.4	68.4	0.8	4.3	0.0	1.8
	3200	975.4	-	-	-	-	-	-
	3250	990.6	17.2	59.7	0.9	6.4	0.1	2.5
	3300	1005.8	14.5	51.3	0.7	5.7	0.1	2.7
	3350	1021.1	7.7	85.9	0.4	2.1	0.0	1.4
	3400	1036.3	11.5	77.6	0.6	4.1	0.0	1.5
	3450	1051.6	10.7	64.4	0.5	3.4	0.0	2.0
	3500	1066.8	11.9	75.2	0.7	6.4	0.1	1.7
	3550	1082.0	15.0	64.5	0.8	5.5	0.1	2.1
	3600	1097.3	16.0	57.0	0.8	6.6	0.1	2.6
	3650	1112.5	14.0	57.7	0.7	5.4	0.1	2.9
	3700	1127.8	-	-	-	-	-	-
	3750	1143.0	13.7	64.1	0.7	5.2	0.0	1.9
Erbistock	3960	1205.0	19.8	51.9	0.8	8.0	0.1	2.3
	4110	1255.0	17.4	60.8	0.8	5.7	0.1	2.1
	4155	1265.0	13.2	62.8	0.7	4.7	0.1	2.1
	4290	1310.0	9.0	68.2	0.5	3.5	0.0	2.6
	4325	1320.0	10.8	59.7	0.6	3.8	0.0	2.4
Milton Green	3723	1134.8	8.1	72.7	0.6	6.2	0.0	2.5
	3725	1135.4	16.1	65.3	1.0	3.1	0.0	2.3
	3726	1135.7	19.0	57.9	1.0	6.0	0.0	2.7
	3728	1136.3	13.5	76.1	0.8	3.7	0.0	2.2
	3729	1136.6	11.9	74.4	0.8	3.3	0.0	2.1

Well	Sample depth	Sample depth	Al$_2$O$_3$	SiO$_2$	TiO$_2$	Fe$_2$O$_3$	MnO	MgO
	(ft)	(m)	%	%	%	%	%	%
	3919.7	1194.7	5.6	59.5	0.4	2.0	0.0	2.6
	3947	1203.0	2.2	17.5	0.2	1.0	0.0	1.4
Point of Ayr 3 Colliery shaft	215	65.5	20.3	53.9	0.9	6.5	0.0	2.6
	341.6	104.1	20.0	46.0	0.8	8.5	0.1	2.6
	350	106.7	17.9	44.5	0.7	8.0	0.1	2.1
	350	106.7	18.9	48.6	0.7	10.3	0.1	2.1
	585	178.3	16.8	60.5	1.0	6.5	0.1	2.2
	607	185.0	19.3	57.9	0.9	6.9	0.1	2.5
	620	189.0	17.0	44.5	0.7	6.1	0.1	2.1
	649	197.8	19.4	54.3	0.9	7.4	0.0	2.4
	696.6	212.3	16.6	42.2	0.6	7.9	0.1	2.0
	1017	310.0	18.2	49.4	0.7	6.9	0.1	2.3
	1067	325.2	16.0	47.3	0.6	6.0	0.0	2.0
	1072	326.7	15.3	46.9	0.6	6.6	0.0	2.0
	1086	331.0	13.5	52.8	0.5	5.5	0.0	2.2
	1095	333.8	12.9	53.7	0.5	5.5	0.0	2.2

Well	Sample depth (ft)	Sample depth (m)	CaO %	Na$_2$O %	K$_2$O %	P$_2$O$_5$ %	Cl %	S %
Blacon East	2400	731.5	0.3	0.0	3.1	0.1	0.0	0.1
	2450	746.8	0.8	0.0	2.1	0.1	0.0	0.1
	2500	762.0	-	-	-	-	-	-
	2550	777.2	0.4	0.6	2.7	0.1	0.0	0.0
	2600	792.5	2.0	1.1	1.9	0.1	0.0	0.1
	2650	807.7	0.5	0.9	2.7	0.1	0.0	0.1
	2700	823.0	0.3	0.0	3.6	0.1	0.0	0.0
	2750	838.2	0.4	0.0	3.2	0.1	0.0	0.1
	2800	853.4	0.3	0.0	2.8	0.1	0.0	0.1
	2850	868.7	0.6	0.5	2.8	0.1	0.0	0.3
	2900	883.9	0.7	0.0	1.9	0.0	0.0	0.3
	2950	899.2	0.9	0.0	1.7	0.0	0.0	0.4
	3000	914.4	0.6	0.0	1.8	0.0	0.0	0.1
	3050	929.6	5.4	0.0	2.8	0.1	0.0	1.2
	3100	944.9	-	-	-	-	-	-
	3150	960.1	0.9	0.0	2.0	0.0	0.0	0.9
	3200	975.4	-	-	-	-	-	-
	3250	990.6	0.6	0.0	3.6	0.1	0.0	1.3
	3300	1005.8	7.1	0.0	3.1	0.2	0.0	1.5
	3350	1021.1	1.3	0.0	1.4	0.0	0.0	0.4
	3400	1036.3	1.1	0.0	1.8	0.0	0.0	0.4
	3450	1051.6	5.3	0.0	1.7	0.1	0.0	0.8
	3500	1066.8	1.0	0.0	1.7	0.0	0.0	0.3
	3550	1082.0	1.1	0.0	2.3	0.1	0.0	0.3
	3600	1097.3	1.9	0.0	2.9	0.1	0.0	1.0
	3650	1112.5	3.5	0.5	2.4	0.1	0.0	0.9
	3700	1127.8	-	-	-	-	-	-
	3750	1143.0	1.4	0.0	2.0	0.1	0.0	0.7
Erbistock	3960	1205.0	0.4	0.0	3.4	0.2	0.1	0.4
	4110	1255.0	0.6	0.0	3.7	0.1	0.1	0.5
	4155	1265.0	4.1	0.0	2.7	0.1	0.1	0.6
	4290	1310.0	4.6	0.0	2.3	0.1	0.1	1.1
	4325	1320.0	7.7	0.0	2.4	0.1	0.0	0.8
Milton Green	3723	1134.8	0.3	0.0	1.2	0.2	0.0	2.0
	3725	1135.4	0.2	0.0	3.6	0.1	0.0	0.3
	3726	1135.7	0.2	0.0	4.3	0.1	0.0	1.8
	3728	1136.3	0.1	0.0	2.7	0.0	0.0	1.0
	3729	1136.6	0.1	0.0	2.6	0.0	0.0	1.0
	3919.7	1194.7	13.3	0.0	1.3	0.1	0.0	1.1
	3947	1203.0	39.2	0.0	0.4	0.0	0.0	0.4

Well	Sample depth (ft)	Sample depth (m)	CaO %	Na$_2$O %	K$_2$O %	P$_2$O$_5$ %	Cl %	S %
Point of Ayr 3 Colliery shaft	215	65.5	0.2	0.0	3.9	0.1	0.0	0.0
	341.6	104.1	2.1	0.0	3.4	0.3	0.0	2.0
	350	106.7	4.2	0.0	2.8	0.1	0.0	2.6
	350	106.7	3.0	0.0	2.9	0.1	0.0	3.9
	585	178.3	0.3	0.6	2.7	0.1	0.0	0.0
	607	185.0	0.2	0.7	3.4	0.1	0.0	0.0
	620	189.0	5.6	0.0	3.0	0.3	0.0	1.4
	649	197.8	0.3	0.0	3.0	0.2	0.0	2.4
	696.6	212.3	6.5	0.0	2.7	0.1	0.0	2.7
	1017	310.0	4.1	0.0	2.5	0.2	0.0	2.4
	1067	325.2	6.5	0.0	2.1	0.1	0.0	2.4
	1072	326.7	7.0	0.0	2.0	0.2	0.0	3.0
	1086	331.0	5.5	0.0	2.1	0.1	0.0	2.2
	1095	333.8	5.3	0.0	1.9	0.1	0.0	2.5

Appendix G: Inorganic trace element geochemical parameters for borehole samples of the Holywell Shale

Well	Sample depth (ft)	Sample depth (m)	As ppm	Ba ppm	Ce ppm	Co ppm	Cr ppm	Cu ppm	Ga ppm
Blacon East	2400	731.5	12.4	467.0	84.2	29.3	117.8	50.6	24.9
	2450	746.8	7.4	293.1	54.0	15.8	83.0	39.1	12.0
	2500	762.0	-	-	-	-	-	-	-
	2550	777.2	8.2	482.7	70.2	18.4	96.9	40.1	19.5
	2600	792.5	11.5	427.2	58.8	9.4	81.3	22.2	8.9
	2650	807.7	10.2	400.5	95.3	18.0	87.5	33.4	17.7
	2700	823.0	4.2	445.7	100.7	16.5	110.8	41.4	24.0
	2750	838.2	6.3	356.6	87.1	24.2	117.8	23.2	20.0
	2800	853.4	8.0	448.3	86.6	24.9	108.6	50.3	17.6
	2850	868.7	6.7	397.7	76.1	21.8	112.5	65.7	15.4
	2900	883.9	5.0	208.3	50.0	10.6	79.2	25.7	6.4
	2950	899.2	7.1	178.2	55.3	9.3	85.6	22.0	5.7
	3000	914.4	4.8	219.3	44.8	9.2	82.7	29.8	6.6
	3050	929.6	15.5	298.1	66.2	16.4	114.2	75.3	16.9
	3100	944.9	-	-	-	-	-	-	-
	3150	960.1	11.2	166.4	69.6	11.2	96.9	20.2	7.9
	3200	975.4	-	-	-	-	-	-	-
	3250	990.6	17.7	284.2	73.9	23.4	114.3	63.4	16.5
	3300	1005.8	13.3	255.7	44.0	20.7	108.2	85.8	12.7
	3350	1021.1	6.9	566.1	21.6	-	47.9	35.2	-
	3400	1036.3	8.1	383.6	47.2	20.5	118.3	40.6	5.7
	3450	1051.6	8.2	371.3	60.5	6.9	80.5	36.2	6.2
	3500	1066.8	8.2	277.2	60.6	32.2	100.3	28.8	-
	3550	1082.0	0.9	335.2	70.8	12.5	99.5	34.2	7.3
	3600	1097.3	12.7	276.7	87.8	21.6	96.2	58.2	15.4
	3650	1112.5	11.2	402.1	80.6	15.2	100.2	75.3	16.9
	3700	1127.8	-	-	-	-	-	-	-
	3750	1143.0	7.4	229.4	58.8	15.3	99.6	49.7	11.8
Erbistock	3960	1205.0	9.5	434.8	73.1	23.0	108.9	58.2	22.7
	4110	1255.0	10.3	402.5	71.4	18.3	116.6	38.9	17.7
	4155	1265.0	13.7	230.2	48.5	12.5	101.9	40.9	10.7
	4290	1310.0	9.2	172.3	51.3	-	83.8	18.0	5.3
	4325	1320.0	7.1	182.6	65.6	22.5	85.6	23.2	7.4
Milton Green	3723	1134.8	12.6	87.8	71.6	16.7	99.0	22.6	5.1
	3725	1135.4	5.8	221.6	91.2	10.4	117.4	25.1	14.0
	3726	1135.7	17.0	203.5	95.2	26.5	136.3	41.4	18.4
	3728	1136.3	4.5	152.4	66.4	12.2	124.7	18.2	7.0
	3729	1136.6	7.5	129.7	73.7	-	107.2	138.6	6.3
	3919.7	1194.7	7.7	66.0	39.3	-	70.8	4.9	-
	3947	1203.0	-	25.8	15.8	-	28.1	-	5.3

Well	Sample depth	Sample depth	As	Ba	Ce	Co	Cr	Cu	Ga
	(ft)	(m)	ppm	ppm	ppm	ppm	ppm	ppm	ppm
Point of Ayr 3 Colliery shaft	215	65.5	4.1	672.9	95.4	24.6	112.1	27.2	25.9
	341.6	104.1	74.4	494.6	95.9	60.7	166.6	185.3	23.9
	350	106.7	69.8	601.6	76.6	28.4	153.5	159.7	23.4
	350	106.7	568.8	419.0	81.2	37.5	139.9	153.0	23.0
	585	178.3	11.9	392.5	79.3	23.2	97.7	40.0	15.3
	607	185.0	7.2	470.5	88.9	20.6	109.2	36.0	20.8
	620	189.0	32.4	445.2	73.7	22.8	289.8	244.4	19.2
	649	197.8	25.1	409.0	77.1	33.7	134.9	128.7	19.5
	696.6	212.3	68.3	386.5	49.9	34.3	211.0	243.2	15.8
	1017	310.0	54.8	321.0	72.8	36.9	174.8	194.3	19.6
	1067	325.2	43.0	381.1	71.6	28.0	134.6	157.3	17.3
	1072	326.7	31.9	523.2	60.9	26.2	130.0	162.5	16.8
	1086	331.0	33.6	255.2	60.6	29.0	182.5	229.5	11.1
	1095	333.8	33.9	244.7	62.1	29.1	148.6	219.0	11.2

Well	Sample depth (ft)	Sample depth (m)	La ppm	Nb ppm	Ni ppm	Pb ppm	Rb ppm	Sr ppm	Th ppm
Blacon East	2400	731.5	38.2	11.8	81.5	15.2	163.2	100.1	14.6
	2450	746.8	21.0	9.0	47.0	8.9	101.2	64.4	10.3
	2500	762.0	-	-	-	-	-	-	-
	2550	777.2	29.1	14.4	52.7	7.8	119.8	101.6	12.2
	2600	792.5	31.3	12.1	34.0	8.8	73.4	81.2	8.3
	2650	807.7	44.0	15.0	47.2	9.2	114.3	105.9	12.4
	2700	823.0	45.9	12.8	61.5	8.3	175.4	126.4	14.7
	2750	838.2	42.6	13.1	67.1	15.8	157.1	83.5	14.6
	2800	853.4	59.0	14.4	61.0	8.6	138.0	80.1	14.1
	2850	868.7	38.7	12.1	60.1	66.5	131.8	85.3	13.2
	2900	883.9	27.6	9.8	29.9	15.8	76.9	44.8	8.3
	2950	899.2	31.7	8.6	26.6	7.9	64.1	43.4	6.0
	3000	914.4	31.9	8.9	26.8	4.8	70.4	42.8	6.0
	3050	929.6	23.4	10.4	69.8	53.7	131.6	108.5	11.2
	3100	944.9	-	-	-	-	-	-	-
	3150	960.1	37.7	10.9	32.2	14.1	78.8	68.4	9.1
	3200	975.4	-	-	-	-	-	-	-
	3250	990.6	38.5	13.5	64.4	30.2	159.6	85.7	13.0
	3300	1005.8	34.3	10.5	63.8	26.8	136.5	156.5	11.0
	3350	1021.1	17.9	4.9	21.9	20.0	53.3	52.1	5.1
	3400	1036.3	26.4	6.3	78.7	23.8	72.1	55.5	6.7
	3450	1051.6	32.1	8.1	37.5	27.9	67.8	131.9	5.0
	3500	1066.8	28.5	8.7	32.2	19.2	68.6	63.2	7.4
	3550	1082.0	42.5	9.9	45.3	240.6	98.6	85.9	11.2
	3600	1097.3	34.4	12.0	57.6	26.9	132.3	97.8	11.6
	3650	1112.5	24.7	11.1	54.4	30.0	109.6	93.8	9.3
	3700	1127.8	-	-	-	-	-	-	-
	3750	1143.0	23.3	10.3	43.4	53.8	88.6	77.7	8.9
Erbistock	3960	1205.0	29.5	11.8	68.8	30.8	150.1	92.8	12.6
	4110	1255.0	34.0	12.1	53.4	49.5	149.3	82.9	11.7
	4155	1265.0	33.9	9.8	44.5	30.1	106.8	99.8	9.4
	4290	1310.0	32.4	7.6	24.4	12.3	66.4	66.0	5.0
	4325	1320.0	30.9	9.2	32.4	36.5	88.3	113.4	7.8
Milton Green	3723	1134.8	39.9	8.4	44.5	10.7	41.5	37.8	6.8
	3725	1135.4	40.6	16.4	31.7	7.4	144.7	76.5	12.8
	3726	1135.7	45.3	16.4	69.2	24.5	196.7	88.0	14.1
	3728	1136.3	-	13.5	25.5	7.5	94.8	42.2	9.9
	3729	1136.6	40.8	11.5	23.3	8.2	81.5	47.1	9.3
	3919.7	1194.7	42.4	5.0	24.8	10.5	45.3	416.4	4.8
	3947	1203.0	12.5	1.4	28.7	5.6	19.0	1300.1	3.6
Point of Ayr 3 Colliery shaft	215	65.5	41.4	13.5	60.6	10.2	194.8	134.2	13.9
	341.6	104.1	58.0	11.0	194.2	131.2	171.3	142.1	13.9
	350	106.7	31.9	9.9	122.5	102.7	154.6	161.1	12.3
	350	106.7	29.7	9.8	127.8	142.5	156.2	140.6	11.6
	585	178.3	32.7	15.2	45.8	7.6	117.3	112.3	11.6

Well	Sample depth	Sample depth	La	Nb	Ni	Pb	Rb	Sr	Th
	(ft)	(m)	ppm	ppm	ppm	ppm	ppm	ppm	ppm
	607	185.0	44.2	15.0	52.8	7.4	162.2	130.4	12.0
	620	189.0	54.2	10.0	153.0	99.4	158.8	170.0	12.8
	649	197.8	48.1	13.9	89.0	60.8	168.9	105.3	15.0
	696.6	212.3	-	8.2	165.0	171.9	146.7	174.8	13.2
	1017	310.0	38.6	10.3	118.5	35.9	139.6	148.0	12.5
	1067	325.2	34.6	8.7	102.9	32.3	120.4	202.4	10.9
	1072	326.7	42.5	8.9	114.2	26.5	119.7	178.3	9.6
	1086	331.0	37.4	7.7	126.9	13.8	108.6	131.2	9.5
	1095	333.8	34.2	6.8	128.9	13.3	102.8	140.1	8.3

Well	Sample depth (ft)	Sample depth (m)	U ppm	V ppm	Y ppm	Zn ppm	Zr ppm
Blacon East	2400	731.5	1.8	148.3	36.3	95.5	137.5
	2450	746.8	1.7	96.6	29.0	44.4	140.1
	2500	762.0	-	-	-	-	-
	2550	777.2	2.1	110.5	37.5	71.4	200.2
	2600	792.5	-	55.7	33.9	53.7	285.7
	2650	807.7	1.7	104.8	39.1	86.4	237.8
	2700	823.0	-	147.5	35.0	76.9	140.7
	2750	838.2	2.1	133.9	38.5	60.6	190.9
	2800	853.4	2.2	110.1	39.8	80.6	216.1
	2850	868.7	3.0	124.4	37.5	67.3	180.5
	2900	883.9	1.7	82.8	29.8	26.1	243.3
	2950	899.2	-	61.8	25.8	21.7	260.5
	3000	914.4	-	57.5	27.0	18.0	272.3
	3050	929.6	4.7	205.3	37.8	49.5	144.2
	3100	944.9	-	-	-	-	-
	3150	960.1	1.3	76.6	31.4	15.9	290.0
	3200	975.4	-	-	-	-	-
	3250	990.6	2.1	143.5	46.5	33.7	183.4
	3300	1005.8	5.2	132.3	45.5	42.8	135.3
	3350	1021.1	-	47.9	14.6	24.7	93.5
	3400	1036.3	1.5	69.3	23.6	32.1	233.6
	3450	1051.6	2.7	86.0	30.6	20.7	254.7
	3500	1066.8	-	69.3	30.0	26.6	291.0
	3550	1082.0	2.2	85.0	39.0	104.5	252.8
	3600	1097.3	3.2	118.1	37.3	42.1	184.0
	3650	1112.5	4.1	122.9	37.1	54.3	201.2
	3700	1127.8	-	-	-	-	-
	3750	1143.0	4.0	81.7	39.2	31.6	231.7
Erbistock	3960	1205.0	1.6	140.0	38.6	237.0	141.3
	4110	1255.0	1.5	116.6	35.4	287.2	163.6
	4155	1265.0	1.3	85.7	33.0	141.7	199.2
	4290	1310.0	-	39.2	26.0	37.2	212.5
	4325	1320.0	1.4	75.2	29.6	161.0	172.9
Milton Green	3723	1134.8	1.0	58.8	38.5	16.5	405.3
	3725	1135.4	-	110.4	38.8	19.9	282.6
	3726	1135.7	2.8	133.0	39.1	28.0	188.6
	3728	1136.3	1.3	106.0	33.7	23.6	382.9
	3729	1136.6	1.5	87.9	37.9	18.5	395.0
	3919.7	1194.7	3.3	59.2	17.1	20.2	93.6
	3947	1203.0	-	-	6.6	10.1	30.4
Point of Ayr 3 Colliery shaft	215	65.5	-	147.6	30.6	86.0	132.3
	341.6	104.1	9.2	193.5	47.9	166.3	124.4
	350	106.7	10.3	356.0	41.7	127.6	104.4
	350	106.7	10.5	324.0	41.3	142.0	106.3
	585	178.3	1.7	113.1	39.6	107.0	275.0

Well	Sample depth	Sample depth	U	V	Y	Zn	Zr
	(ft)	(m)	ppm	ppm	ppm	ppm	ppm
	607	185.0	-	128.7	34.9	82.4	158.4
	620	189.0	17.0	668.0	49.8	202.1	102.0
	649	197.8	17.9	194.5	43.1	88.0	155.8
	696.6	212.3	9.0	590.0	40.9	227.1	95.2
	1017	310.0	12.8	378.0	58.3	88.4	105.5
	1067	325.2	11.6	210.7	36.2	65.1	86.3
	1072	326.7	17.2	234.0	48.5	89.5	87.4
	1086	331.0	11.0	481.0	34.1	107.3	82.8
	1095	333.8	12.0	434.9	33.8	175.7	78.0

References

Aitkenhead, N., Barclay, W.J., Brandon, A., Chadwick, R.A., Chisholm, J.I., Cooper, A.H., Johnson, E.W., 2002, British regional geology: the Pennines and adjacent areas (4th edition), British Geological Survey, Nottingham.

Andrews, I.J., 2013, The Carboniferous Bowland Shale gas study: geology and resource estimation. *British Geological Survey for Department of Energy and Climate Change*, *London, UK*. URI: http://nora.nerc.ac.uk/id/eprint/503839

Aplin, A.C., Macquaker, J.H.S., 2011, Mudstone diversity: Origin and implications for source, seal, and reservoir properties in petroleum systems, *AAPG Bulletin*, 95 (12), pp. 2031-2059. DOI: 10.1306/03281110162

Armitage, P.J., Faulkner, D.R., Worden, R.H., Aplin, A.C., Butcher, A.R., Iliffe, J., 2011, Experimental measurement of, and controls on, permeability and permeability anisotropy of caprocks from the CO2 storage project at the Krechba Field, Algeria, *Journal of Geophysical Research: Solid Earth*, **116**, B12208. DOI: 10.1029/2011JB008385

Armstrong, J.P., Smith, J., D'Elia, V.A.A., Trueblood, S.P., 1997, The occurrence and correlation of oils and Namurian source rocks in the Liverpool Bay- North Wales area, *Geological Society, London, Special Publications*, **124**, pp. 195-211. DOI: 10.1144/GSL.SP.1997.124.01.12

Arthurton, R.S., Johnson, E.W., Mundy, D.J.C., 1988, Geology of the country around Settle, *Memoir of the British Geological Survey*, Sheet 60 (England & Wales).

Behar, F., Beaumont, V., Penteado, H.L.De B., 2001, Rock-Eval 6 Technology: Performances and Developments, *Oil & Gas Science and Technology – Rev. IFP*, **56** (2), pp. 111-134. DOI: 10.2516/ogst:2001013

Blood, R., Lash, G., Bridges, L., 2013, Biogenic Silica in the Devonian Shale Succession of the Appalachian Basin, USA, *AAPG Search and Discovery Article*, **#50864**

Bott, M.H.P., Johnson, G.A.L., 1967, The controlling mechanism of Carboniferous cyclic sedimentation, *Quarterly Journal of the Geological Society of London*, **122**, pp. 421-441. DOI: 10.1144/gsjgs.122.1.0421

Bowker, K. A., 2003, Recent developments of the Barnett Shale play, Fort Worth Basin, *West Texas Geological Society Bulletin*, **42** (6), pp. 4–11.

Bowker, K.A., 2007, Barnett Shale gas production, Fort Worth Basin: Issues and discussion, *AAPG Bulletin*, **91** (4), pp.523-533. DOI: 10.1306/06190606018

Calvert, S.E., 2004, Beware intercepts: interpreting compositional ratios in multi-component sediments and sedimentary rocks, *Organic Geochemistry*, **35**, pp. 981-987. DOI: 10.1016/j.orggeochem.2004.03.001

Castaing, R., 1951, Application des sondes électroniques à une méthode d'analyse ponctuelle chimique et cristallographique, *PhD Thesis, University of Paris*.

Charpentier, R.R., Cook, T.A., 2011, USGS Methodology for Assessing Continuous Petroleum Resources, *U.S. Geological Survey Open-File Report*, pp. 2011–1167.

Church, K.D., Gawthorpe, R.L., 1994, High resolution sequence stratigraphy of the late Namurian in the Widmerpool Gulf (East Midlands, UK), *Marine and Petroleum Geology*, **11**, pp. 528-544. DOI: 10.1016/0264-8172(94)90066-3

Collinson, J.D., 1988, Controls on Namurian sedimentation in the Central Province basins of northern England, *in Sedimentation in a Synorogenic Basin Complex: the Upper Carboniferous of Northwest Europe (eds Besly B. M., Kelling G)*, Blackie, Glasgow, pp. 85–101, ISBN: 0216920256.

Cope, J.C.W., Guion, P.D., Sevastopulo, G.D., Swan, A.R.H., 1992, Carboniferous *in Atlas of Palaeogeography and Lithofacies, Geological Society, London, Memoirs*, **13**, pp. 67-86. DOI: 10.1144/GSL.MEM.1992.013.01.9

Craig, L.C., Connor, C.W., Brobst, D.A., Cohee, G.V., De Witt, W., Dutro, J.T., Gordon, M., Huddle, J.W., McGrew, L.W., Sable, E.G., Varnes, K.L., 1979, Paleotectonic Investigations of the Mississippian System in the United States: Part II. Interpretive study and special features of the Mississippian System, *USGS Geological Survey Professional Paper 1010*, 559 pages.

Curtis, M.E., Sondergeld, C.H., Ambrose, R.J., Rai, C.S., 2012, Microstructural investigation of gas shales in two and three dimensions using nanometer-scale resolution imaging, *AAPG Bulletin*, **96** (4), pp.665-677. DOI: 10.1306/08151110188

Davies, S.J., Hampson, G.J., Elliott, T., Flint, S.S., 1999, Continental-scale sequence stratigraphy of the Namurian, Upper Carboniferous and its applications to reservoir prediction, *Petroleum Geology of NW Europe: Proceedings of the 5th Conference, edited by A. J. Fleet and S. A. R. Boldy*, pp. 757–770, Geol. Soc., London. DOI: 10.1144/0050757

Davies, J.R., Wilson, D., Williamson, I.T., 2004, Geology of the Country around Flint, *Memoir for 1:50000 Geological Sheet 108 (England and Wales)*, British Geological Survey, ISBN: 085272487-X.

Davies, S.J., Leng, M.J., Macquaker, J.H.S., Hawkins, K., 2012, Sedimentary process control on carbon isotope composition of sedimentary organic matter in an ancient shallow-water shelf succession, *Geochemistry Geophysics Geosystems*, **13** (1), Q0AI04. DOI: 10.1029/2012GC004218

Dembicki, H., 2009, Three common source rock evaluation errors made by geologists during prospect or play appraisals, *AAPG Bulletin*, **93** (3), pp. 341-356. DOI: 10.1306/10230808076

Dembicki, H., 2013, Shale Gas Geochemistry Mythbusting, *AAPG Search and Discovery Article*, **#80294**

Dewhurst, D.N., Aplin, A.C., Sarda, J.P., Yang, Y.L., 1998, Compaction-driven evolution of porosity and permeability in natural mudstones: An experimental study, *Journal of Geophysical Research: Solid Earth*, **103** (B1), pp. 651-661. DOI: 10.1029/97JB02540

Dow, W.G., 1977, Kerogen studies and geological interpretations, *Journal of Geochemical Exploration*, **7**, pp.79-99. DOI: 10.1016/0375-6742(77)90078-4

Espitalié, J., Laporte, J.L., Madec, M., Marquis, F., Leplat, P., Paulet, J., Boutefeu, A., 1977, Rapid method for source rock characterization, and for determination of their petroleum potential and degree of evolution, *Oil & Gas Science and Technology - Revue de l'Institut Français du Pétrole*, **32 (**1), pp. 23-42. DOI: 10.2516/ogst:1977002

Fielding, C.R., Frank, T.D., Birgenheier, L.P., Rygel, M.C., Jones, A.T., Roberts, J., 2008, Stratigraphic imprint of the Late Paleozoic Ice Age in eastern Australia: A record

of alternating glacial and nonglacial climate regime, *Papers in the Earth and Atmospheric Sciences*, Paper **103**. http://digitalcommons.unl.edu/geosciencefacpub/103

Fisher, Q.J., Wignall, P.B., 2001, Palaeoenvironmental controls on the uranium distribution in an Upper Carboniferous black shale (*Gastrioceras listeri* Marine Band) and associated strata; England, *Chemical Geology*, **175**, pp. 605-621. DOI: 10.1016/S0009-2541(00)00376-4

Folk, R.L., 1980, Petrology of Sedimentary Rocks, *Hemphill Publishing, Austin, TX*, 184 pages. ISBN: 0-914696-14-9

Frank, T.D., Birgenheier, L.P., Montañez, L.P., Fielding, C.R., Rygel, M.C., 2008, Late Paleozoic climate dynamics revealed by comparison of ice-proximal stratigraphic and ice-distal isotopic records, in Fielding, C.R., Frank, T.D., and Isbell, J.L., eds., Resolving the Late Paleozoic Ice Age in Time and Space: *Geological Society of America Special Paper*, **441**. DOI: 10.1130/2008.2441(23).

Fraser, A.J., Gawthorpe, R.L., 1990, Tectono-stratigraphic development and hydrocarbon habitat of the Carboniferous in northern England, *Geological Society, London, Special Publications*, **55**, pp. 49-86. DOI: 10.1144/GSL.SP.1990.055.01.03

Fraser, A.J., Gawthorpe, R.L., 2003, An Atlas of Carboniferous Basin Evolution in Northern England, *Geological Society Memoirs*, **28**, 88 pages. ISBN: 1862391351

Gale, J.F.W., Reed, R.M., Holder, J., 2007, Natural fractures in the Barnett Shale and their importance for hydraulic fracture treatments, *AAPG Bulletin*, **91** (4), pp. 603-622. DOI: 10.1306/11010606061

Gale, J.F.W., Laubach, S.E., Olson, J.E., Eichhubl, P., Fall, A., 2014, Natural fractures in shale: A review and new observations, *AAPG Bulletin*, **98** (11), pp. 2165-2216. DOI: 10.1306/08121413151

Gasparik, M., Ghanizadeh, A., Bertier, P., Gensterblum, Y., Bouw, S., Krooss, B.M., 2012, High-Pressure Methane Sorption Isotherms of Black Shales from The Netherlands, *Energy & Fuels*, **26** (8), pp. 4995-5004. DOI: 10.1021/ef300405g

Gilman, J., Robinson, C., 2011, Success and Failure in Shale Gas Exploration and Development: Attributes that Make the Difference, *AAPG Search and Discovery Article*, **#80132**.

González, C.R., 2001, New data on the late Paleozoic glaciations in Argentina: *Newsletter on Carboniferous Stratigraphy*, **19**, pp. 44–45.

Gordon, M., 1962, Species of Goniatites in the Caney Shale of Oklahoma, *Journal of Paleontology*, **36** (2), pp. 355-357. URL: http://www.jstor.org/stable/1301116

Gross, D., Sachsenhofer, R.F., Bechtel, A., Pytlak, L., Rupprecht, B., Wegerer, E., 2015, Organic geochemistry of Mississippian shales (Bowland Shale Formation) in central Britain: Implications for depositional environment, source rock and gas shale potential, *Marine and Petroleum Geology*, **59**, pp. 1-21. DOI: http://dx.doi.org/10.1016/j.marpetgeo.2014.07.022

Guion, P.D., Fielding, C.R., 1988, Westphalian A and B sedimentation in the Pennine Basin, UK, *in Sedimentation in a Synorogenic Basin Complex: the Upper Carboniferous of Northwest Europe (eds Besly B. M., Kelling G)*, Blackie, Glasgow, pp. 85–101, ISBN: 0216920256

Hampson, G.J., Elliott, T., Flint, S.S., 1996, Critical application of high resolution sequence stratigraphic concepts to the Rough Rock Group (Upper Carboniferous) of northern England, *Geological Society, London, Special Publications*, **104**, p. 221-246. DOI: 10.1144/GSL.SP.1996.104.01.14

Hart, B.S., Macquaker, J.H.S., Taylor, K.G., 2013, Mudstone ("shale") depositional and diagenetic processes: Implications for seismic analyses of source-rock reservoirs, *Interpretation (SEG)*, **1**(1), B7-B26. DOI: 10.1190/INT-2013-0003.1

Heckel, P.H., 1986, Sea-level curve for Pennsylvanian eustatic marine transgressive-regressive depositional cycles along midcontinent outcrop belt, North America, *Geology*, **14**, pp. 330-334. DOI: 10.1130/0091-7613(1986)14<330:SCFPEM>2.0.CO;2

Holdsworth B.K., Collinson J.D., 1988, Millstone Grit cyclicity revisited. In: Besly B.M., Kelling G. (eds) Sedimentation in a Synorogenic Basin Complex: The Upper Carboniferous of Northwest Europe. Blackie, Glasgow, 132–152.

House, M.R., 1996, Juvenile goniatite survival strategies following Devonian extinction events, *From* Hart, M. B. (ed.), 1996, *Biotic Recovery from Mass Extinction Events*, Geological Society Special Publication, **102**, pp. 163-185.

Isbell, J.L., Miller, M.F., Wolfe, K.L., Lenaker, P.A., 2003, Timing of late Paleozoic glaciation in Gondwana: Was glaciation responsible for the development of Northern Hemisphere cyclothems?: in Chan, M.A., and Archer, A.W., eds., Extreme Depositional Environments: Mega End Members in Geologic Time: *Geological Society of America Special Paper* **370**, pp. 5–24.

Jarvie, D.M., Baker, D.R., 1984, Application of the Rock-Eval III Oil Show Analyzer to the study of gaseous hydrocarbons in an Oklahoma gas well, 187th ACS National Meeting, St. Louis Missouri, April 8-13 (1984).

Jarvie, D.M., Hill, R.J., Ruble, T.E., Pollastro, R.M., 2007, Unconventional shale-gas systems: The Mississippian Barnett Shale of north-central Texas as one model for thermogenic shale-gas assessment, *AAPG Bulletin*, **91** (4), pp. 475-499. DOI: 10.1306/12190606068

Jarvie, D.M., 2011, Unconventional Oil Petroleum Systems: Shales and Shale Hybrids, *AAPG Search and Discovery Article*, #80131.

Jarvie, D.M., 2012, Shale resource systems for oil and gas: Part 1—Shale-gas resource systems, *in Shale reservoirs—Giant resources for the 21st century (ed Breyer J. A.).* AAPG Memoir, **97**, pp. 69–87.

Jerrett, R.M., Hampson, G.J., 2007, Sequence stratigraphy of the upper Millstone Grit (Yeadonian, Namurian), North Wales, *Geological Journal*, **42**, pp. 513-530. DOI: 10.1002/gj.1089

Johnson, E.W., Soper, N.J., Burgess, I.C., 2001, Geology of the country around Ulverston, *Memoir of the British Geological Survey*, Sheet 48 (England & Wales).

Jones, R.C.B., Lloyd, W., 1942, The stratigraphy of the Millstone Grit of Flintshire, *Journal of the Manchester Geological Association*, **13**, pp. 78-99.

Jones, M., 1980, Deltaic sedimentation in the Roaches Grit and associated sediments (Namurian R2b) in the south-west Pennines, *Proceedings of the Yorkshire Geological Society*, **43**, pp, 39-67. DOI: 10.1144/pygs.43.1.39

Jones, B., Manning, D.A.C., 1994, Comparison of geochemical indexes used for the interpretation of palaeoredox conditions in ancient mudstones, *Chemical Geology*, **111** (1-4), pp. 111-129. DOI: 10.1016/0009-2541(94)90085-X

Junium, C.K., Arthur, M.A., 2007, Nitrogen cycling during the Cretaceous, Cenomanian–Turonian Oceanic Anoxic Event II, *Geochemistry, Geophysics,Geosystems*, **8** (3), Q03002. DOI: 10.1029/2006GC001328

Koch, P.L., Zachos, J.C., Gingerich, P.D., 1992, Correlation between isotope records in marine and continental carbon reservoirs near the Palaeocene/Eocene boundary, *Nature*, **358**, pp. 319-322.

Könitzer, S.F., Davies, S.J., Stephenson, M.H., Leng, M.J., Gabbott, S.E., Angiolini, L., Macquaker, J.H.S., Vane, C.H., Millward, D., Kane, I.A., 2011, Primary Controls on Organic Carbon Content in UK Upper Mississippian Gas Shales, *AAPG Search and Discovery Article*, **#80175**.

Könitzer, S.F., Davies, S.J., Stephenson, M.H., Leng, M.J., 2014a, Depositional controls on mudstone lithofacies in a basinal setting: implications for the delivery of sedimentary organic matter, *Journal of Sedimentary Research*, **84**, pp.198-214. DOI: 10.2110/jsr.2014.18

Könitzer, S.F., 2014b, Primary Biological Controls on UK Lower Namurian Shale Gas Prospectivity: A Step Towards Understanding A Major Potential UK Unconventional Gas Resource, *PhD Thesis at the University of Leicester*.

Lazar, O.R., Bohacs, K.M., Macquaker, J.H.S., Schieber, J., Demko, T.M., 2015a, Capturing key attributes of fine-grained sedimentary rocks in outcrops, cores, and thin sections: nomenclature and description guidelines, *Journal of Sedimentary Research*, **85**, pp 230-246. DOI: 10.2110/jsr.2015.11

Lazar, O.R., Bohacs, K.M., Macquaker, J.H.S., Schieber, J., Demko, T.M., 2015b, Mudstone Primer: Lithofacies variations, diagnostic criteria, and sedimentologic-

stratigraphic implications at lamina to bedset scales, *SEPM Concepts in Sedimentology and Palaeontology* **#12**, 198 pages.

Leeder, M.R., McMahon, A.H., 1988, Upper Carboniferous (Silesian) basin subsidence in northern Britain, *in:* Besly, B.M., Kelling, G. (eds), *Sedimentation in a Synorogenic Basin Complex: the Upper Carboniferous of Northwest Europe*, Blackie, Glasgow, pp. 43-52.

Lewan, M.D., 1986, Stable carbon isotopes of amorphous kerogens from Phanerozoic sedimentary-rocks, *Geochimica et Cosmochimica Acta*, **50** (8), pp. 1583-1591. DOI: 10.1016/0016-7037(86)90121-3

Loucks, R.G., Reed, R.M., Ruppel, S.C., Hammes, U., 2012, Spectrum of pore types and networks in mudrocks and a descriptive classification for matrix-related mudrock pores, *AAPG Bulletin*, **96** (6), pp. 1071-1098. DOI: 10.1306/08171111061

Macquaker, J.H.S., Adams, A.E., 2003, Maximising information from fine-grained sedimentary rocks: an inclusive nomenclature for mudstones, *Journal of Sedimentary Research*, **73** (5), pp.735-744. DOI: 10.1306/012203730735

Macquaker, J.H.S., Taylor, K.G., Gawthorpe, R.L., 2007, High-Resolution Facies Analyses of Mudstones: Implications for Paleoenvironmental and Sequence Stratigraphic Interpretations of Offshore Ancient Mud-Dominated Successions, *Journal of Sedimentary Research*, **77** (4), pp. 324-339. DOI: 10.2110/jsr.2007.029

Magraw, D., 1954, Fossils specimens collected from Point of Ayr colliery shaft number 3, identified and held at the British Geological Survey, Keyworth (UK).

Martinsen, O.J., Collinson, J.D., Holdsworth, B.K., 1995, Millstone Grit cyclicity revisited, II: sequence stratigraphy and sedimentary responses to changes of relative sea-level, *Sedimentary Facies Analysis*: *A Tribute to the Research and Teaching of Harold G. Reading (ed A. G. Plint)*, Blackwell Publishing Ltd., Oxford, UK. DOI: 10.1002/9781444304091.ch13

Maynard, J.B., 1981, Carbon isotopes as indicators of dispersal patterns in Devonian-Mississippian shales of the Appalachian Basin, *Geology*, **9**, pp. 262-265.

McCarthy, K., Rojas, K., Niemann, M., Palmowski, D., Peters, K., Stankiewicz, A., 2011, Basic Petroleum Geochemistry for Source Rock Evaluation, *Schlumberger Oilfield Review*, **23** (2), pp. 32-43.

Meyers, P.A., Bernasconi, S.M., Yum, J-G., 2009, 20 My of nitrogen fixation during deposition of mid-Cretaceous black shales on the Demerara Rise, equatorial Atlantic Ocean, *Organic Geochemistry*, **40** (2), pp. 158-166. DOI: 10.1016/j.orggeochem.2008.11.006

Michael, G.E., Packwood, J., Holba, A., 2013, Determination of In-situ Hydrocarbon Volumes in Liquid Rich Shale Plays, *Unconventional Resources Technology Conference*, **1573030**, 7 pages.

Milliken, K.L., Esch, W.L., Reed, R.M., Zhang, T.W., 2012, Grain assemblages and strong diagenetic overprinting in siliceous mudrocks, Barnett Shale (Mississippian), Fort Worth Basin, Texas, *AAPG Bulletin*, **96** (8), pp. 1553-1578. DOI: 10.1306/12011111129

Milliken, K.L., 2014, A compositional classification for grain assemblages in fine-grained sediments and sedimentary rocks, *Journal of Sedimentary Research*, **84**, pp.1185-1199. DOI: 10.2110/jsr.2014.92

Montgomery, S.L., Jarvie, D.M., Bowker, K.A., Pollastro, R.M., 2005, Mississippian Barnett Shale, Fort Worth basin, north-central texas: Gas-shale play with multi-trillion cubic foot potential, *AAPG Bulletin*, **89** (2), pp. 155-175. DOI: 10.1306/09170404042

Murphy, A.E., Sageman, B.B., Hollander, D.J., 2000, Eutrophication by decoupling of the marine biogeochemical cycles of C, N, and P: A mechanism for the Late Devonian mass extinction, *Geology*, **28** (5), pp.427-430. DOI: 10.1130/0091-7613(2000)28<427:EBDOTM>2.0.CO;2

Newport, L.P., Aplin, A.C., Gluyas, J.G., Greenwell, H.C., Gröcke, D.R., 2016, Geochemical and lithological controls on a potential shale reservoir: Carboniferous Holywell Shale, Wales, *Marine and Petroleum Geology*, **71**, pp. 198-210. DOI: 10.1016/j.marpetgeo.2015.11.026

Orr, W.L., 1986, Kerogen/asphaltene/sulphur relationships in sulphur-rich Monterey oils, *Organic Geochemistry*, **10** (1-3), pp. 499-516. DOI: 10.1016/0146-6380(86)90049-5

Passey, Q. R., Bohacs, K. M., Esch, W. L., Klimentidis, R., Sinha, S., 2010, From oil-prone source rock to gas-producing shale reservoir: Geologic and petrophysical characterization of unconventional shale-gas reservoirs: International Oil and Gas Conference and Exhibition in China, Beijing, China, June 8–10, 2010, SPE Paper 131350, 29 p.

Penn, I.E., 1987, Geophysical logs in the stratigraphy of Wales and adjacent offshore and onshore areas, *Proceedings of the Geologists' Association*, **98**(4), pp. 275-313.

Peters, K.E., Moldowan, J.M., 1993, The biomarker guide: Interpreting molecular fossils in petroleum and ancient sediments, *Prentice Hall*, 363 pages. ISBN-10: 0130867527

Peters-Kottig, W., Strauss, H., Kerp, H., 2006, The land plant δ^{13}C record and plant evolution in the Late Palaeozoic, *Palaeogeography Palaeoclimatology Palaeoecology*, **240** (1-2), pp. 237-252. DOI: 10.1016/j.palaeo.2006.03.051

Philibert, J., 1963, A method for calculating the absorption correction in electron-probe microanalysis, *From:* H.H. Pattee, V.E. Coslett, A. Engstrom (Eds.), Proc. Symposium on X-ray Optics and X-ray Microanalysis, Academic Press, New York, pp. 379–392.

Pouchou J.L., Pichoir F., 1984, A new model for quantitative X-ray-microanalysis, Part 1. Application to the analysis of homogeneous samples, *La Recherche Aérospatiale*, **3**, pp. 167-192.

Ramsbottom, W.H.C., 1974, The Namurian of North Wales, *in Owen, T.R., The Upper Palaeozoic and post-Palaeozoic of North Wales*, Cardiff University Press, 426 pages, ISBN: 0-7083-0555-5.

Ramsbottom, W.H.C., 1977, Major cycles of transgression and regression (mesothems) in the Namurian, *Proceedings of the Yorkshire Geological Society*, **41**, pp. 261-291.

Ramsbottom, W.H.C., 1978, Namurian mesothems in South Wales and northern France, *Journal of the Geological Society*, **135**, pp. 307-312. DOI: 10.1144/gsjgs.135.3.0307

Rexer, T.F.T., Benham, M.J., Aplin, A.C., Thomas, K.M., 2013, Methane Adsorption on Shale under Simulated Geological Temperature and Pressure Conditions, *Energy & Fuels*, **27** (6), pp. 3099-3109. DOI: 10.1021/ef400381v

Rider, M.H., Kennedy, M., 2011, The geological interpretation of well logs, *Rider-French Consulting Limited; 3rd Revised edition edition*, 440 pages. ISBN: 0954190688

Rivera, K., Quan, T. M., 2013, Thermal maturation effects on the nitrogen isotopes in marine shales: a case study of the Woodford Shale, *AAPG Annual Convention and Exhibition*. Abstract published as Search and Discovery article #50920 (2014).

Rose, W.C.C., Dunham, K.C., 1977, Geology and hematite deposits of South Cumbria, *Economic Memoir of the British Geological Survey*, Sheet 58, Part 48.

Ross, D.J.K., Bustin, R.M., 2006, Sediment geochemistry of the Lower Jurassic Gordondale Member, northeastern British Columbia, *Bulletin of Canadian Petroleum Geology*, **54**, pp. 337–365.

Ross, D.J.K., Bustin, R.M., 2009, Investigating the use of sedimentary geochemical proxies for paleoenvironmental interpretation of thermally mature organic-rich strata: Examples from the Devonian-Mississippian shales, Western Canadian Sedimentary Basin, *Chemical Geology*, **260**, pp. 1-19. DOI: 10.1016/j.chemgeo.2008.10.027

Rygel, M.C., Fielding, C.R., Frank, T.D., Birgenheier, L.P., 2008, The magnitude of late Palaeozoic glacioeustatic fluctuations: a synthesis, *Journal of Sedimentary Research*, **78** (7-8), pp. 500-511. DOI: 10.2110/jsr.2008.058

Schieber, J., Southard, J.B., Thaisen, K., 2007, Accretion of Mudstone Beds from Migrating Floccule Ripples, *Science*, **318**, p. 1760-1763. DOI: 10.1126/science.1147001

Schieber, J., Southard, J.B., Schimmelmann, A., 2010, Lenticular Shale Fabrics Resulting from Intermittent Erosion of Muddy Sediments − Comparing Observations

from Flume Experiments to the Rock Record, *Journal of Sedimentary Research*, **80**, p. 119-128. DOI: 10.2110/jsr.2010.005

Słowakiewicz, M., Tucker, M.E., Vane, C.H., Harding, R., Collins, A., Pancost, R.D., 2015, Shale-Gas Potential of the Mid-Carboniferous Bowland-Hodder Unit in the Cleveland Basin (Yorkshire), Central Britain, *Journal of Petroleum Geology*, **38**(1), pp.59-76. DOI: 10.1111/jpg.12598

Smith, N.J.P., Kirby, G.A., Pharaoh, T.C., 2005, The structure and evolution of the south-west Pennine Basin and adjacent area, *British Geological Survey*, 129 pages.

Stephenson, M.H., Millward, D., Leng, M.J., Vane, C.H., 2008, Palaeoecological and possible evolutionary effects of early Namurian (Serpukhovian, Carboniferous) glacioeustatic cyclicity, *Journal of the Geological Society, London,* **165**, pp. 993-1005. DOI: 10.1144/0016-76492007-153

Schieber, J., Krinsley, D., Riciputi, L., 2000, Diagenetic origin of quartz silt in mudstones and implications for silica cycling, *Nature*, **406**, p. 981-985. DOI: 10.1038/35023143

Stewart, D.R., 1986, Petroleum Engineering Factual Report (LM1-1) Erbistock-1, W48 File, *Completion Report, United Kingdom Land Well Records (dti)*.

Sutton, M.A., Li, N., Joy, D.C., Reynolds, A.P., Li, X., 2007, Scanning electron microscopy for quantitative small and large deformation measurements part i: SEM imaging at magnifications from 200 to 10,000, *Experimental Mechanics*, **47** (6), pp.775-787.

Tissot, B.P., Welte, D.H., 1984, Petroleum Formation and Occurrence: a new approach to oil and gas exploration [2nd Edition], *Springer-Verlag, New York*, pp.538, ISBN 978-3642878152

Tyson, R.V., 1995, Sedimentary Organic Matter: organofacies and palynofacies, *Chapman & Hall*, 615 pages. ISBN 0-412-36350-X

Tyson, R.V., Follows, B., 2000, Palynofacies prediction of distance from sediment source: A case study from the Upper Cretaceous of the Pyrenees, *Geology*, **28** (6), pp. 569-571. DOI: 10.1130/0091-7613(2000)28<569:PPODFS>2.0.CO;2

Van Krevelen, D.W., 1950, Graphical-statistical method for the study of structure and reaction processes of coal, *Fuel*, **29**, pp.269-84

Van Mooy, B.A.S., Keil, R.G., Devol, A.H., 2002, Impact of suboxia on sinking particulate organic carbon: enhanced carbon flux and preferential degradation of amino acids via denitrification, *Geochimica et Cosmochimica Acta*, **66** (3), pp.457–465. DOI: 10.1016/S0016-7037(01)00787-6

Verardo, D.J., MacIntyre, A., 1994, Production and destruction: control of biogenous sedimentation in the tropical Atlantic 0–300,000 years B.P., *Paleoceanography*, **9** (1), pp.63–86. DOI: 10.1029/93PA02901

Waters, C.N., Waters, R.A., Barclay, W.J., Davies, J.R., 2009, A lithostratigraphical framework for the Carboniferous successions of southern Great Britain (Onshore), *British Geological Survey Research*, Report RR/09/01.

Waters, C.N., 2009, Carboniferous geology of Northern England, *Journal Open University Geological Society*, **30** (2), pp. 5-16. URI: http://nora.nerc.ac.uk/id/eprint/10713

Waters, C.N., Condon, D.J., 2012, Nature and timing of Late Mississippian to Mid-Pennsylvanian glacio-eustatic sea-level changes of the Pennine Basin, UK, *Journal of the Geological Society*, **169** (1), pp. 37-51. DOI: 10.1144/0016-76492011-047

Wedepohl, K.H., 1971, Environmental influences on the chemical composition of shales and clays. In: Ahrens, L.H., Press, F., Runcorn, S.K., Urey, H.C. (Eds.), Physics and Chemistry of the Earth, vol. 8, Pergamon, Oxford, pp. 305–333.

Wells, M.R., Allison, P.A., Hampson, G.J., Piggott, M.D., Pain, C.C., 2005, Modelling ancient tides: the Upper Carboniferous epi-continental seaway of Northwest Europe, *Sedimentology*, **52** (4), pp. 715-735. DOI: 10.1111/j.1365-3091.2005.00718.x

Williams, L.A., 1984, Subtidal stromatolites in Monterey formation and other organic-rich rocks as suggested source contributors to petroleum formation, *AAPG Bulletin*, **68** (12), pp. 1879-1893. DOI:

Williams, G.D., Eaton, G.P., 1993, Stratigraphic and structural analysis of the Late Palaeozoic-Mesozoic of NE Wales and Liverpool Bay: implications for hydrocarbon

prospectivity, *Journal of the Geological Society*, **150** (3), pp. 489-499. DOI: 10.1144/gsjgs.150.3.0489

Woodcock, N., Strachan, R.., 2009, Geological History of Britain and Ireland, *Blackwell Publishing*, 423 pages.

Wright, W.B., Sherlock, R.L., Wray, D.A., Lloyd, W., Tonks, L.H., 1927, The geology survey of the Rossendale Anticline, *Memoir of the Geological Survey, Great Britain,* Sheet 76 (England & Wales), 182 pages.

Yang, Y.L., Aplin, A.C., 2007, Permeability and petrophysical properties of 30 natural mudstones, *Journal of Geophysical Research: Solid Earth*, **112** (B3), B03206. DOI: 10.1029/2005JB004243

Yang, Y.L., Aplin, A.C., 2010, A permeability-porosity relationship for mudstones, *Marine and Petroleum Geology*, **27** (8), pp. 1692-1697. DOI: 10.1016/j.marpetgeo.2009.07.001